

US EPA ARCHIVE DOCUMENT

UV- Epifluorescence Microscopy Analysis of Sediments Recovered from the Kalamazoo River

by

**Kenneth Lee, Jay Bugden, Susan Cobanli, Tom King, Claire McIntyre, Brian
Robinson, Scott Ryan and Gary Wohlgeschaffen**

**Centre for Offshore Oil, Gas and Energy Research (COOGER)
Fisheries and Oceans Canada
Bedford Institute of Oceanography
P.O. Box 1006, 1 Challenger Drive
Dartmouth, Nova Scotia
Canada B2Y 4A2**

October 24, 2012

Table of Contents

1.0 ABSTRACT 3

2.0 INTRODUCTION..... 3

3.0 MATERIALS AND METHODS 5

 3.1 *Sample coding and information* 5

 3.2 *Epifluorescence microscopy* 7

 3.3 *Visual observation of source oil under UV light* 7

 3.4 *Testing for the creation of oil-mineral aggregates* 7

 3.5 *Preparation of sediment samples for epifluorescence microscopy*..... 7

 3.6 *Microscopy and photomicrography* 8

 3.7 *Sample preparation for chemical analyses* 8

 3.8 *GC-FID analysis of TPH*..... 8

 3.9 *Introspect analysis of saturates, aromatics, resins and asphaltenes (SARA)* 8

 3.10 *Three dimensional UV fluorescence analysis*..... 8

 3.11 *Purification of selected extracts for fluorescence* 9

4.0 RESULTS AND DISCUSSION 9

 4.1 *Visual observation of source oil under UV light* 9

 4.2 *Formation of oil-mineral aggregates* 9

 4.3 *Sediment sample epifluorescence micrographs* 11

 4.4 *Microscopic observations of oil in sediment samples under UV epifluorescence* 14

 4.5 *Comparison of epifluorescence microscopy with TPH oil chemistry* 17

 4.6 *Total petroleum hydrocarbons* 17

 4.7 *Alpha Labs data* 18

 4.8 *Thin-layer chromatogram scanning flame ionization (TLC/FID)* 19

 4.9 *Three dimensional fluorescence* 21

5.0 CONCLUSIONS 24

6.0 REFERENCES 25

Appendix A 28

Appendix B 34

1.0 ABSTRACT

An ultraviolet (UV) epifluorescence microscopy technique was used to determine the presence of residual hydrocarbons and the potential formation of oil-mineral aggregates (OMA) in samples of sediments recovered from the Kalamazoo River impacted by the Enbridge Pipeline. Laboratory experiments with weathered KEB source oil and a sediment sample designated as a reference unoiled sample (based on AECOM data that were provided) verified oil fluorescence under UV illumination and the formation of OMA following agitation. The field samples were subsequently observed to contain what could be the fluorescent mineral aragonite, as well as other sources of organic material including petroleum hydrocarbons.

To support the interpretation of the UV-epifluorescence results, the field samples were also analyzed for petroleum hydrocarbons using a variety of qualitative and semi-quantitative analytical techniques. The results revealed that there were potentially other sources of petroleum in addition to the diluted bitumen product released into the Kalamazoo River from the Line 6B Enbridge pipeline spill. In comparison to the weathered source oil sample provided, the hydrocarbon profiles from gas chromatograph flame ionization detection (GC-FID) for many of the field samples was characteristic of advanced stages of weathering. Iatroscan thin-layer chromatography (TLC) analysis was also conducted to determine the percent-contribution of the major components typically detected in crude oil: saturates, aromatics, resins, and asphaltenes. The results confirmed the presence of contaminant petroleum hydrocarbons from multiple sources within the sediments and provided an indication of their extent of weathering. These results supported the work by Alpha Labs that used gas chromatography-mass spectroscopy (GC-MS) analysis of biomarkers (e.g., hopanes and steranes) to enable the identification and quantification of Line 6B oil from other sources of petroleum hydrocarbons within the sediment samples.

Due to the limited numbers of samples (scored positive for oil under UV-epifluorescence microscopy) and the relatively low level of oil fluorescence observed as oil droplets within OMA (as a result of mobilization and dilution of the petroleum hydrocarbons within the sediments from the spill response measures), a correlation could not be made with oil detected by GC-FID, Iatroscan TLC and GC-MS analysis as total petroleum hydrocarbons or individual classes of constituents. Furthermore, UV fluorescence analysis of the weathered KEB source oil and contaminated sediment samples suggested that quenching inhibited the effectiveness of the UV-fluorescence monitoring techniques that might be used. This hypothesis was subsequently proven by analysis of sample extracts following silica gel solid phase extraction. As a result of quenching, it is recommended that methods based on image analysis of UV-fluorescence in sediments (with the exception of bulk oil) are not a reliable means of identifying and quantifying time-series changes in residual hydrocarbons within the sediments.

2.0 INTRODUCTION

In the summer of 2010, Line 6B of the Enbridge pipeline ruptured, spreading 800,000 gallons of a diluted bitumen product over a 30 mile stretch of the Kalamazoo River in Michigan, USA. Extensive dredging has been required in an attempt to remediate the site.

During the initial phases of the spill response operation, sediment cores were collected and split to collect samples for contaminant hydrocarbon analysis. When the split cores were observed under UV illumination, an estimate of the level of oil contamination could be made by image analysis (Fig. X. *Thomas Graan to add in example photographs*). As oil spill response operations proceeded, largely based on the agitation of sediments to mobilize the oil for physical recovery, it was noted that oil was no longer observed in the analysis of split cores under UV illumination. It was hypothesized that this could be due to: 1) physical removal of oil from the sediments by the remedial operations, 2) the emission/excitation wavelengths for analysis were no longer within the optimal ranges for detection as natural weathering of the oil might have altered its fluorescence characteristics, 3) the oil formed oil-mineral aggregates (OMA) that were distributed and diluted throughout the core to concentrations below the detection limits for the whole core image analysis system. To address this issue, the Centre for

Offshore Oil, Gas and Energy Research (COOGER) offered its in-kind services to the US EPA to conduct analysis of representative sediment cores by UV-epifluorescence microscopy and chemical analysis to: 1) determine if the Line 6B source oil would form OMA in the presence of Kalamazoo River sediments when agitated, 2) to conduct 3D fluorescence spectra analysis of the source oil and field sediments known to be heavily weathered so that optimal excitation/emission wavelengths for UV analysis of the residual oil in sediments could be identified, and 3) to verify the effectiveness of UV fluorescence as a means of identifying and quantifying residual oil concentrations in sediments during spill response operations.

Laboratory examination of the interaction of oil and minerals, and their formation into particulates, began in the late 1980s (Delvigne et al., 1987; Payne et al., 1989). In laboratory studies that followed the *Exxon Valdez* spill, it was observed that an emulsion of micron-sized droplets of oil interacted with mineral fines in the presence of seawater in a process termed “clay-oil flocculation” that reduced the adhesion of oil to sediments, and enabled it to be readily transported away from an oiled shoreline by gentle wave action (Bragg and Yang, 1995; Owens et al., 1994). This process provided an explanation for the unexpected high levels of natural cleansing that occurred on very sheltered, low wave-energy shorelines in Prince William Sound from 1989-1990. These particles, also described as “oil-suspended-particulate-matter aggregates” (Sun and Zheng, 2009) among other names, have now been widely recognized under the term “oil-mineral aggregates” (OMA) by COOGER, which has done much of the pioneering research and development on the use of OMA as an oil spill countermeasure.

Studies of OMA formation have demonstrated that both mineral fines and organic particles can stabilize oil droplets within the water column. Various types of aggregates can be formed depending on the physicochemical properties of the particles, the type of oil, and the environmental conditions (Lee et al., 1998; Muschenheim and Lee, 2002; Stoffyn-Egli and Lee, 2002). Both controlled laboratory experiments (Cloutier et al., 2002; Omotoso et al., 2002; Stoffyn-Egli and Lee, 2002) and shoreline field trials (Lunel et al., 1997; Owens et al., 2003a; Prince et al., 2003) have demonstrated that OMA enhances the natural dispersion of oil spilled in the environment and reduces its environmental persistence. Thus, OMA formation is an integral part of natural attenuation processes, and is a potential process to enhance cleanup techniques used in the remediation of the sea surface and shorelines contaminated by oil (Kepkay et al., 2002; Lee, 2002; Stoffyn-Egli and Lee, 2002; Venosa et al., 2002b). The oil droplets that are incorporated in OMA are easily transported into the water column by wave energy (Payne et al., 2003), and more nutrients, dissolved oxygen, and oil-degrading microorganisms can reach the oil due to the reduced size and increased surface area of the droplets, which in turn can accelerate biodegradation (Lee et al., 1997; Owens and Lee, 2003; Owens et al., 2003b; Weise et al., 1999).

OMA formation has been observed at numerous field sites that have ranged from the rivers of Bolivia (Lee et al., 2001) to the shores of Svalbard Island in the high Arctic (Guénette et al., 2003; Sergy et al., 1998). Numerical models support the hypothesis that OMA can form rapidly (Hill et al., 2002; Khelifa et al., 2003), as long as sufficient mixing-energy is available. Detailed chemical analysis of samples recovered from coastal waters following surf-washing operations after the Sea Empress spill in the United Kingdom conclusively demonstrated that OMA formation enhanced the biodegradation rates of the residual oil (Colcomb et al., 1997; Lee et al., 1997), because the stabilization of oil droplets by mineral fines increased the oil-water interface where microbial activity primarily occurs. Thus, this remediation process may not only effectively dilute oil spilled into the environment to concentrations below toxicity threshold limits, but also effectively eliminate many of the components of environmental concern.

COOGER has been evaluating the feasibility of an oil spill countermeasure technique that is based on the enhanced formation and dispersion of OMA in marine oil spill incidents (Lee et al., 2009a). The advantages of this technology include: 1) enhanced dispersion of oil slicks and stabilization of dispersed oil droplets in the water column, 2) reduction of oil concentrations below toxic threshold limits, 3) reduced re-coalescence of droplets and adhesion properties of oil, and 4) enhanced oil biodegradation rates.

Studies have suggested that turbulent energy, dispersant type, mineral type and salinity influence the amount of oil incorporated into the mineral phase to form OMA (Ajijolaiya et al., 2006; Guyomarch et al., 2002; Khelifa et al., 2005b; Stoffyn-Egli and Lee, 2002). Recent studies by Ma et al. (2008) showed that higher levels of turbulent energy enhanced the interaction between oil and minerals (Ma et al., 2008).

Based on this supporting evidence, it is hypothesized that the agitation procedure used in the spill cleanup operations in the Kalamazoo River following the Line 6B spill resulted in a significant amount of OMA formation in addition to the mobilization of bulk oil.

On 16 August 2012, the Centre for Offshore Oil, Gas and Energy Research received a number of sediment samples from AECOM to evaluate for the presence of petroleum hydrocarbon residues using UV epifluorescence microscopy. The samples came from coring sites in the Kalamazoo River that had been impacted by the Line B MP 608 Marshall pipeline release. The purpose of the study was to evaluate the onsite use of fluorescence to detect either bitumen or other sources of contaminant hydrocarbons in the sediments. A number of standard chemical assays were conducted to validate the presence of hydrocarbons detected by UV-epifluorescence microscopy. These additional analyses included the detection of total petroleum hydrocarbons by gas chromatograph flame ionization detection (GC-FID), percent chemical group composition using thin-layer chromatography with flame ionization detection (latroscan TLC), and 3D oil fluorescence spectra analysis.

Fourteen of the forty-one sample jars containing sediments from AECOM were broken during transit. A portion of the sample in these containers had leaked; however, most of the sediments were intact. When received, the ice packs surrounding the samples had completely thawed. A sample of reference weathered oil labelled "KEB source oil" was also received along with the sample shipments.

3.0 MATERIALS AND METHODS

3.1 Sample coding and information

Two sample shipments were received on 16 August 2012 along with documentation for chain of custody (Appendix A). A second batch of samples was received later the same day, and a copy of the chain of custody is also given in Appendix A. COOGER and AECOM's sample code identifiers along with sample descriptions and their condition of their arrival following shipment were recorded (Table 1).

Table 1. COOGER laboratory sample coding, with field descriptions provided by AECOM.

COOGER Sample ID	Site ID (SSCG)	Mile Post	Geomorphic Strata	Client/Field Sample ID Target Oiling	Target Oiling Level	Actual Poling Result
EB-1	STRATIFIED-003	20.00 - 20.25	Anthro Channel	SEKR2025C702S072412DX	Heavy	Heavy
EB-2				SEKR2025C702S072412D005	Heavy	Heavy
EB-36	STRATIFIED-061	18.75 - 19.00	Anthro Channel	SEKR1900C701S072512DX	None	None
EB-41				SEKR1900C701S072512D005	None	None
EB-35				SEKR1900C701S072512D009	None	None
EB-3	STRATIFIED-081	35.25 - 35.50	Backwater	SEKR3650C701S072512DX	Heavy	No Poling
EB-4				SEKR3650C701S072512D006	Heavy	No Poling
EB-28				SEKR3650C701S072512D010	Heavy	No Poling
EB-5	STRATIFIED-082	37.25 - 37.50	Backwater	SEKR3750C701S072512DX	Heavy	No Poling
EB-6				SEKR3750C701S072512D006	Heavy	No Poling

EB-33				SEKR3750C701S072512D010	Heavy	No Poling
EB-38	STRATIFIED-121	4.25 - 4.50	Backwater	SEKR0425C701S072512DX	Light	Light
EB-20				SEKR0425C701S072512D007	Light	Light
EB-7	STRATIFIED-161	37.50 - 37.75	Channel Deposit	SEKR3775C702S072712DX	Heavy	Moderate
EB-8				SEKR3775C702S072712D005	Heavy	Moderate
EB-26				SEKR3775C702S072712D009	Heavy	Moderate
EB-32	STRATIFIED-301	28.50 - 28.75	Cutoff/Oxbow	SEKR2850C701S072412DX	None	None
EB-34				SEKR2850C701S072412D003	None	None
EB-9	STRATIFIED-481	15.50 - 15.75	Impoundment	SEKR1575C701S072612DX	Heavy	Heavy
EB-16				SEKR1575C701S072612D007	Heavy	Heavy
EB-24				SEKR1575C701S072612D007 dup	Heavy	Heavy
EB-15				SEKR1575C701S072612D013	Heavy	Heavy
EB-23				SEKR1575C701S072612D013 dup	Heavy	Heavy
EB-18				SEKR1575C701S072612D019	Heavy	Heavy
EB-25				SEKR1575C701S072612D019 dup	Heavy	Heavy
EB-10	STRATIFIED-503	15.50 - 15.75	Impoundment	SEKR1575C702S072612DX	Moderate	Heavy
EB-14				SEKR1575C702S072612D005	Moderate	Heavy
EB-19				SEKR1575C702S072612D010	Moderate	Heavy
EB-39	STRATIFIED-583	39.25 - 39.50	Lake	SEKR3950C701S072612DX	None	None
EB-17				SEKR3950C701S072612D007	None	None
EB-27				SEKR3950C701S072612D013	None	None
EB-37				SEKR3950C701S072612D013 dup	None	None
EB-11	STRATIFIED-661	37.75 - 38.00	ML Fan	SEKR3800C707S072712DX	None	Moderate
EB-12				SEKR3800C707S072712D004	None	Moderate
EB-21				SEKR3800C707S072712D009	None	Moderate
EB-29				SEKR3800C707S072712D014	None	Moderate
EB-13	STRATIFIED-663	37.75 - 38.00	ML Fan	SEKR3800C709S072712DX	None	Light
EB-30				SEKR3800C709S072712D006	None	Light
EB-22				SEKR3800C709S072712D011	None	Light
EB-31				SEKR3800C709S072712D011 dup	None	Light
KEB Source Oil				Weathered Crude		

Standard						
EB-40	OxBow			MP2125 OxBow		

[3.2 Epifluorescence microscopy](#)

Sediment samples were maintained at 4°C until processed for microscopic analysis. Samples were examined using UV epifluorescence microscopy (excitation wavelengths 340-380 nm; emission wavelengths 400-430 nm) for evidence of residual oil and formation of oil-mineral aggregates (OMA) according to Ma et al. (2008).

[3.3 Visual observation of source oil under UV light](#)

Prior to examining the sediment samples for evidence of oil (the KEB weathered source oil that was provided), a small sample was smeared onto a glass slide using a metal spatula, covered with a glass cover slip and examined under UV epifluorescence. Observations of the color, shape, and size of the fluorescent oil droplets were noted and photographed to aid with identification of residual oil in the sediment samples.

[3.4 Testing for the creation of oil-mineral aggregates](#)

To determine whether the sediments had the ability to create oil-mineral aggregates with the weathered source oil, a sediment sample that did not show oil after poling was identified as a reference unoled sediment for use in subsequent laboratory studies to assess the potential for OMA formation. The sample was given COOGER laboratory identity (ID) EB-41. The field label ID was SEKR1900C701S072512D005. On 21 August 2012, the unoled sediment (40.06 g) was weighed into a tared, 250 mL baffled Erlenmeyer flask (Pyrex Corning 4450-250). Milli-Q deionized, distilled water was added to the flask (80.00g). The flask was covered and placed on an orbital shaker (ThermoScientific MaxQ 2000) at 200 rpm for 10 minutes. A 10 mL sample of supernatant with suspended particulates was removed from the baffled flask and added to a 20 mL scintillation vial with the KEB source oil (0.04 g) previously weighed into the tared vial by dripping from a metal spatula. The vial was labelled as Spiked 1, and shaken by hand for 3 minutes. Subsamples (2 × 15 µL) were removed from the vial using an Eppendorf pipette with 1 cm of the tip cut back to increase its bore size. Subsamples were dispensed into the top and bottom chamber of a Levy Haemocytometer (Hausser Scientific, 19044) and covered with a cover slip in such a way as to exclude air bubbles.

Subsampling of the Spiked 1 vial was repeated after sitting for 48 hours at 4°C (Spiked 2). The vial was removed from the refrigerator and gently shaken. Subsamples were taken from the bottom of the vial and examined for OMA formation as described above.

[3.5 Preparation of sediment samples for epifluorescence microscopy](#)

For the large sediment samples EB-1 through EB-26 and EB-41, a primary dilution was prepared by weighing 1.00 ± 0.01 g of wet sediment into a tared, 20 mL glass scintillation vial, and suspending in 10 ± 0.05 g of MilliQ, deionized distilled water. For samples EB-27 through EB-40, which had a much smaller available mass, 0.50 ± 0.02 g of sediment was weighed into a tared, 20 mL glass scintillation vial and suspended in 5.62 ± 0.63 g of MilliQ, deionized distilled water (6.25 g water was added to EB-39). The water was dispensed into the vial with a Nicheryo pipette and the weight of water was recorded (Table 2). The vial was capped and shaken by hand for one minute. Subsamples (2 × 15 µL) were removed from the vial using an Eppendorf pipette with 1 cm of its tip removed to increase bore size. Subsamples were dispensed into the top and bottom chamber of a Levy Haemocytometer (Hausser Scientific, 19044) and covered with a glass cover slip in such a way as to exclude air bubbles. If the primary dilution was determined to be too dense, a further 1:10 dilution (final dilution of 1:100) was prepared for analysis.

[3.6 Microscopy and photomicrography](#)

The haemocytometer was placed onto the stage of a Leitz Orthoplan UV-epifluorescence microscope (USH-50W mercury bulb) equipped with motorized stage and an Optiscan controller. The integrated imaging system consisted of an Olympus DP70 camera controlled by Image ProPlus software (Ver. 5.1.0.20, Media Cybernetics, 1993-2004).

The sediments in the upper chamber were first examined using 128× magnification under UV light to determine whether oil was present in the sample. An area of interest (evidence of oil or OMA), or a representative area of the sample was photographed under UV epifluorescence. The same area was photographed under epifluorescence and transmitted white light to include non-fluorescing objects in the same field. Finally, the area was photographed under transmitted white light only. Areas of interest (possible oil or OMA) were examined further using 320× magnification and photographed in the same manner. For each of the two chambers of the haemocytometer, 3 replicate optical fields were photographed under the 3 lighting conditions for a minimum total of 18 photomicrographs per sample. Three additional photomicrographs of a replicate resulted when the higher magnification was used.

[3.7 Sample preparation for chemical analyses](#)

The method employed was a modified version of Cortes et al. (2012). Briefly, wet sediment samples were homogenized with a metal spatula and a 5 g subsample was removed and placed in a 50 mL Teflon centrifuge tube. Anhydrous sodium sulphate was added (10-20 g) until the sediment was dry. The sediment sample was then extracted by adding 10 mL of dichloromethane and mixing on a Vortex-Genie for 30 seconds. The solvent was removed with a Pasteur pipette, passed through glass wool and collected in a 50 mL glass tube. This process was repeated an additional two times for a total of 30 mL of solvent extract. Extract volume was then reduced to 2 mL under a gentle stream of nitrogen using an N-Evap. This concentrated extract was split, with 1 mL for GC-FID and Iatroscan analysis, and a separate 1 mL for analysis using the scanning fluorometer. This type of extraction permits rapid assessment of oil contamination in sediments. The approach was designed to generate semi-quantitative data.

[3.8 GC-FID analysis of TPH](#)

The GC-FID system consisted of an Agilent 6890 gas chromatograph with flame ionization detector and a 7683 auto-sampler. The column used for separations was a Supelco MDN-5s 30 m x 250 µm x 0.25 µm (length x inside diameter x film thickness) with a 1 m retention gap of deactivated fused silica. The sample was injected using the cool-on-column mode with a sample injection volume of 1 µL. Helium was used as a carrier gas with a flow rate of 1.0 mL/min. The initial oven temperature was 50°C, held for 2 min, followed by an increase to 300°C at 30°C/min, and held at 300°C for 10 min, with the total run time of 22.33 min. The FID detector was operated at 320°C with the hydrogen flow set at 40 mL/min and the air flow set at 450 mL/min. A seven point calibration was generated using standards prepared from weathered oil, and peak quantification was performed using the total area under the curve.

[3.9 Iatroscan analysis of saturates, aromatics, resins and asphaltenes \(SARA\)](#)

All oils were characterized using thin-layer chromatography (TLC) followed by scanning flame ionization detection using the IATROSCAN MK6 (Shell, USA) (Yamamoto and Kawanobe, 1984, Parts I and II; Leazar, 1986). Briefly, 3 µL of the concentrated sample extract was spotted onto one end of the silica coated TLC rods. The rods were then placed into a series of developing chambers to separate the 4 fractions of crude oil. The developing order was 18 minutes in hexane, 8 minutes in toluene and 2 minutes in 20:1 dichloromethane:methanol, with 10 minutes in a humidity chamber between each developing chamber.

[3.10 Three dimensional UV fluorescence analysis](#)

The 1.0 mL DCM extract, split from the hydrocarbon extraction, was made up to a final volume of 3.0 mL prior to fluorescence analysis. The technique employed was similar to that of Bugden et al. (2008).

3.11 Purification of selected extracts for fluorescence

The weathered crude oil and EB-37 were chosen for separation of asphaltenes and resins to determine whether or not these components contributed to the overall fluorescence of the samples. The weathered crude oil and EB-37 extracts were exchanged into hexane prior to silica gel solid phase extraction. The hexane extracts (1.0 mL) were passed through 4.0 grams of 1% deactivated silica gel. The samples were then eluted from the silica gel with 30% (v/v) dichloromethane:hexane. The purified extracts were concentrated just to dryness and made up in dichloromethane prior to fluorescence analyses. The remaining hexane insolubles not passed through the silica gel were dissolved in dichloromethane and also analyzed using UV fluorescence.

4.0 RESULTS AND DISCUSSION

4.1 Visual observation of source oil under UV light

The weathered KEB source oil without sediment was observed to fluoresce yellow under the UV light. It formed distinct, round droplets (Figure 1).

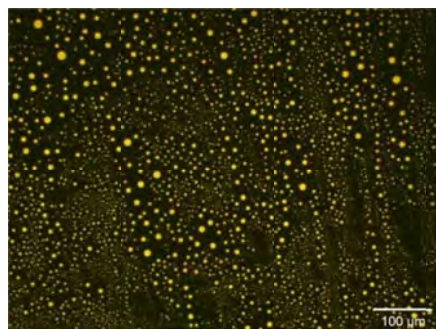


Figure 1. KEB weathered source oil at 128x magnification under UV light.

4.2 Formation of oil-mineral aggregates

A small number of oil-mineral aggregates (OMA) were readily observed in the initial Spiked1 subsamples. Figure 2 illustrates an OMA photographed at magnification factors of 128x and 320x, and under three types of illumination: 1) a combination of bright-field transmitted light and UV-epifluorescence, 2) UV-epifluorescence alone, and 3) bright-field transmitted light only. Figure 2A is the OMA with both bright-field transmitted and UV epifluorescence illumination to highlight the attachment of sediment particles (dark patches) to the oil (bright yellow). Figure 2B shows the same OMA under UV-epifluorescence illumination only; notice that only the oil droplets are visible. Figure 2C shows the OMA under bright-field transmitted light to show the fine mineral particles associated with the oil droplets.

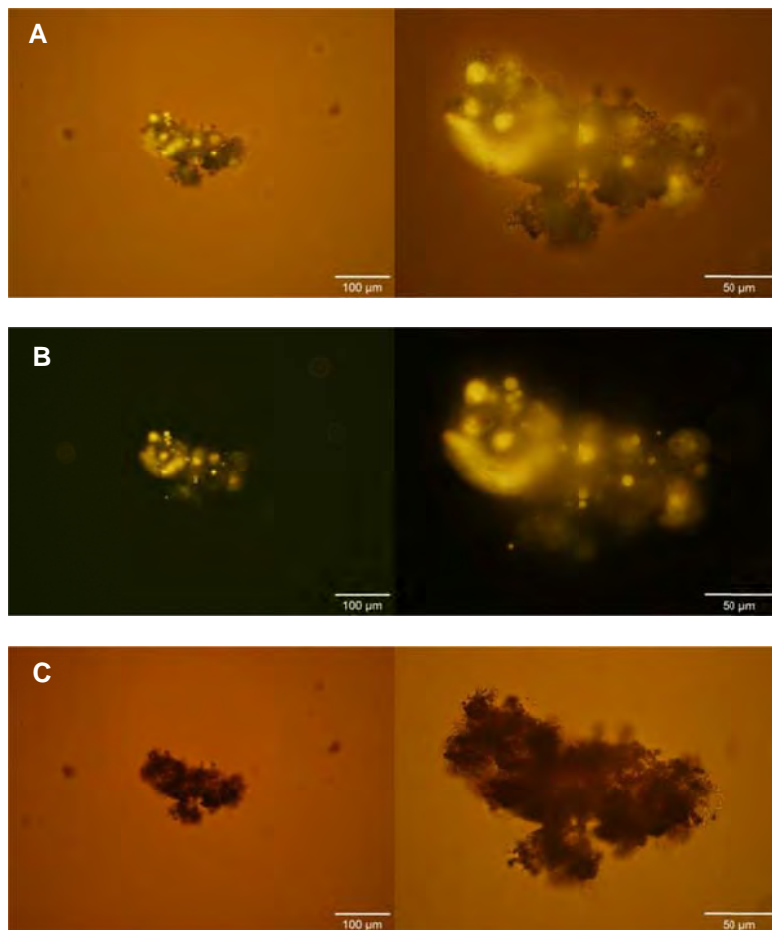
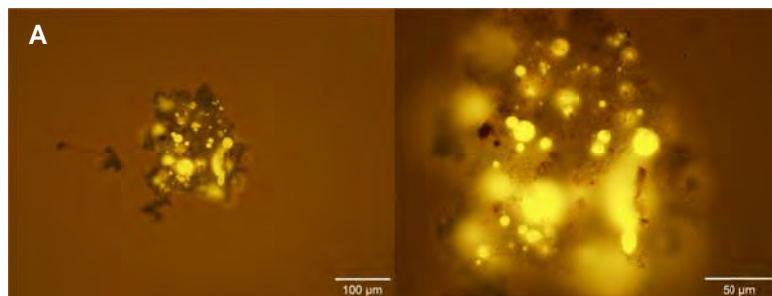


Figure 2. Formation of OMA when weathered KEB source oil was added to unoiled sediment. Image magnifications are 128x on the left and 320x on the right. (A) UV and transmitted light; (B) UV only; (C) transmitted light only. Sample is KEB Spiked 1-6.

When the vial was subsampled again two days later, an abundance of larger OMA had formed with the weathered source oil and the unoiled sediment collected from the site. Photomicrographs from these later subsamples were labelled as Spiked2 (Figure 3).



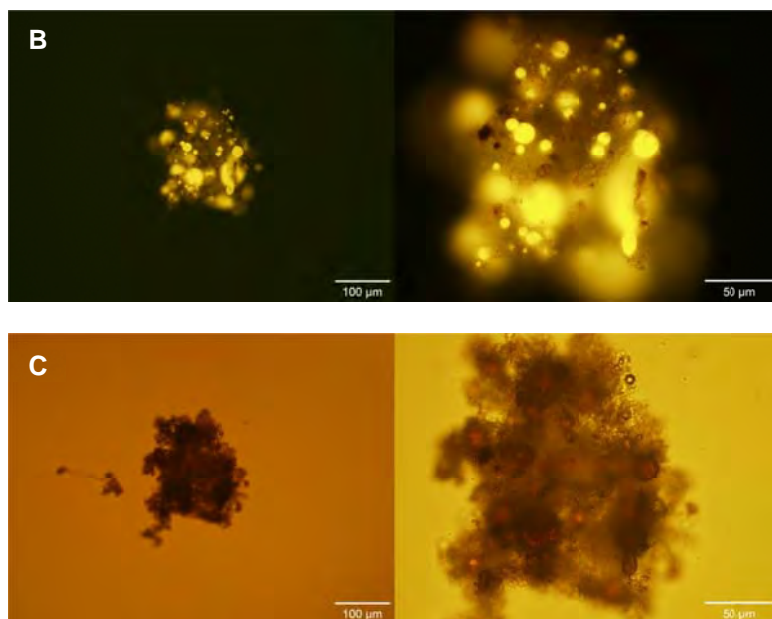


Figure 3. Formation of OMA 48 h after weathered KEB source oil was added to unoiled sediment. Image magnifications are 128x on the left and 320x on the right. (A) UV and transmitted light; (B) UV only; (C) transmitted light only. Sample is KEB Spiked 2-3.

4.3 Sediment sample epifluorescence micrographs

Photographs of each sediment sample were made under the various types of illumination and photographed as previously described in the methods. A photographic record of 1,042 samples observed in this study is included Appendix C. The images shown in this Results and Discussion section of the report were selected as typical examples of what was observed.

The sediment samples varied in grain size and quantity of organic material present. Table 2 outlines the differences in the sample matrix conditions observed. Variability between sites was significant due to factors such as the concentration of organic material due to the presence of detrital material such as dead leaves and roots. It is important to note that numerous samples contained an abundance of green fluorescent material that could be the carbonate mineral aragonite, which is known to fluoresce green under UV light (Figure 4). This is well illustrated by Figure 5 that contained a high concentration of green fluorescent material (sample EB-6). The fluorescent material was not considered to be dispersed oil, because the laboratory experiments with source oil showed that free oil droplets resulting from physical dispersion or in the form of OMA were spherical in shape and fluoresced yellow.

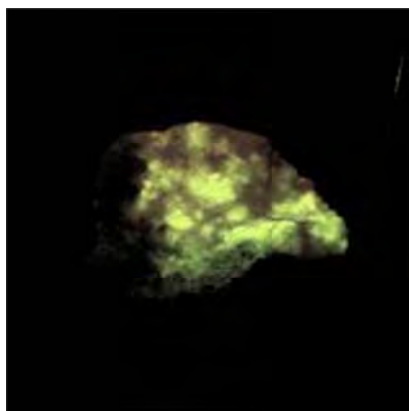


Figure 4. This referenced photomicrograph shows a specimen of aragonite from Texas, taken under shortwave UV light (<http://www.mindat.org/photo-317408.html>).

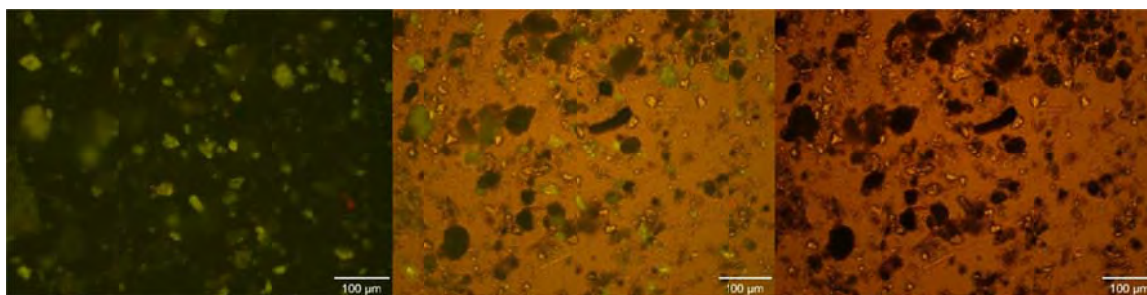


Figure 5. Sample EB-6, showing an abundance of green fluorescent material, photographed under UV epifluorescence (left), UV and transmitted light (middle), and transmitted light only (right).

Table 2. Description of microscope samples photographed under UV and transmitted light.

Lab ID	Field ID	Mass of Sample (g)	Mass of Water (g)	Comments
EB-1	SEKR2025C702S072412DX	1.00	10.05	
EB-2	SEKR2025C702S072412D005	1.00	10.02	
EB-36	SEKR1900C701S072512DX	0.50	5.00	sand and silt
EB-41	SEKR1900C701S072512D005	1.00	10.01	this sample was also used to spike with the weathered KEB source oil
EB-35	SEKR1900C701S072512D009	0.50	5.00	very sandy, water almost clear
EB-3	SEKR3650C701S072512DX	1.01	10.07	
EB-4_diluted	SEKR3650C701S072512D006	1.00	10.00	many roots, organic material
EB-28	SEKR3650C701S072512D010	0.49	5.00	sample very thick
EB-28_diluted	SEKR3650C701S072512D010	1.11	9.03	Primary dilution was 0.49 g sediment in 5.00 g water. Secondary dilution for photographs was 9.03 g water added to 1.11 g of primary dilution.

EB-5	SEKR3750C701S072512DX	1.00	10.02	
EB-6	SEKR3750C701S072512D006	1.00	10.03	
EB-33	SEKR3750C701S072512D010	0.50	5.01	
EB-38	SEKR0425C701S072512DX	0.50	5.01	
EB-20	SEKR0425C701S072512D007	1.00	10.03	oil observed in all replicates
EB-7	SEKR3775C702S072712DX	1.00	10.03	
EB-8	SEKR3775C702S072712D005	1.00	10.04	
EB-26	SEKR3775C702S072712D009	1.00	10.01	oil observed in replicates 1, 2, and 5, with OMA in replicate 4
EB-32	SEKR2850C701S072412DX	0.52	5.01	rocky sample
EB-34	SEKR2850C701S072412D003	0.51	5.03	sandy sample
EB-9	SEKR1575C701S072612DX	1.00	10.00	
EB-16	SEKR1575C701S072612D007	1.00	10.09	possible oil observed at edge of slide in replicate 5
EB-15	SEKR1575C701S072612D013	1.00	10.03	oil observed in replicates 1 to 4, and possibly 5 and 6
EB-18	SEKR1575C701S072612D019	1.00	10.01	possible oil observed in replicates 1 and 2
EB-10	SEKR1575C702S072612DX	1.01	10.00	sample mostly water
EB-14	SEKR1575C702S072612D005	1.00	10.00	oil observed in replicates 2, 5 and 6
EB-19	SEKR1575C702S072612D010	1.00	10.06	oil observed in all replicates; very good example of oiled sample
EB-39	SEKR3950C701S072612DX	0.50	6.25	
EB-17	SEKR3950C701S072612D007	1.00	10.06	oil observed
EB-27	SEKR3950C701S072612D013	0.50	4.99	
EB-11	SEKR3800C707S072712DX	1.00	10.02	
EB-12	SEKR3800C707S072712D004	1.00	10.00	
EB-21	SEKR3800C707S072712D009	1.00	10.12	
EB-29	SEKR3800C707S072712D014	0.50	5.02	oil observed in replicates 3, 4 and 7
EB-13	SEKR3800C709S072712DX	1.00	10.07	oil observed in replicate 6
EB-30	SEKR3800C709S072712D006	0.51	5.00	
EB-22	SEKR3800C709S072712D011	1.00	10.12	
EB-24	SEKR1575C701S072612D007	0.99	10.01	
EB-23	SEKR1575C701S072612D013	1.00	10.01	
EB-25	SEKR1575C701S072612D019	1.00	10.03	
EB-37	SEKR3950C701S072612D013	0.50	5.05	
EB-31	SEKR3800C709S072712D011	0.50	5.00	
EB-40	OxBow	0.50	5.00	OMA observed in replicates 2, 4, 5 and 6

4.4 Microscopic observations of oil in sediment samples under UV epifluorescence

Of the 41 sediment samples received for analysis, only 11 were deemed to show any evidence of oil fluorescence (Figure 6 through Figure 16). (Note that all 1,042 sample photographs can be found in Appendix C.) Figure 6 to Figure 16 are selected photomicrographs of samples deemed to have positive evidence of dispersed oil droplets (spherical shape with yellow fluorescence). Observations were made at 320x magnification under UV epifluorescence (left), UV with transmitted light (middle), and transmitted light alone (right). The COOGER laboratory sample number has been used for brevity with the replicate number, Target Oiling Level, and Actual Poling result included in parentheses.

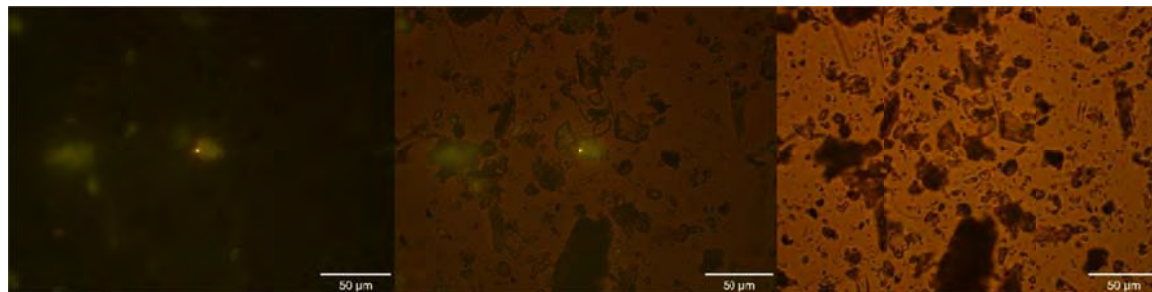


Figure 6. EB-13 (replicate 6, Target Oiling Level = None, Actual Poling = Light).

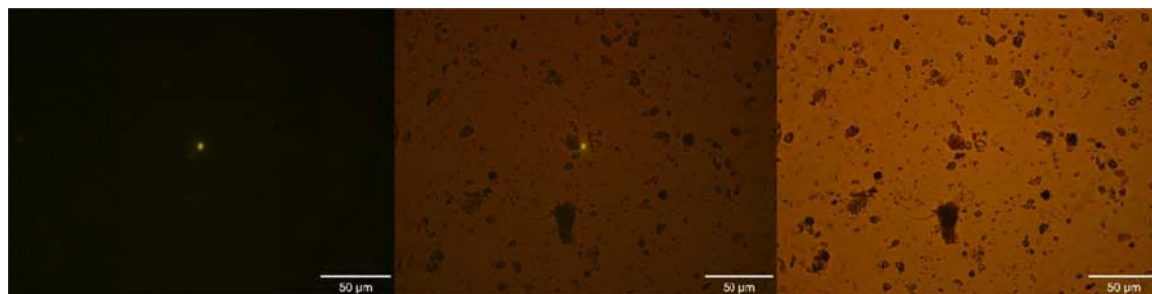


Figure 7. EB-14 (replicate 2, Target Oiling Level = Moderate, Actual Poling = Heavy).

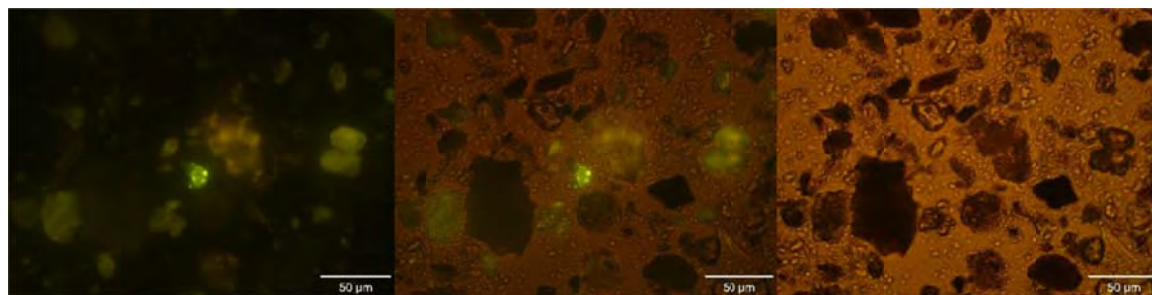


Figure 8. EB-15 (replicate 2, Target Oiling Level = Heavy, Actual Poling = Heavy).

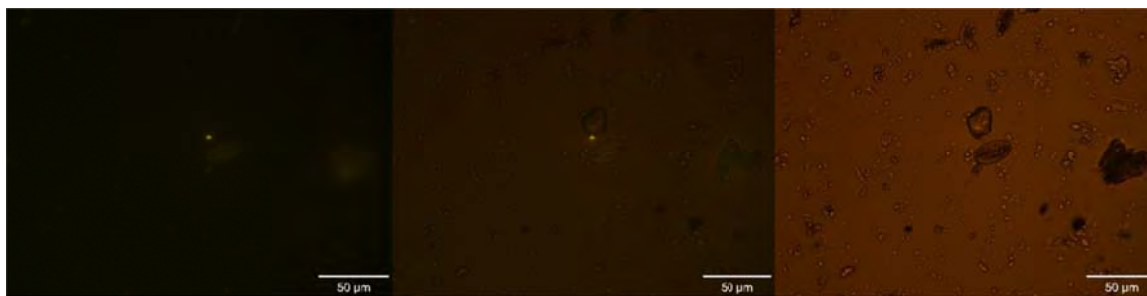


Figure 9. EB-16 (replicate 6, Target Oiling Level = Heavy, Actual Poling = Heavy).

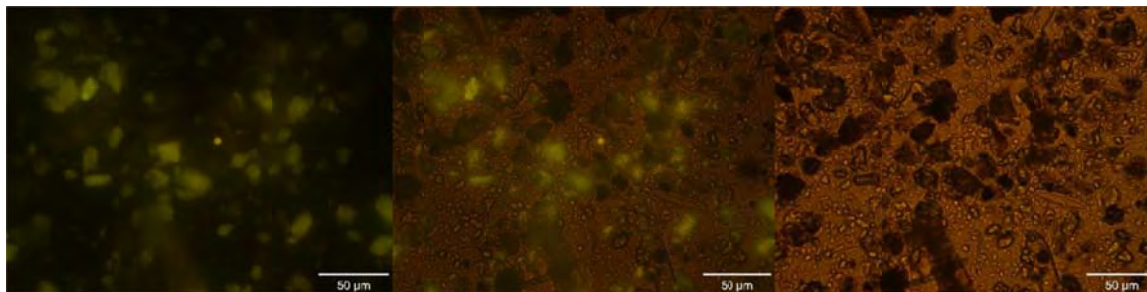


Figure 10. EB-17 (replicate 6 Target Oiling Level = None, Actual Poling = None).

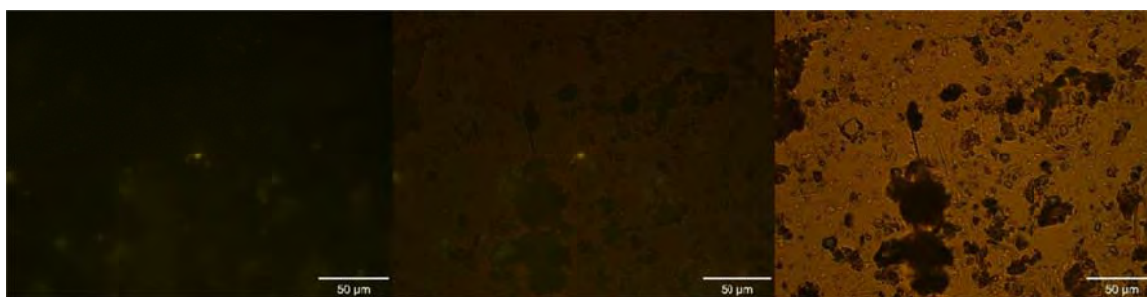


Figure 11. EB-18 (replicate 2, Target Oiling Level = Heavy, Actual Poling = Heavy).

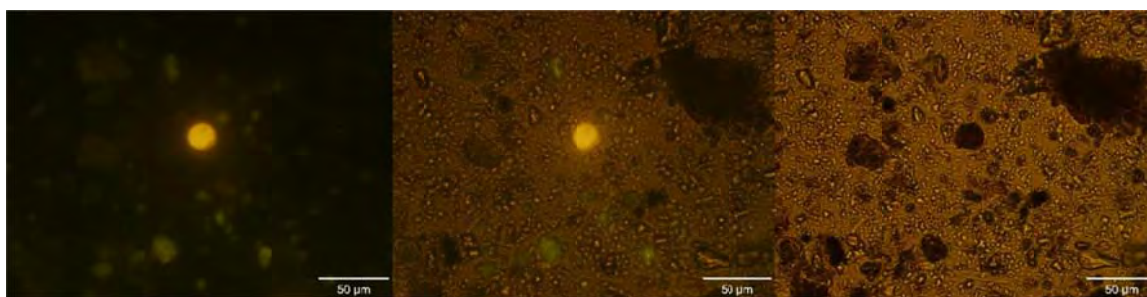


Figure 12. EB-19 (replicate 4, Target Oiling Level = Moderate, Actual Poling = Heavy).

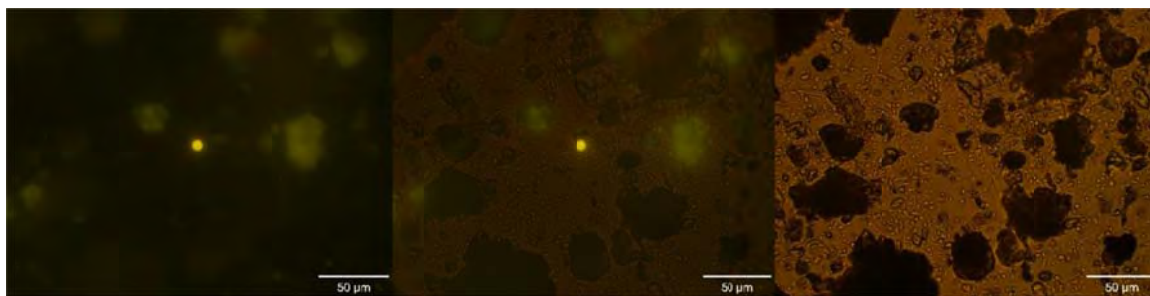


Figure 13. EB-20 (replicate 3, Target Oiling Level = Light, Actual Poling = Light).

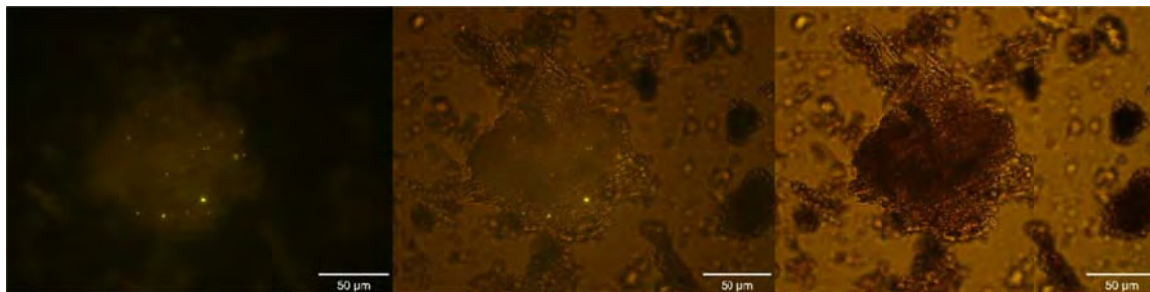


Figure 14. EB-26 (replicate 4, Target Oiling Level = Heavy, Actual Poling = Moderate). This could possibly be an OMA.

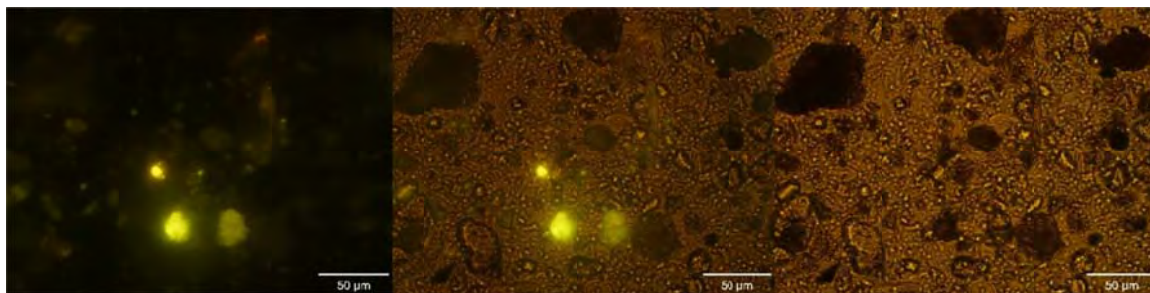


Figure 15. EB-29 (replicate 7, Target Oiling Level = None, Actual Poling = Moderate).

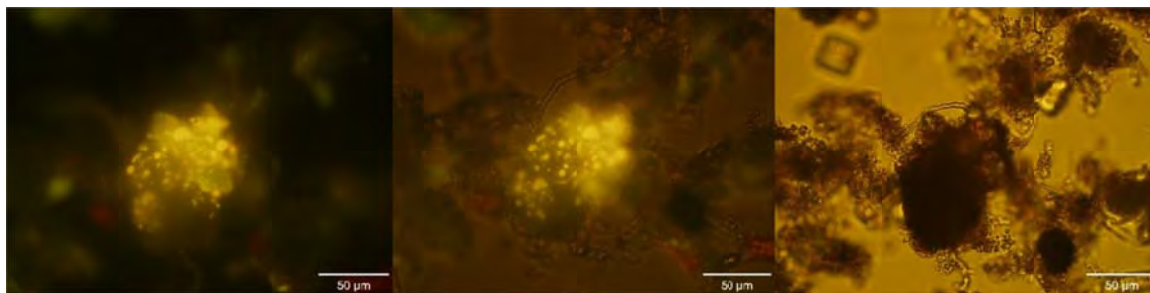


Figure 16. EB-40 (replicate 6) showing OMA. There was no Target Oiling Level or Actual Poling result for this sample.

4.5 Comparison of epifluorescence microscopy with TPH oil chemistry

Due to the low numbers or lack of oil droplets observed in the majority of samples observed, which precluded the collection of quantitative data by image analysis (without doing image analysis on 100's of fields for each sample for statistical analysis) a strong correlation could not be drawn between the epifluorescence microscopy and analytical oil chemistry results.

It is important to note that beyond the presence or absence of yellow fluorescent spherically shaped particles – presumed to be dispersed droplets of petroleum hydrocarbons – the interpretation of the UV-epifluorescence data is limited as they cannot provide information on the state of weathering of the oil, or the source of the oil.

As noted, due to the irregular frequency of occurrence of fluorescent oil-like bodies, there was no attempt to make semi-quantitative estimations of oil concentrations within the sediment from the image analysis data provided by UV-epifluorescence microscopy.

4.6 Total petroleum hydrocarbons

The results of the total petroleum hydrocarbon analysis are illustrated in Figure 17. These results were compared to the data obtained from Alpha Labs. The difference in the results are most likely due to the fact that COOGER's data were reported based on wet weight of sediment, rather than dry weight which was used by Alpha Labs. COOGER could not present the data on a dry weight basis, because many of the sample jars were damaged and leaked during transport, which also presents the possibility that some of the broken samples suffered cross-contamination. In addition, COOGER labs did not have samples of oils that were used to correct TPH results. The corrected TPH values presented by Alpha Labs are found in Appendix B.

The gas chromatographic profiles generated by COOGER were not comparable to the reference weathered crude oil sample provided due to the potential presence of other petroleum sources and a greater extent of weathering for the detected hydrocarbons.

It is important to note that the oil chemistry data collected by COOGER on the specific samples that were provided was only intended to be used as a reference point to compare to the corresponding measurements from UV-epifluorescence microscopy. COOGER's aim was to provide supporting data to validate the link between the presence of residual petroleum hydrocarbons and observed fluorescence – not to provide an estimate for the Line 6B oil released during the Kalamazoo spill.

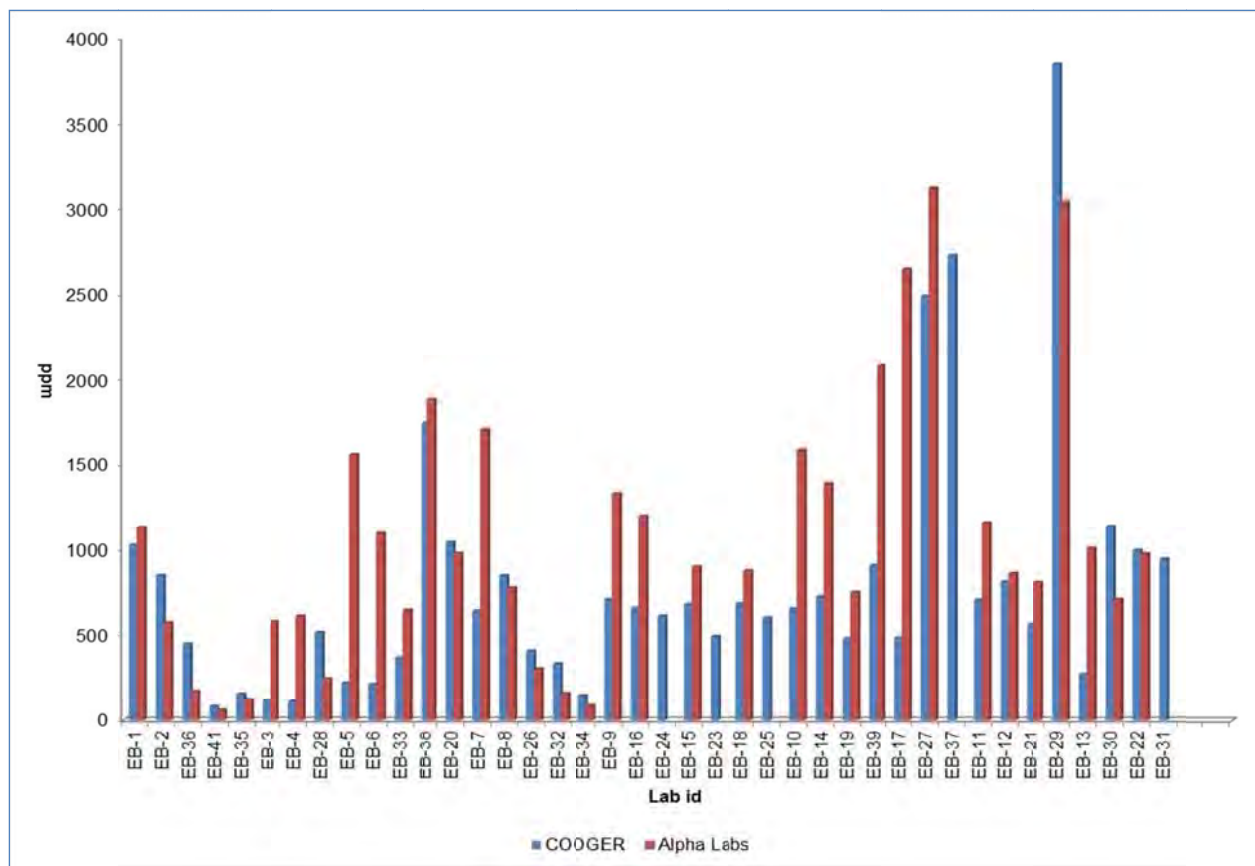


Figure 17. Total petroleum hydrocarbon results.

4.7 Alpha Labs data

A table showing the results from Alpha Labs is presented in Appendix B. By measuring biomarkers (hopanes and steranes) using gas chromatography-mass spectrometry (GC-MS), Alpha Labs was capable of distinguishing Line 6B oil from other potential oil sources detected in the samples. Figure 18 illustrates the graphical distribution of total oil (a different data set than the TPH values used in Figure 17), line 6B oil, contributions of the sum of saturates and aromatics, and the sum of resins and asphaltenes in the samples collected in the vicinity of the spill. There are no obvious trends between the various fractions of components in the data illustrated in Figure 18. This is likely due to the presence of other sources of petroleum in the sediments.

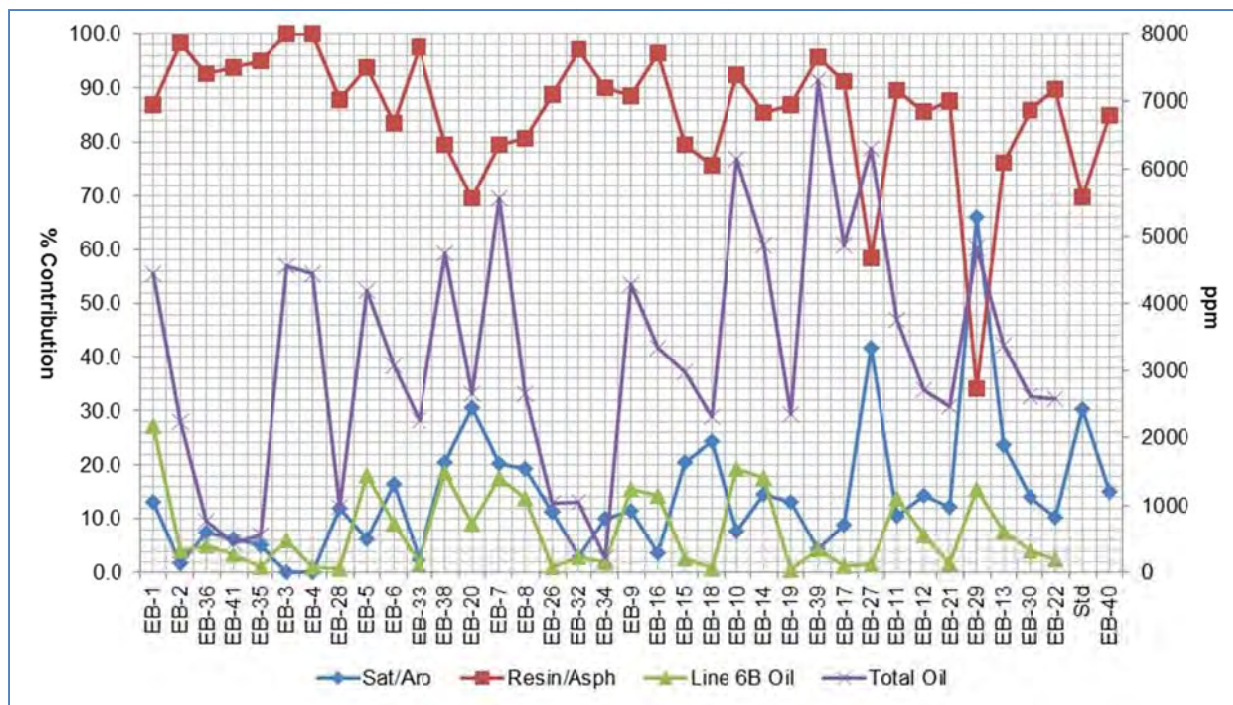


Figure 18. Concentrations of total oil and line 6B oil in sediment samples collected near the spill. The percent contribution of saturates plus aromatics (Sat/Aro), and resins plus asphaltenes (Resin/Asph) for each sample is also shown.

4.8 Thin-layer chromatogram scanning flame ionization (TLC/FID)

Thin-layer chromatography (TLC) coupled with flame ionization (FID) analyses (Iatroscan) is presented in Table 3. The detection of oil components in sediment sample EB-29 illustrated a very different profile compared to that found in the reference weathered crude oil sample (Figure 19). Contrary to the reference weathered oil sample, EB-29 appears to have a lower percentage of high molecular weight resins and asphaltenes relative to low molecular weight saturates and aromatics. The technique of TLC/FID has been employed by other researchers to demonstrate oil degradation (Stephen et al., 1998; Maki et al., 2001). In general these studies suggest that an advanced extent of weathering results in a greater percentage of resins and asphaltenes. This can be attributed to the fact that the larger molecules of resins and asphaltenes in oil are apt to degrade more slowly compared to low molecular weight polycyclic aromatic hydrocarbons and saturates (Hozumi et al., 2000). Based on this assumption, it is deemed that samples exhibiting a very low percent contribution (<2%) of asphaltenes likely contained another highly weathered petroleum source rather than Line 6B source oil. Samples containing a percent contribution of asphaltenes ranging from 2 to 20% were most likely comprised of a mixture of petroleum products that may include an unknown proportion of weathered petroleum hydrocarbons from the Kalamazoo River spill.

Table 3. Results for crude oil component analysis. In the comments column, 'no' indicates most likely non-aromatic, and 'yes' indicates the presence of aromatics.

COOGER	Crude Oil Component Analysis (%Contribution)				Comments on Iatroscan Aromatic Results
	Saturates	Aromatics	Resins	Asphaltenes	
Sample id					
EB-1	7.5	5.7	73.0	13.8	yes

EB-2	0.2	1.6	80.4	17.8	based on chromatogram, yes likely
EB-36	0.2	7.2	91.9	0.6	yes
EB-41	2.5	3.7	72.5	21.2	based on chromatogram, not likely
EB-35	2.2	2.9	57.7	37.2	yes
EB-3	0.0	0.0	11.9	88.1	no
EB-4	0.0	0.0	32.5	67.5	no
EB-28	8.4	3.6	82.8	5.2	based on chromatogram, not likely
EB-5	0.5	5.7	59.7	34.1	based on chromatogram, not likely
EB-6	9.4	7.0	73.4	10.2	yes
EB-33	2.3	0.2	97.2	0.2	no
EB-38	15.4	5.1	71.5	8.0	yes
EB-20	14.2	16.3	59.6	9.9	yes
EB-7	15.0	5.4	73.7	5.8	yes
EB-8	11.3	8.1	72.9	7.8	yes
EB-26	8.4	2.9	61.2	27.5	based on chromatogram, not likely
EB-32	2.3	0.7	78.6	18.4	no
EB-34	8.5	1.5	82.4	7.6	no
EB-9	8.8	2.7	79.9	8.6	based on chromatogram, not likely
EB-16	0.2	3.4	75.9	20.5	yes
EB-24	8.7	0.0	81.4	10.0	no
EB-15	13.2	7.4	67.1	12.4	yes
EB-23	19.6	5.9	74.0	0.5	yes
EB-18	20.4	4.0	70.5	5.2	based on chromatogram, not likely
EB-25	22.9	2.1	65.0	10.0	based on chromatogram, not likely
EB-10	7.6	0.0	84.9	7.4	no
EB-14	7.2	7.4	66.9	18.5	yes
EB-19	10.2	2.8	83.0	3.9	based on chromatogram, not likely
EB-39	1.0	3.3	89.8	5.9	yes
EB-17	8.7	0.1	61.9	29.2	no
EB-27	35.6	6.1	53.2	5.1	yes
EB-37	37.4	9.9	36.5	16.2	yes
EB-11	7.9	2.7	57.4	32.0	yes
EB-12	10.1	4.2	78.9	6.8	yes
EB-21	9.3	3.0	75.7	12.0	based on chromatogram, not likely
EB-29	45.4	20.6	32.9	1.1	yes
EB-13	12.1	11.7	67.7	8.5	yes
EB-30	9.3	4.8	80.4	5.6	yes
EB-22	9.6	0.7	88.1	1.6	no

EB-31	13.4	4.2	55.8	26.6	yes
Std	17.7	12.5	47.1	22.7	Weathered crude oil
EB-40	8.6	6.4	79.0	6.0	yes

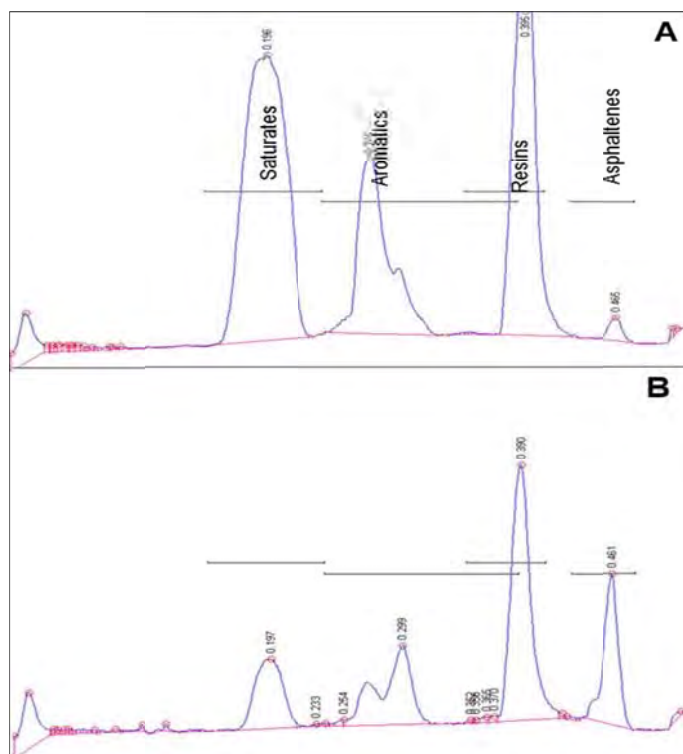


Figure 19. TLC/FID chromatograms of (A) EB-29, (B) weathered source oil from the Line 6B spill.

4.9 Three dimensional fluorescence

COOGER conducted 3D fluorescence analysis on the reference weathered source oil sample as well as representative samples of contaminated sediments recovered from the Kalamazoo River to accomplish the following: 1) to determine the optimal excitation/emission wavelengths for the identification of the weathered Line 6B source oil, 2) to determine if there was a difference in optimal excitation/emission wavelengths for fluorescent contaminant hydrocarbons within the sediments as a result of other contaminant petroleum hydrocarbon sources or further oil weathering processes, and 3) to identify physicochemical processes that may interfere with the fluorescence of oil in the presence of sedimentary material.

The 3D fluorescence data are presented in Figure 20 and Figure 21. The contour plots show that fluorescence intensity was greater in samples containing lower TPH concentrations which suggested that fluorescence quenching was occurring. Fluorescence spectra for crude oils typically consist of a broad band in the visible region, at about 350 to 650 nm, which reflects the overlapping of emissions from different fluorophores present in the matrix (Sotelo et al., 2008).

Oils are classified by the American Petroleum Institute as light, medium or heavy depending on their API gravity value. In general, light oils (high API gravities) will have narrow, intense emission bands while heavy oils (low API gravities) tend to have broad, less intense bands (Sotelo et al., 2008). This is due to the high concentration of fluorophores in heavy oils, which is characterized by a high rate of collisional energy transfer, and a shift toward red in the emission spectrum.

The nature of the fluorophores in a heavy oil, and the presence of reabsorbing molecules (that absorb light emitted from the fluorescent molecule), lead to quenching resulting in low fluorescence intensities (Sotelo et al., 2008). In addition to differences in oil composition, fluorescence signatures are also influenced by the degree of chemical and physical dispersion, and degree of weathering that may be influenced by environmental factors such as temperature, influence of microbial degradation and the presence of ultra-violet light.

The two primary quenching processes of concern are collisional (dynamic) quenching and static (complex formation) quenching. Collisional quenching occurs when the excited fluorophore experiences contact with an atom or molecule that can facilitate non-radiative transitions to the ground state. Common quenchers include O_2 , I^- , Cs^+ and acrylamide. In static quenching the fluorophore can form a stable complex with another molecule. If this *ground-state* is non-fluorescent then we say that the fluorophore has been statically quenched. Sediments recovered from the Kalamazoo River for analysis in this project are likely experiencing dynamic quenching, since the levels of fluorescence increased after the sample extracts were purified by silica gel solid phase extraction (Figure 21). This indicated that there were reabsorbing molecules in the oil that were causing the quenching. The presence of what appeared to be aragonite in the microscopic analysis was unlikely to have been a confounding factor since it would have been left behind in the sediment during the dichloromethane extraction. These results suggest that UV-fluorescence analysis of sediments in field samples could under-estimate the petroleum that is present, or even generate false non-detectable levels of petroleum.

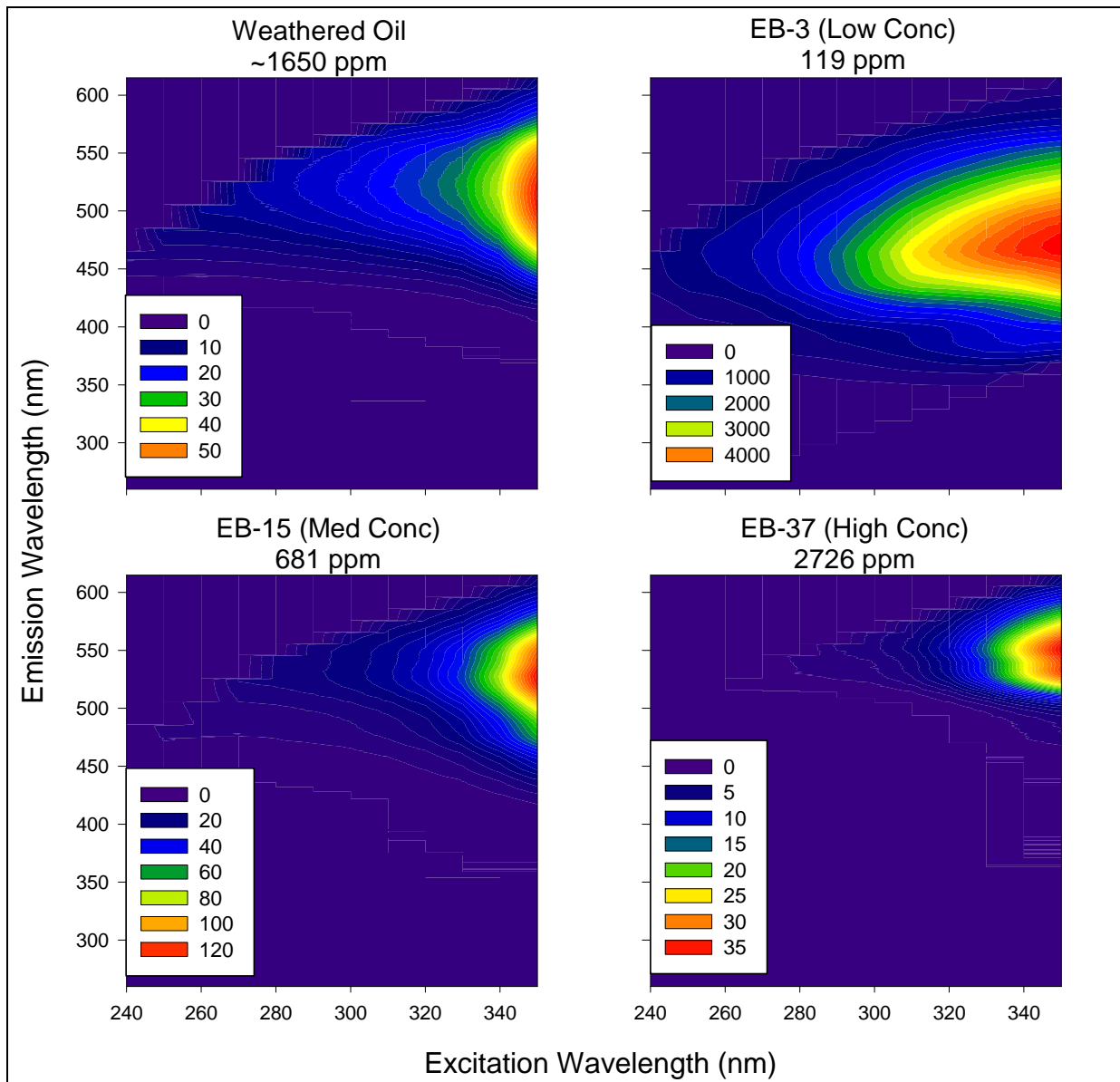


Figure 20. Contour plots of the weathered crude oil and a few selected samples.

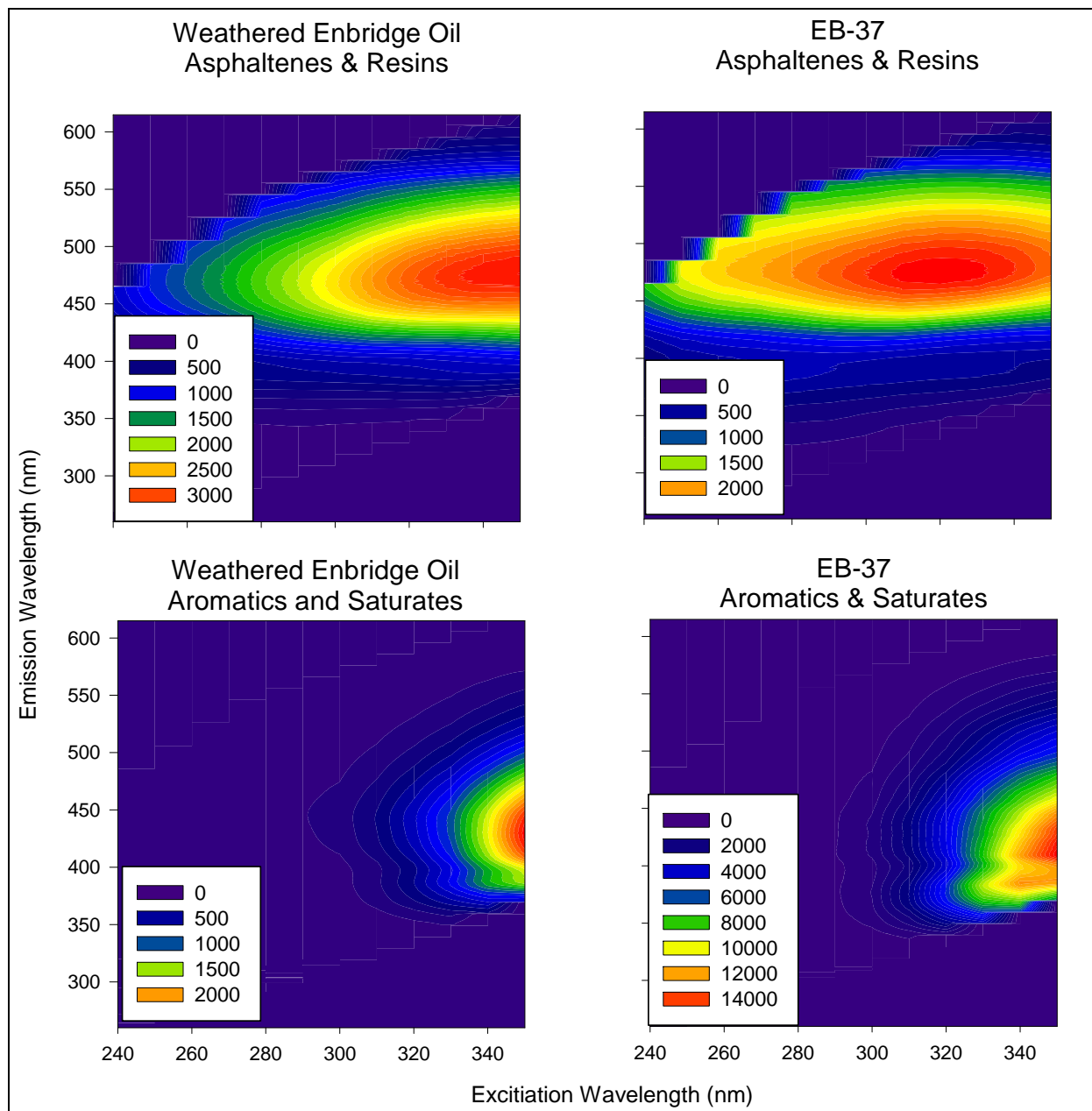


Figure 21. Contour plots of purified weathered crude and EB-37.

5.0 CONCLUSIONS

Epifluorescence microscopy by UV irradiation showed that the weathered KEB source oil and Kalamazoo River sediments readily formed OMA. These OMA were stable, as indicated by observations of the spiked sample after two days. The presence of dispersed oil droplets and OMA were detected in a number of samples; however, there was no clear pattern of detection when compared with sample oil chemistry due to 1) the dilution of the petroleum hydrocarbons within the sediments to concentrations below detection limits that may be attributed to the application of an agitation strategy to mobilize oil entrained within the

sediments, 2) weathering of the oil that modified its fluorescence characteristics (i.e., excitation/emission wavelengths for monitoring were no longer within the optimal range for detection), and 3) the occurrence of fluorescence quenching that diminished sensitivity and selectivity.

Based on prior knowledge on the limitations of the methodology, it was known that UV-epifluorescence microscopy analysis could not be used to determine the state of weathering of contaminant hydrocarbons within the sediments or their source. The qualitative and semi-quantitative techniques employed by COOGER proved to be beneficial in providing a rapid evaluation of contamination by petroleum hydrocarbons in the spill area, and a percent fractionation of the major components detected in crude oils for each sample extract. Iatroscan (TLC/FID) analysis suggested that the contaminant hydrocarbons in most of the samples were in a more advanced stage of weathering relative to the reference source oil provided for this study. The data also supported the conclusions of the GC/MS data from Alpha Labs, that involved the profiling and quantification of biomarkers such as hopanes and steranes against other target compounds, to resolve Line 6B residual oil against the presence of other sources of oil contamination within the sediments.

3D fluorescence analysis of the weathered reference source oil and selected sediment samples (with and without extractive sample cleanup) provided a means of identifying the optimal excitation/emission wavelengths for detection of residual petroleum hydrocarbons in the sediments. The 3D technique also demonstrated that dynamic quenching significantly reduces our capacity to employ UV fluorescence as a time-series monitoring methodology for remedial operations.

In conclusion, it appears that in the initial stages of the cleanup operations, UV-fluorescence was able to highlight the presence of bulk oil within the split sediment cores. However, as cleanup operations proceeded by the use of strategies such as sediment agitation, oil within the sediments was reduced to low concentrations by a combination of the recovery of the mobilized oil, and dilution and dispersion of oil within the sediments through the natural process of OMA formation. This, coupled with quenching of dispersed oil droplets, resulted in our subsequent inability to detect traces of the residual oil by image analysis of whole sediment cores under UV illumination.

6.0 REFERENCES

- Ajjolaiya, L. O., P. S. Hill, A. Khelifa, R. M. Islam and K. Lee. 2006. Laboratory investigation of the effects of mineral size and concentration on the formation of oil-mineral aggregates. *Marine Pollution Bulletin* 52: 920-927.
- Bragg, J. R. and S. H. Yang. 1995. Clay-oil flocculation and its effects on the rate of natural cleansing in Prince William Sound following the *Exxon Valdez* oil spill. In Wells, P.G., Butler, J.N. and Hughes, J.S. (eds.), *Exxon Valdez Oil Spill - Fate and Effects in Alaskan Waters*. American Society for Testing and Materials, Philadelphia, PA.
- Bugden, J., Yeung, W., Kepkay, P., and Lee, K. 2008. Application of ultra-violent fluorometry and excitation-emission matrix spectroscopy (EEMS) to fingerprint oil and chemically dispersed oil in seawater. *Marine Pollution Bulletin*, 56:677-685.
- Cloutier, D., C. L. Amos, P. R. Hill and K. Lee. 2002. Oil erosion in an annular flume by seawater of varying turbidities: A critical bed shear stress approach. *Spill Science & Technology Bulletin* 8: 83-93.
- Colcomb, K., D. Bedborough, T. Lunel, R. Swannell, P. Wood, J. Rusin, N. Bailey, C. Halliwell, L. Davis, M. Sommerville, A. Dobie, D. Michell, M. McDonagh, S. Shimwell, B. Davies, D. Harries and K. Lee. 1997. Shoreline cleanup and waste disposal issues during the *Sea Empress* Incident. In *Proceedings of the 1997 International Oil Spill Conference*, Fort Lauderdale, FL, USA: 195-203.
- Cortes, J., Suspes, S., González C., and Castro, H. 2012. Total petroleum hydrocarbons by gas chromatography in Columbian waters and soils. *American Journal of Environmental Science*, 8(4):396-402.

- Delvigne, G. A. L., J. A. Van del Stel and C. E. Sweeney. 1987. *Measurements of Vertical Turbulent Dispersion and Diffusion of Oil Droplets and Oil Particles*. Report No. MMS 87-111. US Department of the Interior, Minerals Management Service, Anchorage, Alaska. 501 p.
- Guénette, C. C., G. A. Sergy, E. H. Owens, R. C. Prince and K. Lee. 2003. Experimental design of the Svalbard shoreline field trials. *Spill Science and Technology Bulletin* 8: 245-256.
- Guyomarch, J., S. Le Floch and F. X. Merlin. 2002. Effect of suspended mineral load, water salinity and oil type on the size of oil-mineral aggregates in the presence of chemical dispersant. *Spill Science and Technology Bulletin* 8: 95-100.
- Hill, P. S., A. Khelifa and K. Lee. 2002. Time scale for oil droplet stabilization by mineral particles in turbulent suspensions. *Spill Science and Technology Bulletin* 8: 73-81.
- Hozumi, T., Tsutsumi, H., and Kono, M. 2000. Bioremediation on the shore after an oilspill from the Nakhodka in the Sea of Japan. I. Chemistry and characteristics of heavy oil loaded on the Nakhodka and biodegradation tests by a bioremediation agent with microbiological cultures in the laboratory. *Marine Pollution Bulletin*, 40(4):308-314.
- Kepkay, P. E., J. B. C. Bugden, K. Lee and P. Stoffyn-Egli. 2002. Application of ultraviolet fluorescence spectroscopy to monitor oil-mineral aggregate formation. *Spill Science and Technology Bulletin* 8: 101-108.
- Khelifa, A., P. S. Hill and K. Lee. 2003. A stochastic model to predict the formation of oil-mineral aggregates. In *Proceedings of the 26th Arctic and Marine OilSpill Program (AMOP) Technical Seminar*. Victoria, Canada. Environment Canada, Ottawa, Ontario. pp. 893-910.
- Khelifa, A., P. Stoffyn-Egli, P. S. Hill and K. Lee. 2005b. Effects of salinity and clay type on oil-mineral aggregation. *Marine Environmental Research* 59: 235-254.
- Leazar, L.L. (1986). Quantitative Analysis of Petroleum Residues and Heavy Oil by TLC/FID. *J. Chromatographic Science*. 24:340
- Lee, K. 2002. Oil-particle interactions in aquatic environments: Influence on the transport, fate, effect and remediation of oil spills. *Spill Science and Technology Bulletin* 8: 3-8.
- Lee, K., Z. Li, H. Niu, P. Kepkay, Y. Zheng, M. Boufadel and Z. Chen. 2009a. *Enhancement of oil-mineral-aggregate formation to mitigate oil spills in offshore oil and gas activities*. Final Report (Contract No. M07PC13035) submitted to Minerals Management Service. March 30, 2009. 99 pp.
- Lee, K., T. Lunel, P. Wood, R. Swannell and P. Stoffyn-Egli. 1997. Shoreline cleanup by acceleration of clay-oil flocculation processes In *Proceedings of the 1997 International Oil Spill Conference*, Fort Lauderdale, FL, USA: 235-240.
- Lee, K., P. Stoffyn-Egli, P. Wood and T. Lunel. 1998. Formation and structure of oil-mineral fines aggregates in coastal environments. In *Proceedings of the 21st Arctic and Marine Oilspill Program (AMOP) Technical Seminar*. Environment Canada, Ottawa, Ontario, pp. 911-921.
- Lunel, T., R. Swannell and J. Rusin. 1997. Monitoring the effectiveness of response operations during the Sea Empress incident: a key component of the successful. *Oceanographic Literature Review* 44: 1570-1570.
- Ma, X., A. Cogswell, Z. Li and K. Lee. 2008. Particle size analysis of dispersed oil and oil-mineral aggregates with an automated ultraviolet epi-fluorescence microscopy system. *Environmental Technology* 29: 739-748.
- Maki, H. Sasaki, T. and Harayama, S. 2001. Photo-oxidation of biodegraded crude oil and toxicity of the photo-oxidized products. *Chemosphere*, 44:1145-1151.
- Omotoso, O. E., V. A. Munoz and R. J. Mikula. 2002. Mechanisms of crude oil-mineral interactions. *Spill Science & Technology Bulletin* 8: 45-54.
- Owens, E. H., B. Humphrey and G. A. Sergy. 1994. Natural cleaning of oiled coarse sediment shorelines in Arctic and Atlantic Canada. *Spill Science and Technology Bulletin* 1: 37-52.

Owens, E. H. and K. Lee. 2003. Interaction of oil and mineral fines on shorelines: review and assessment. *Marine Pollution Bulletin* 47: 397-405.

Owens, E. H., G. A. Sergy, C. C. Gu nette, R. C. Prince and K. Lee. 2003a. The reduction of stranded oil by in situ shoreline treatment options. *Spill Science and Technology Bulletin* 8: 257-272.

Owens, E. H., G. A. Sergy, C. C. Gu nette, R. C. Prince and K. Lee. 2003b. The reduction of stranded oil by *in-situ* shoreline treatment options. *Spill Science and Technology Bulletin* 8: 257-272.

Payne, J. R., J. R. Clayton Jr. and B. E. Kirstein. 2003. Oil/suspended particulate material interactions and sedimentation. . *Spill Science and Technology Bulletin* 8: 201-221.

Payne, J. R., J. R. Clayton Jr., G. D. McNabb, B. E. Kirstein, C. L. Clary, R. T. Redding, J. S. Evans, E. Reimnitz and E. W. Kempema. 1989. Oil-Ice-Sediment Interactions during Freeze-up and Break-up. Outer Continental Shelf Environmental Assessment Program, Final Reports of Principal Investigators. U.S. Department of Commerce, NOAA, OCSEAP. Final Report 64, 382 p.

Prince, R. C., R. E. Bare, R. M. Garrett, M. J. Grossman, C. E. Haith, L. G. Keim, K. Lee, G. J. Holtom, P. Lambert, G. A. Sergy, E. H. Owens and C. C. Gu nette. 2003. Bioremediation of stranded oil on an arctic shoreline. *Spill Science and Technology Bulletin* 8: 303-312.

Sergy, G. A., C. C. Guenette and E. H. Owens. 1998. The Svalbard shoreline oilspill field trials. *In Proceedings of the 21st Arctic and Marine Oilspill Program (AMOP) Technical Seminar*, Environment Canada, Ottawa, pp. 873-889.

Sotelo, F., Pantoja, P., Lopez-Gejo, J., Le Roux, G., Quina, F., and Nascimento, C. 2008. Application of fluorescence spectroscopy for spectral discrimination of crude oil samples. *Brazilian Journal of Petroleum and Gas*, 2(2):63-71.

Stephens, F., Bonner, J., Autenrieth, R., and McDonald, T. 1998. TLC/FID analysis of compositional hydrocarbon changes associated with biodegradation. In proceeding of the International Oil Spill Conference. 1998, #264.

Stoffyn-Egli, P. and K. Lee. 2002. Formation and characterization of oil-mineral aggregates. *Spill Science and Technology Bulletin* 8: 31-44.

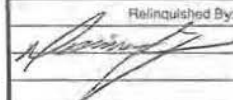
Sun, J. and X. Zheng. 2009. A review of oil-suspended particulate matter aggregation-a natural process of cleansing spilled oil in the aquatic environment. *Journal of Environmental Monitoring* 11: 1801-1809.

Venosa, A. D., M. T. Suidan, K. Lee, S. E. Cobanli, S. Garcia-Blanco and J. R. Haines. 2002b. Bioremediation of oil-contaminated coastal freshwater and saltwater wetlands. In: *Coastal Environment: Environmental Problems in Coastal Regions IV*, C.A. Brebbia (ed.). WIT Press, Southampton, pp. 139-150.

Weise, A. M., C. Nalewajko and K. Lee. 1999. Oil-mineral fine interactions facilitate oil biodegradation in seawater. *Environmental Technology* 20: 811-824.

Yamamoto, V. and Kawanobe, T. (1984). Analysis of Heavy Oils by FID-TLC (Part 1) Rapid Method for Determination of Asphaltene Contents. *Sekiyu Gakkaishi* 27:269.

Yamamoto, V. and Kawanobe, T. (1984). Analysis of Heavy Oils by FID-TLC (Part 2) Rapid Method for Determination of Heavy Oils. *Sekiyu Gakkaishi* 27:373.

MANSFIELD CHAIN OF CUSTODY						PAGE 3 OF 4		Date Rec'd in Lab:		ALPHA Job #:			
 <p>Westborough, MA TEL: 508-898-9220 FAX: 508-898-9193 Mansfield, MA TEL: 508-822-9300 FAX: 508-822-3288</p>		Project Information				Report Information		Data Deliverables		Billing Information			
		Project Name: Enbridge				<input type="checkbox"/> FAX <input type="checkbox"/> EMAIL <input type="checkbox"/> ADEX <input type="checkbox"/> Add'l Deliverables		<input type="checkbox"/> Same as Client Info PO #:					
Client Information		Project Location:				Regulatory Requirements/Report Limits							
Client: AECOM		Project #: Quantification Study				State/Fed Program			Criteria				
Address: 250 Apollo Dr		Project Manager: Robert Kennedy				ANALYSIS Epifluorescence/UV Wavelength						SAMPLE HANDLING <input type="checkbox"/> Done <input type="checkbox"/> Not Needed <input type="checkbox"/> Lab to do Preservation <input type="checkbox"/> Lab to do (Please specify below)	TOTAL # BOTTLES
Chelmsford MA 01824		ALPHA Quote #:											
Phone: 978-905-2269		Turn-Around Time				Sample Specific Comments							
Fax: 978-905-2100		<input type="checkbox"/> Standard <input type="checkbox"/> Rush (ONLY IF PRE-APPROVED)											
Email: robert.kennedy@aecom.com		Due Date: Time:				Other Project Specific Requirements/Comments/Detection Limits: <input type="checkbox"/> MS/MSD (at unit cost) will be omitted unless you check here							
<input type="checkbox"/> These samples have been Previously analyzed by Alpha													
ALPHA Lab ID (Lab Use Only)	Sample ID	Collection		Sample Matrix	Sampler's Initials	[Grid for Analysis Results]						TOTAL # BOTTLES	
		Date	Time										
1208010-04	SEKR1575C702S072612D010	07/26/12	07/27/12	SED	15:11	[Grid]							1
1208010-05	SEKR1575C701S072612DX	07/26/12	07/27/12	SED	15:06	[Grid]							1
1208010-06	SEKR1575C701S072612D007	07/26/12	07/27/12	SED	15:23	[Grid]							2
1208010-07	SEKR1575C701S072612D013	07/26/12	07/27/12	SED	15:26	[Grid]							2
1208010-08	SEKR1575C701S072612D019	07/26/12	07/27/12	SED	15:29	[Grid]							2
1208010-09	SEKR3800C707S072712DX	07/27/12	07/28/12	SED	13:37	[Grid]							1
1208010-10	SEKR3800C707S072712D004	07/27/12	07/28/12	SED	13:43	[Grid]							1
1208010-11	SEKR3800C707S072712D009	07/27/12	07/28/12	SED	13:45	[Grid]							1
1208010-12	SEKR3800C707S072712D014	07/27/12	07/28/12	SED	13:46	[Grid]							1
1208010-13	SEKR3800C709S072712DX	07/27/12	07/28/12	SED	14:28	[Grid]							1
					Container Type	-							
					Preservative	-							
Relinquished By:					Date/Time	Received By:					Date/Time		
					8/13/12 1615	URS Date for off-site and on-site Enbridge Project T.G.					8/13/12		
Please print clearly, legibly and completely. Samples can not be logged in and turnaround time clock will not start until any ambiguities are resolved. All samples submitted are subject to Alpha's Payment Terms.													

In reference to the first shipment of samples sent in 2 coolers (Mansfield Chain of Custody 1) from AECOM (ALPHA LAB), the Centre for Offshore Oil, Gas and Energy Research received the samples in the conditions stated below.

The ID's of damaged samples were as follows:

- 1) SEKR1575C701S072612D019 1 of 2 Broken, bottom of jar detached
- 2) SEKR1575C701S072612D019 2 of 2 Broken, bottom of jar detached
- 3) SEKR0425C701S072512D007 Large crack, bottom of jar about to detach
- 4) SEKR1575C702S072612D010 Broken, bottom of jar detached
- 5) SEKR3775C702S072712D009 Crack, sample may have leaked
- 6) SEKR3800C707S072712D009 Broken, bottom of jar detached
- 7) SEKR1575C702S072612D005 Broken, bottom of jar detached
- 8) SEKR1575C701S072612D013 1 of 2 Small crack visible on jar
- 9) SEKR1575C701S072612D013 2 of 2 Small crack visible on jar
- 10) SEKR3800C709S072712D011 2 of 2 Crack, sample may have leaked
- 11) SEKR3950C701S072612D007 Broken, bottom of jar detached
- 12) SEKR1575C701S072612D007 1 of 2 Small crack visible on jar
- 13) SEKR1575C701S072612D007 2 of 2 Broken, bottom of jar detached
- 14) SEKR3950C701S072612D013 1 of 2 Broken, bottom of jar detached

In addition, all ice packs were melted and the samples were near room temperature. All samples were isolated from the two shipment coolers and placed in the fridge at 4 degrees Celsius.

Appendix B

Alpha Labs Data

NewFields Interpretation of Alpha Labs Data (10/11/12) (results reported in mg/kg sediment, dry weight basis)																	
Site ID (SSCG)	Mile Post	Geomorphic State	Client/Field Sample ID	Target Oiling Level	Actual Oiling Result	Visual Observation %	UV Observation %	Visibly Impacted (yes/no)	Sample From	Sample To	Center of Sample Depth Interval	USCS	TPH	TPH (corrected for oil response factor)	Total Oil	Line 6B Oil	Line 6B Oil % of total oil)
STRATIFIED-003	20.00 - 20.25	Arthro Channel	SFR02026270S0724 2DX	Heavy	Heavy	0	0	N	0.00	0.10	0.05	ML	1135	2877	4444	2174	48.9%
STRATIFIED-061	18.75 - 19.00	Arthro Channel	SFR02026270S0724 2DX005	Heavy	Heavy	0	0	N	0.0	0.50	0.30	ML	577	1550	2238	332	14.8%
			SFR0300270S0725 2DX	None	None	0	0	N	0.00	0.08	0.04	SP	172	585	775	405	52.2%
			SFR0300270S0725 2DX005	None	None	0	0	N	0.08	0.50	0.23	SP	61	321	439	278	63.4%
			SFR0300270S0725 2DX009	None	None	0	0	N	0.50	0.90	0.70	SP	123	468	562	74	13.2%
STRATIFIED-081	36.25 - 36.50	Backwater	SFR03050270S0725 2DX	Heavy	No Poling	0	0	N	0.00	0.10	0.05	ML	564	1565	4549	475	10.4%
			SFR03050270S0725 2DX006	Heavy	No Poling	0	0	N	0.10	0.60	0.35	ML	612	1633	4448	91	2.0%
			SFR03050270S0725 2DX010	Heavy	No Poling	0	0	N	0.60	1.00	0.80	ML	247	765	969	59	6.1%
STRATIFIED-082	37.25 - 37.50	Backwater	SFR030750270S0725 2DX	Heavy	No Poling	0	0	Y	0.00	0.10	0.05	ML	1564	3899	4190	1458	34.8%
			SFR030750270S0725 2DX006	Heavy	No Poling	0	0	N	0.10	0.60	0.35	ML	1102	2800	3072	730	23.8%
			SFR030750270S0725 2DX010	Heavy	No Poling	0	0	N	0.60	1.00	0.80	ML	647	1717	2247	145	6.4%
STRATIFIED-021	4.25 - 4.50	Backwater	SFR04046270S0725 2DX	Light	Light	0	0	N	0.00	0.10	0.05	ML	1885	4664	4748	1491	31.4%
			SFR04046270S0725 2DX007	Light	Light	0	0	N	0.10	0.70	0.40	ML	961	2511	2644	739	27.9%
STRATIFIED-011	37.50 - 37.75	Channel Deposit	SFR03156270S0724 2DX	Heavy	Moderate	0	0	N	0.00	0.08	0.04	ML	1707	4241	5569	1423	25.6%
			SFR03156270S0724 2DX003	Heavy	Moderate	0	0	N	0.08	0.50	0.29	ML	778	2028	2654	1111	41.9%
			SFR03156270S0724 2DX005	Heavy	Moderate	0	0	N	0.50	0.90	0.70	ML	306	903	1034	79	7.7%
STRATIFIED-301	2.850 - 2.875	Cutoff/Diow	SFR02806270S0724 2DX	None	None	0	0	N	0.00	0.08	0.04	OL	160	556	1056	234	22.2%
			SFR02806270S0724 2DX003	None	None	0	0	N	0.08	0.25	0.17	OL	89	387	224	151	67.2%
STRATIFIED-481	15.50 - 15.75	Impoundment	SFR03156270S0726 2DX	Heavy	Heavy	0	2	N	0.00	0.08	0.04	ML	1335	3354	4282	1235	28.8%
			SFR03156270S0726 2DX007	Heavy	Heavy	0	0	N	0.08	0.65	0.35	ML	1202	3038	3329	1147	34.5%
			SFR03156270S0726 2DX013	Heavy	Heavy	0	0	N	0.65	1.25	0.95	ML	901	2222	2973	219	7.4%
			SFR03156270S0726 2DX019	Heavy	Heavy	0	0	N	1.25	1.65	1.55	ML	878	2267	2303	69	3.0%
STRATIFIED-503	15.50 - 15.75	Impoundment	SFR03156270S0726 2DX	Moderate	Heavy	0	0	N	0.00	0.10	0.05	OL	1581	3965	6145	1543	25.1%
			SFR03156270S0726 2DX005	Moderate	Heavy	0	0	N	0.10	0.50	0.30	OL	1395	3498	4864	1412	29.0%
			SFR03156270S0726 2DX010	Moderate	Heavy	0	0	N	0.50	1.00	0.75	OL	751	1963	2340	48	2.1%
STRATIFIED-583	39.25 - 39.50	Lane	SFR03050270S0726 2DX	None	None	0	0	N	0.00	0.10	0.05	ML	2083	5136	7308	357	4.9%
			SFR03050270S0726 2DX007	None	None	0	0	N	0.10	0.70	0.40	ML	2647	6478	4853	103	2.1%
			SFR03050270S0726 2DX013	None	None	0	0	N	0.70	1.30	1.00	ML	3120	7604	6296	130	2.1%
STRATIFIED-661	37.75 - 38.00	ML Fan	SFR0300270S0727 2DX	None	Moderate	0	0	N	0.00	0.10	0.05	ML	1162	2944	3763	1102	29.3%
			SFR0300270S0727 2DX004	None	Moderate	0	<1	N	0.10	0.40	0.25	ML	863	2231	2709	567	20.9%
			SFR0300270S0727 2DX009	None	Moderate	0	0	N	0.40	0.90	0.65	ML	810	2104	2464	138	5.6%
			SFR0300270S0727 2DX014	None	Moderate	0	0	N	0.90	1.40	1.15	ML	3039	7413	4820	1238	25.7%
STRATIFIED-663	37.75 - 38.00	ML Fan	SFR0300270S0727 2DX	None	Light	0	0	N	0.00	0.10	0.05	ML	1011	2582	3376	607	18.0%
			SFR0300270S0727 2DX006	None	Light	0	0	N	0.10	0.60	0.35	ML	711	1869	2608	339	13.0%
			SFR0300270S0727 2DX011	None	Light	0	0	N	0.60	1.10	0.85	ML	977	2503	2574	202	7.9%

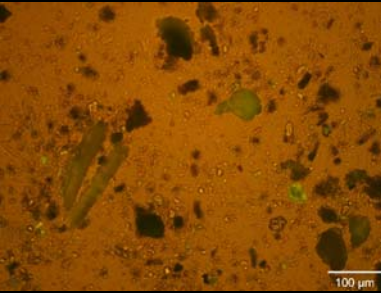
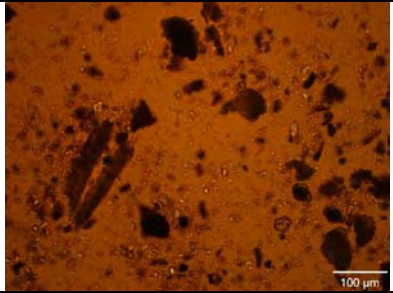
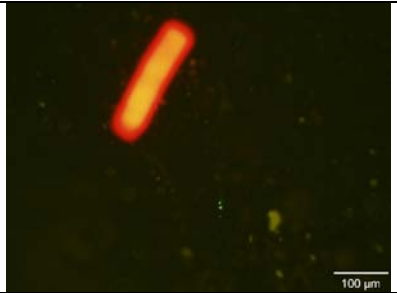
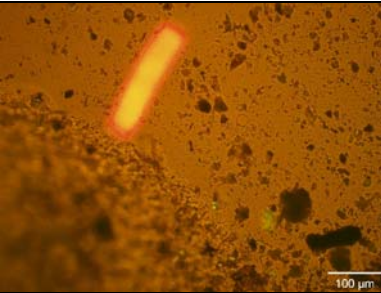
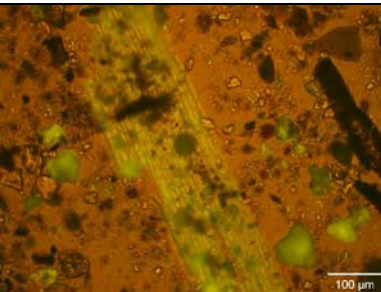
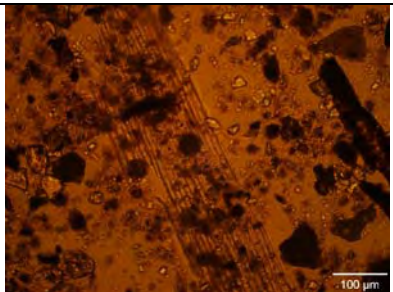
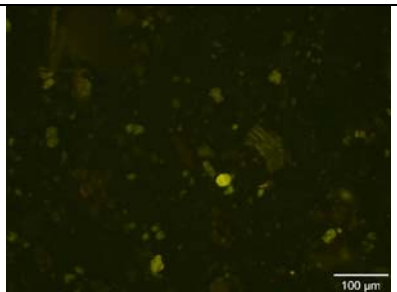
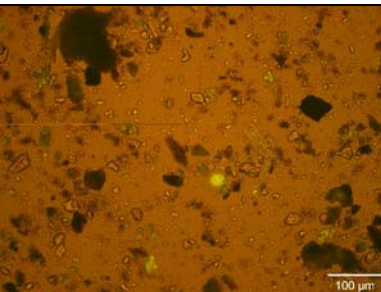
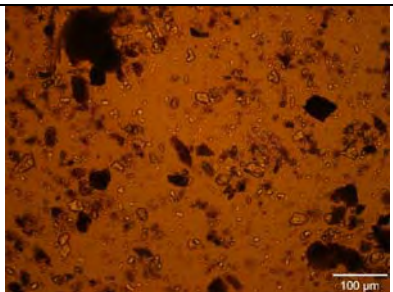
Appendix C: Kalamazoo River Sediment Sample Photographs

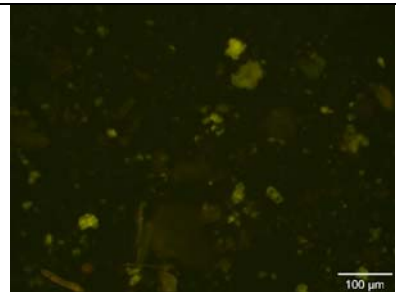
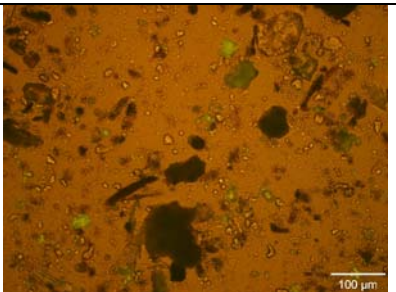
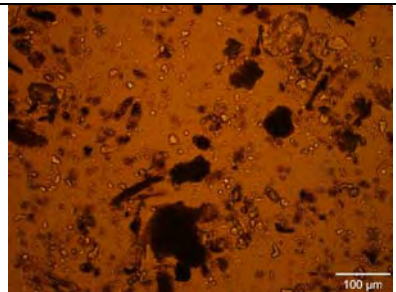
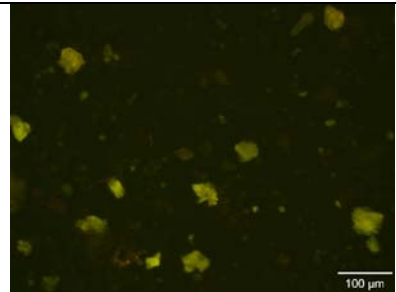
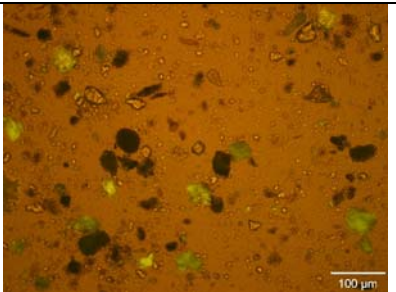
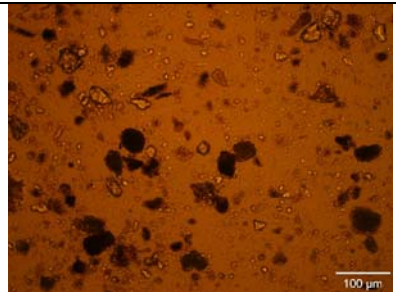
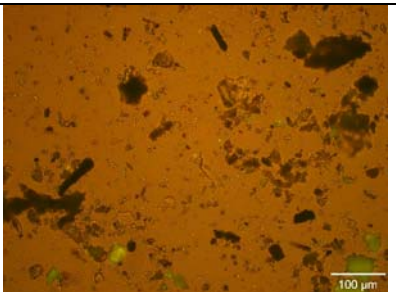
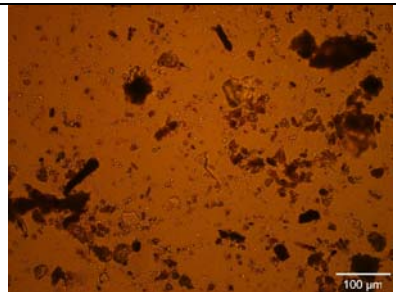
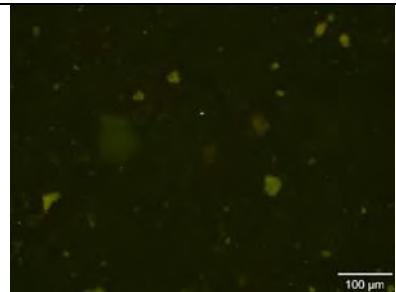
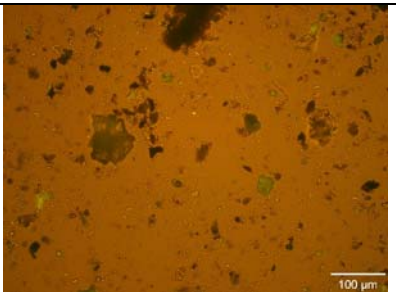
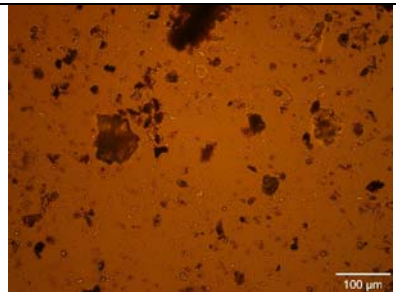
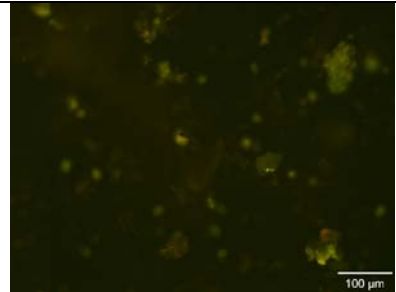
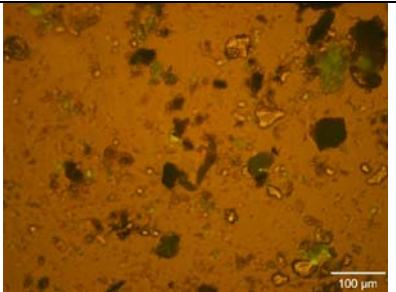
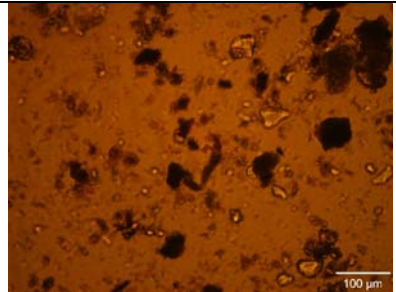
The following table contains all the photographs taken of the sediment samples. The corresponding field ID is provided, magnification (100µM scale bar = 128x and the 50 µM scale bar = 320x) and light conditions:

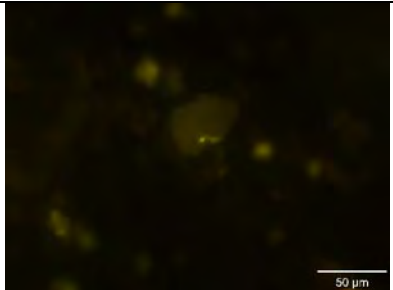
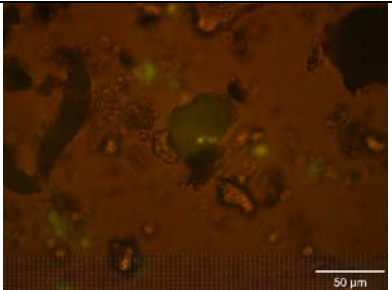
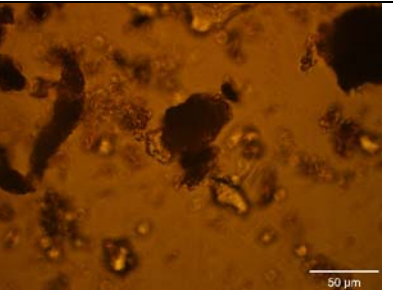
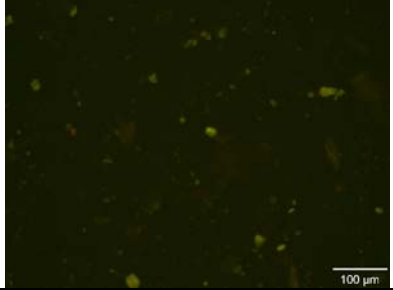
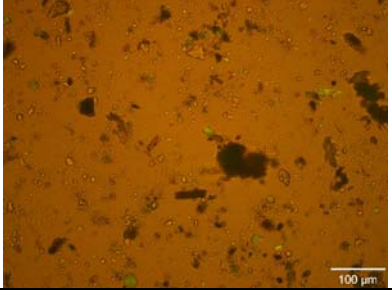
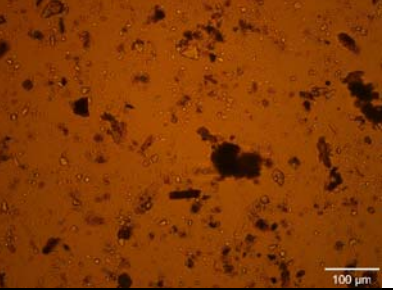
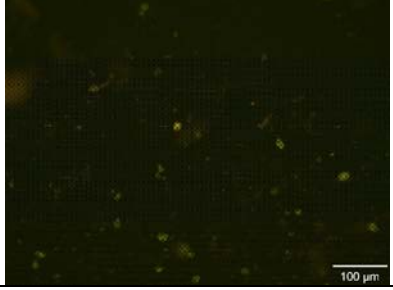
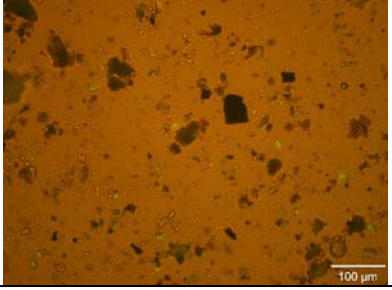
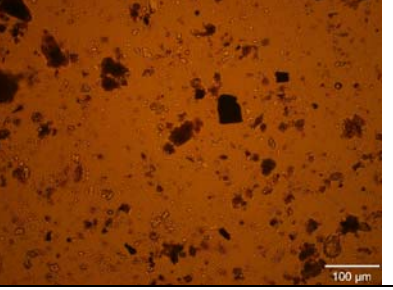
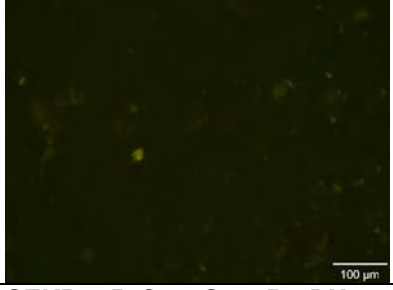
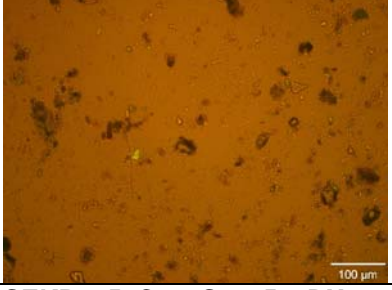
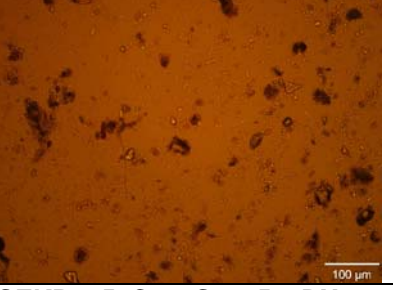
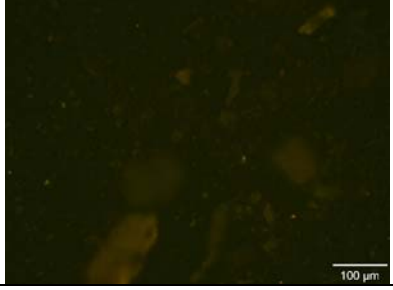
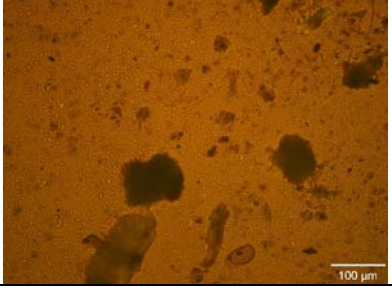
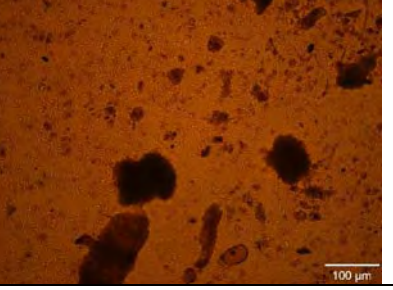
A = UV Epifluorescence

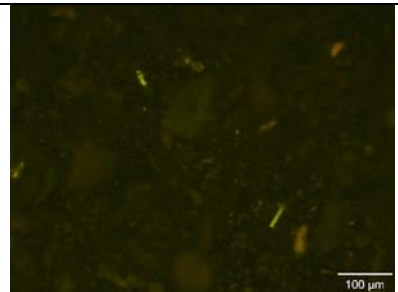
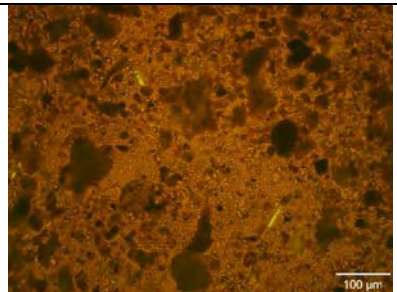
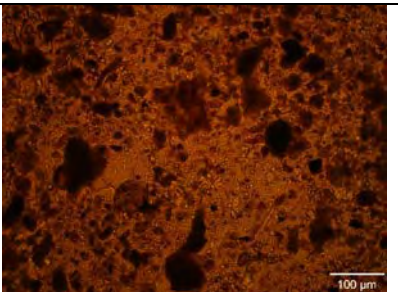
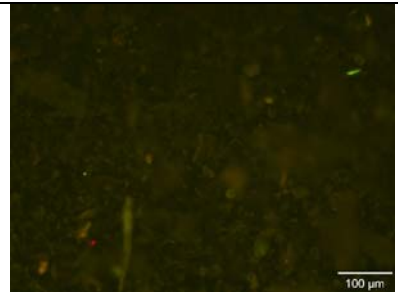
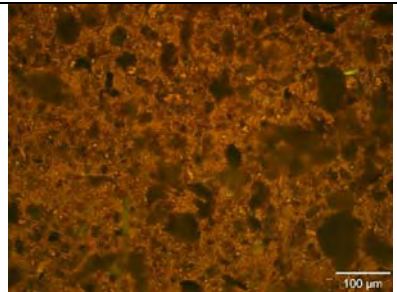
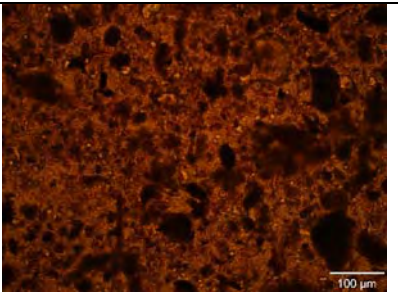
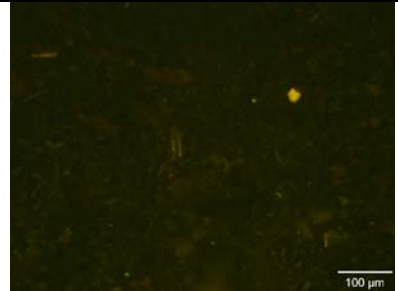
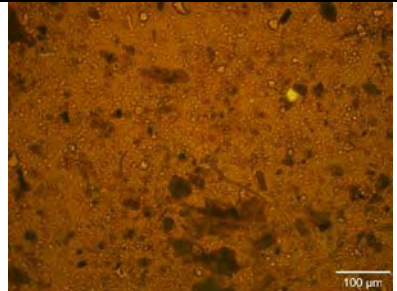
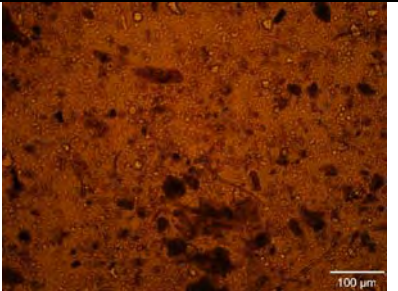
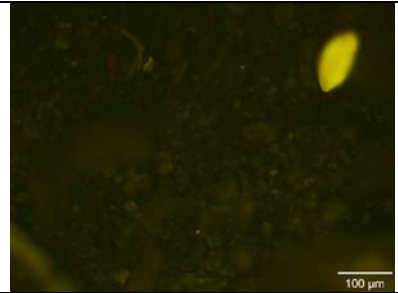
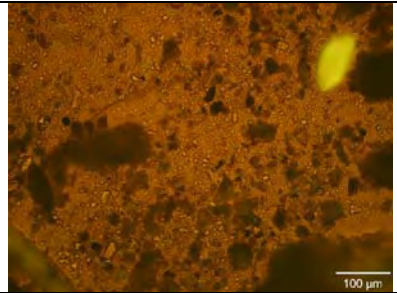
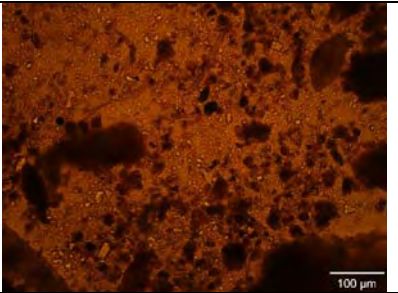
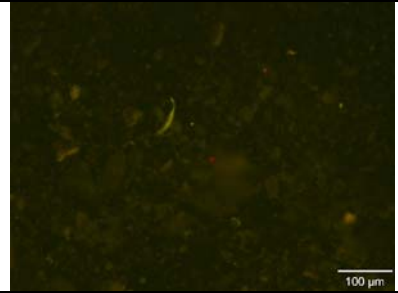
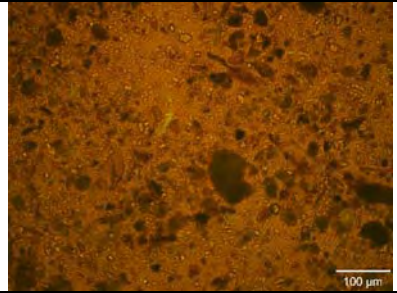
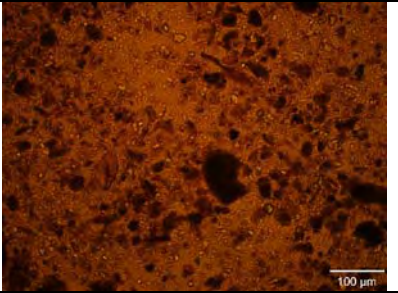
B = UV Epifluorescence and Transmitted Light

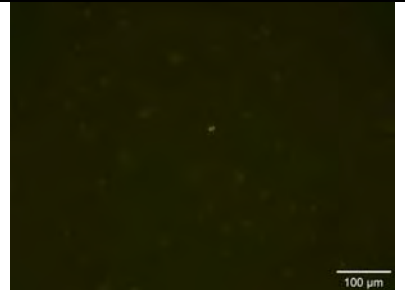
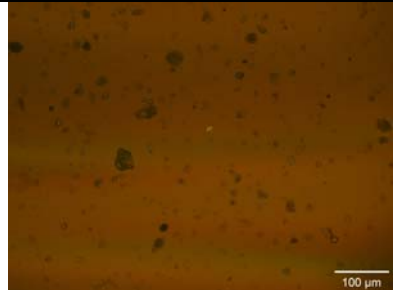
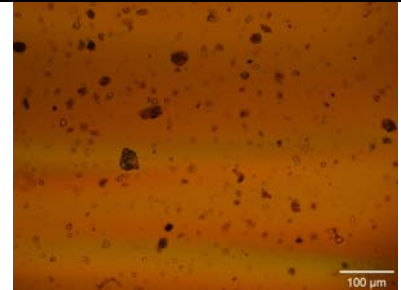
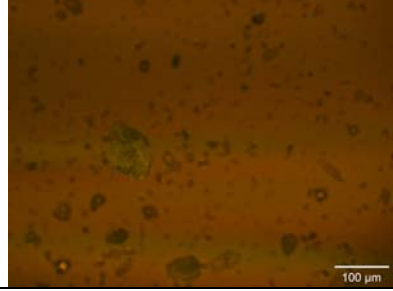
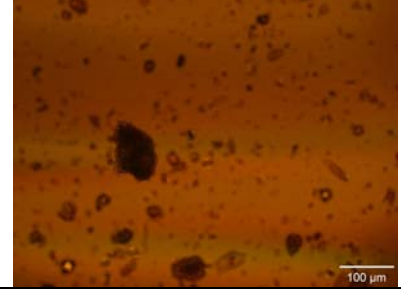
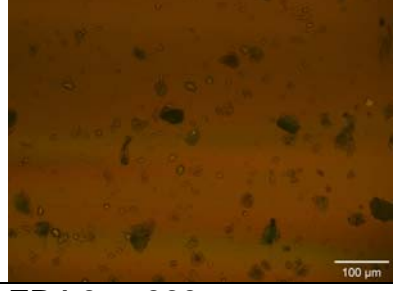
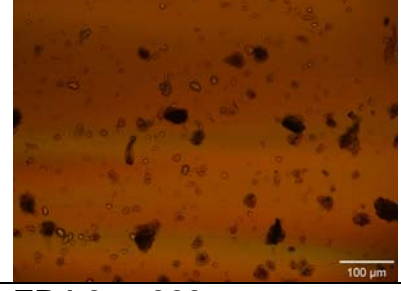
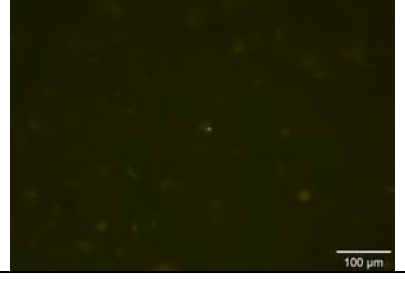
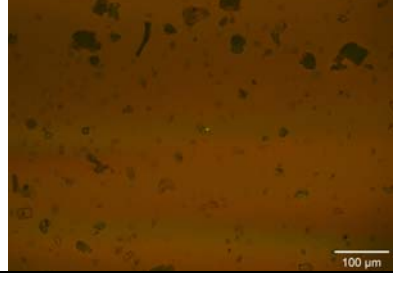
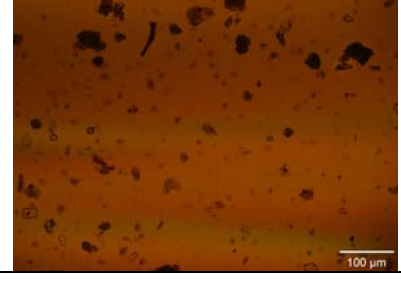
C = Transmitted Light

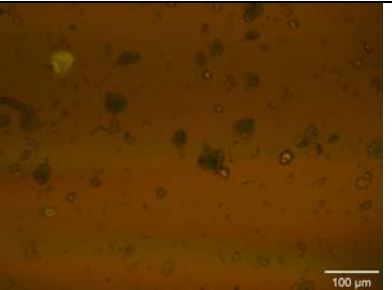
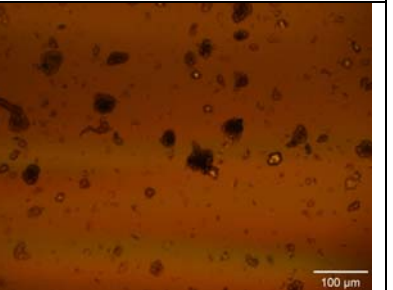
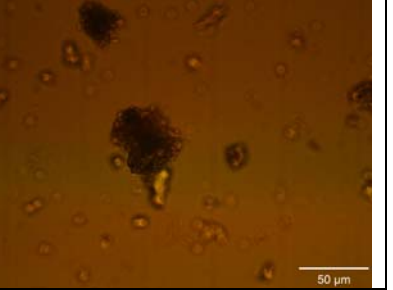
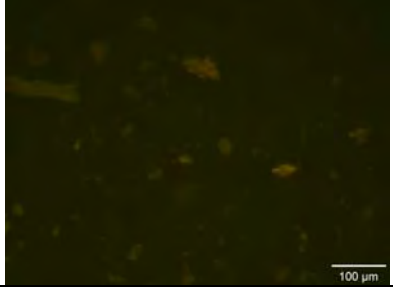
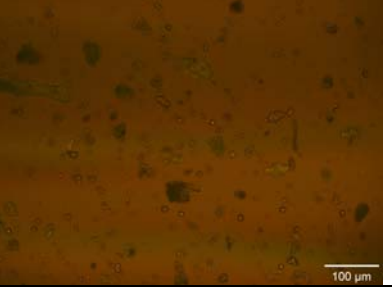
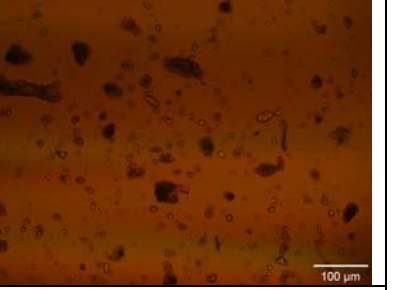
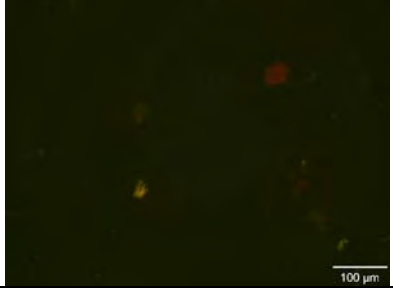
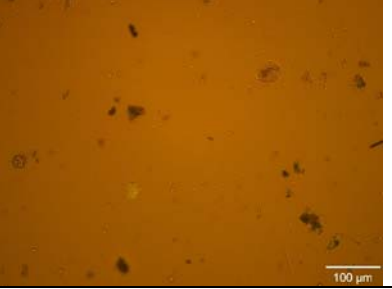
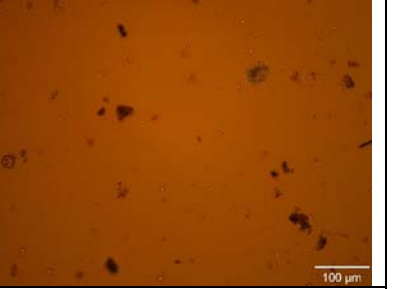
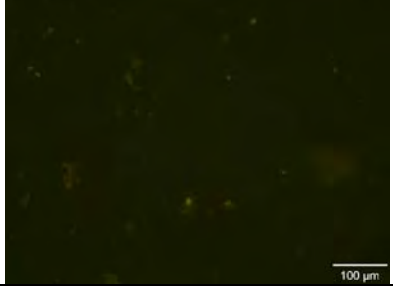
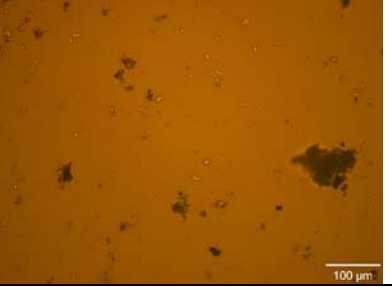
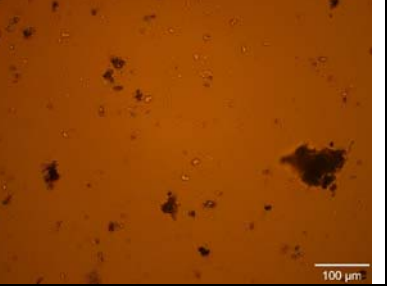
SEKR2025C702S07241DX EB1-1 A	SEKR2025C702S07241DX EB-1 B	SEKR2025C702S07241DX EB1-1 C
		
EB1-2	EB1-2	EB1-2
		
EB1-3	EB1-3	EB1-3
		
EB1-4	EB1-4	EB1-4
		

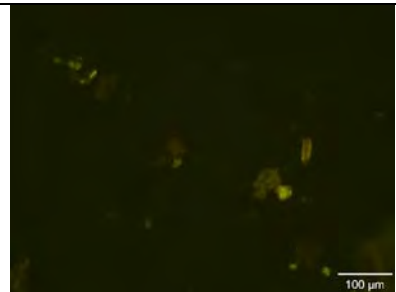
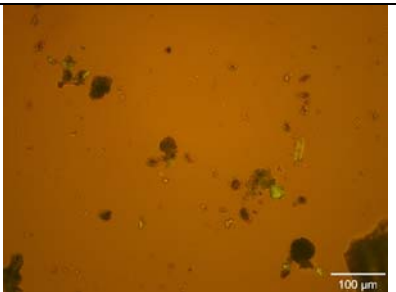
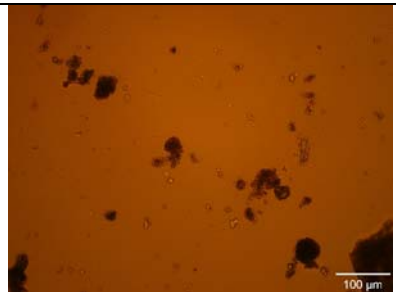
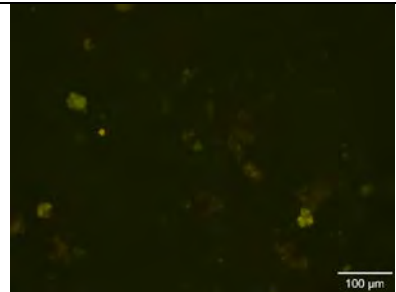
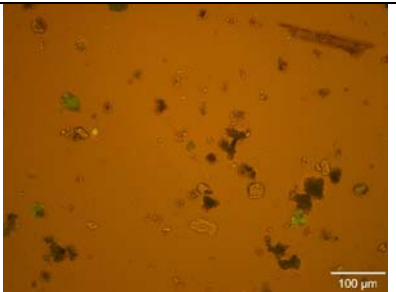
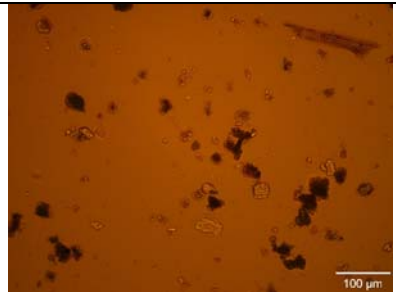
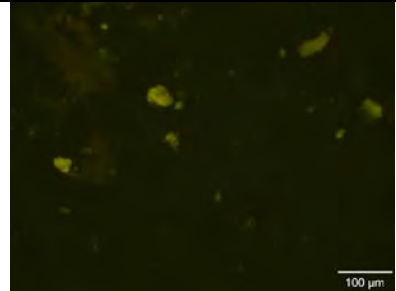
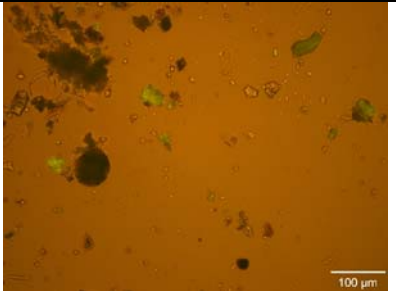
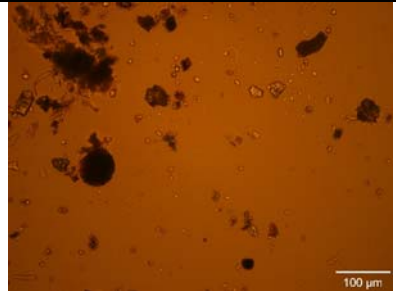
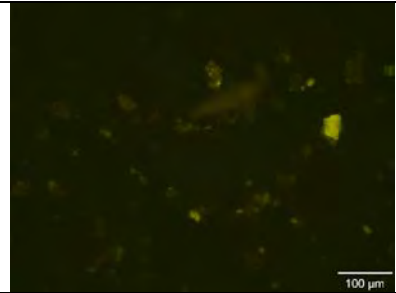
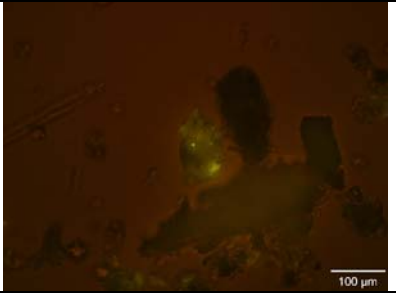
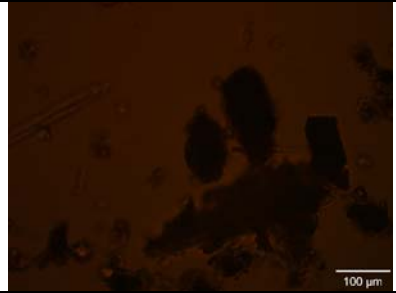
EB1-5 	EB1-5 	EB1-5 
EB1-6 	EB1-6 	EB1-6 
SEKR2025C702S072412D005 EB2-1 A	SEKR2025C702S072412D005 EB2-1 B	SEKR2025C702S072412D005 EB2-1 C
		
EB2-2 	EB2-2 	EB2-2 
EB2-3 	EB2-3 	EB2-3 

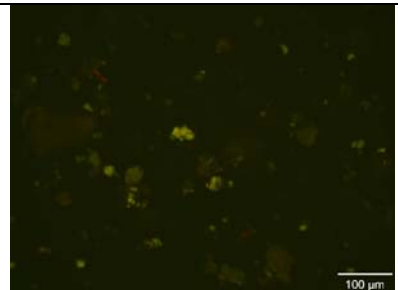
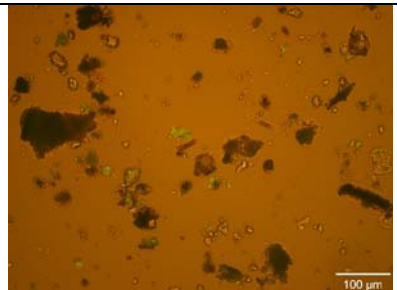
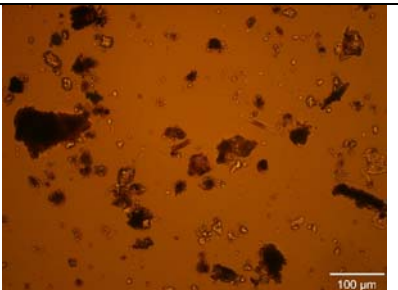
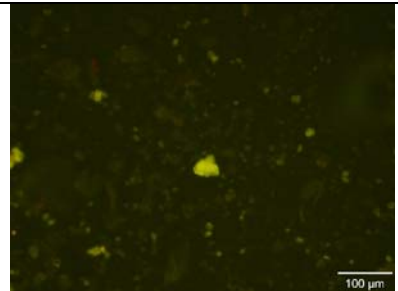
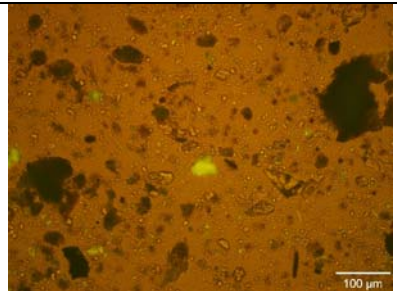
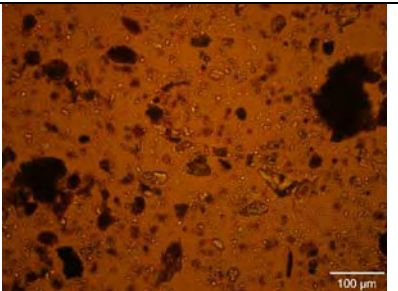
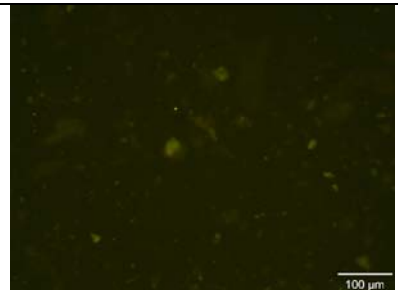
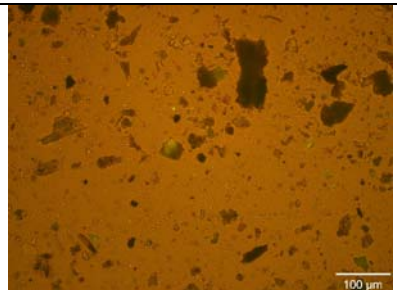
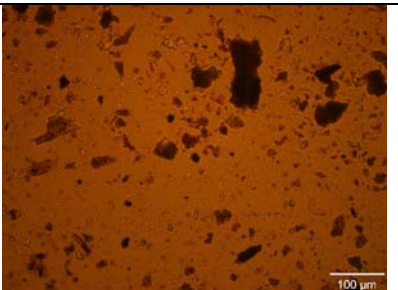
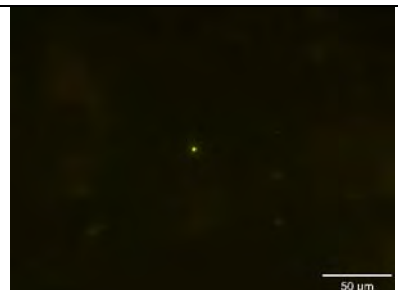
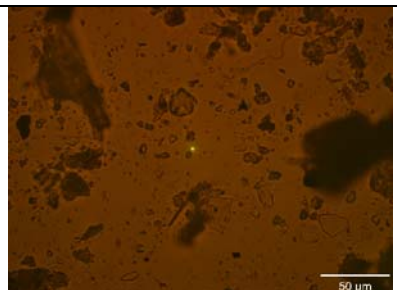
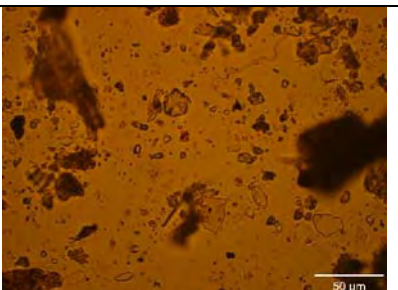
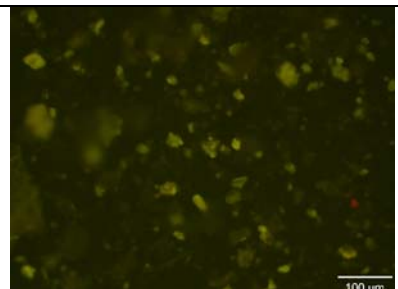
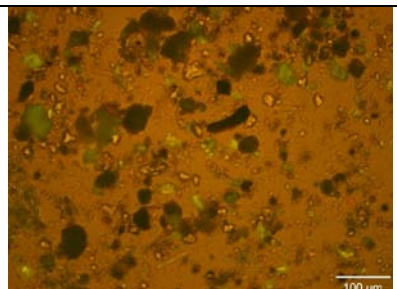
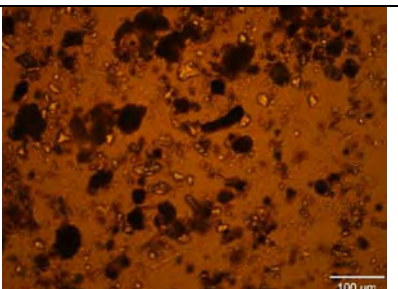
EB2-3 at 320x	EB2-3 at 320x	EB2-3 at 320x
		
EB2-4	EB2-4	EB2-4
		
EB2-5	EB2-5	EB2-5
		
EB2-6	EB2-6	EB2-6
		
SEKR3650C701S072512DX EB3-1 A	SEKR3650C701S072512DX EB3-1 B	SEKR3650C701S072512DX EB3-1 C
		

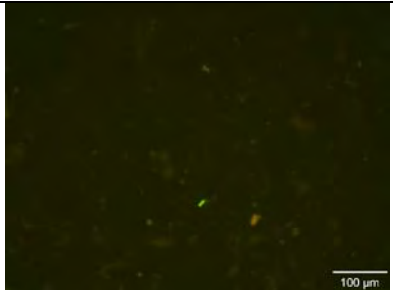
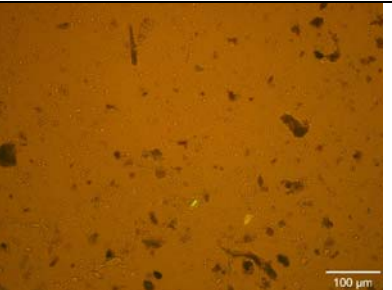
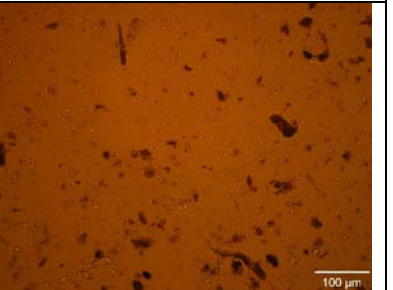
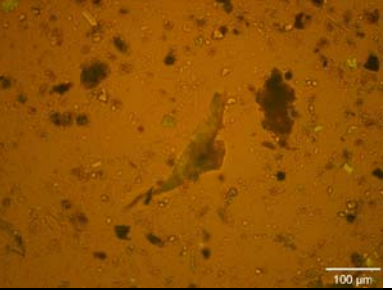
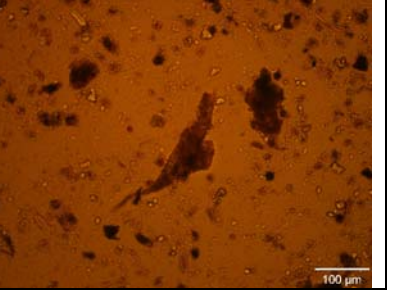
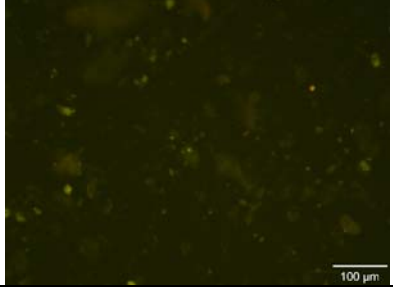
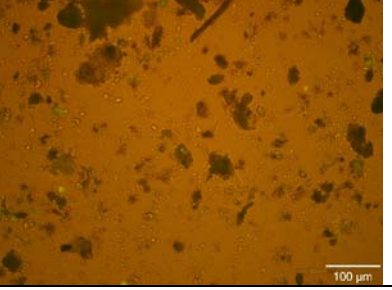
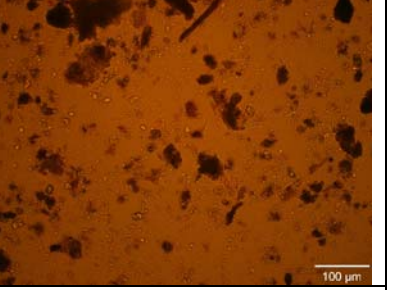
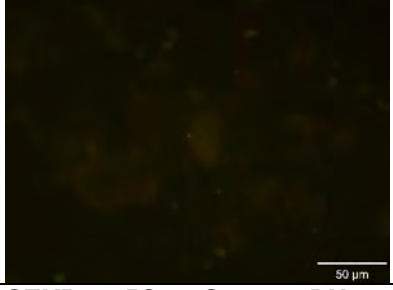
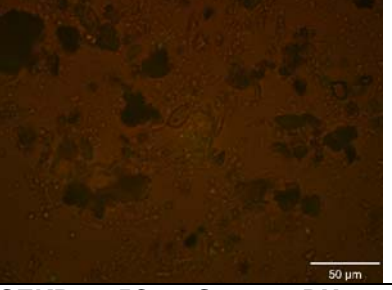
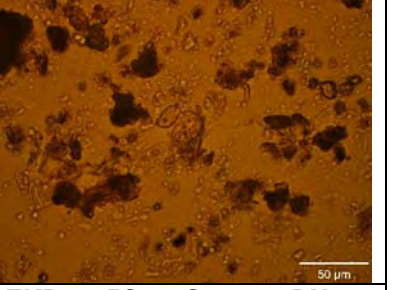
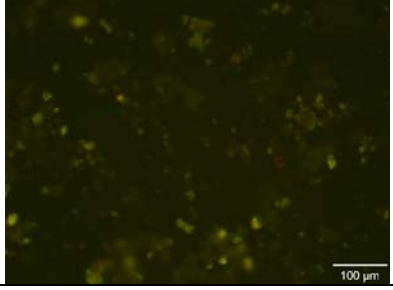
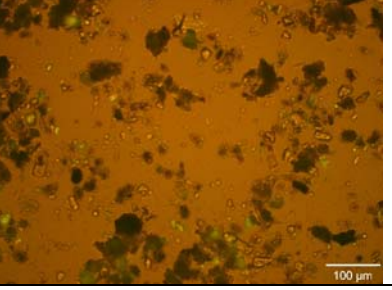
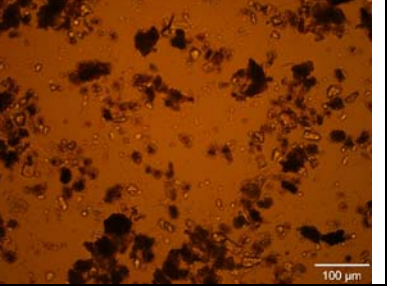
EB3-2 	EB3-2 	EB3-2 
EB3-3 	EB3-3 	EB3-3 
EB3-4 	EB3-4 	EB3-4 
EB3-5 	EB3-5 	EB3-5 
EB3-6 	EB3-6 	EB3-6 

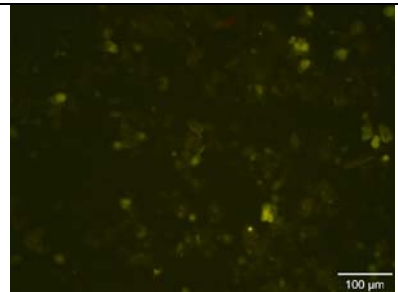
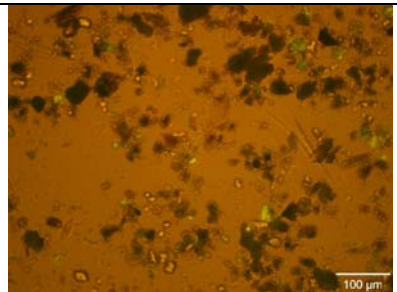
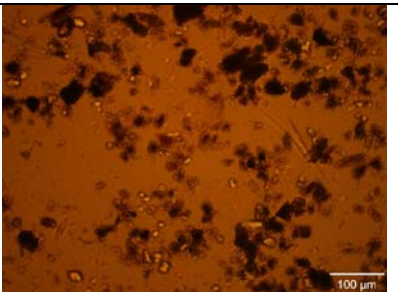
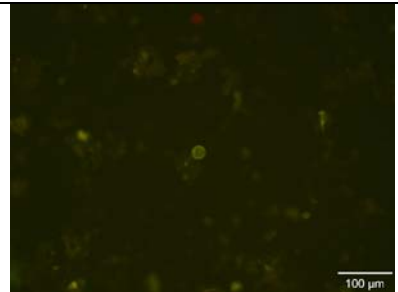
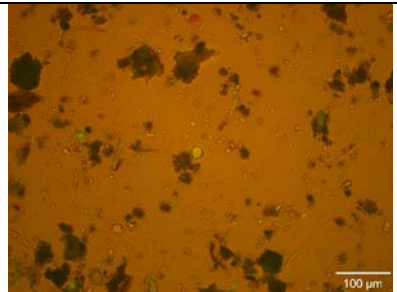
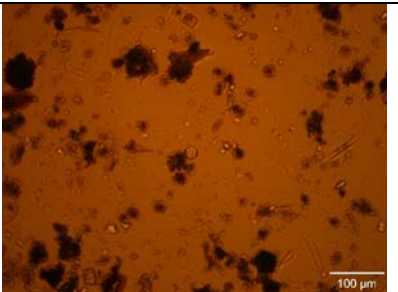
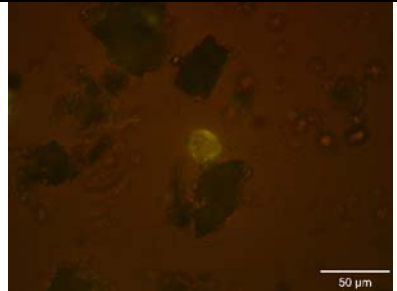
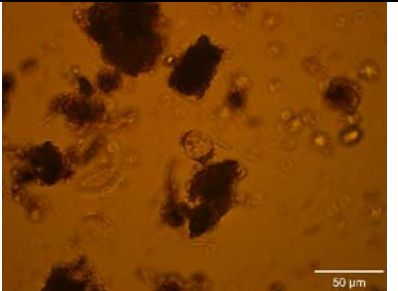
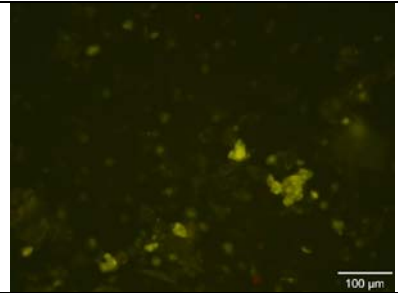
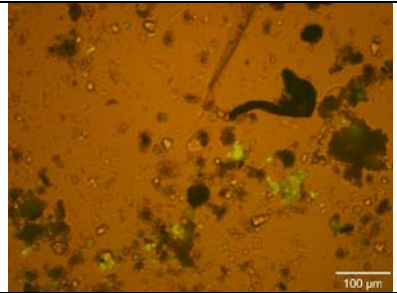
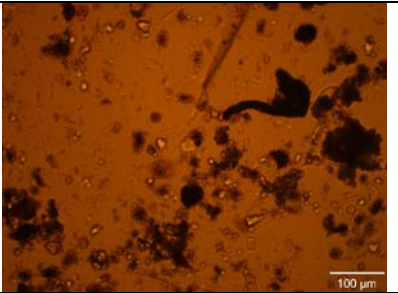
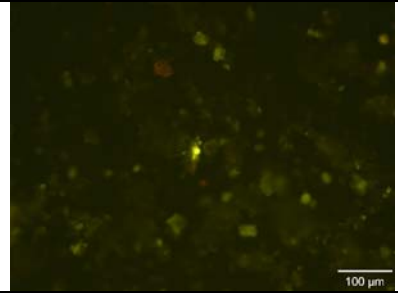
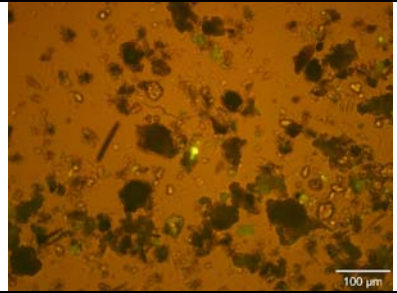
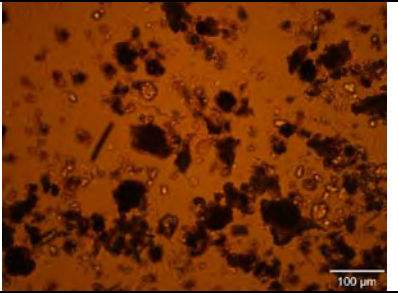
SEKR3650C701S072512D006 EB4-1 A	SEKR3650C701S072512D006 EB4-1 B	SEKR3650C701S072512D006 EB4-1 C
 100 µm	 100 µm	 100 µm
EB4-2	EB4-2	EB4-2
 100 µm	 100 µm	 100 µm
EB4-3	EB4-3	EB4-3
 100 µm	 100 µm	 100 µm
EB4-3 at 320x	EB4-3 at 320x	EB4-3 at 320x
 50 µm	 50 µm	 50 µm
EB4-4	EB4-4	EB4-4
 100 µm	 100 µm	 100 µm

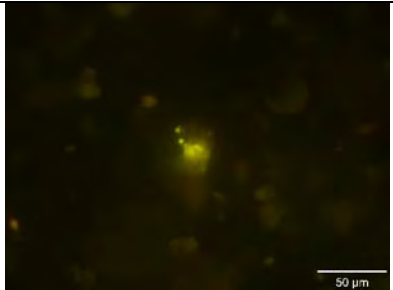
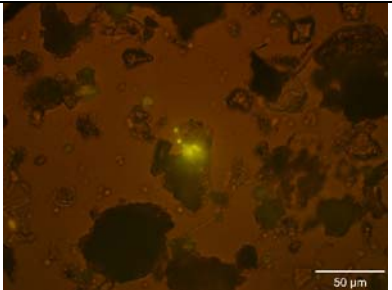
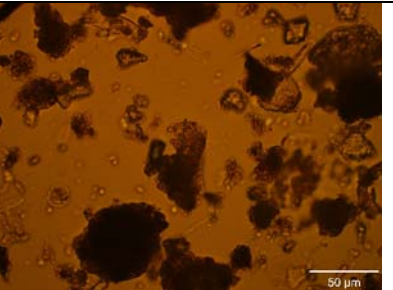
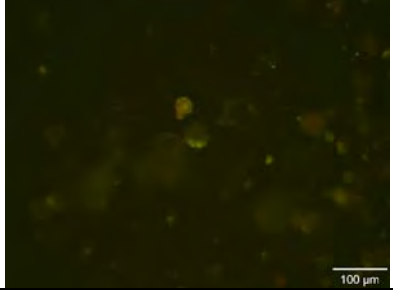
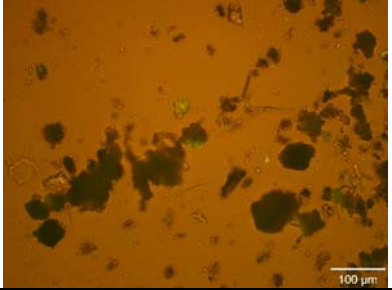
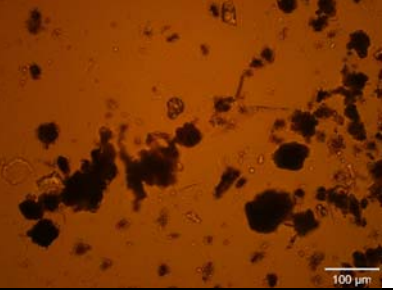
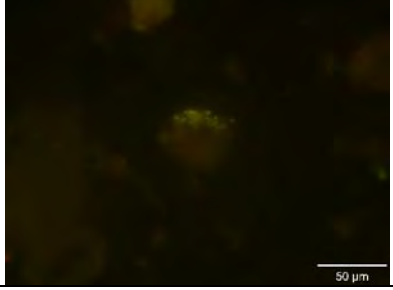
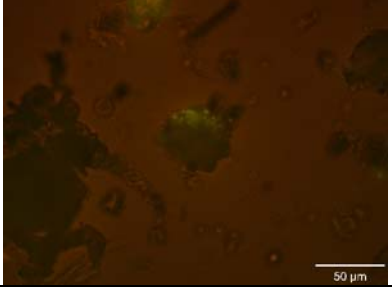
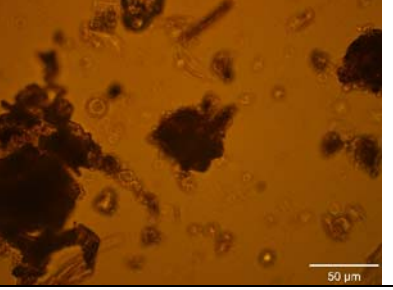
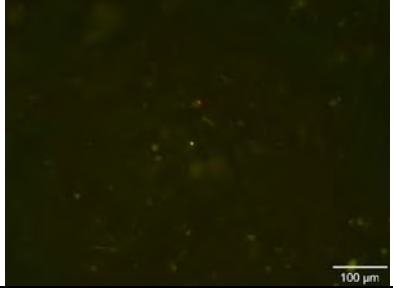
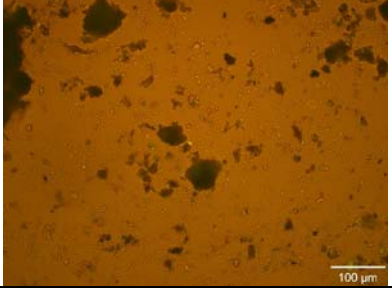
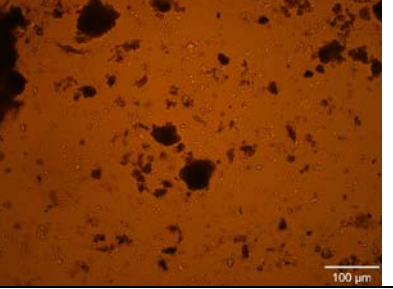
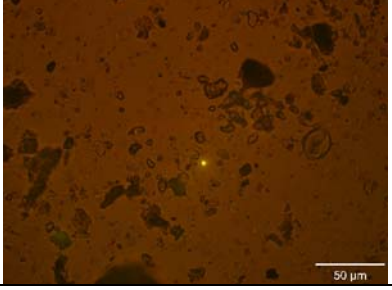
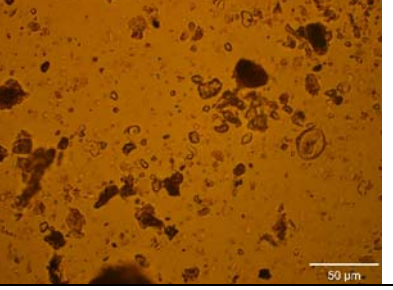
EB4-5 	EB4-5 	EB4-5 
EB4-5 at 320x 	EB4-5 at 320x 	EB4-5 at 320x 
EB4-6 	EB4-6 	EB4-6 
SEKR3750C701S072512DX EB5-1 A	SEKR3750C701S072512DX EB5-1 B	SEKR3750C701S072512DX EB5-1 C
		
EB5-2 	EB5-2 	EB5-2 

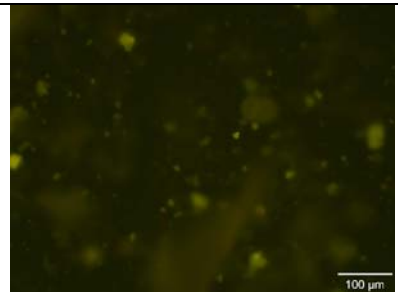
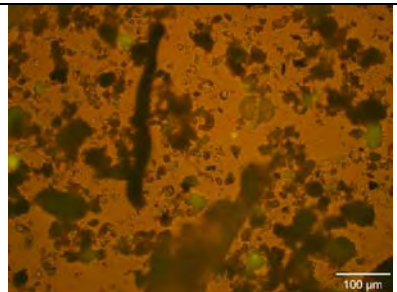
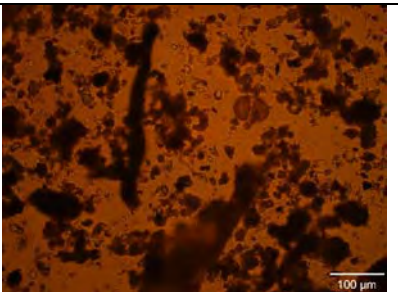
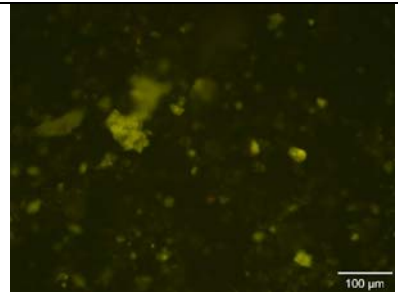
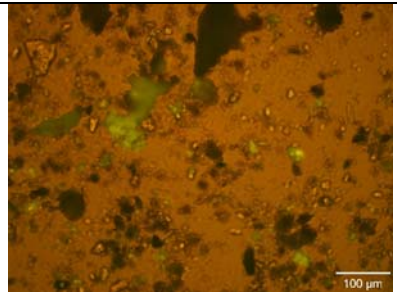
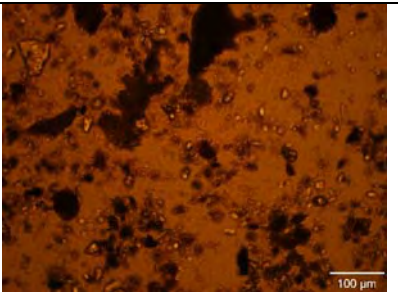
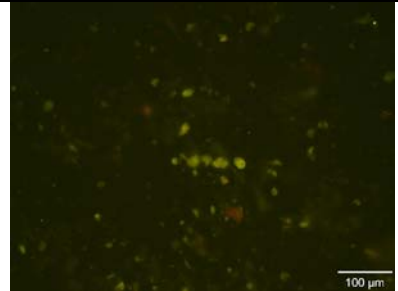
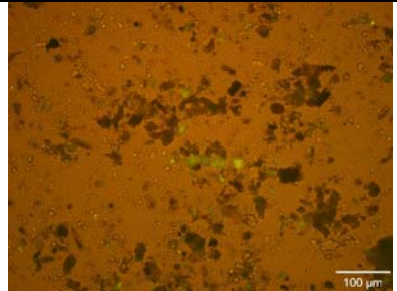
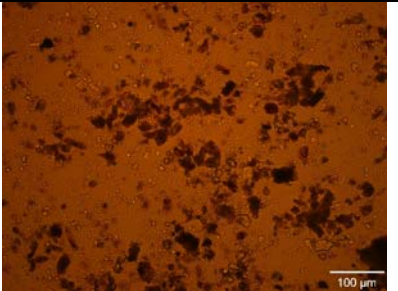
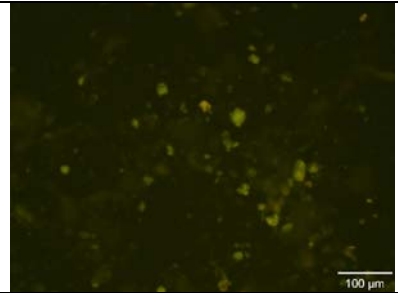
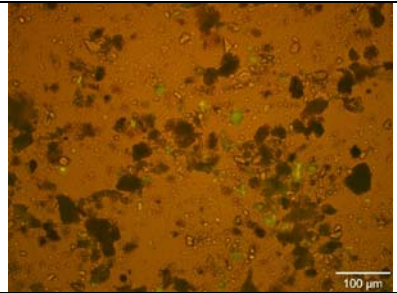
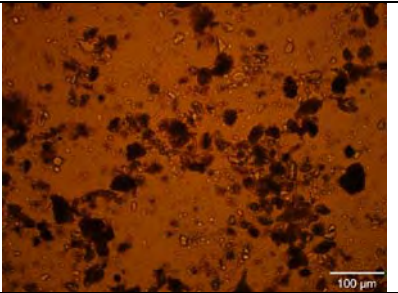
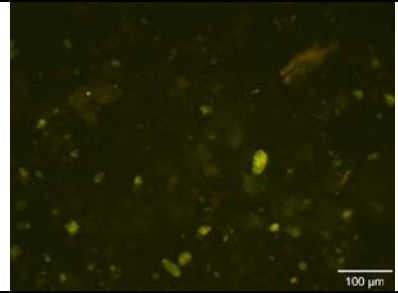
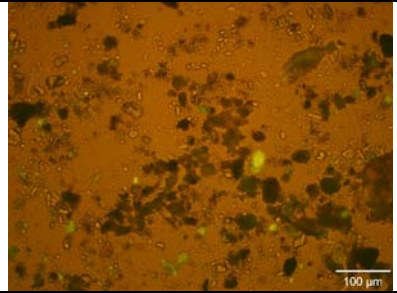
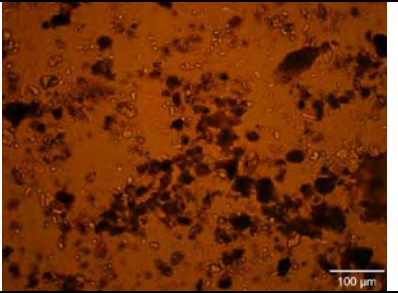
EB5-3 	EB5-3 	EB5-3 
EB5-4 	EB5-4 	EB5-4 
EB5-5 	EB5-5 	EB5-5 
EB5-6 	EB5-6 	EB5-6 
EB5-6 at 320x 	EB5-6 at 320x 	EB5-6 at 320x 

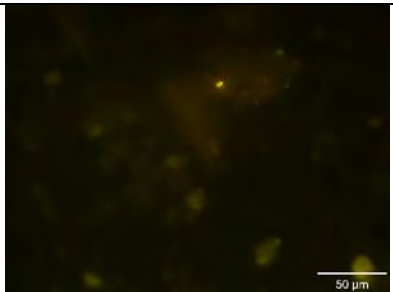
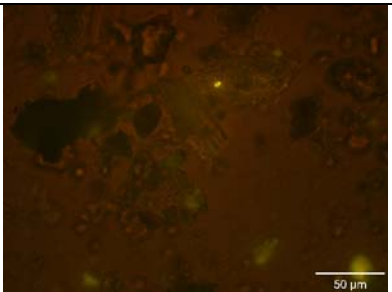
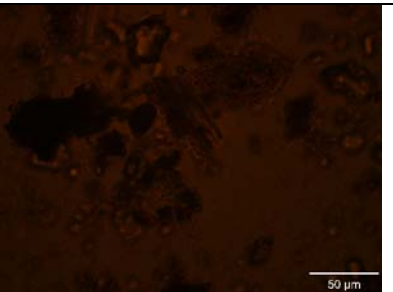
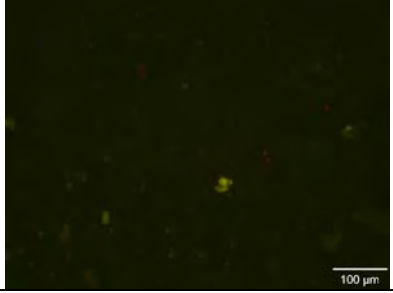
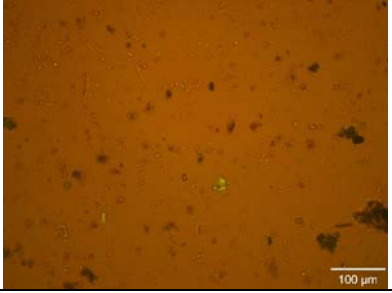
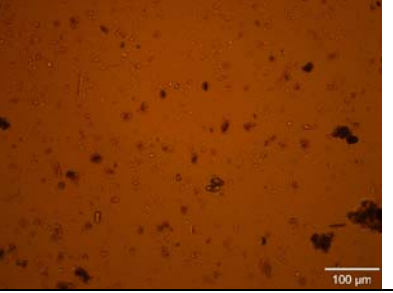
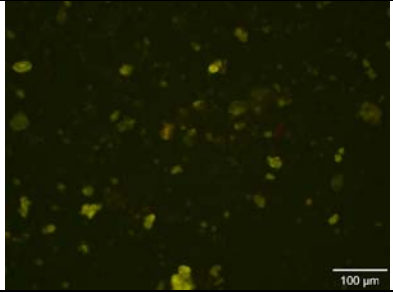
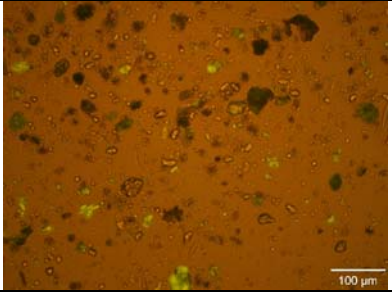
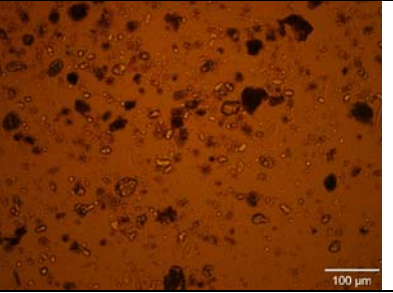
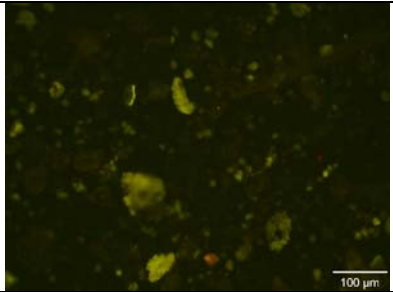
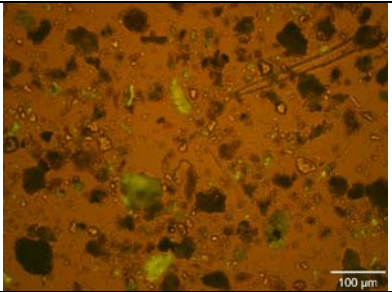
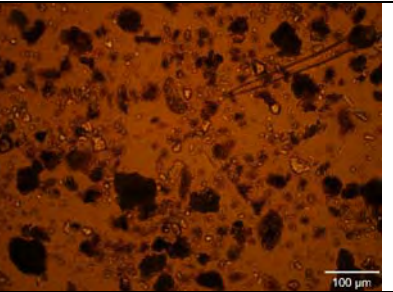
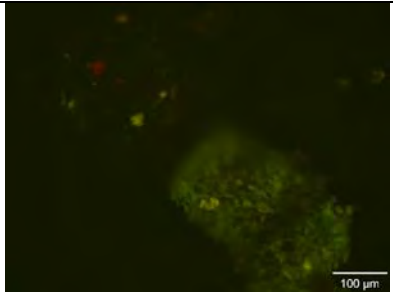
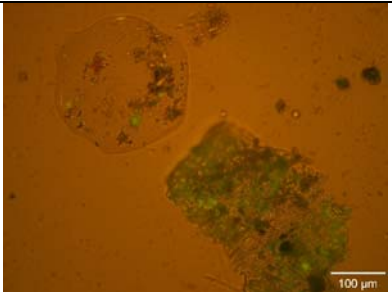
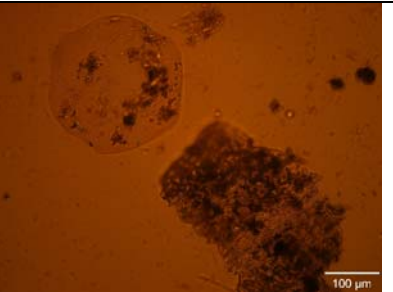
EB5-7 	EB5-7 	EB5-7 
SEKR3750C701S072512D006 EB6-1 A	SEKR3750C701S072512D006 EB6-1 B	SEKR3750C701S072512D006 EB6-1 C
		
EB6-2	EB6-2	EB6-2
		
EB6-2 at 320x	EB6 at 320x	EB6 at 320x
		
EB6-3	EB6-3	EB6-3
		

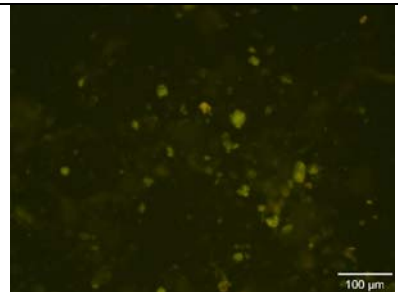
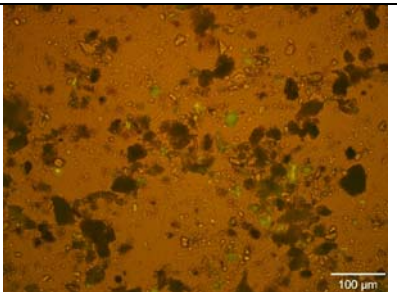
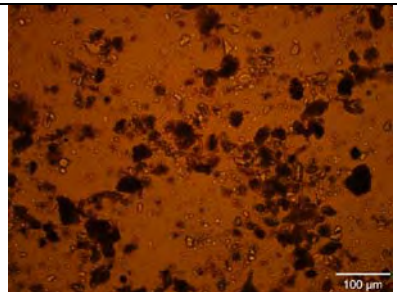
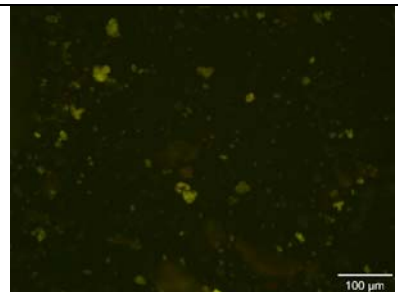
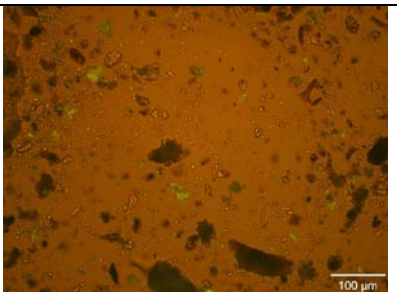
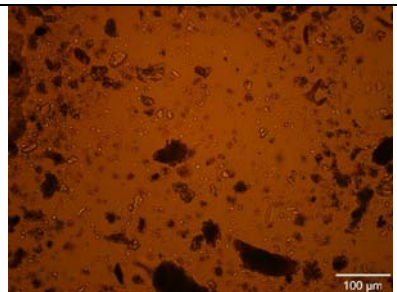
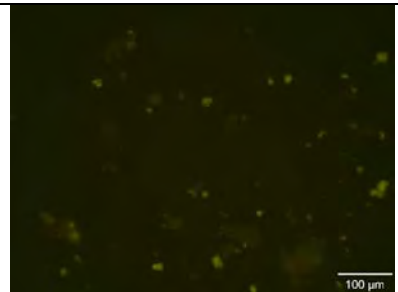
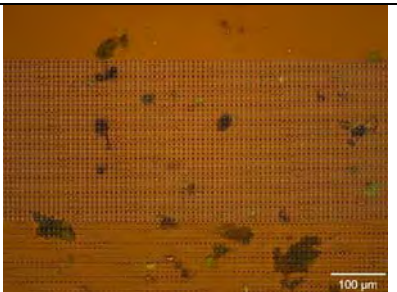
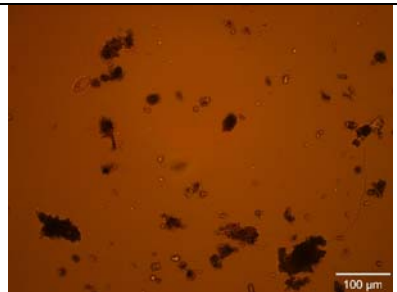
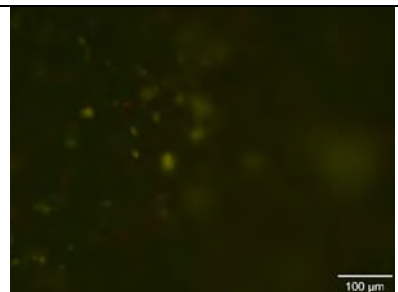
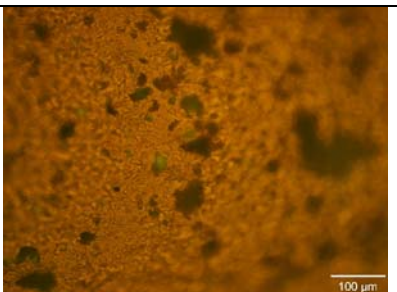
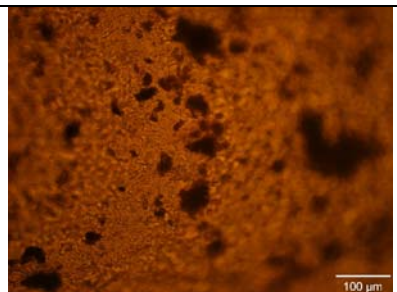
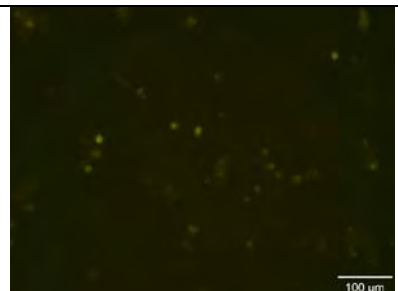
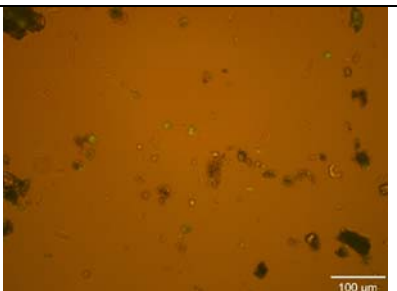
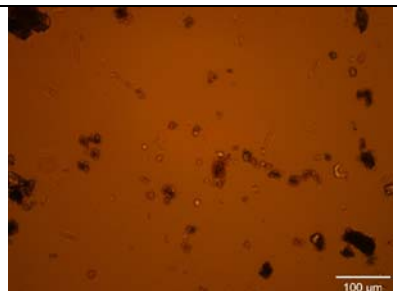
EB6-4 	EB6-4 	EB6-4 
EB6-5 	EB6-5 	EB6-5 
EB6-6 	EB6-6 	EB6-6 
EB6-6 at 320x 	EB6 at 320x 	EB6 at 320x 
SEKR3775C702S072712DX EB7-1 A	SEKR3775C702S072712DX EB7-1 B	SEKR3775C702S072712DX EB7-1 C
		

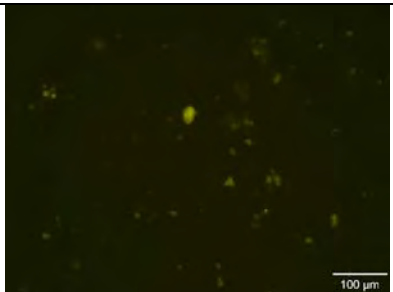
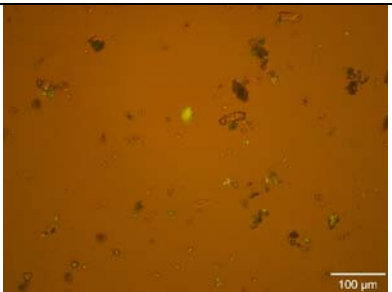
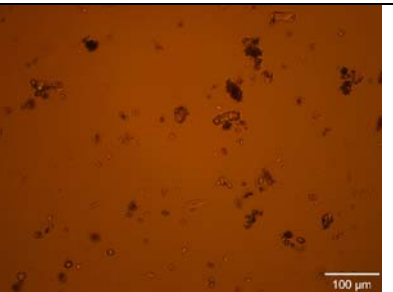
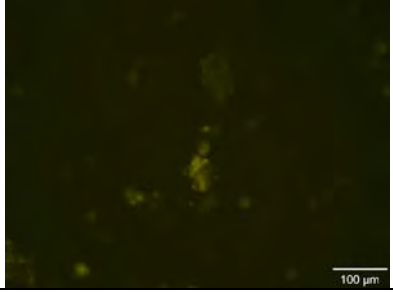
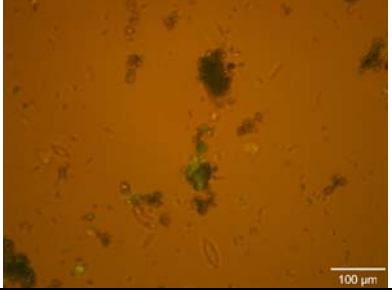
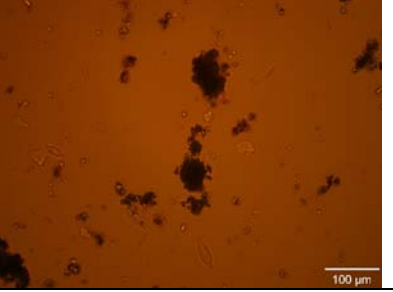
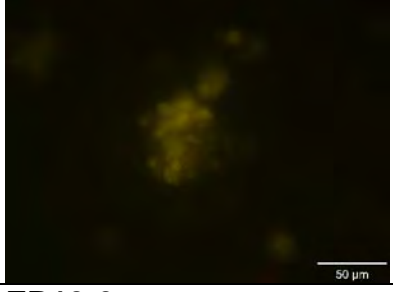
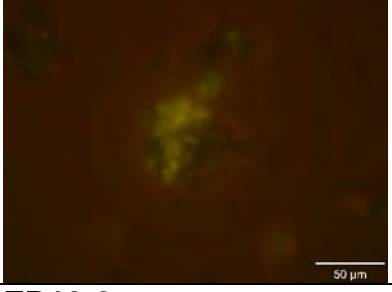
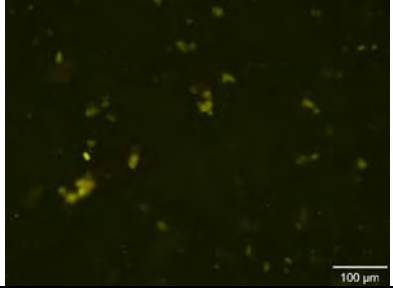
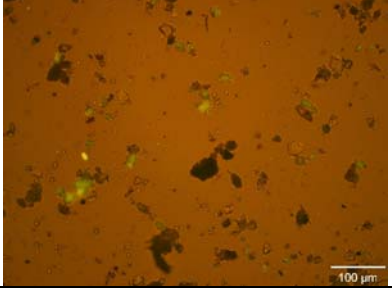
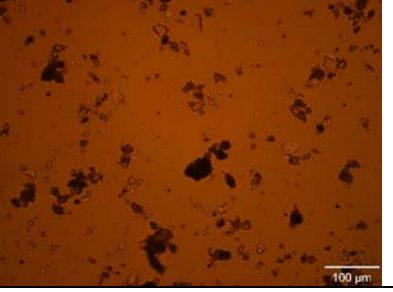
EB7-2 	EB7-2 	EB7-2 
EB7-3 	EB7-3 	EB7-3 
EB7-3 at 320x 	EB7-3 at 320x 	EB7-3 at 320x 
EB7-4 	EB7-4 	EB7-4 
EB7-5 	EB7-5 	EB7-5 

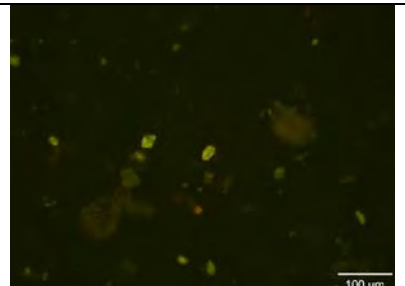
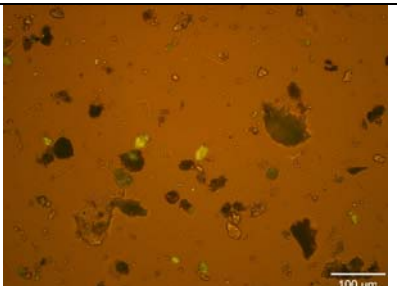
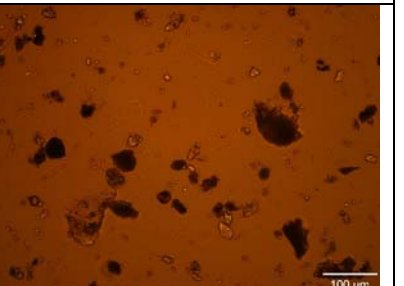
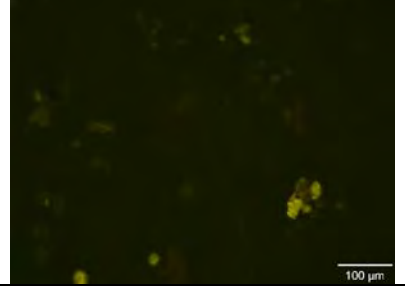
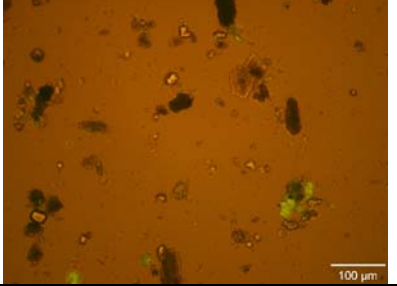
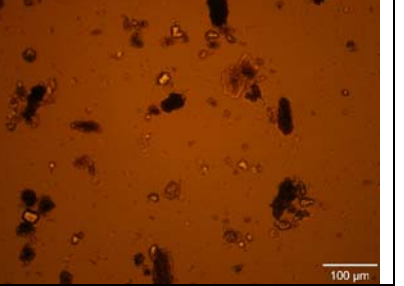
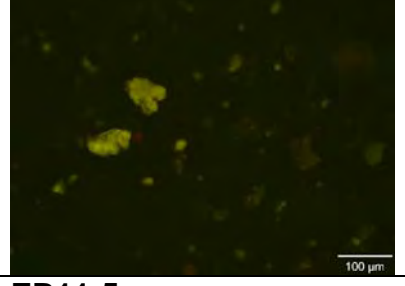
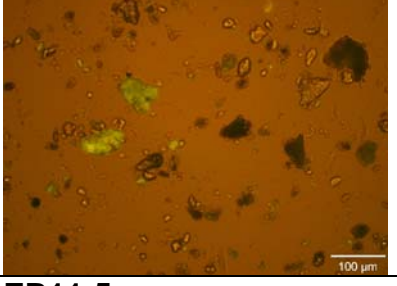
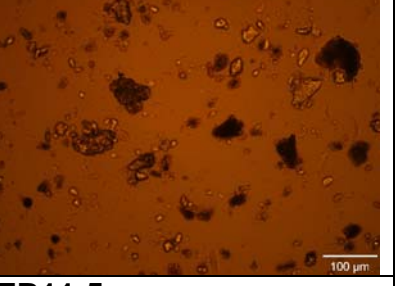
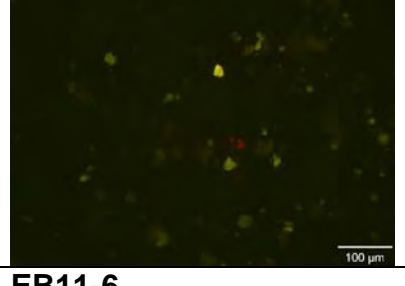
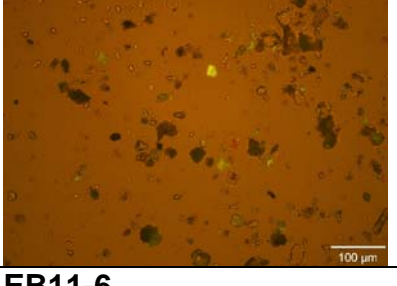
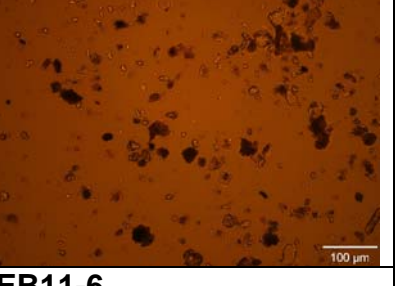
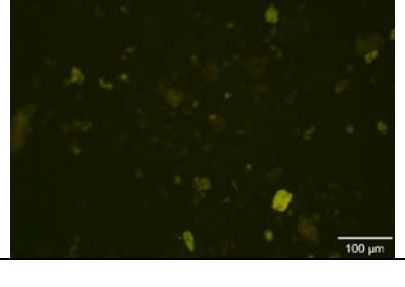
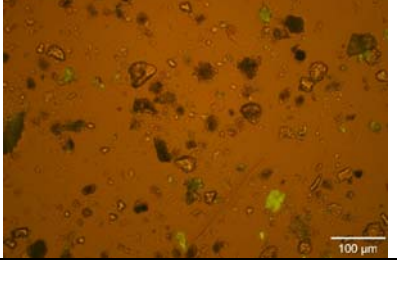
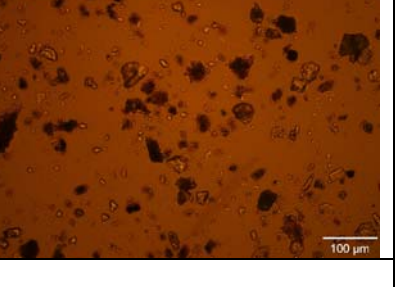
EB7-5 at 320x	EB7-5 at 320x	EB7-5 at 320x
		
EB7-6	EB7-6	EB7-6
		
EB7-6 at 320x	EB7-6 at 320x	EB7-6 at 320x
		
SEKR3775C702S072712D005 EB8-1 A	SEKR3775C702S072712D005 EB8-1 B	SEKR3775C702S072712D005 EB8-1 C
		
EB8-1 at 320x	EB8-1 at 320x	EB8-1 at 320x
		

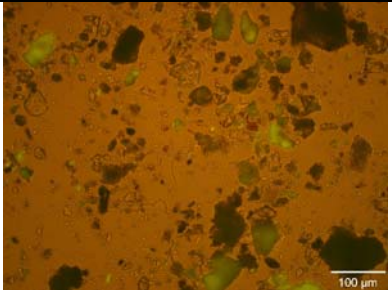
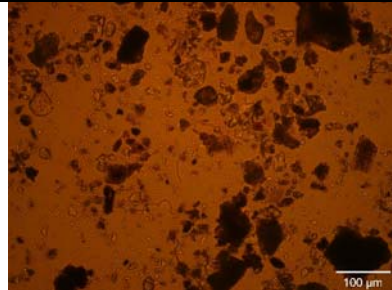
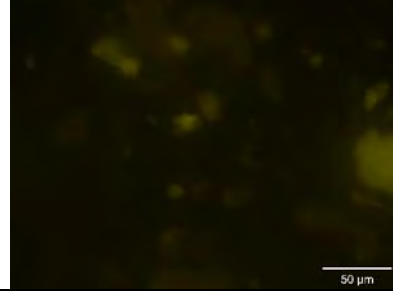
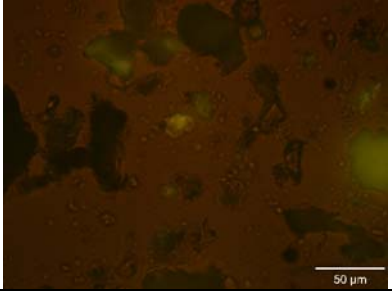
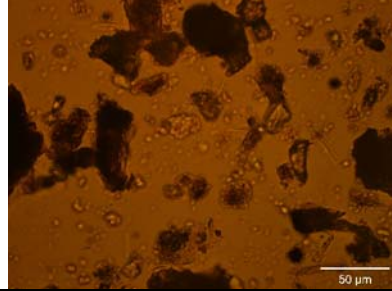
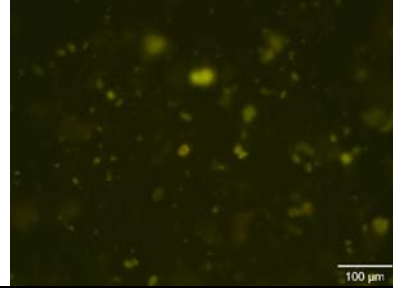
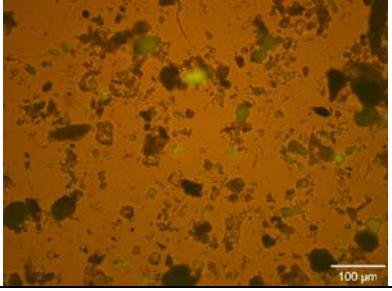
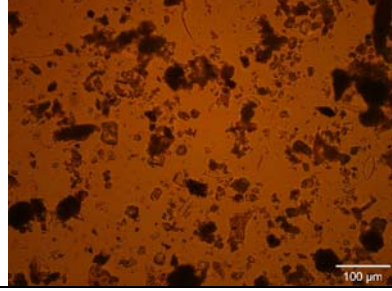
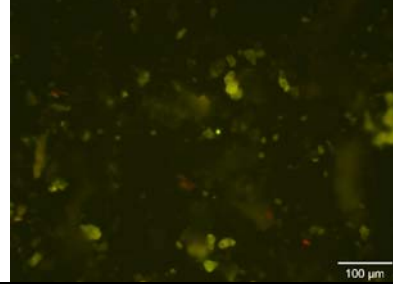
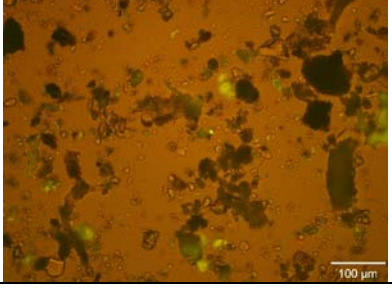
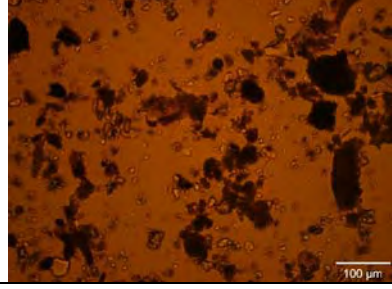
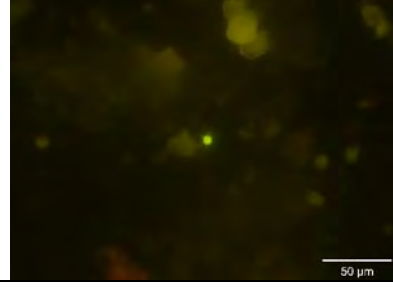
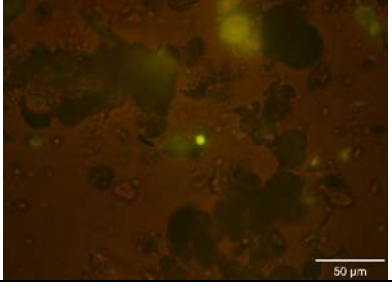
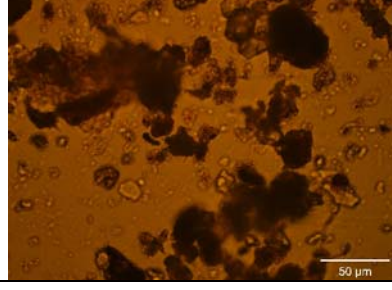
EB8-2 	EB8-2 	EB8-2 
EB8-3 	EB8-3 	EB8-3 
EB8-4 	EB8-4 	EB8-4 
EB8-5 	EB8-5 	EB8-5 
EB8-6 	EB8-6 	EB8-6 

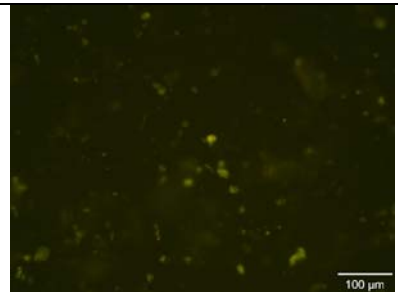
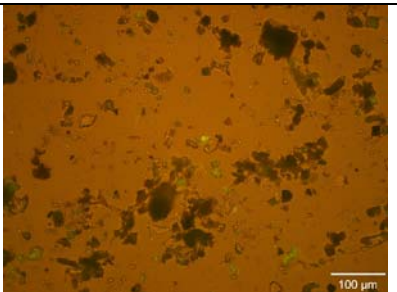
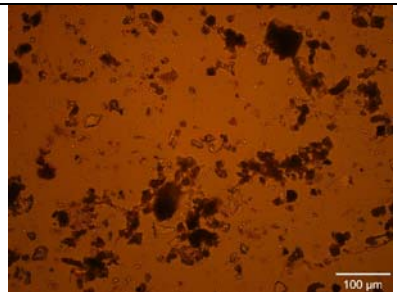
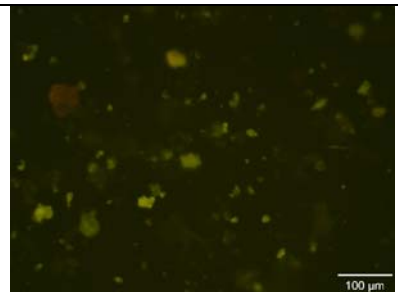
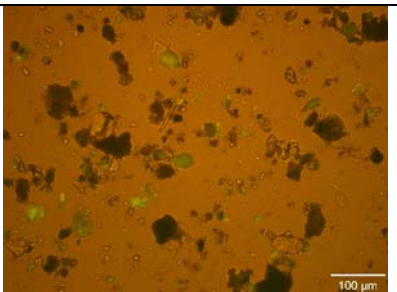
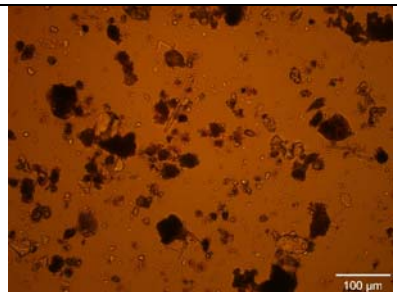
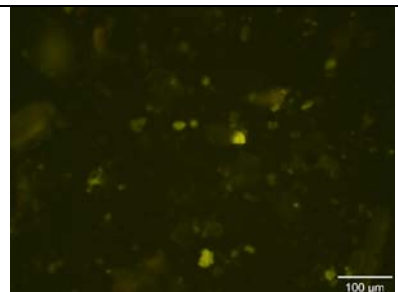
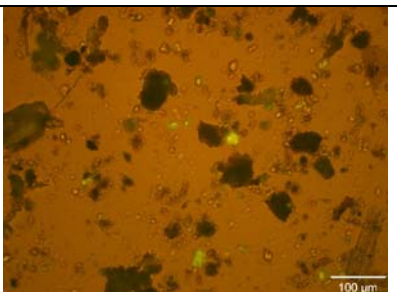
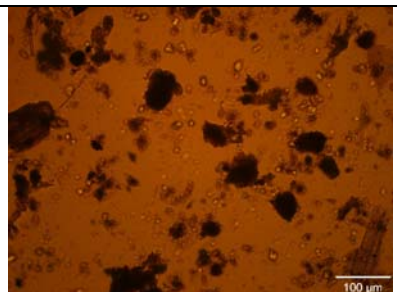
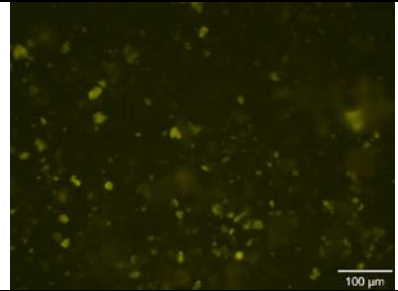
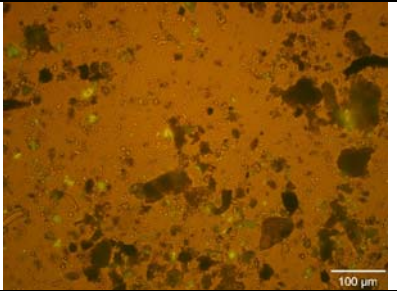
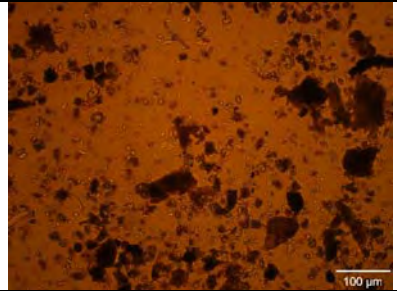
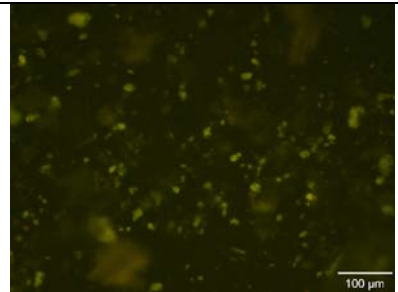
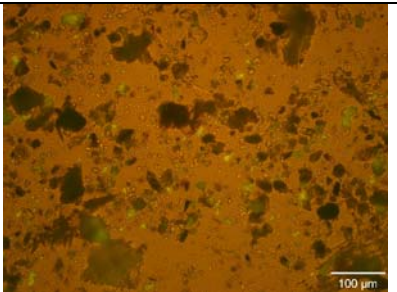
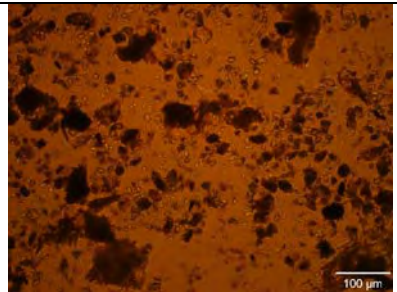
EB8-6 at 320x	EB8-6 at 320x	EB8-6 at 320x
		
SEKR1575C701S072612DX EB9-1 A	SEKR1575C701S072612DX EB9-1 B	SEKR1575C701S072612DX EB9-1 C
		
EB9-2	EB9-2	EB9-2
		
EB9-3	EB9-3	EB9-3
		
EB9-4	EB9-4	EB9-4
		

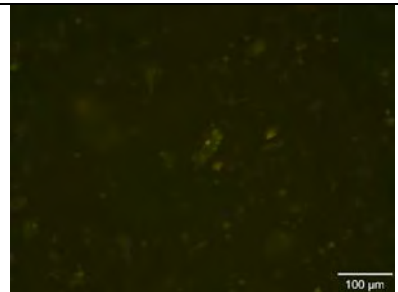
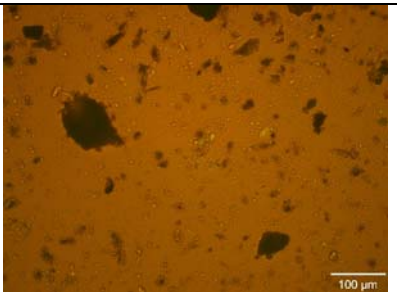
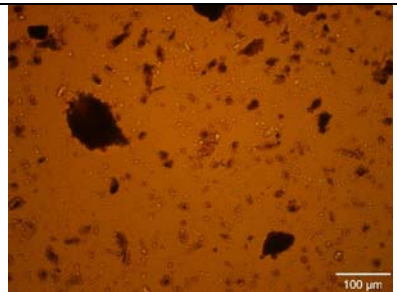
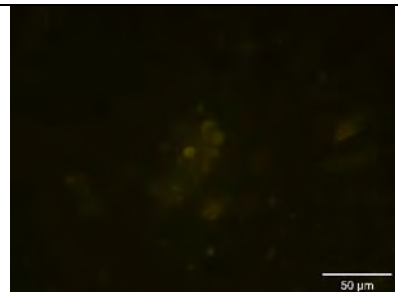
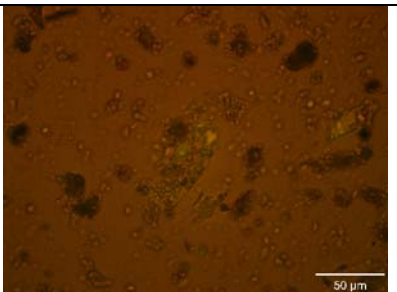
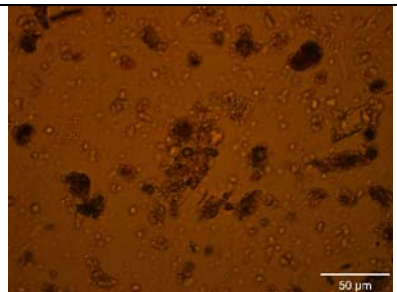
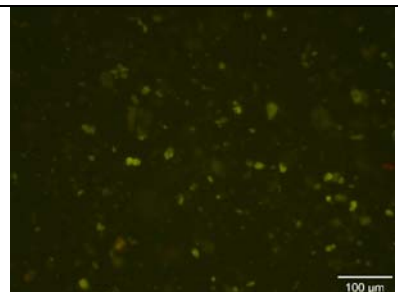
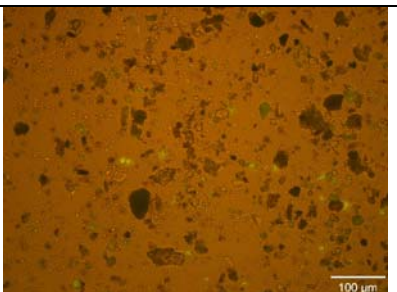
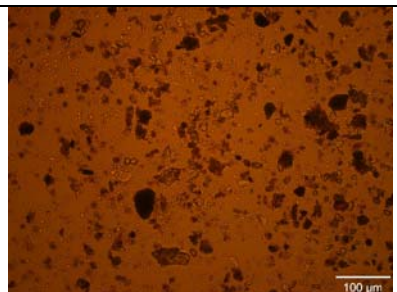
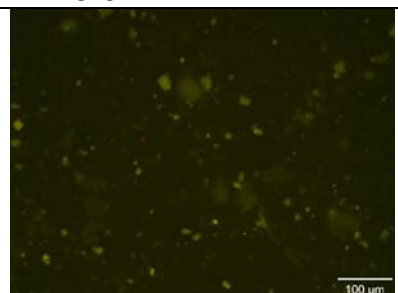
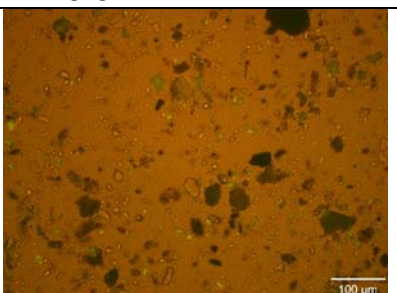
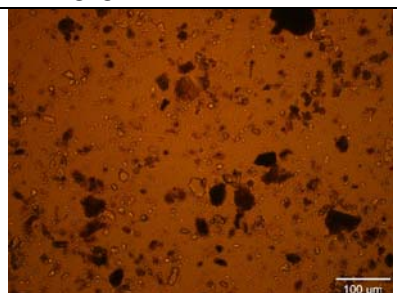
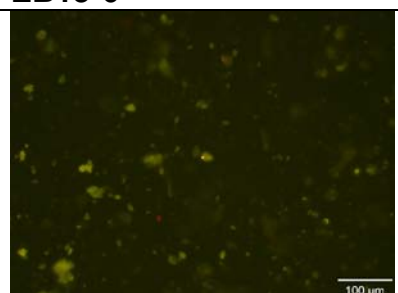
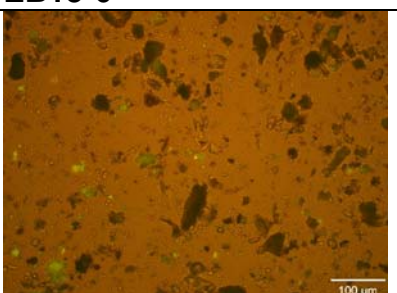
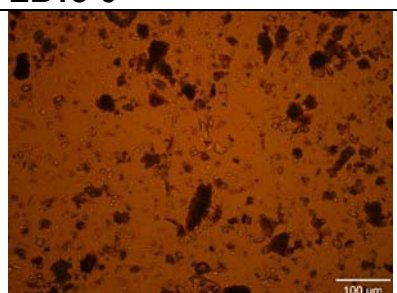
EB9-5 	EB9-5 	EB9-5 
EB9-6 	EB9-6 	EB9-6 
SEKR1575C702S072612DX EB10-1 A 	SEKR1575C702S072612DX EB10-1 B 	SEKR1575C702S072612DX EB10-1 C 
EB10-2 	EB10-2 	EB10-2 
EB10-3 	EB10-3 	EB10-3 

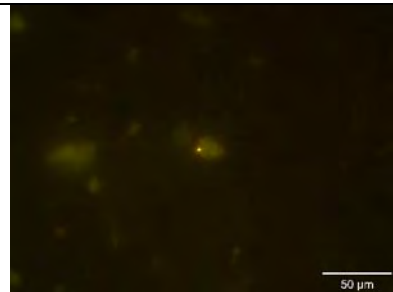
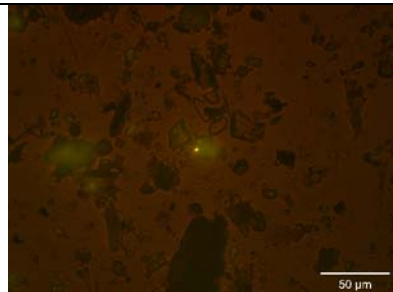
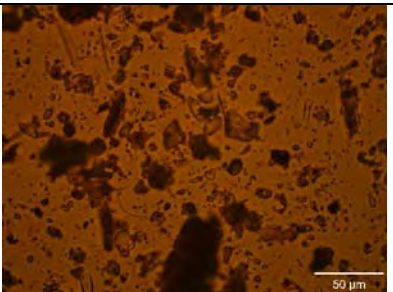
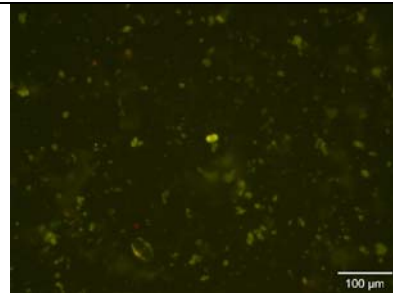
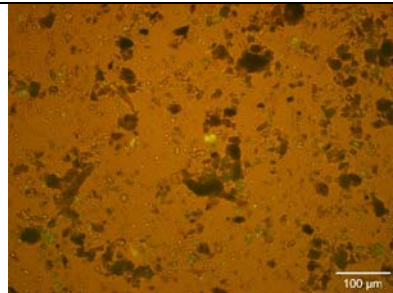
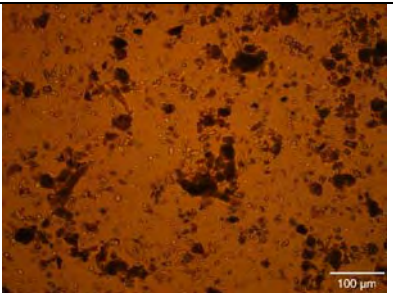
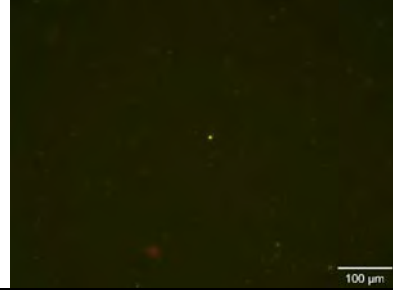
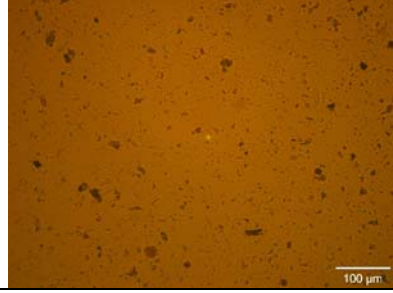
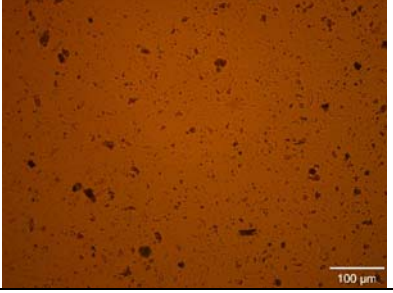
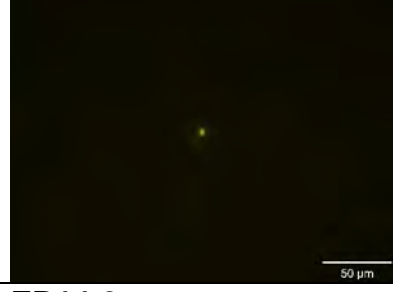
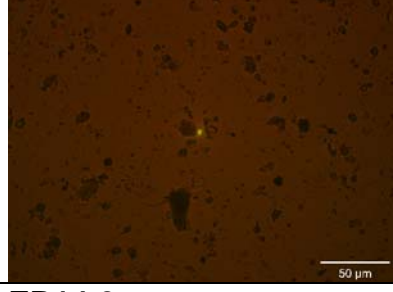
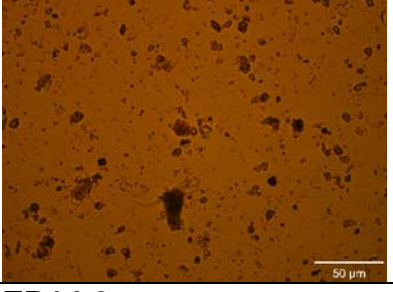
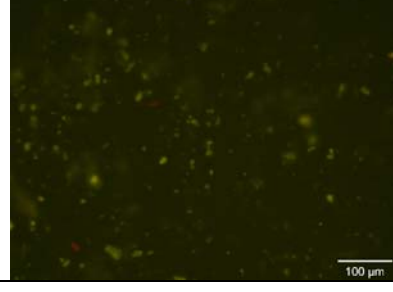
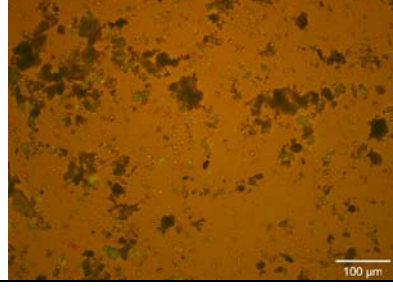
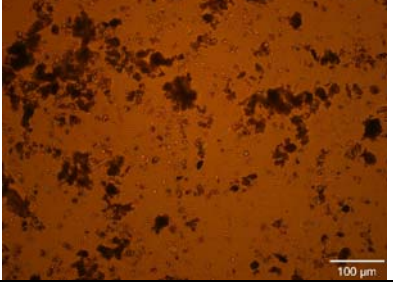
EB10-4 	EB10-4 	EB10-4 
EB10-5 	EB10-5 	EB10-5 
EB10-5 at 320x 	EB10-5 at 320x 	EB10-5 at 320x 
EB10-6 	EB10-6 	EB10-6 
SEKR3800C707S072712DX EB11-1 A	SEKR3800C707S072712DX EB11-1 B	SEKR3800C707S072712DX EB11-1 C
		

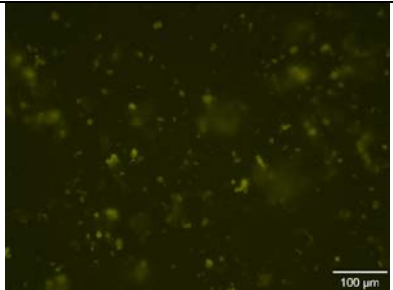
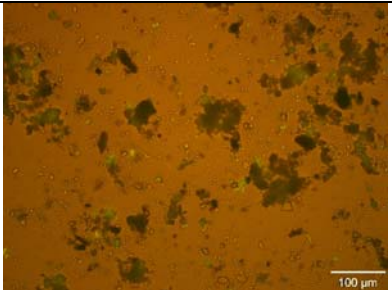
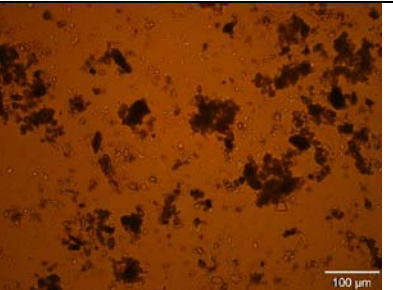
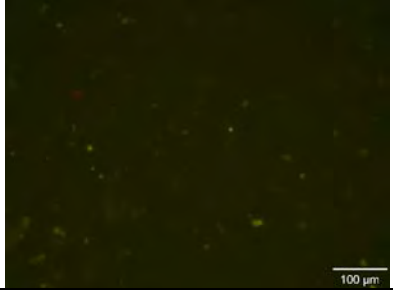
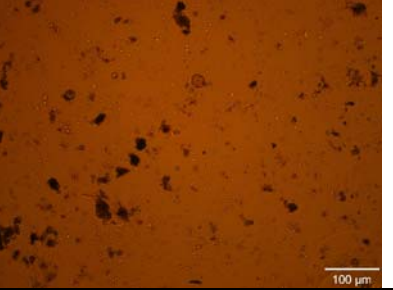
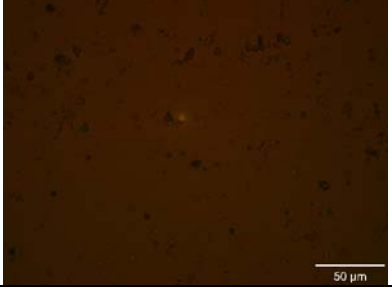
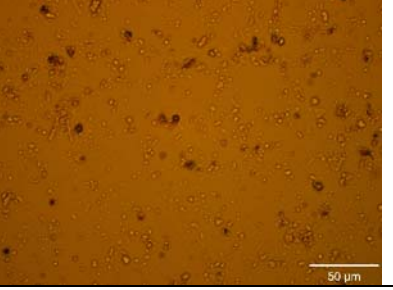
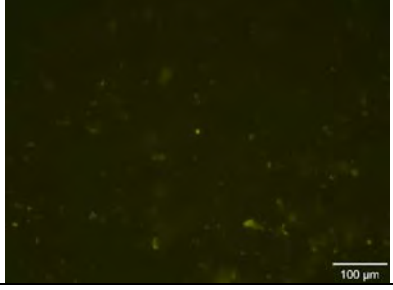
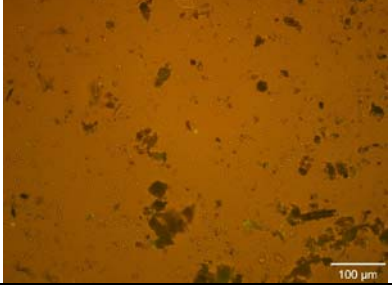
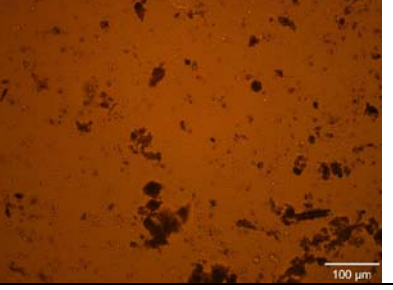
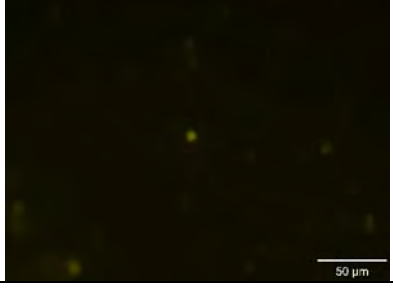
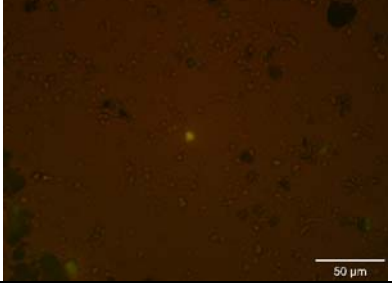
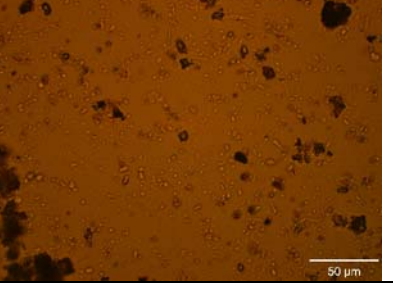
<p>EB11-2</p> 	<p>EB11-2</p> 	<p>EB11-2</p> 
<p>EB11-3</p> 	<p>EB11-3</p> 	<p>EB11-3</p> 
<p>EB11-4</p> 	<p>EB11-4</p> 	<p>EB11-4</p> 
<p>EB11-5</p> 	<p>EB11-5</p> 	<p>EB11-5</p> 
<p>EB11-6</p> 	<p>EB11-6</p> 	<p>EB11-6</p> 

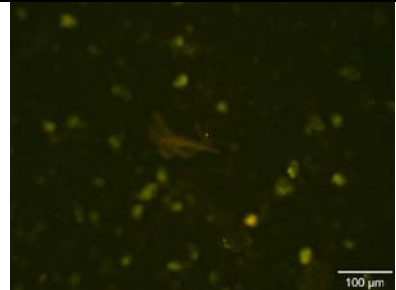
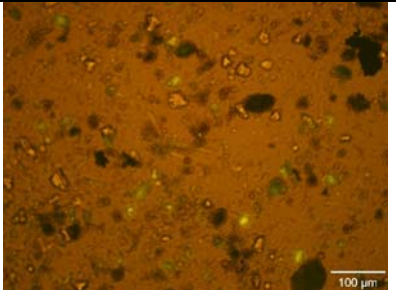
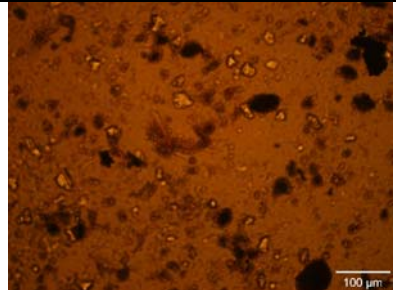
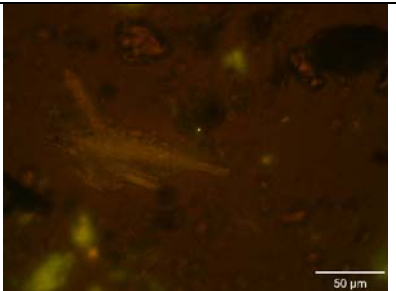
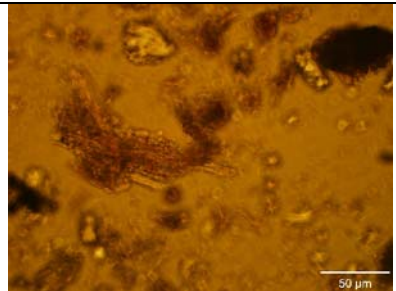
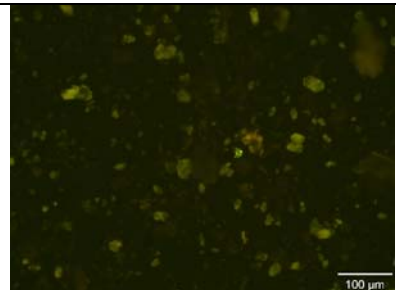
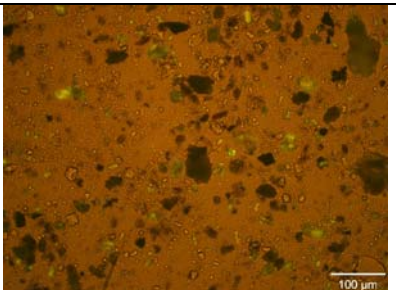
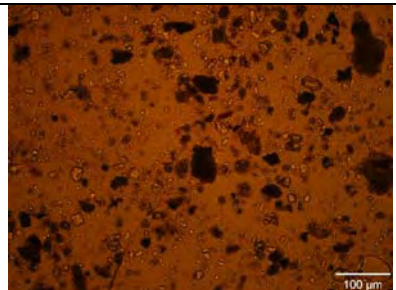
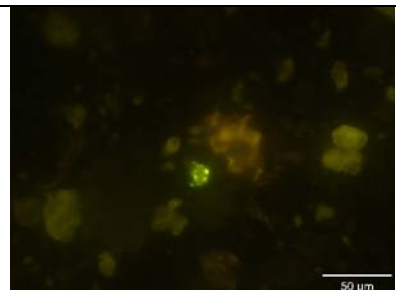
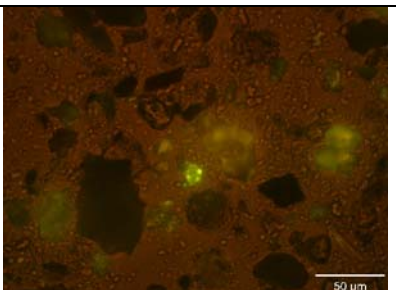
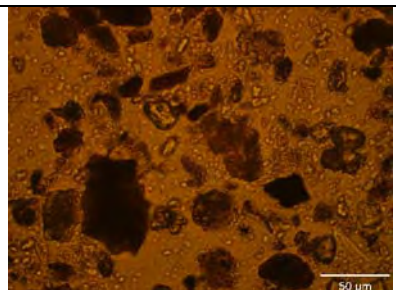
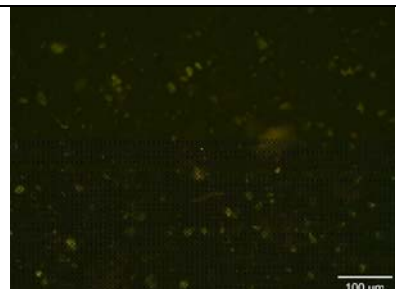
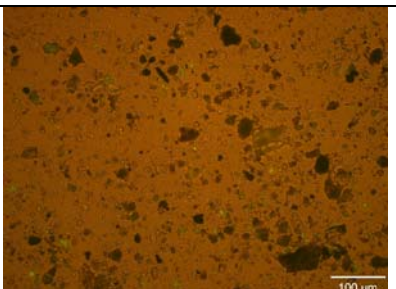
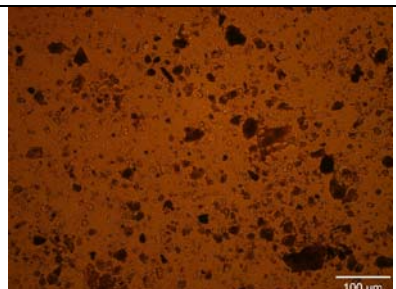
SEKR3800C707S072712D004 EB12-1 A	SEKR3800C707S072712D004 EB12-1 B	SEKR3800C707S072712D004 EB12-1 C
		
EB12-1 at 320x	EB12-1 at 320x	EB12-1 at 320x
		
EB12-2	EB12-2	EB12-2
		
EB12-3	EB12-3	EB12-3
		
EB12-3 at 320x	EB12-3 at 320x	EB12-3 at 320x
		

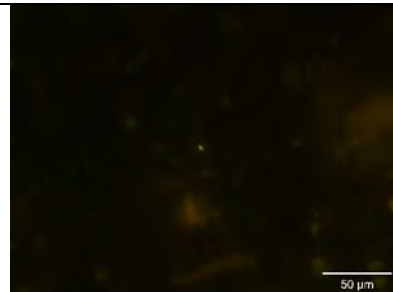
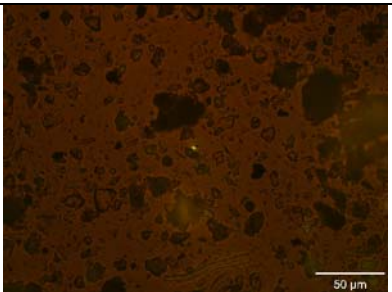
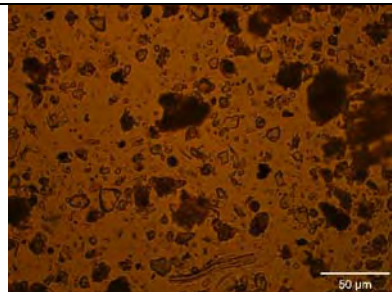
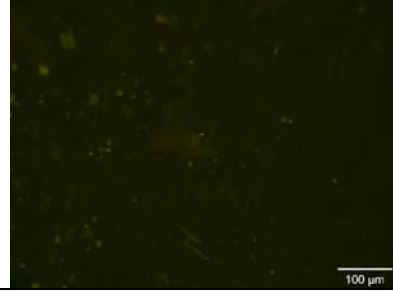
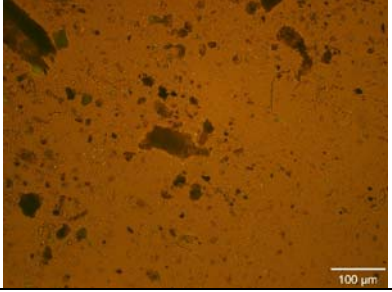
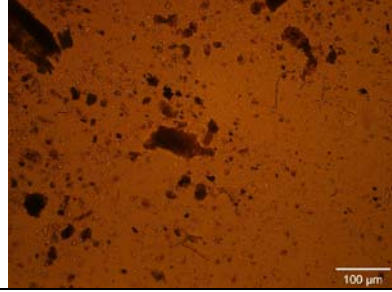
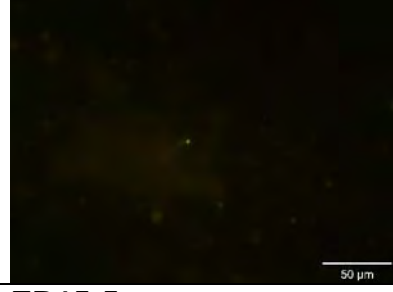
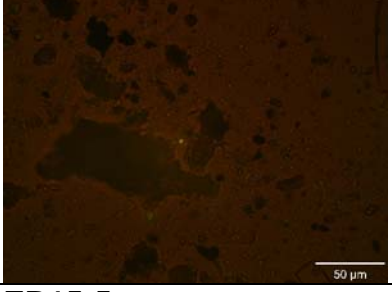
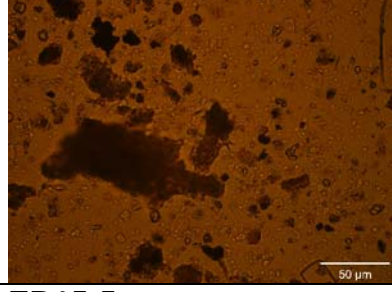
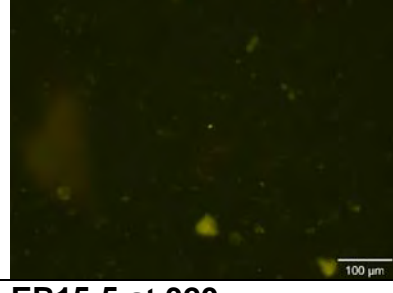
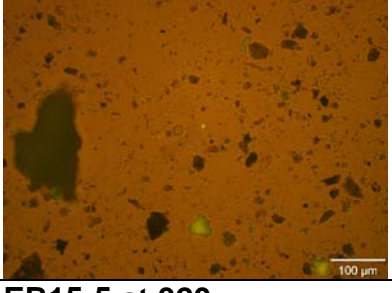
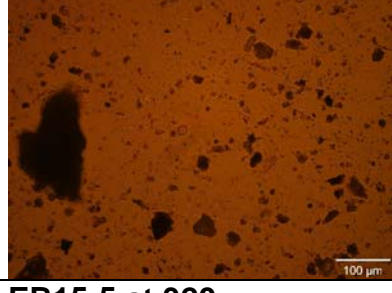
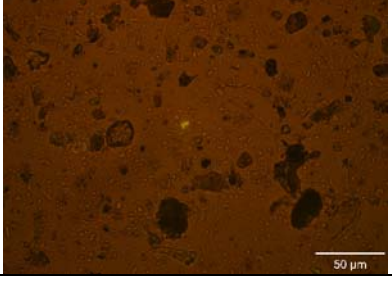
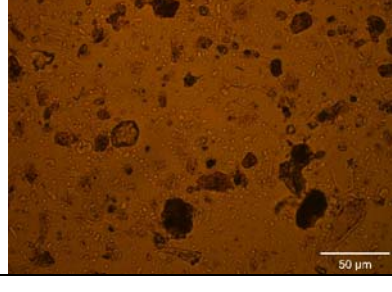
EB12-4	EB12-4	EB12-4
		
EB12-5	EB12-5	EB12-5
		
EB12-6	EB12-6	EB12-6
		
SEKR3800C709S072712DX EB13-1 A	E SEKR3800C709S072712DX EB13-1 B	SEKR3800C709S072712DX EB13-1 C
		
EB13-2	EB13-2	EB13-2
		

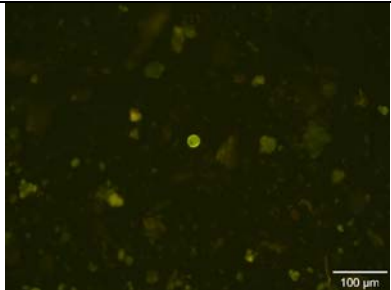
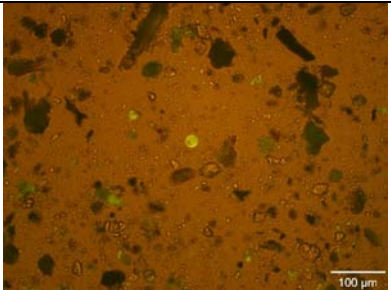
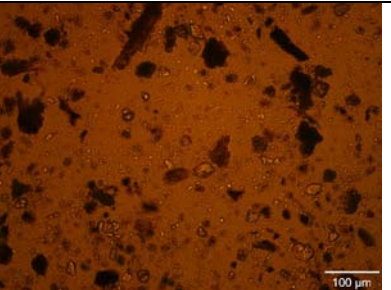
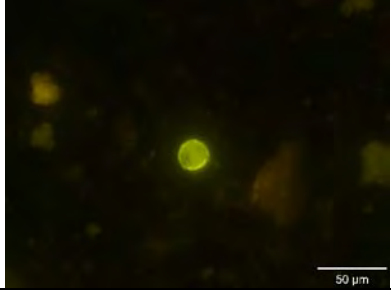
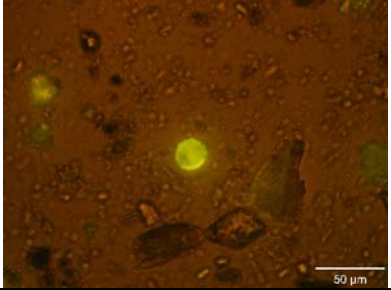
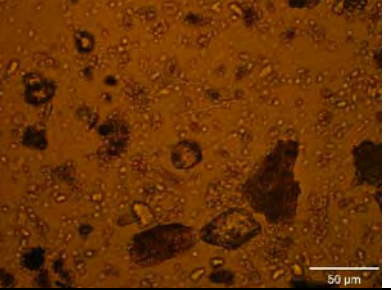
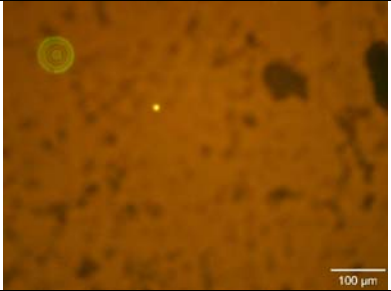
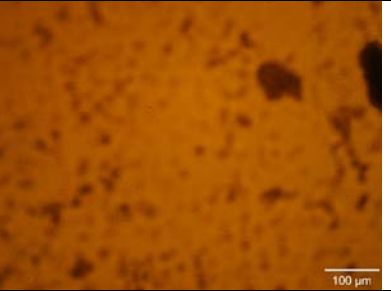
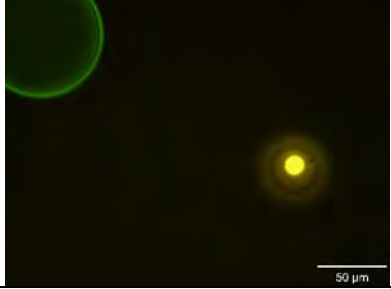
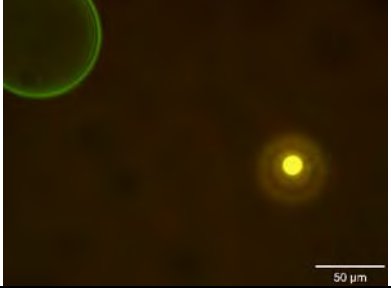
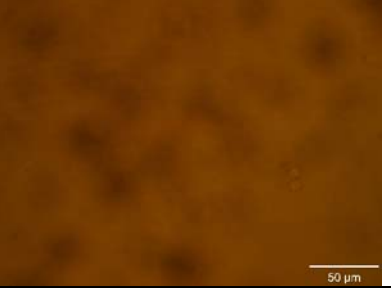
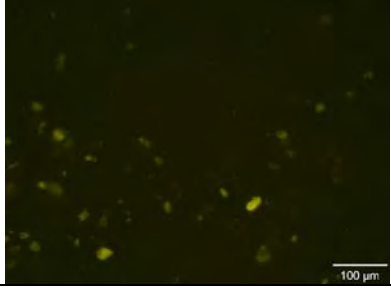
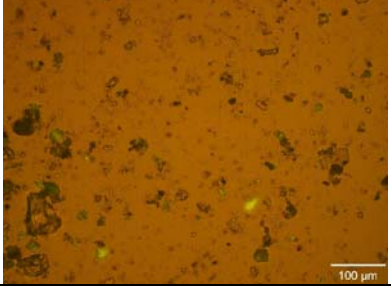
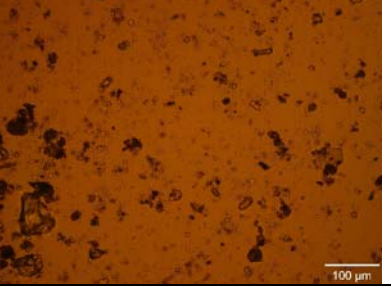
EB13-3 	EB13-3 	EB13-3 
EB13-3 x320 	EB13-3 	EB13-3 
EB13-4 	EB13-4 	EB13-4 
EB13-5 	EB13-5 	EB13-5 
EB13-6 	EB13-6 	EB13-6 

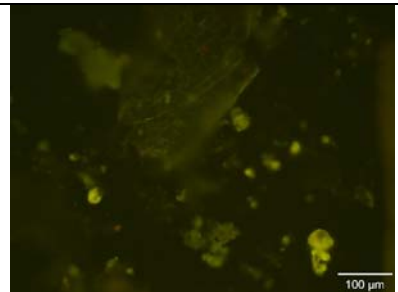
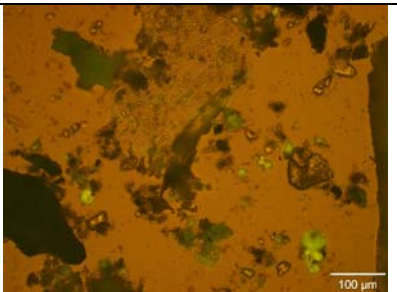
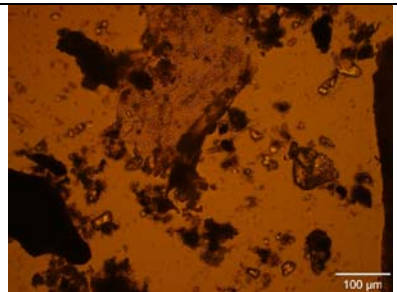
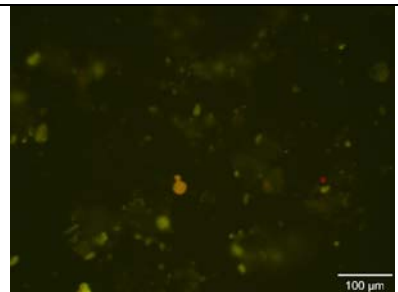
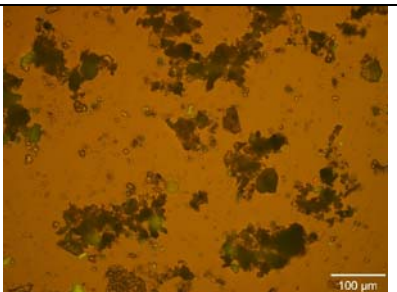
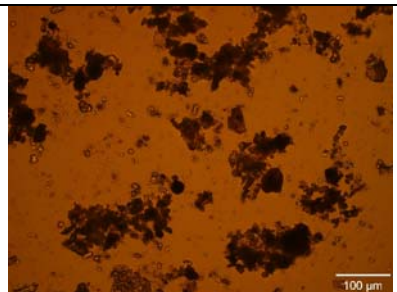
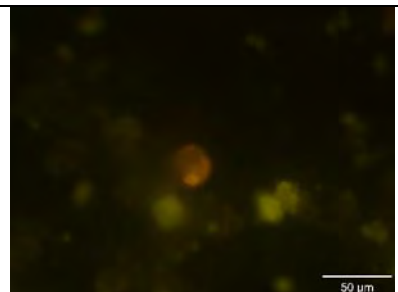
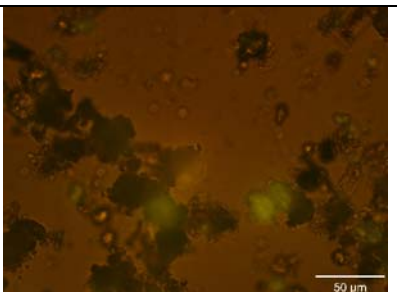
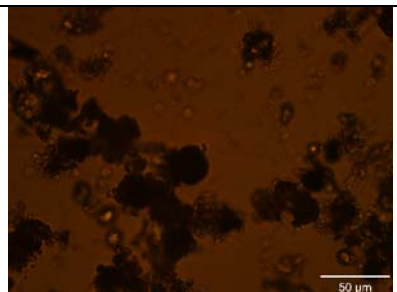
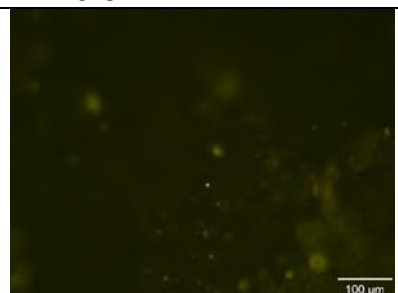
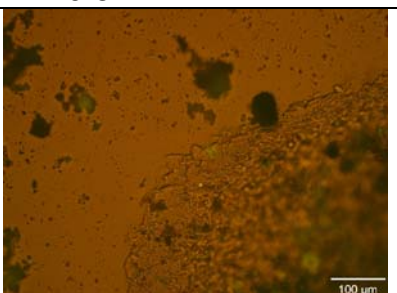
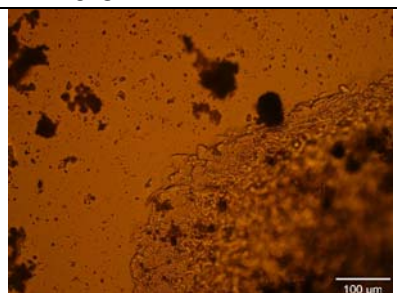
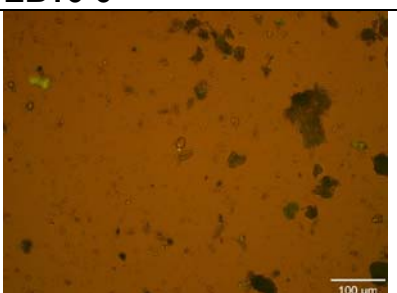
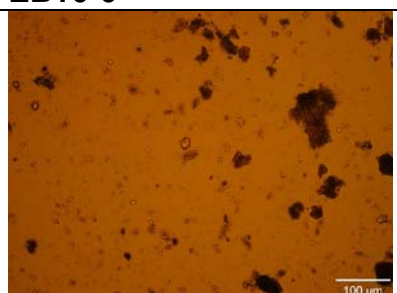
EB13-6 at 320x	EB13-6 at 320x	EB13-6 at 320x
		
SEKR1575C702S072612D005 EB14-1 A	SEKR1575C702S072612D005 EB14-1 B	SEKR1575C702S072612D005 EB14-1 C
		
EB14-2	EB14-2	EB14-2
		
EB14-2 at 320x	EB14 at 320x	EB14 at 320x
		
EB14-3	EB14-3	EB14-3
		

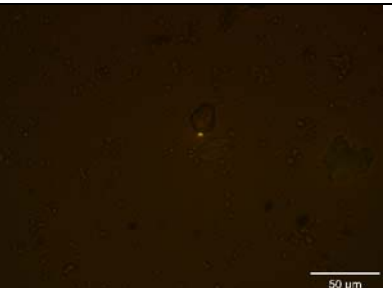
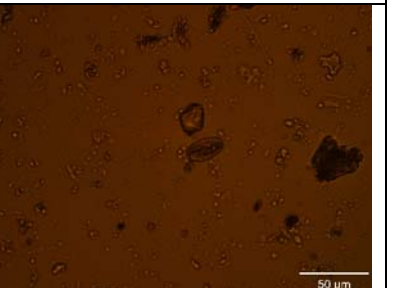
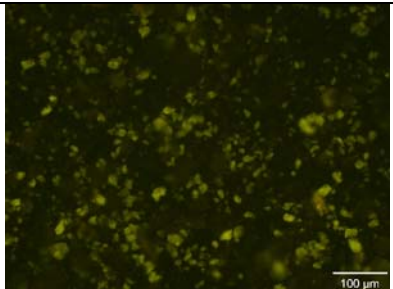
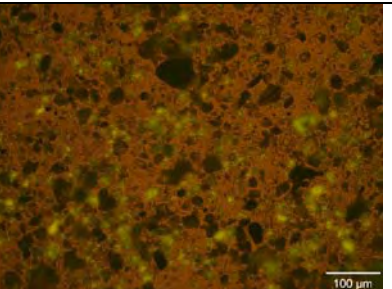
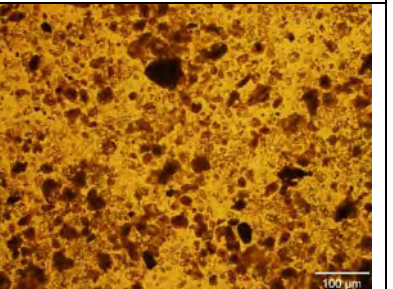
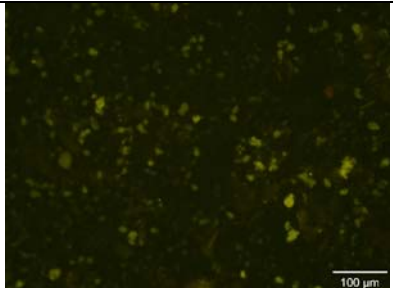
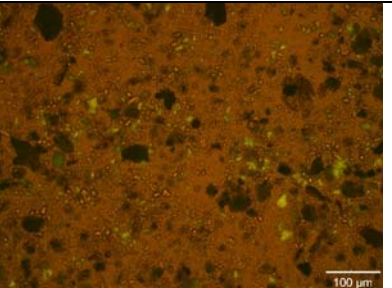
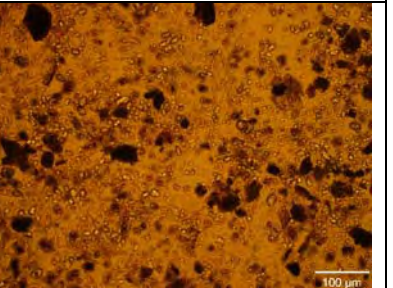
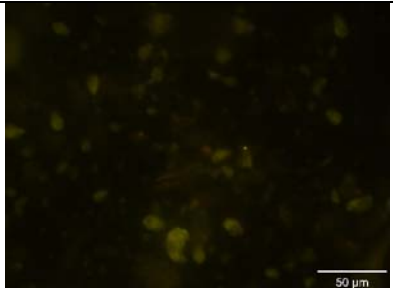
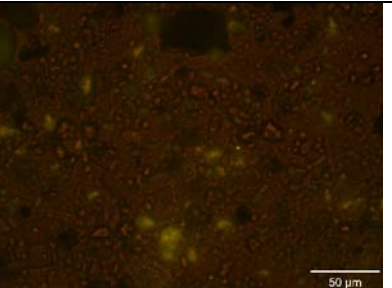
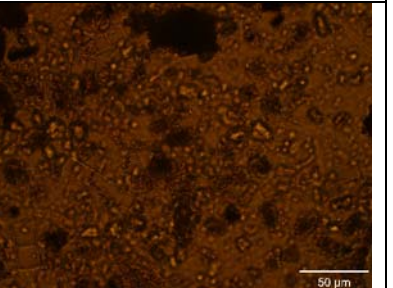
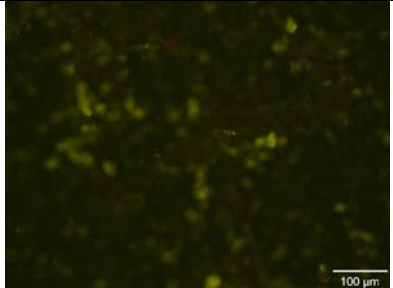
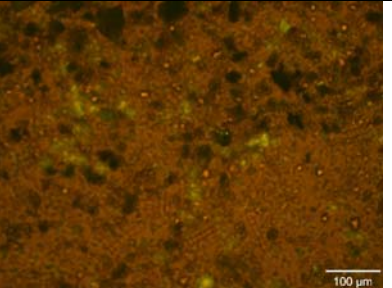
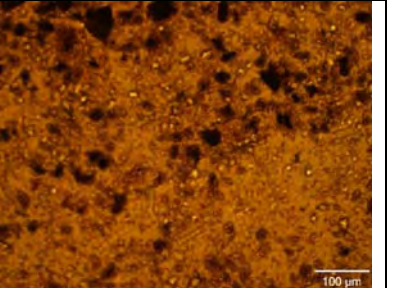
EB14-4 	EB14-4 	EB14-4 
EB14-5 	EB14-5 	EB14-5 
EB14-5 at 320x 	EB14-5 at 320x 	EB14-5 at 320x 
EB14-6 	EB14-6 	EB14-6 
EB14-6 at 320x 	EB14-6 at 320x 	EB14-6 at 320x 

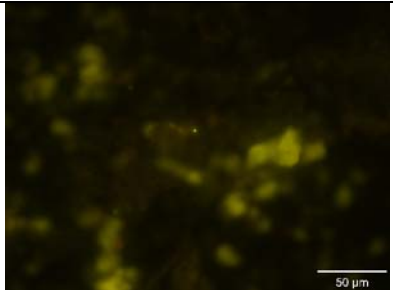
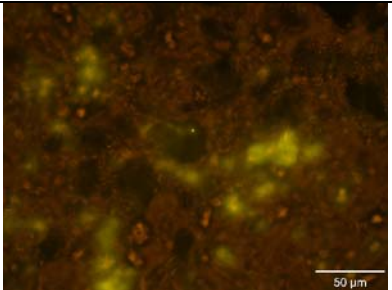
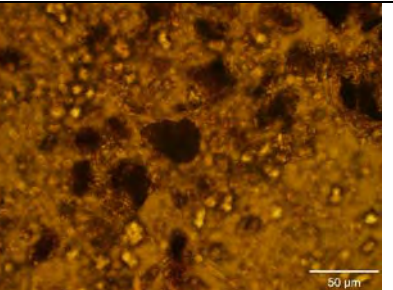
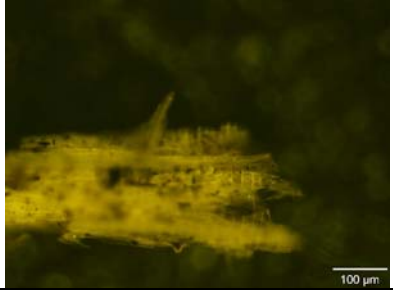
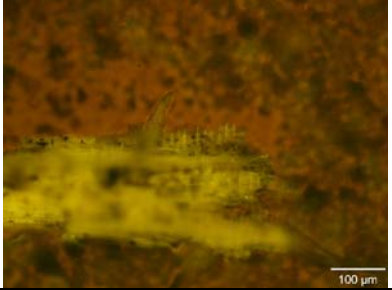
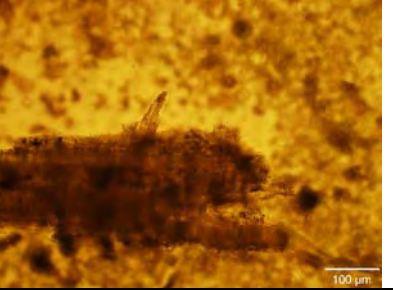
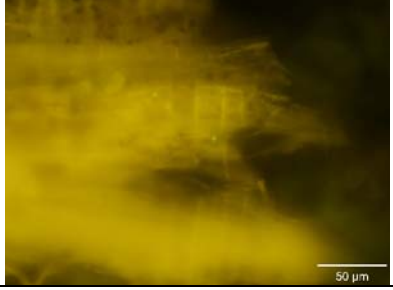
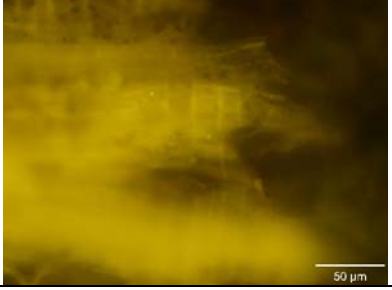
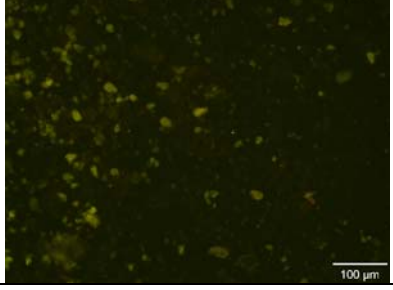
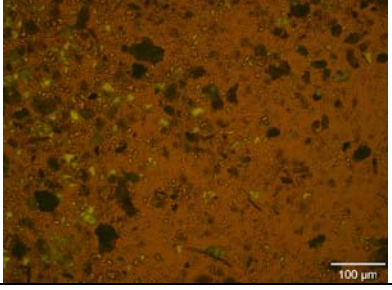
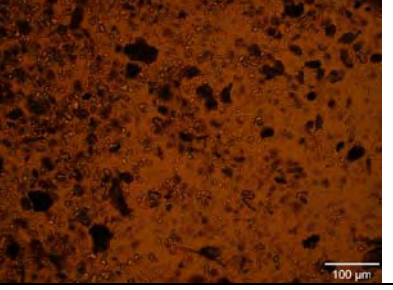
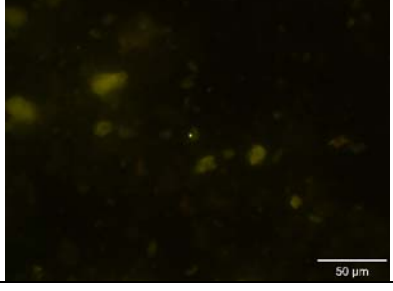
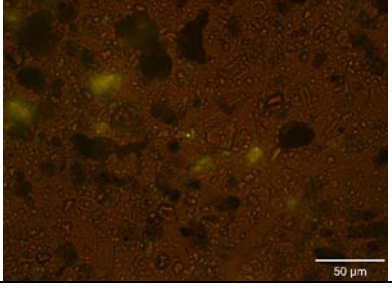
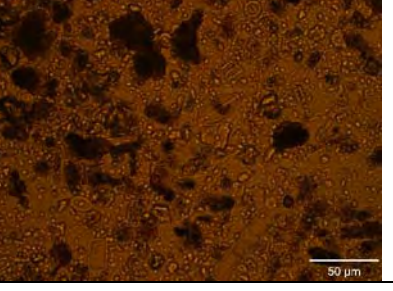
SEKR1575C701S072612D013 EB15-1 A	SEKR1575C701S072612D013 EB15-1 B	SEKR1575C701S072612D013 EB15-1 C
		
EB15-1 at 320x	EB15-1 at 320x	EB15-1 at 320x
		
EB15-2	EB15-2	EB15-2
		
EB15-2 at 320x	EB15-2 at 320x	EB15-2 at 320x
		
EB15-3	EB15-3	EB15-3
		

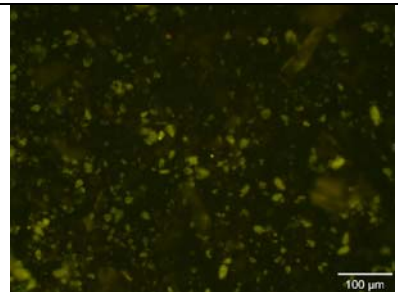
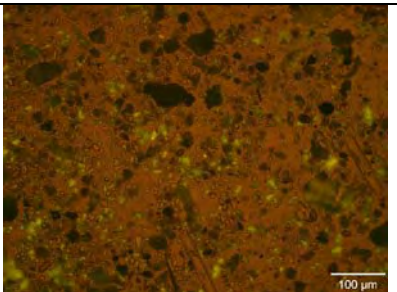
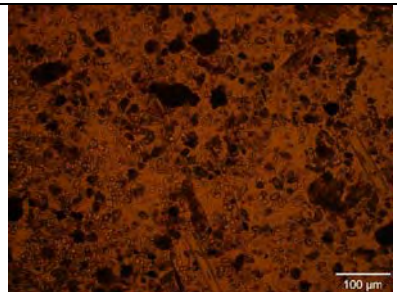
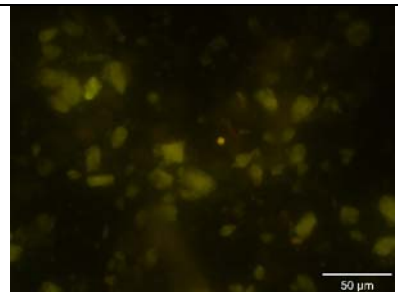
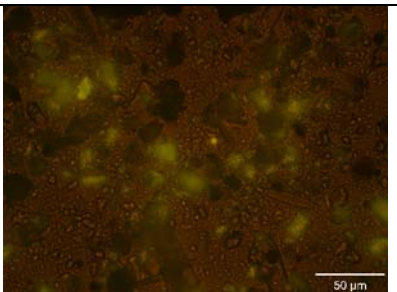
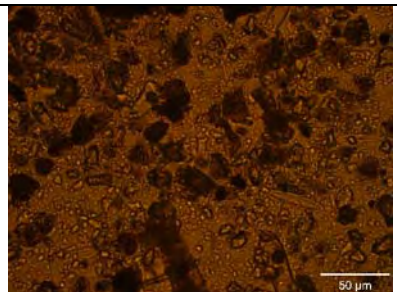
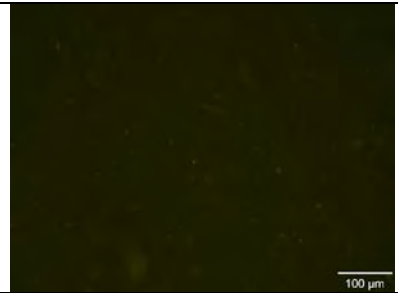
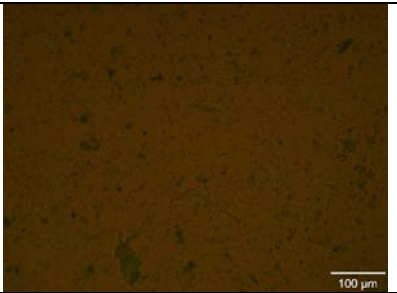
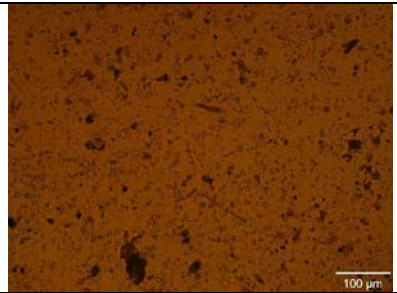
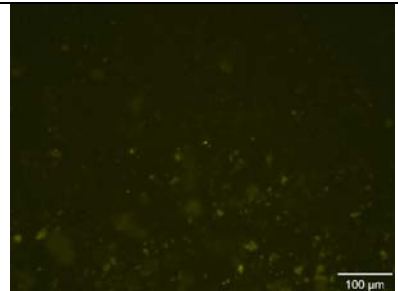
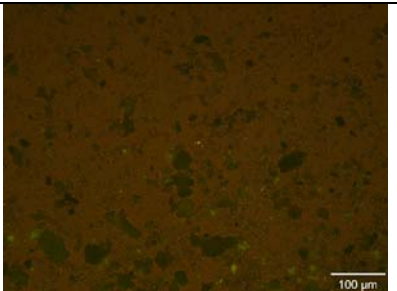
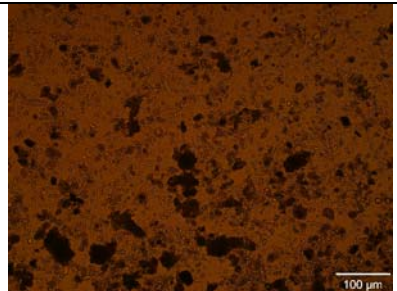
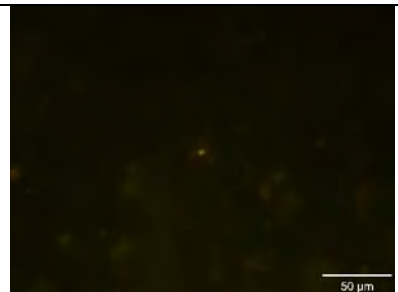
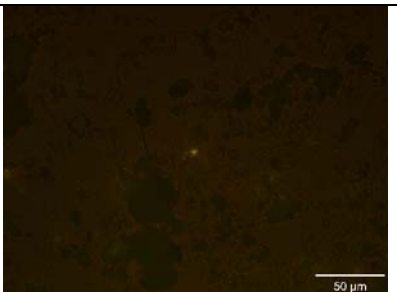
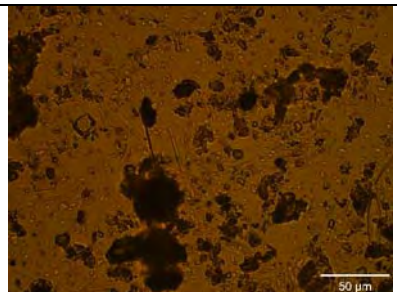
EB15-3 at 320x	EB15-3 at 320x	EB15-3 at 320x
		
EB15-4	EB15-4	EB15-4
		
EB15-4 at 320x	EB15-4 at 320x	EB15-4 at 320x
		
EB15-5	EB15-5	EB15-5
		
EB15-5 at 320x	EB15-5 at 320x	EB15-5 at 320x
		

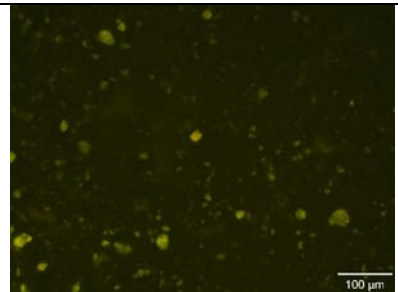
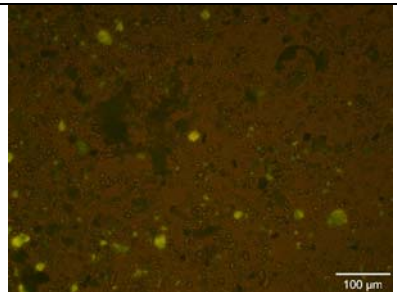
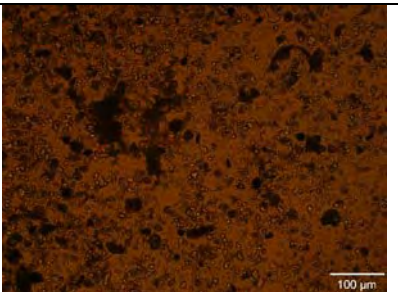
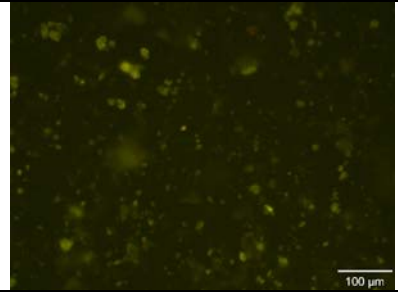
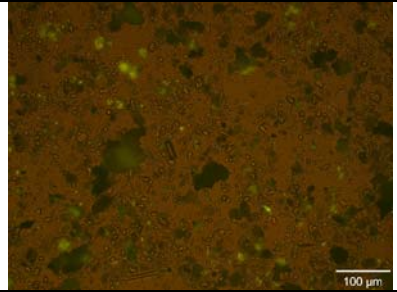
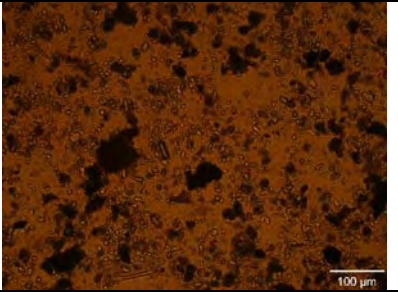
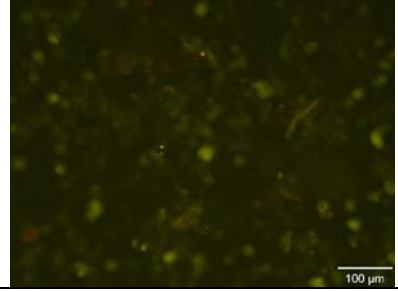
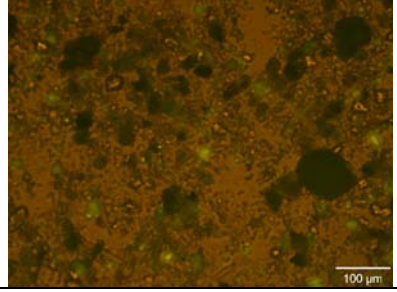
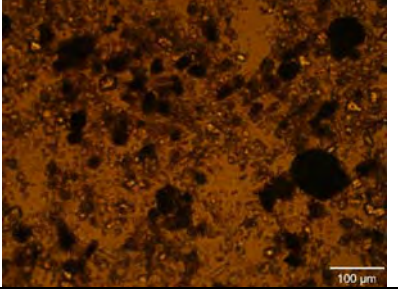
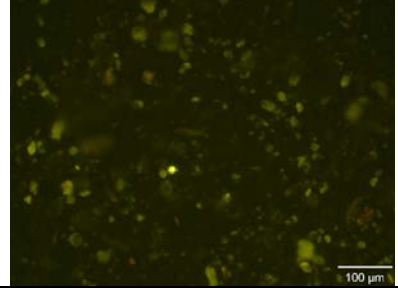
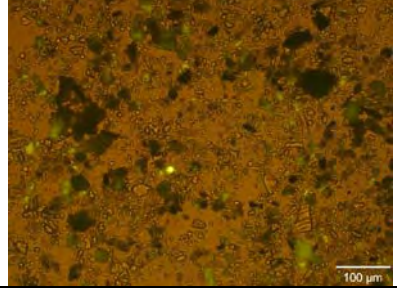
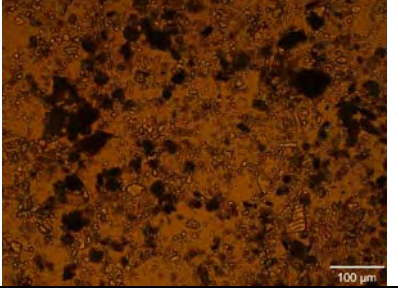
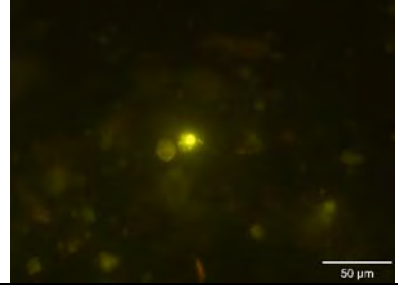
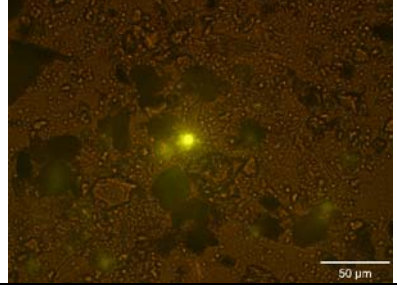
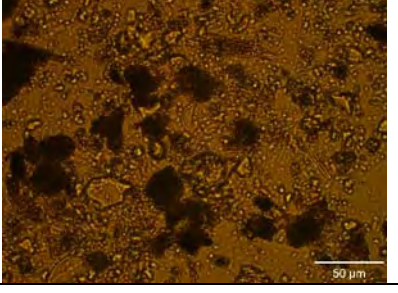
EB15-6 	EB15-6 	EB15-6 
EB15-6 at 320x 	EB15-6 at 320x 	EB15-6 at 320x 
SEKR1575C701S072612D007 EB16-1 A	SEKR1575C701S072612D007 EB16-1 B	SEKR1575C701S072612D007 EB16-1 C
		
EB16-1 at 320x 	EB16-1 at 320x 	EB16-1 at 320x 
EB16-2 	EB16-2 	EB16-2 

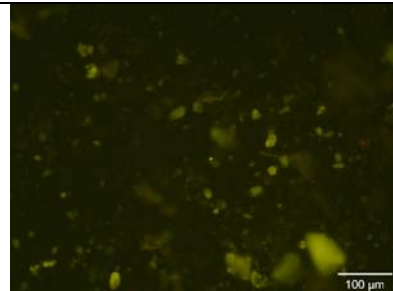
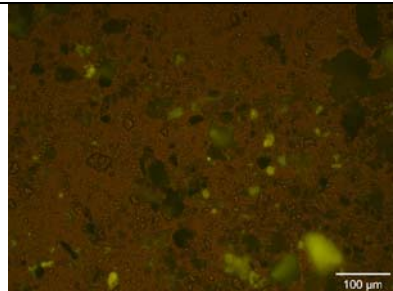
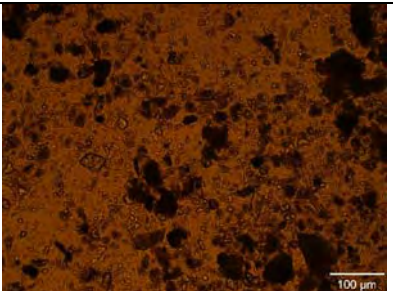
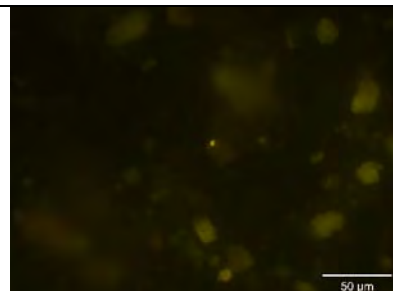
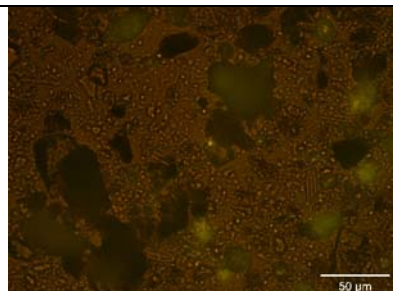
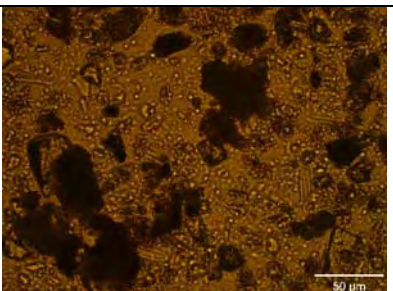
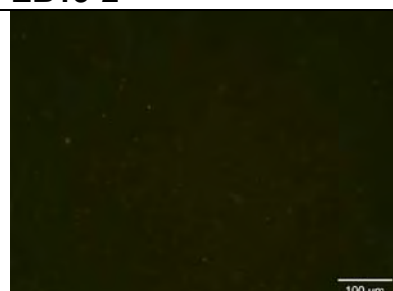
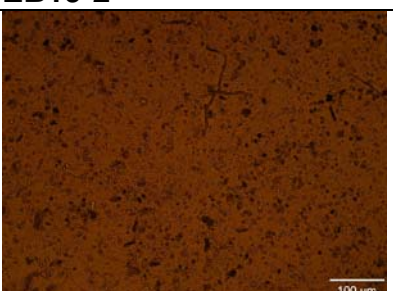
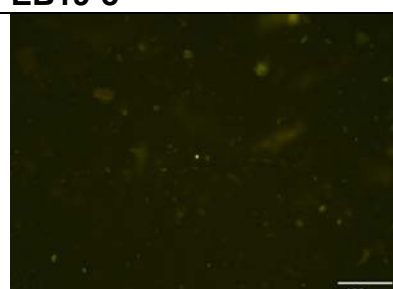
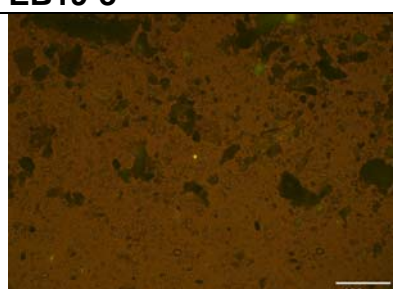
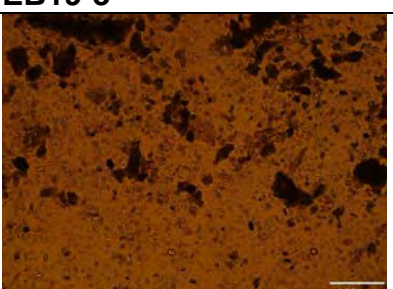
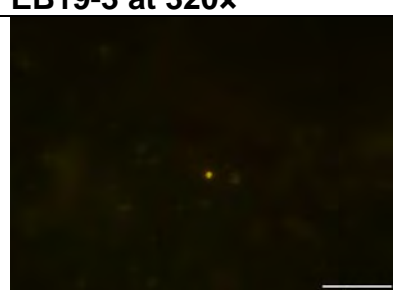
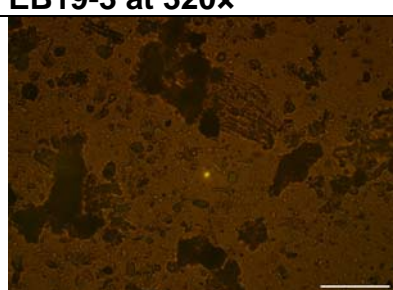
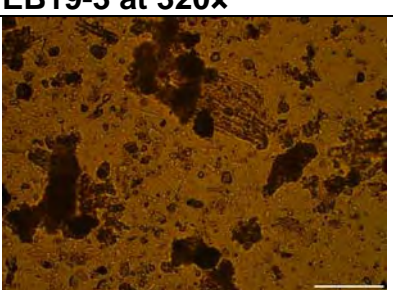
EB16-3 	EB16-3 	EB16-3 
EB16-4 	EB16-4 	EB16-4 
EB16-4 at 320x 	EB16-4 at 320x 	EB16-4 at 320x 
EB16-5 	EB16-5 	EB16-5 
EB16-6 	EB16-6 	EB16-6 

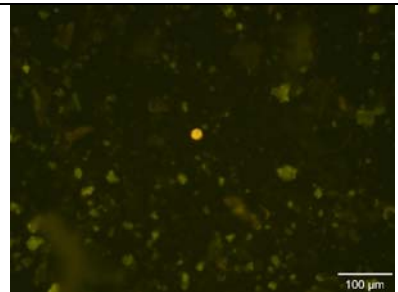
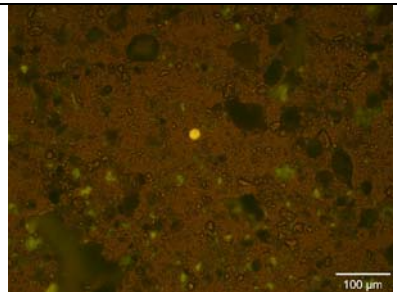
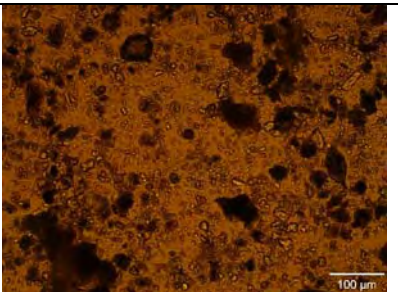
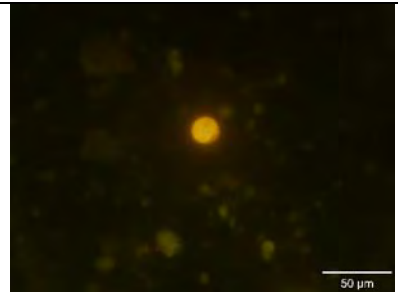
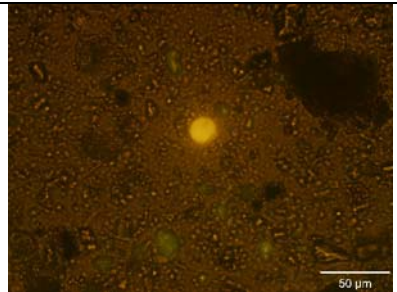
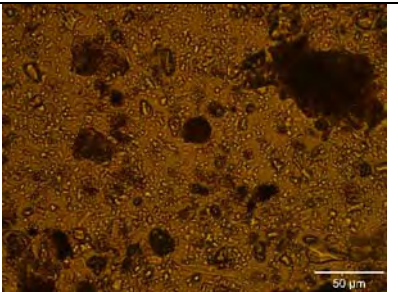
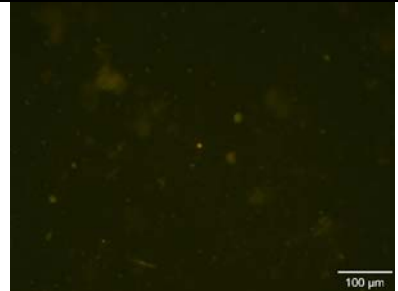
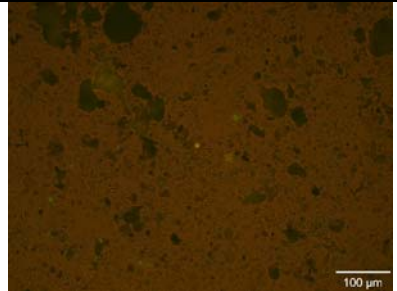
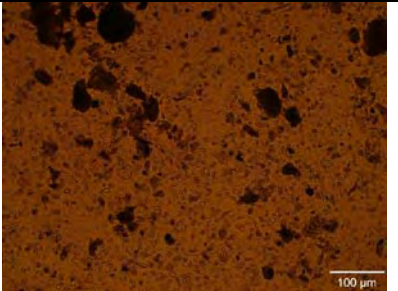
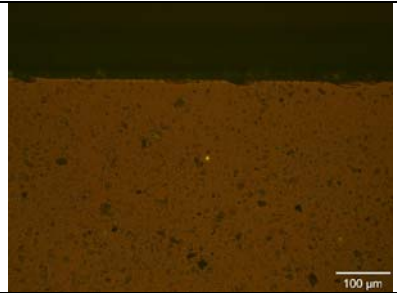
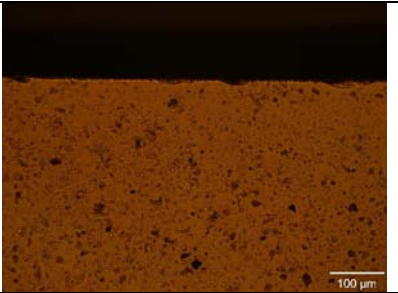
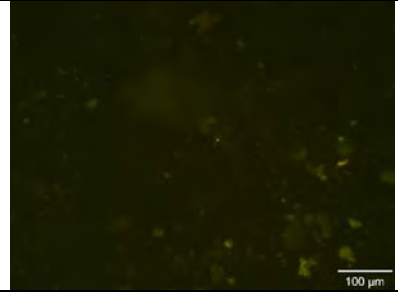
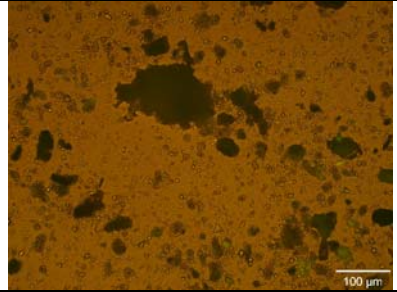
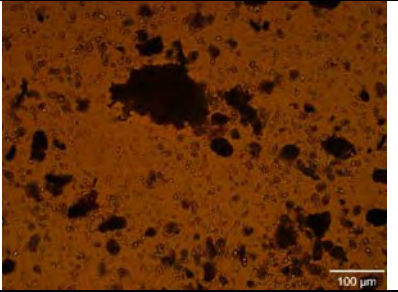
EB16-6 at 320x	EB16-6 at 320x	EB16-6 at 320x
		
SEKR3950C701S072612D007 EB17-1 A	SEKR3950C701S072612D007 EB17-1 B	SEKR3950C701S072612D007 EB17-1 C
		
EB17-2	EB17-2	EB17-2
		
EB17-2 at 320x	EB17-2 at 320x	EB17-2 at 320x
		
EB17-3	EB17-3	EB17-3
		

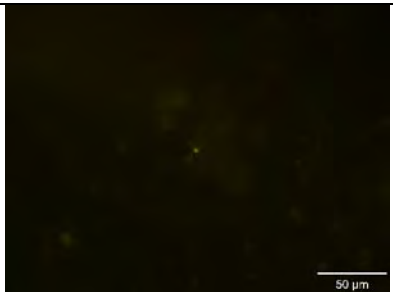
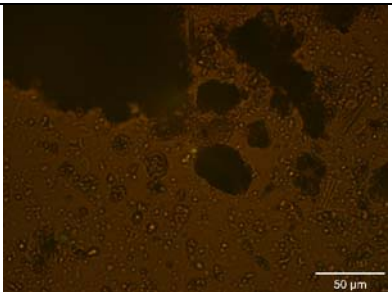
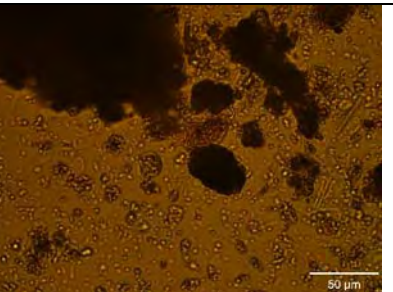
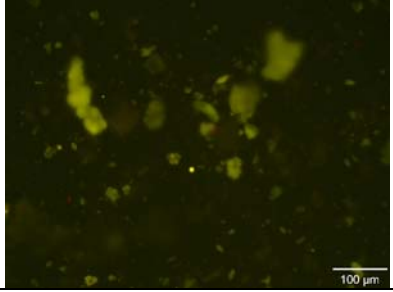
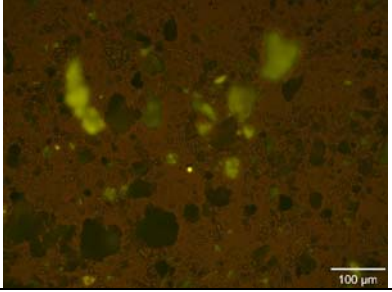
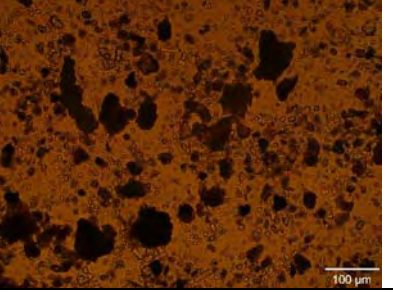
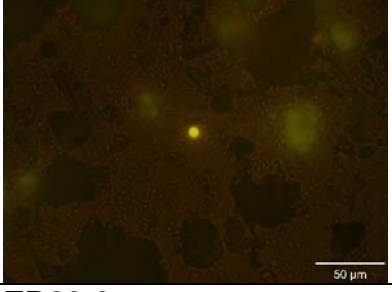
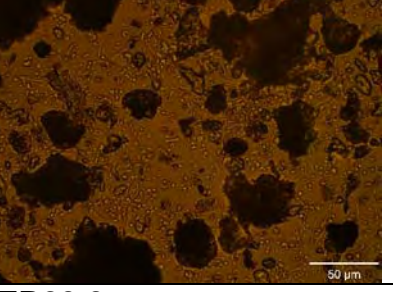
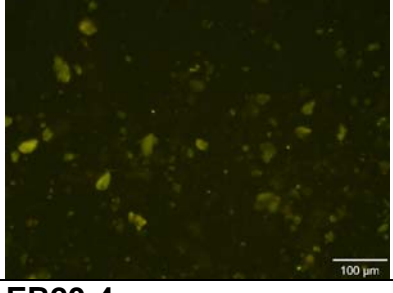
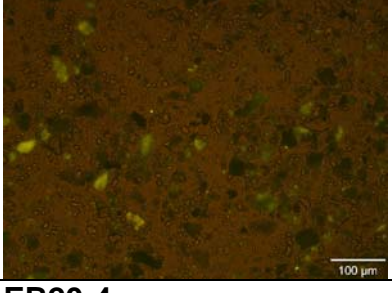
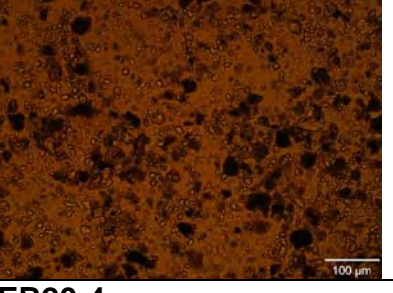
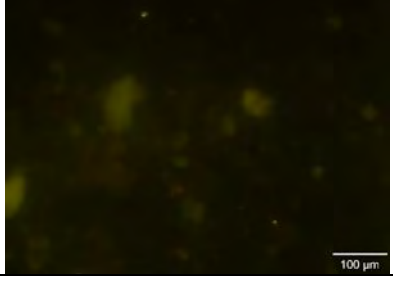
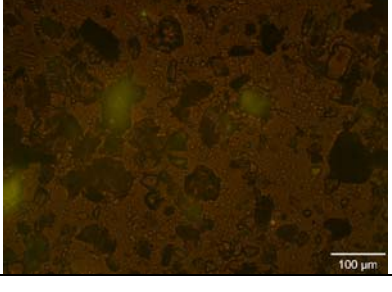
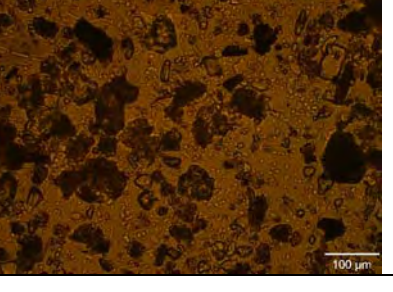
EB17-3 at 320x	EB17-3 at 320x	EB17-3 at 320x
		
EB17-4	EB17-4	EB17-4
		
EB17-4 at 320x	EB17-4 at 320x	EB17-4 at 320x
		
EB17-5	EB17-5	EB17-5
		
EB17-5 at 320x	EB17-5 at 320x	EB17-5 at 320x
		

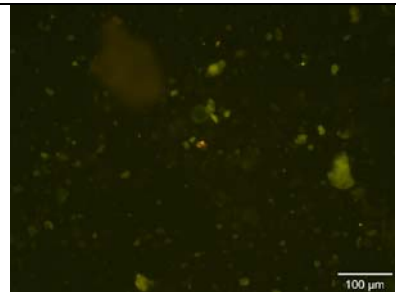
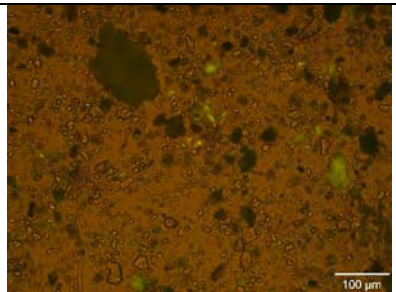
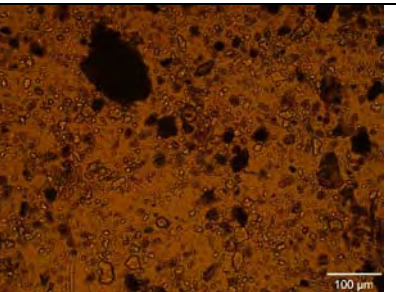
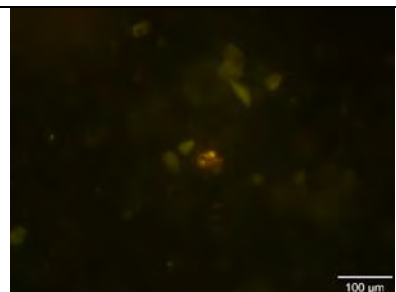
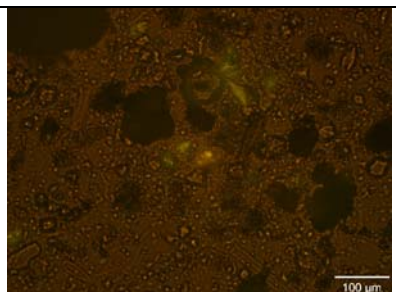
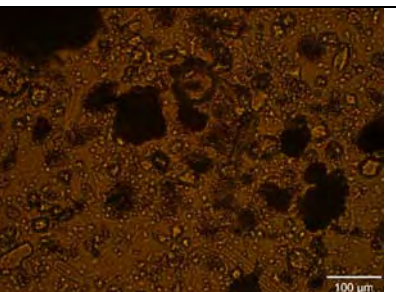
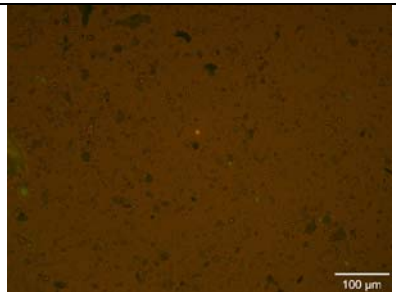
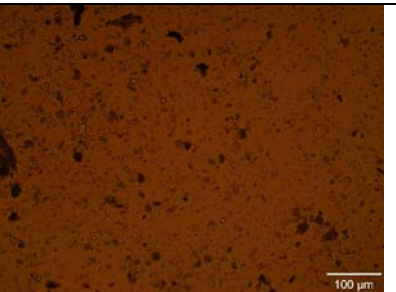
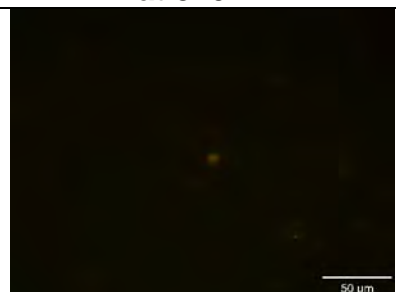
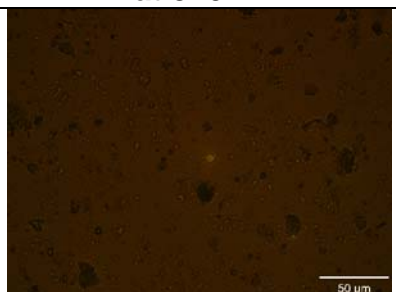
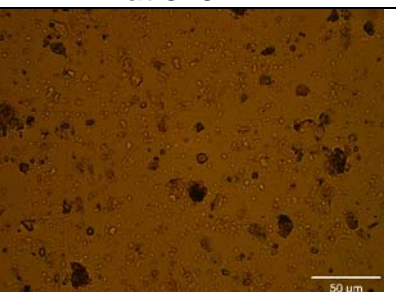
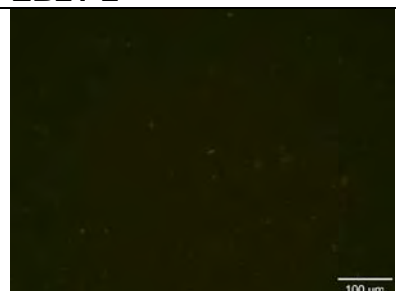
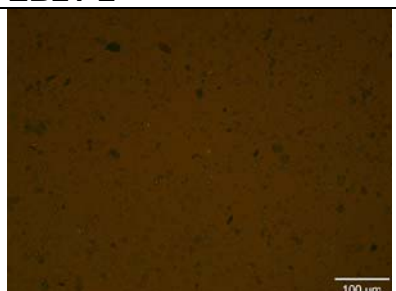
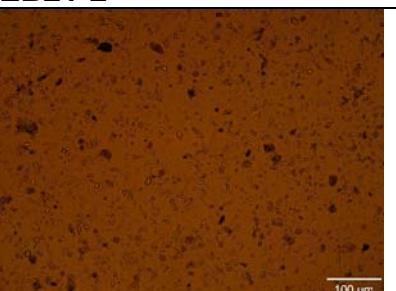
EB17-6  100 µm	EB17-6  100 µm	EB17-6  100 µm
EB17-6 at 320x  50 µm	EB17-6 at 320x  50 µm	EB17-6 at 320x  50 µm
SEKR1575C701S072612D019 EB18-1 A  100 µm	SEKR1575C701S072612D019 EB18-1 B  100 µm	SEKR1575C701S072612D019 EB18-1 C  100 µm
EB18-2  100 µm	EB18-2  100 µm	EB18-2  100 µm
EB18-2 at 320x  50 µm	EB18-2 at 320x  50 µm	EB18-2 at 320x  50 µm

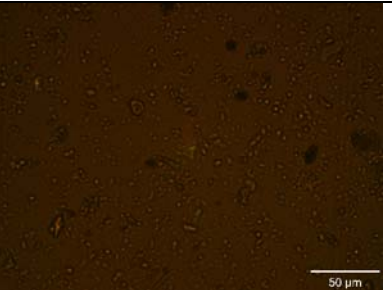
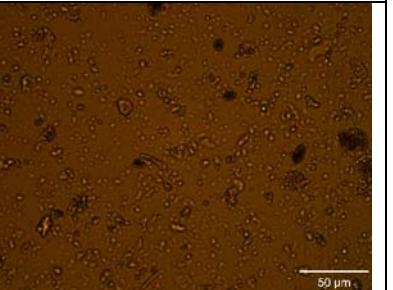
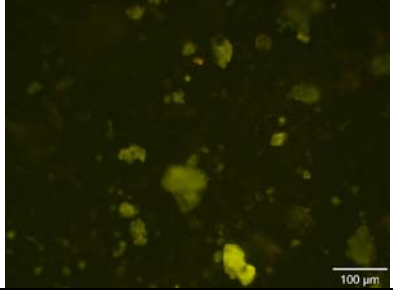
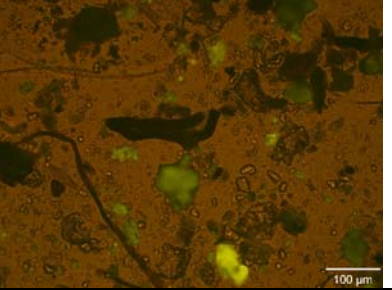
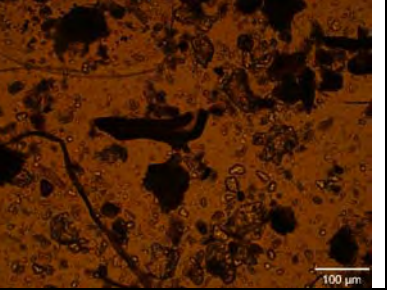
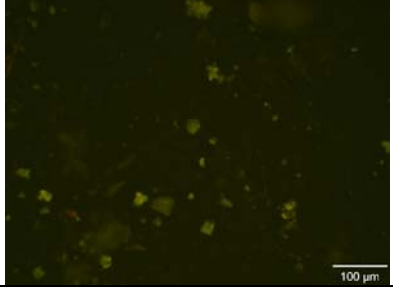
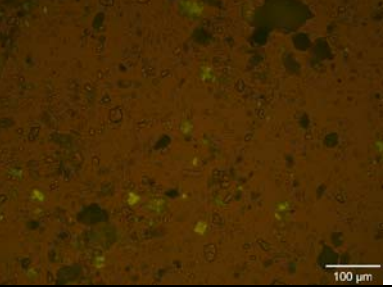
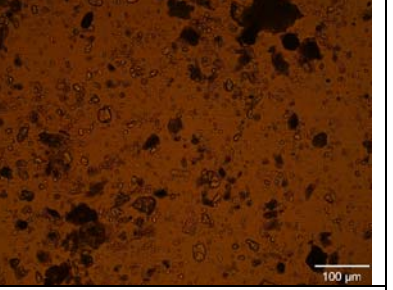
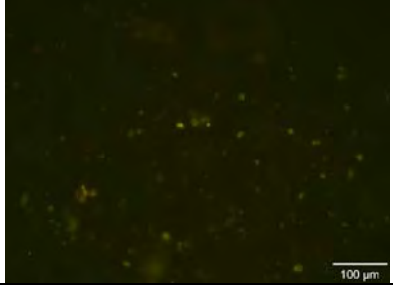
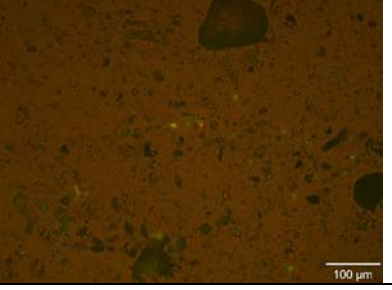
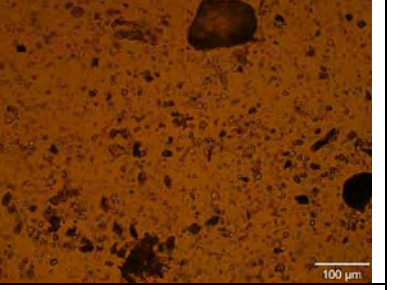
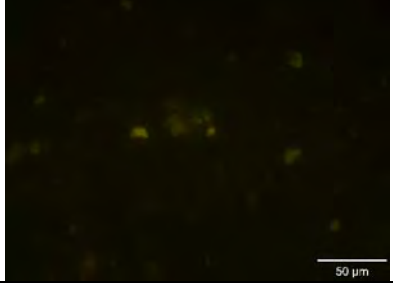
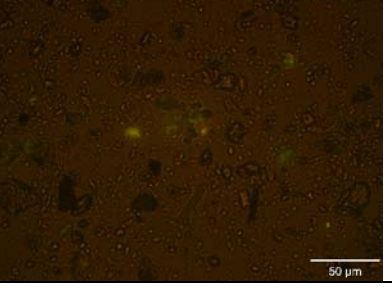
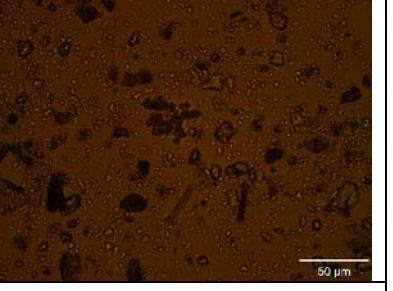
EB18-3 	EB18-3 	EB18-3 
EB18-4 	EB18-4 	EB18-4 
EB18-5 	EB18-5 	EB18-5 
EB18-6 	EB18-6 	EB18-6 
EB18-6 at 320x 	EB18-6 at 320x 	EB18-6 at 320x 

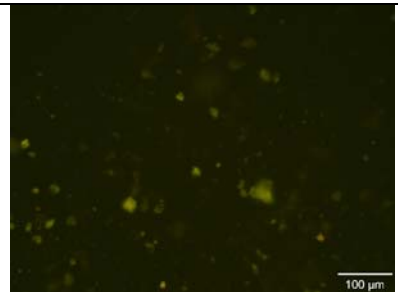
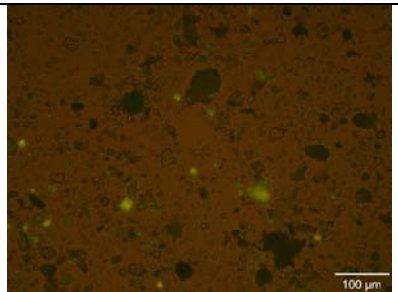
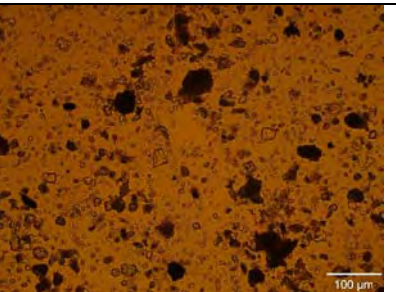
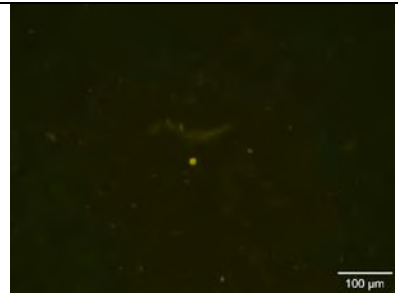
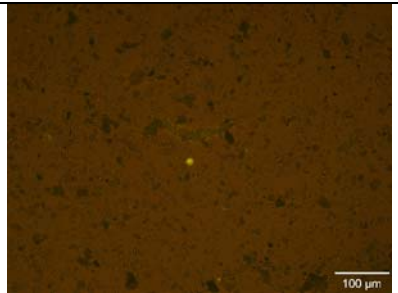
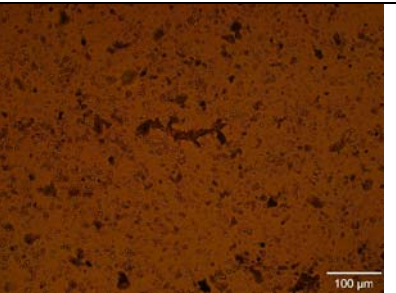
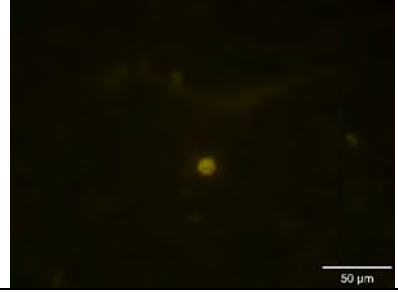
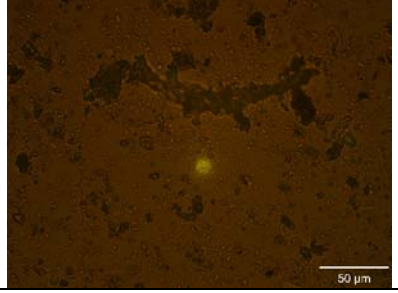
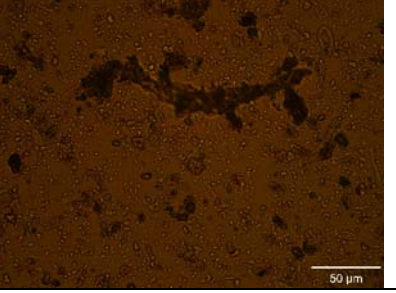
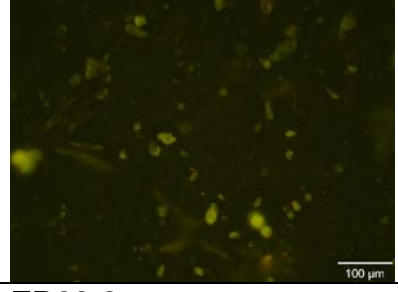
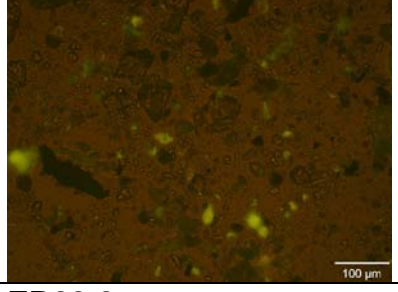
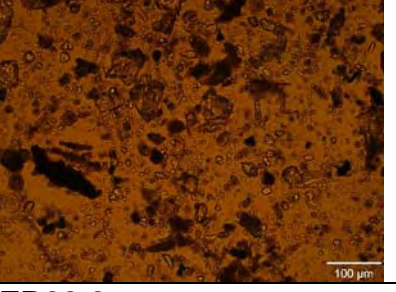
SEKR1575C702S072612D010 EB19-1 A	SEKR1575C702S072612D010 EB19-1 B	SEKR1575C702S072612D010 EB19-1 C
		
EB19-1 at 320x	EB19-1 at 320x	EB19-1 at 320x
		
EB19-2	EB19-2	EB19-2
		
EB19-3	EB19-3	EB19-3
		
EB19-3 at 320x	EB19-3 at 320x	EB19-3 at 320x
		

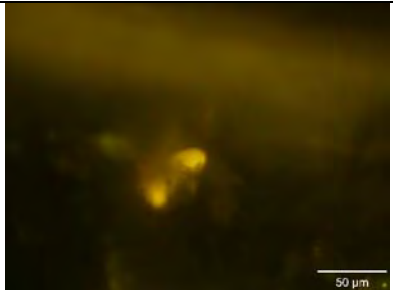
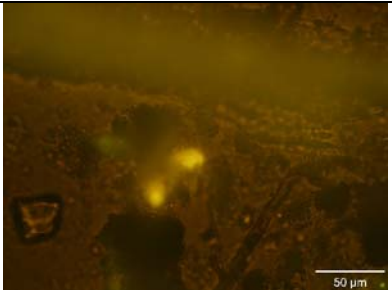
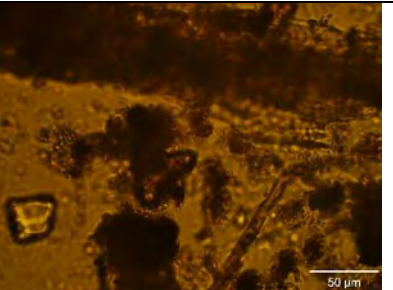
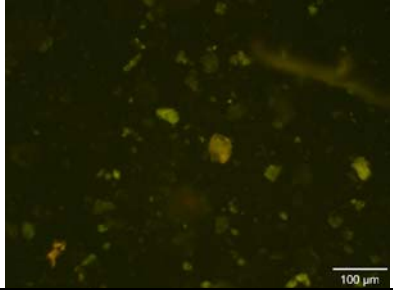
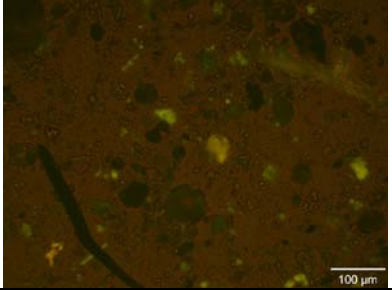
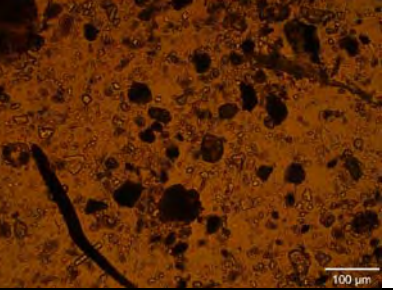
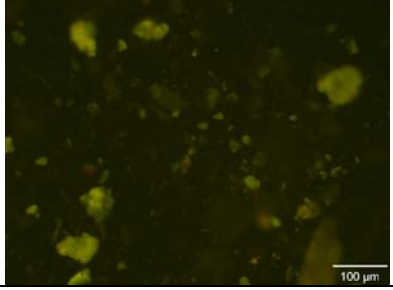
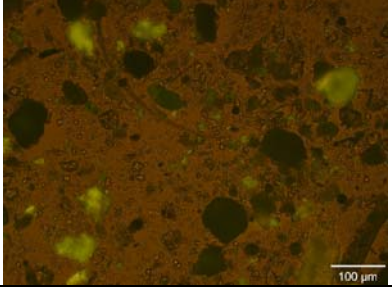
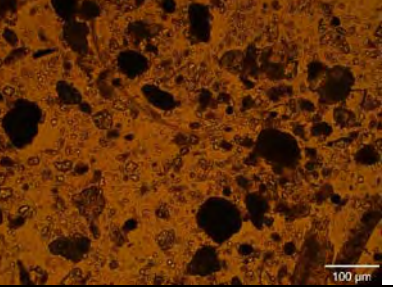
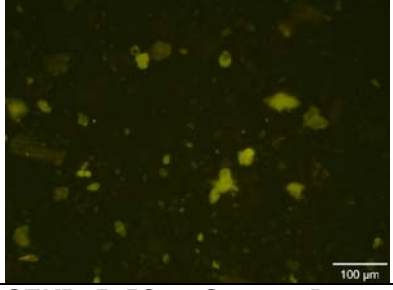
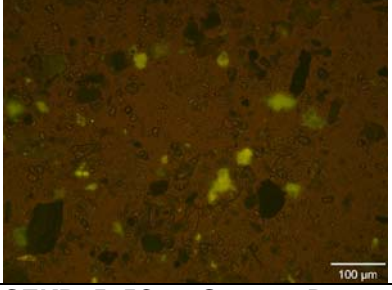
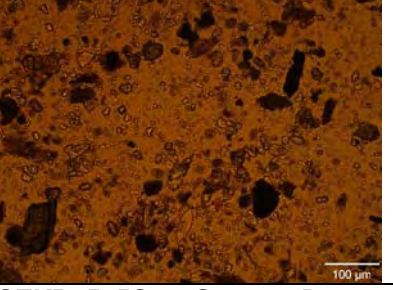
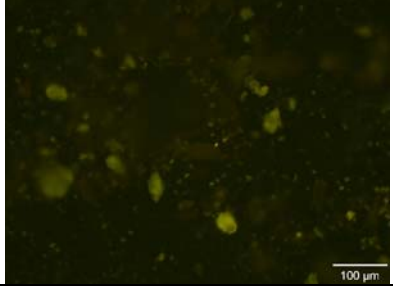
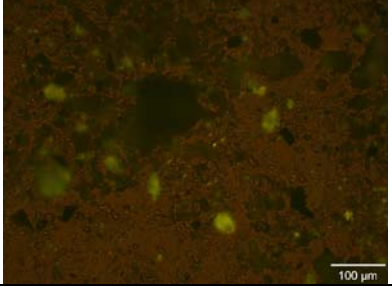
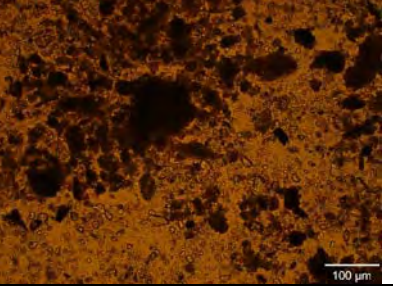
EB19-4 	EB19-4 	EB19-4 
EB19-4 at 320x 	EB19-4 at 320x 	EB19-4 at 320x 
EB19-5 	EB19-5 	EB19-5 
EB19-6 	EB19-6 	EB19-6 
SEKR0425C701S072512D007 EB20-1 A	SEKR0425C701S072512D007 EB20-1 B	SEKR0425C701S072512D007 EB20-1 C
		

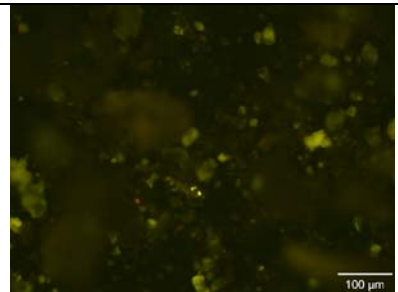
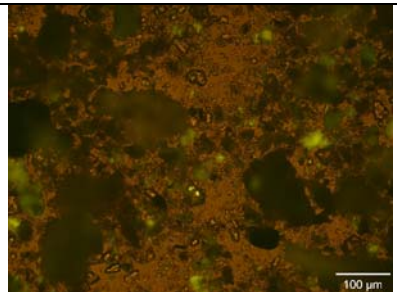
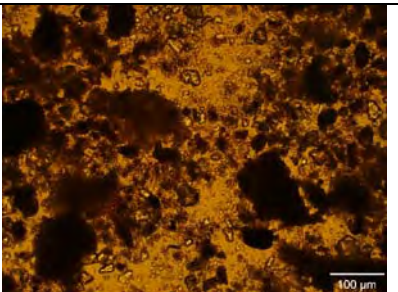
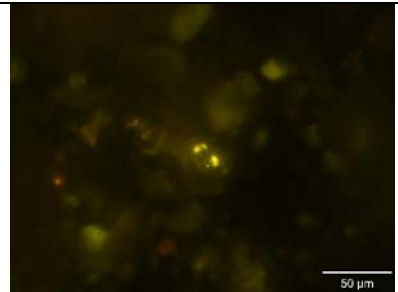
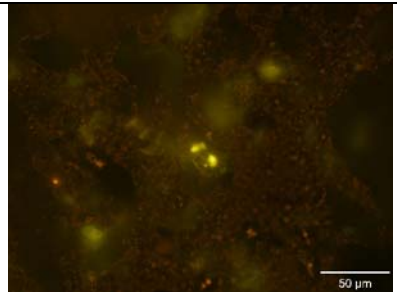
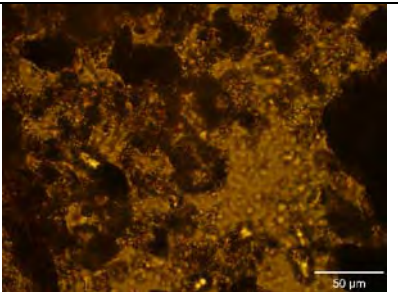
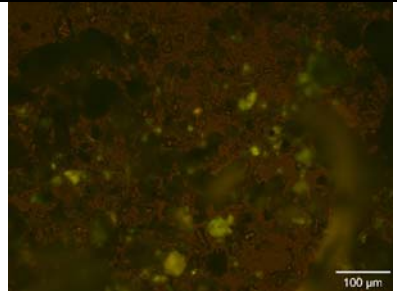
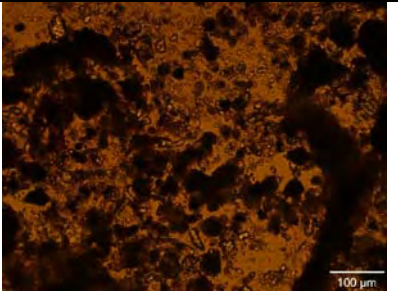
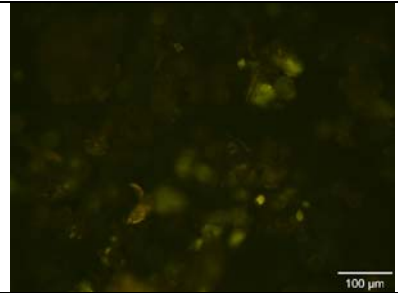
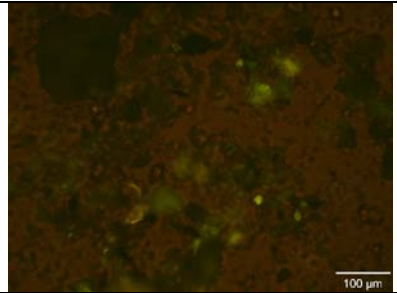
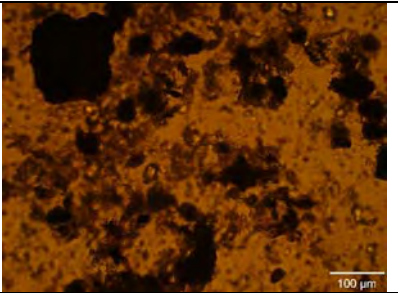
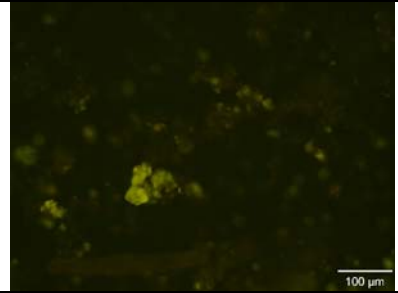
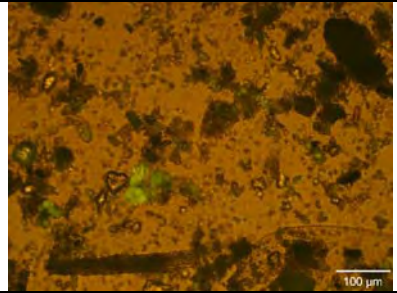
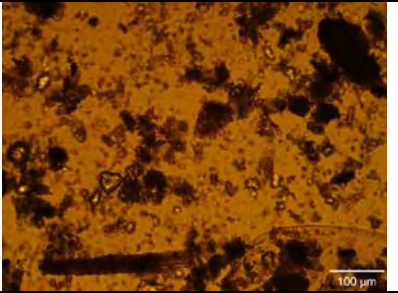
EB20-1 at 320x	EB20-1 at 320x	EB20-1 at 320x
		
EB20-2	EB20-2	EB20-2
		
EB20-2 at 320x	EB20-2 at 320x	EB20-2 at 320x
		
EB20-3	EB20-3	EB20-3
		
EB20-4	EB20-4	EB20-4
		

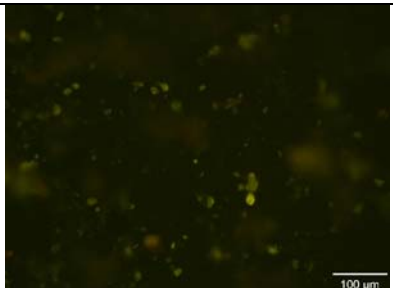
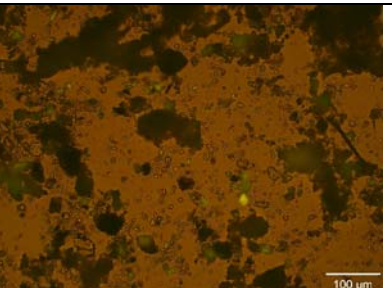
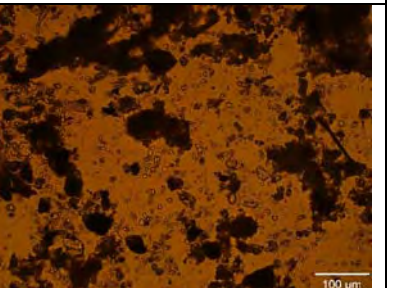
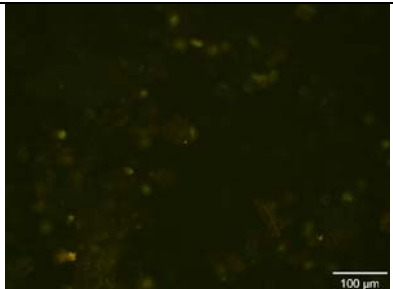
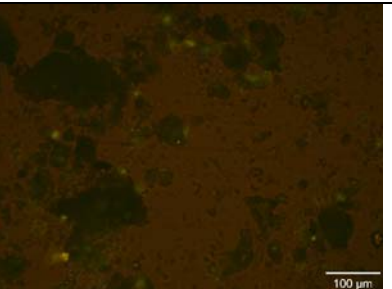
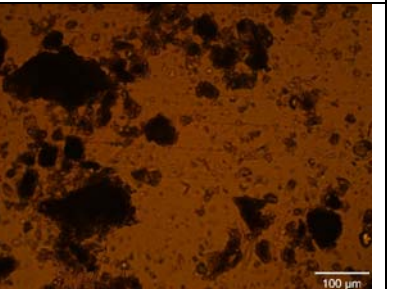
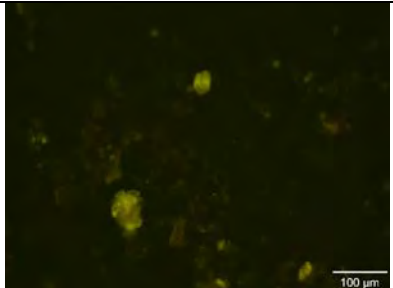
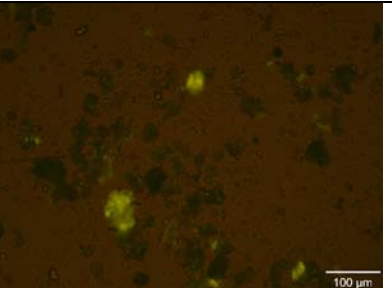
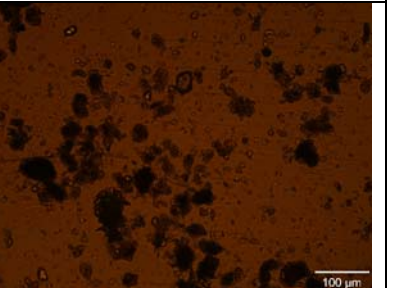
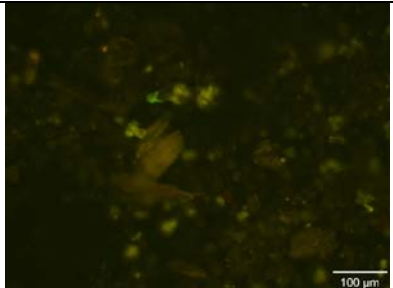
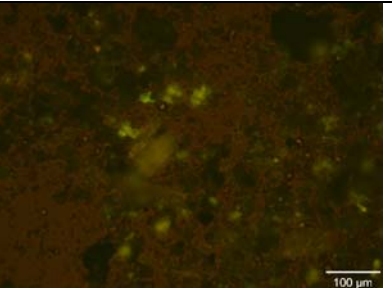
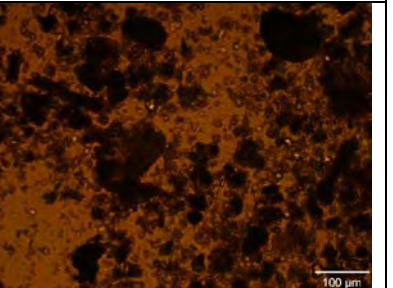
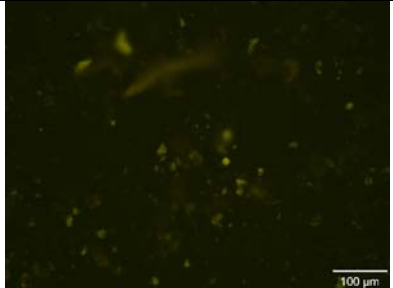
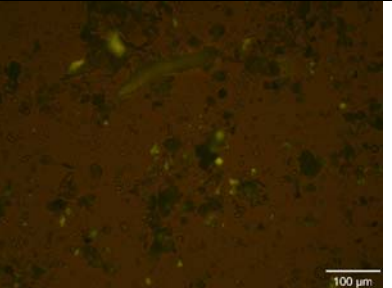
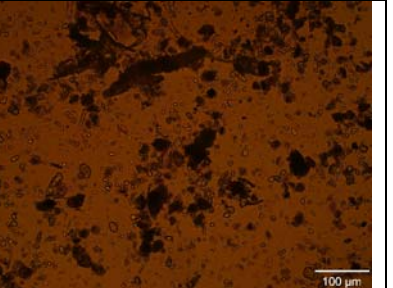
EB20-5 	EB20-5 	EB20-5 
EB20-6 	EB20-6 	EB20-6 
SEKR3800C707S072712D009 EB21-1 A	SEKR3800C707S072712D009 EB21-1 B	SEKR3800C707S072712D009 EB21-1 C
		
EB21-1 at 320x	EB21-1 at 320x	EB21-1 at 320x
		
EB21-2	EB21-2	EB21-2
		

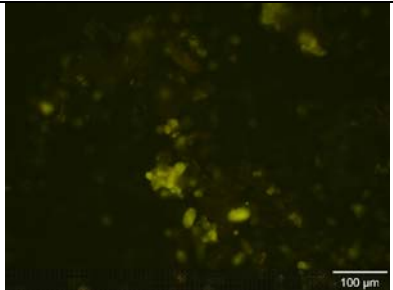
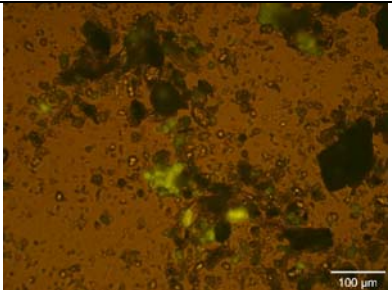
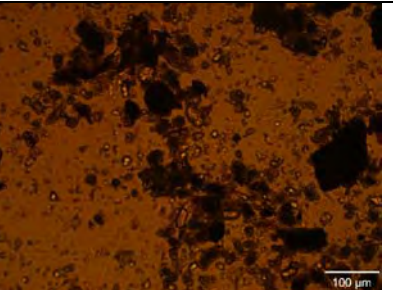
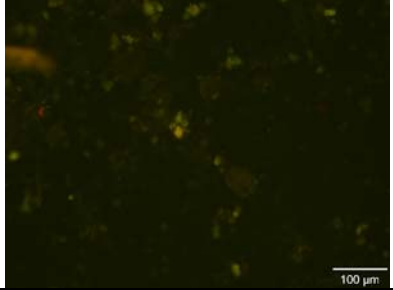
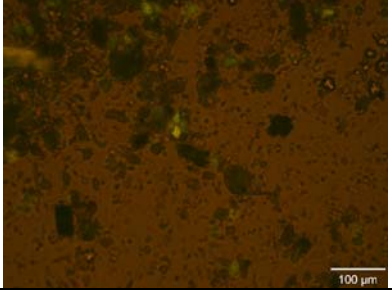
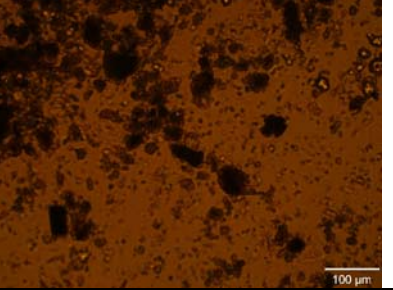
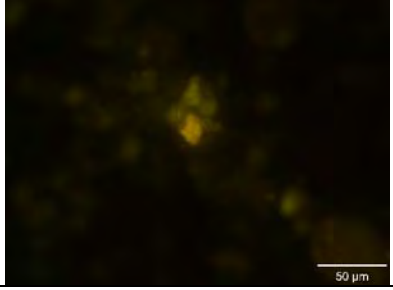
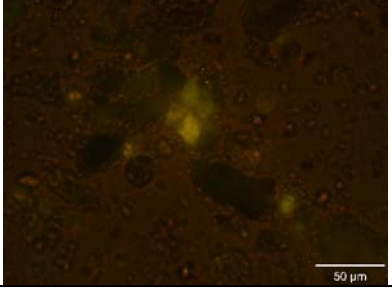
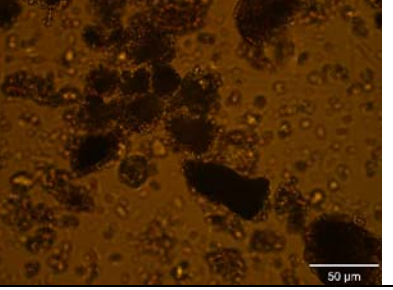
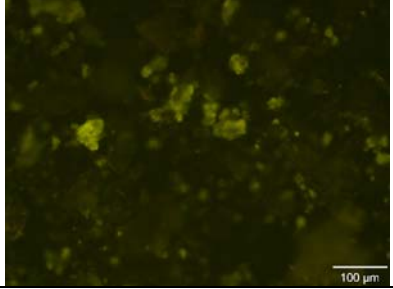
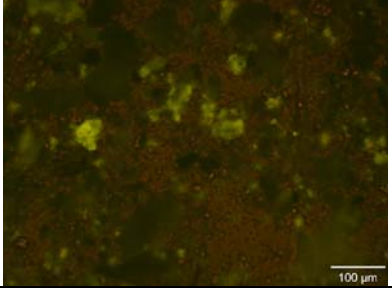
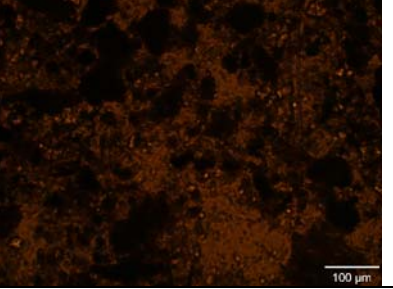
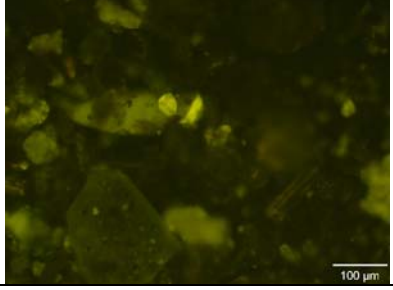
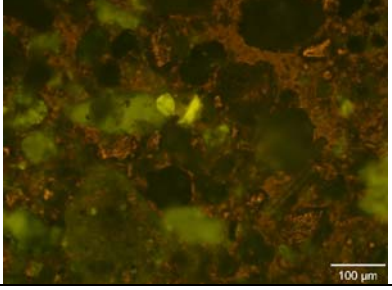
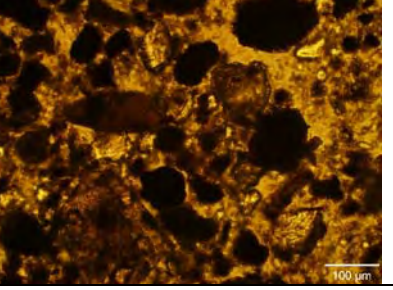
EB21-2 at 320x 	EB21-2 at 320x 	EB21-2 at 320x 
EB21-3 	EB21-3 	EB21-3 
EB21-4 	EB21-4 	EB21-4 
EB21-5 	EB21-5 	EB21-5 
EB21-5 at 320x 	EB21-5 at 320x 	EB21-5 at 320x 

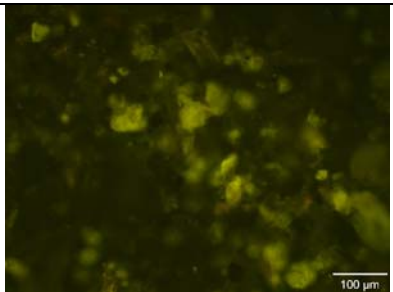
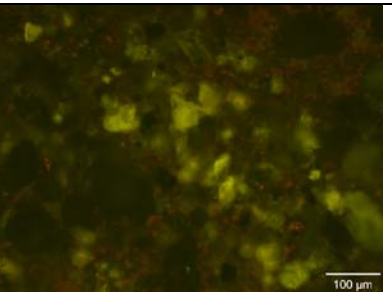
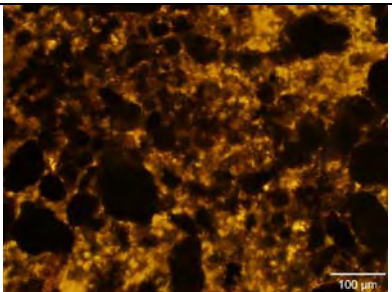
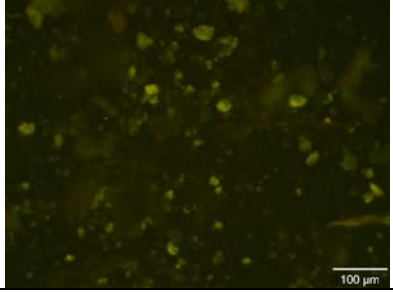
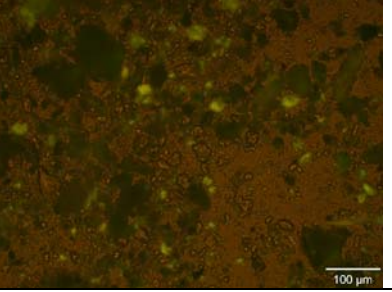
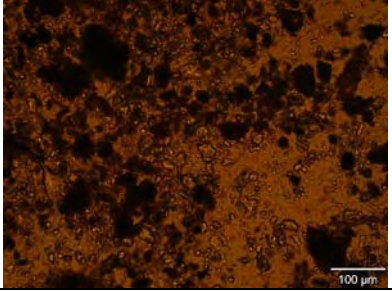
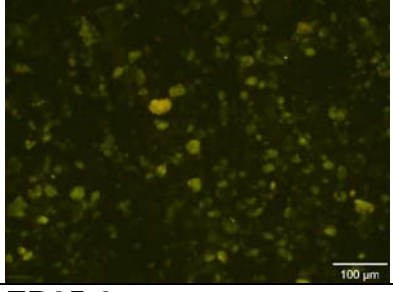
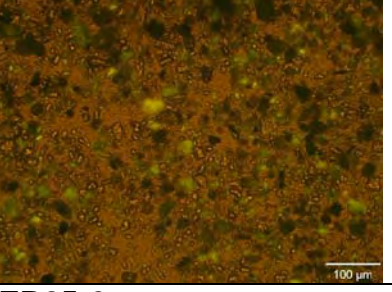
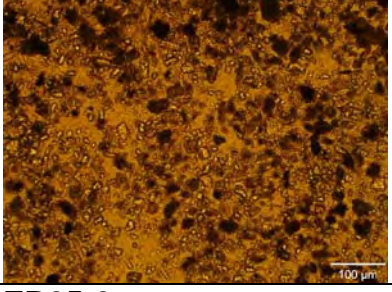
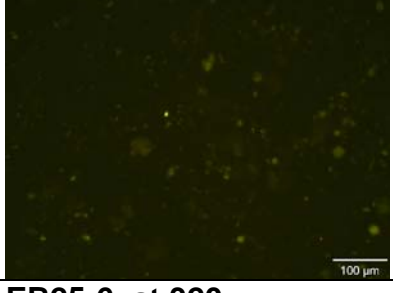
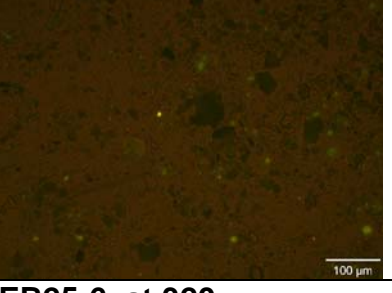
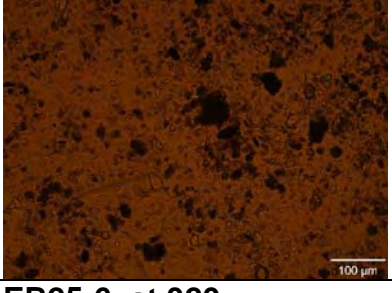
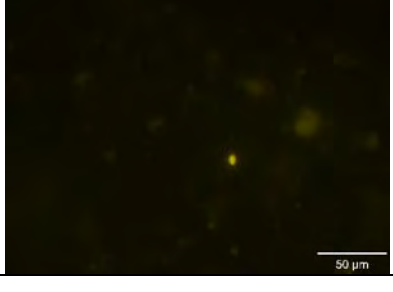
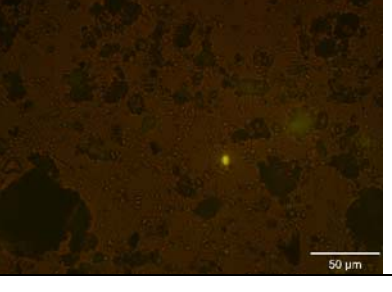
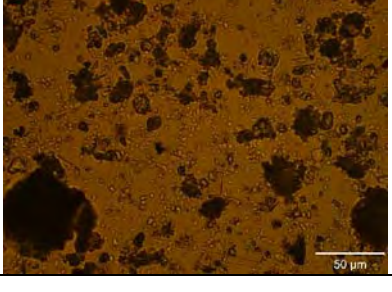
EB21-6	EB21-6	EB21-6
		
SEKR3800C709S072712D011 EB22-1 A	SEKR3800C709S072712D011 EB22-1 B	SEKR3800C709S072712D011 EB22-1 C
		
EB22-1 at 320x	EB22-1 at 320x	EB22-1 at 320x
		
EB22-2	EB22-2	EB22-2
		
EB22-3	EB22-3	EB22-3

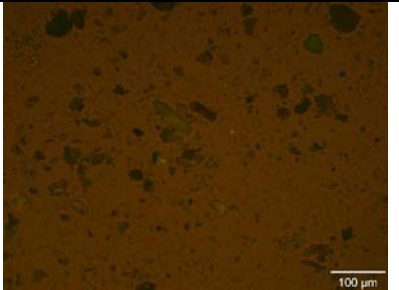
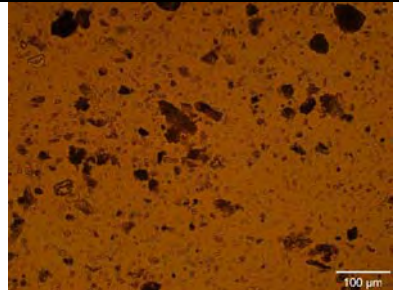
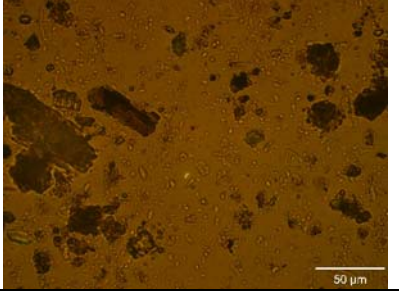
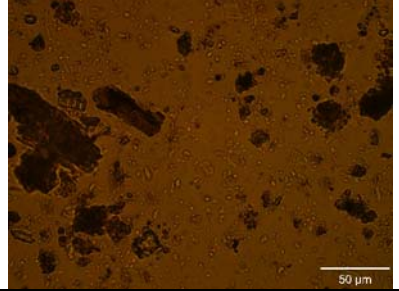
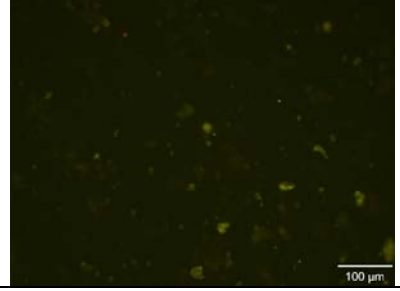
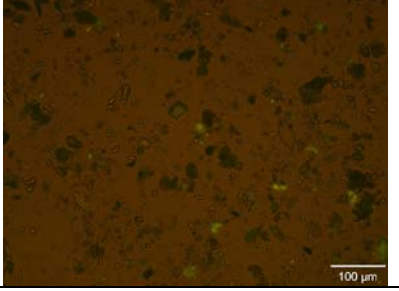
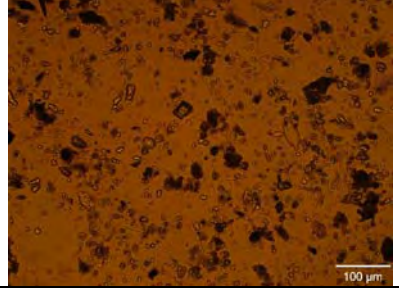
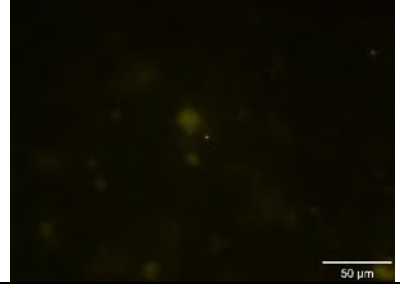
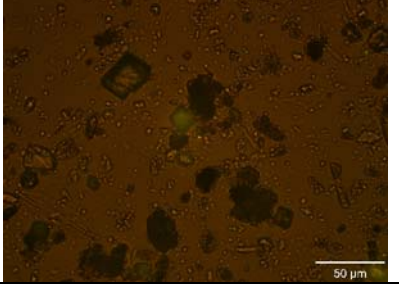
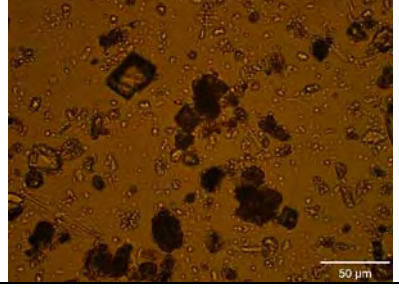
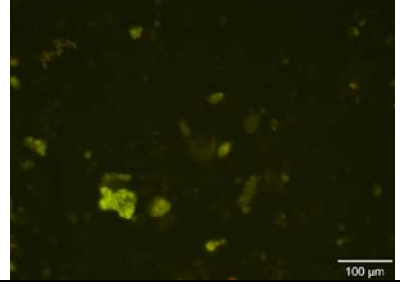
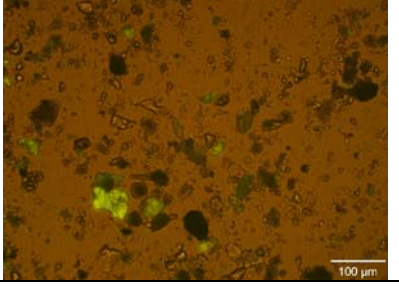
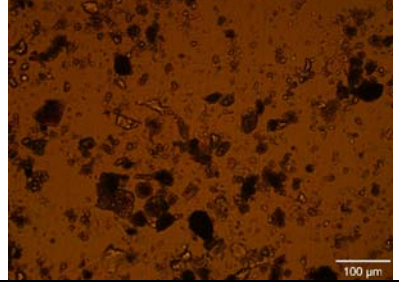
EB22-3 at 320x	EB22-3 at 320x	EB22-3 at 320x
		
EB22-4	EB22-4	EB22-4
		
EB22-5	EB22-5	EB22-5
		
EB22-6	EB22-6	EB22-6
		
SEKR1575C701S072612D013 EB23-1 A	SEKR1575C701S072612D013 EB23-1 B	SEKR1575C701S072612D013 EB23-1 C
		

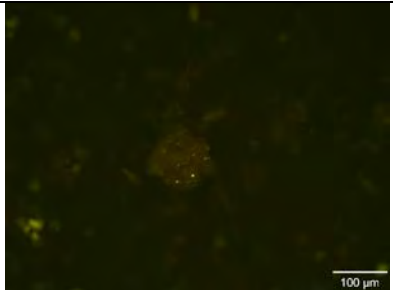
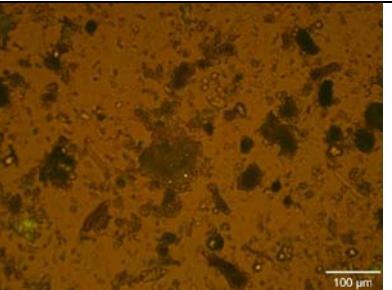
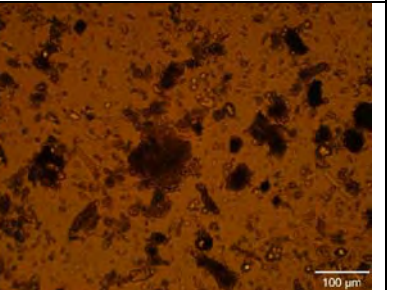
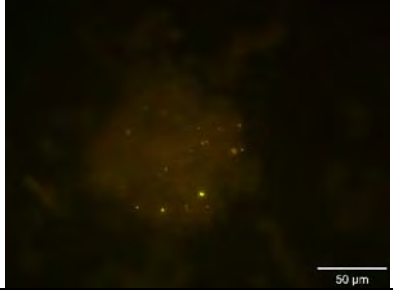
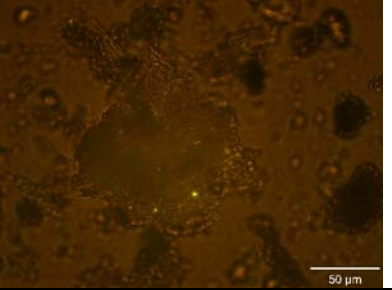
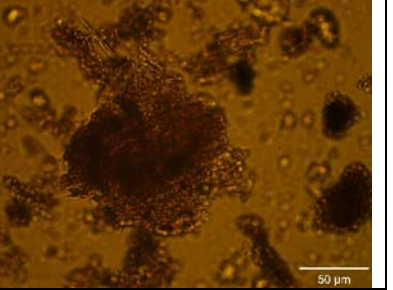
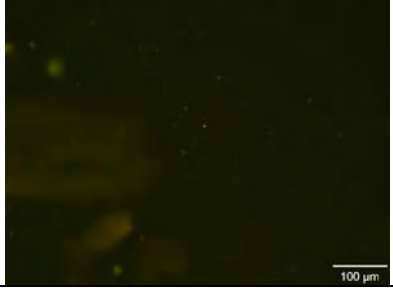
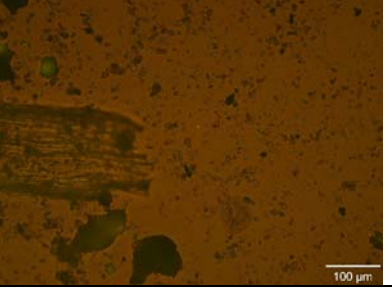
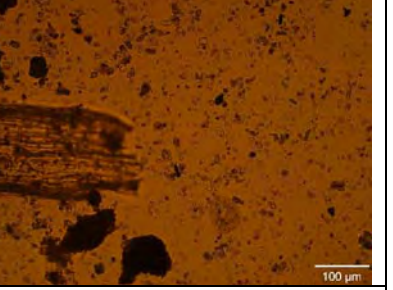
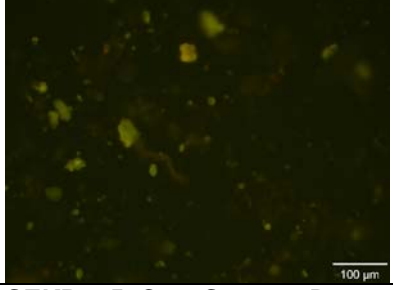
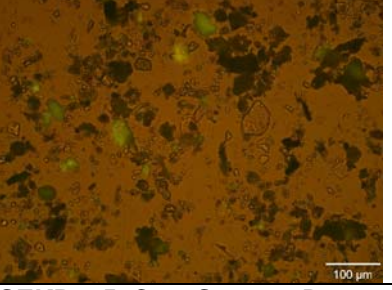
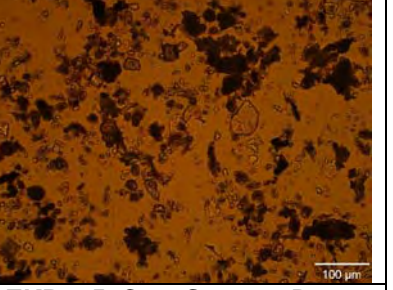
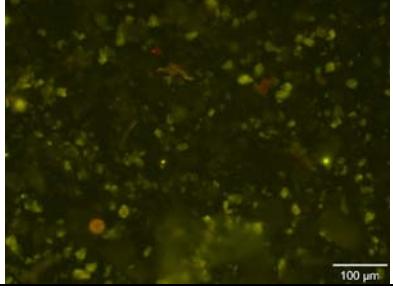
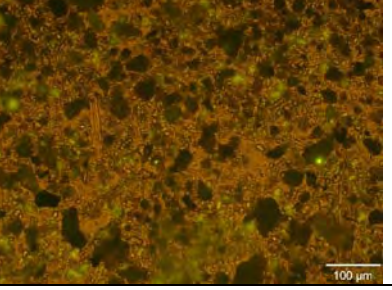
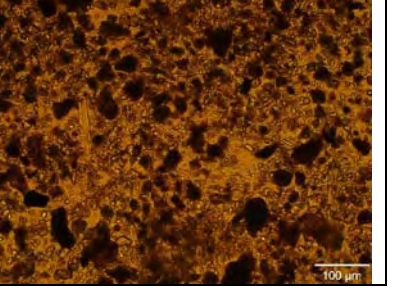
EB23-2	EB23-2	EB23-2
		
EB23-2 at 320x	EB23-2 at 320x	EB23-2 at 320x
		
EB23-3	EB23-3	EB23-3
		
EB23-4	EB23-4	EB23-4
		
EB23-5	EB23-5	EB23-5
		

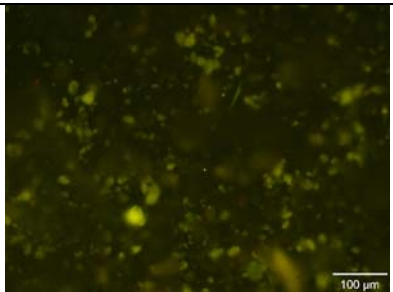
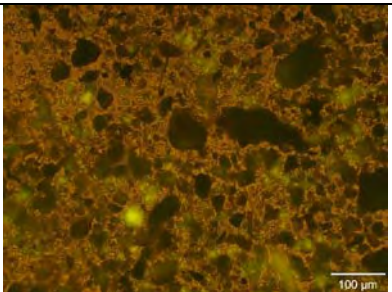
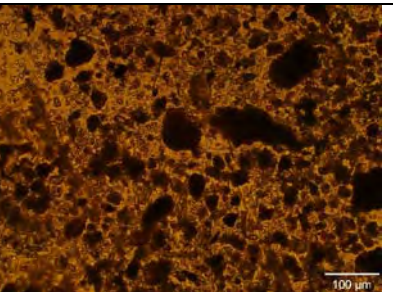
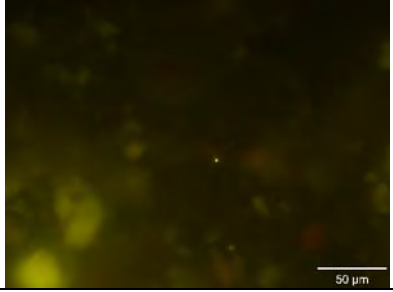
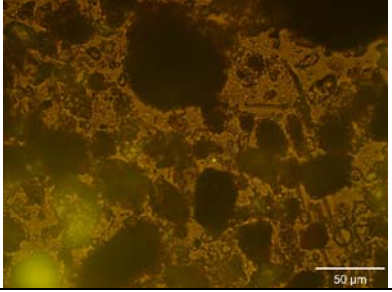
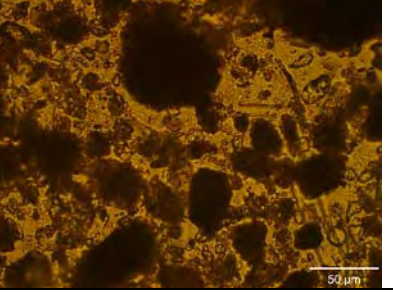
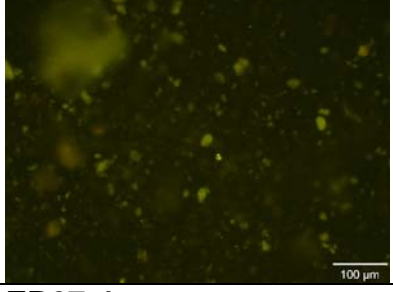
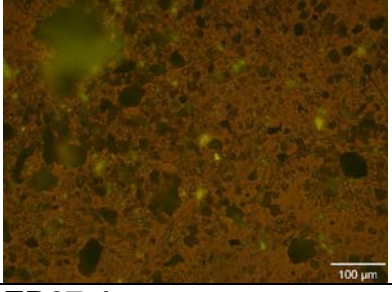
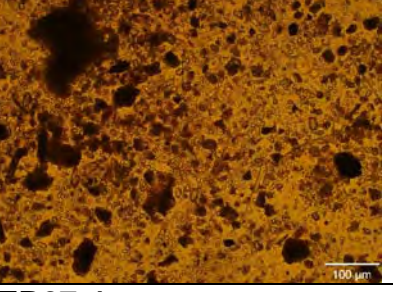
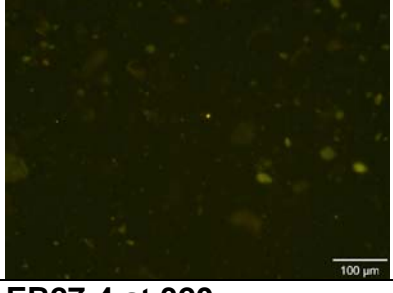
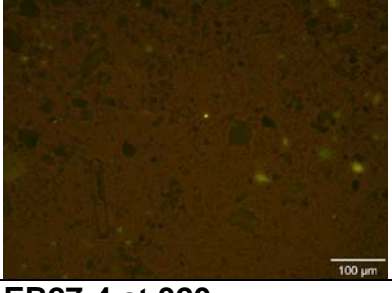
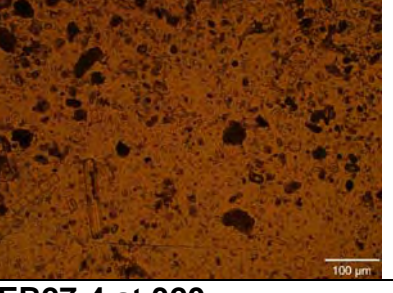
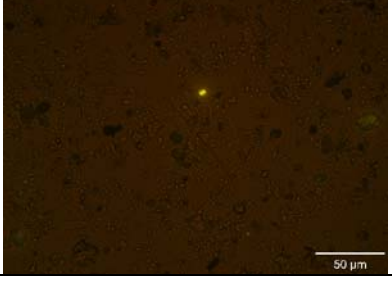
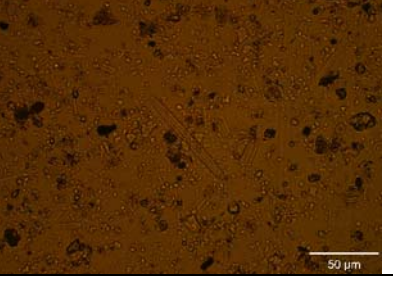
EB23-6	EB23-6	EB23-6
		
SEKR1575C701S072612D007 EB24-1 A	SEKR1575C701S072612D007 EB24-1 B	SEKR1575C701S072612D007 EB24-1 C
		
EB24-2	EB24-2	EB24-2
		
EB24-3	EB24-3	EB24-3
		
EB24-4	EB24-4	EB24-4
		

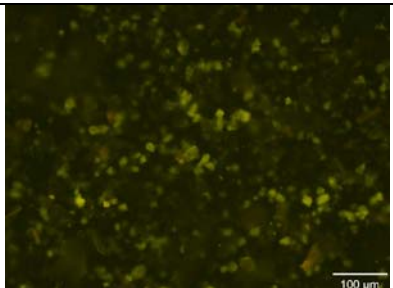
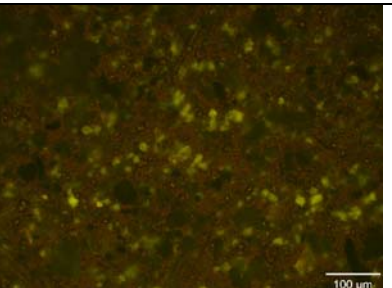
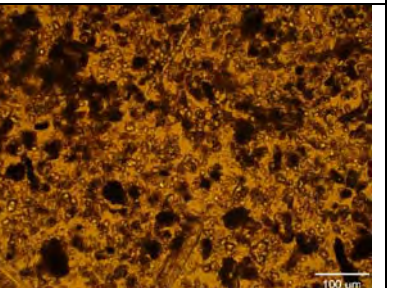
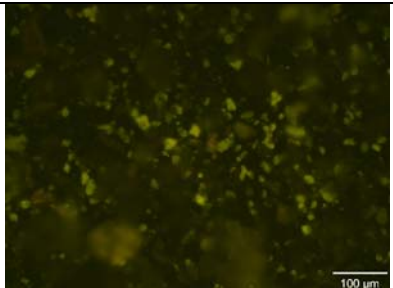
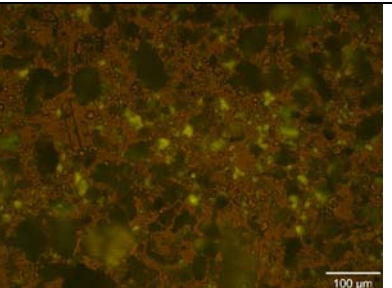
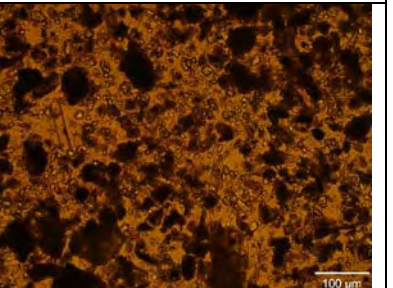
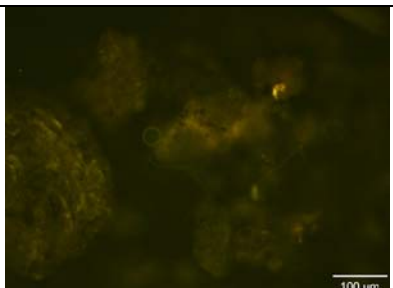
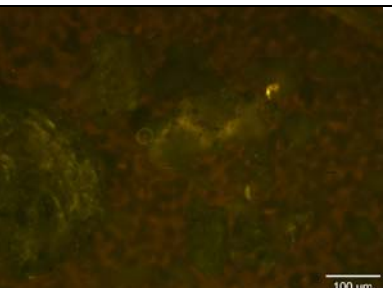
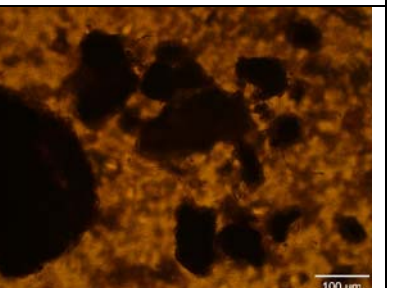
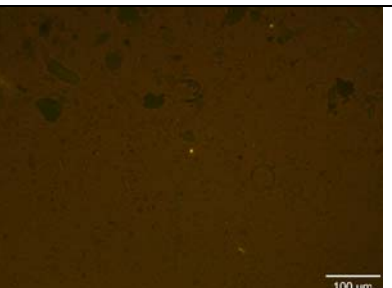
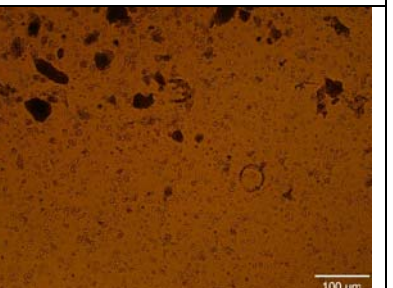
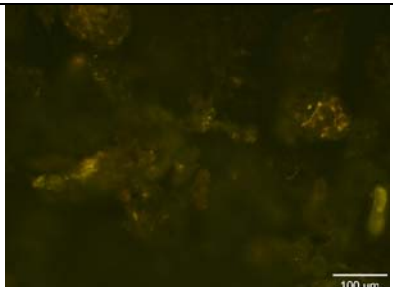
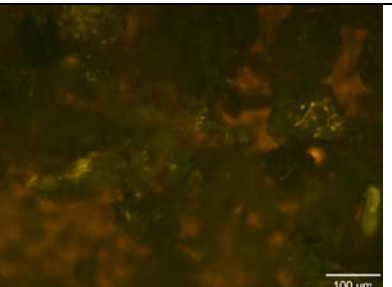
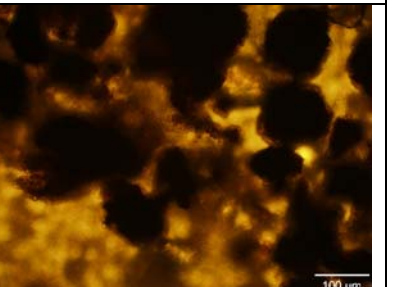
EB24-5 	EB24-5 	EB24-5 
EB24-6 	EB24-6 	EB24-6 
EB24-6 at 320x 	EB24-6 at 320x 	EB24-6 at 320x 
SEKR1575C701S072612D019 EB25-1 A	SEKR1575C701S072612D019 EB25-1 B	SEKR1575C701S072612D019 EB25-1 C
		
EB25-2 	EB25-2 	EB25-2 

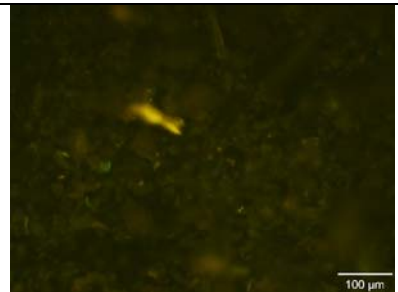
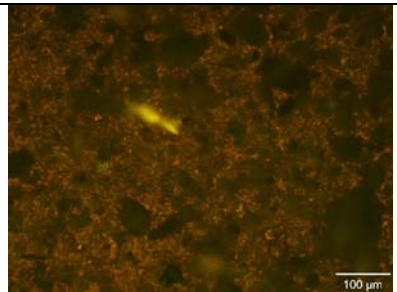
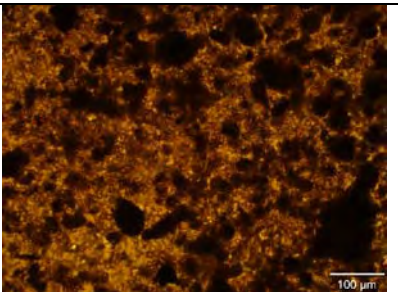
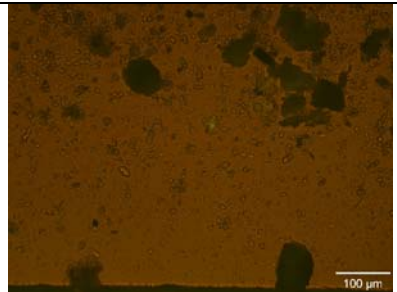
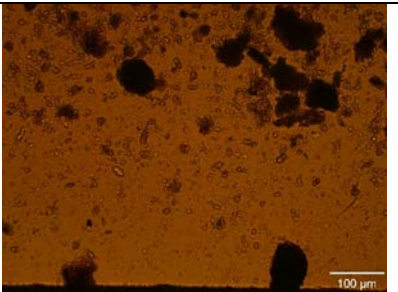
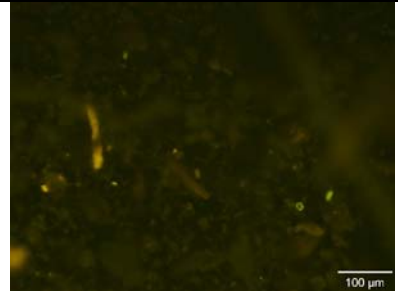
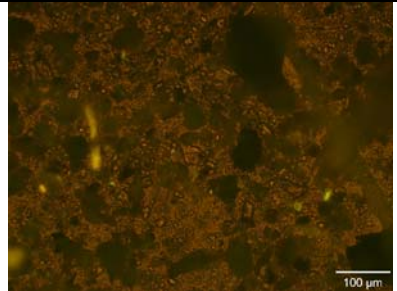
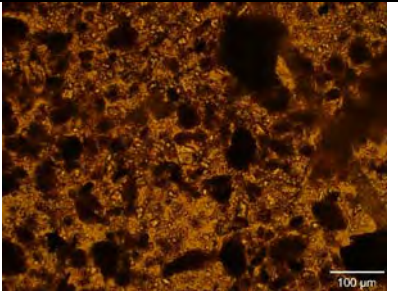
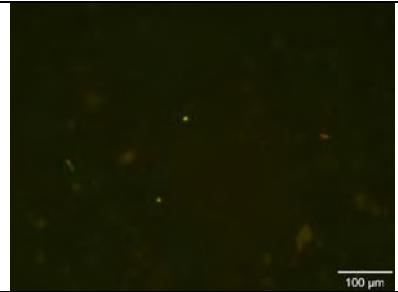
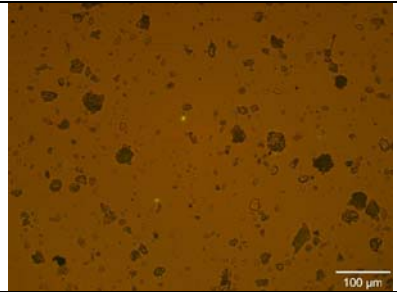
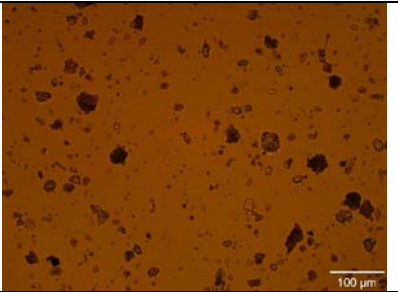
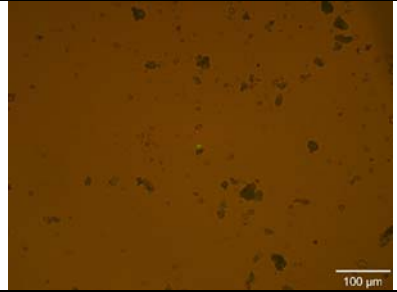
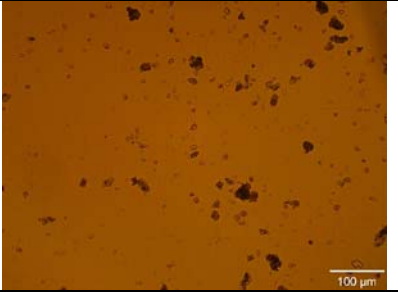
EB25-3 	EB25-3 	EB25-3 
EB25-4 	EB25-4 	EB25-4 
EB25-5 	EB25-5 	EB25-5 
EB25-6 	EB25-6 	EB25-6 
EB25-6 at 320x 	EB25-6 at 320x 	EB25-6 at 320x 

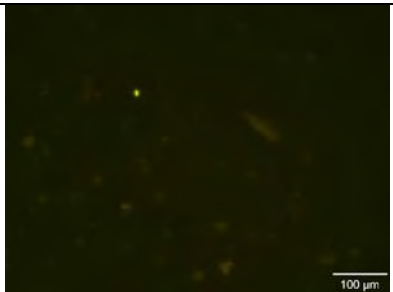
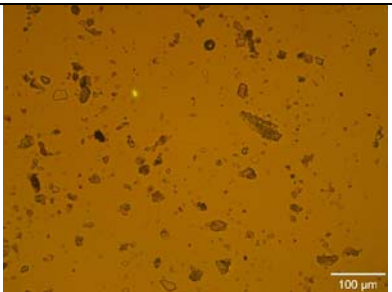
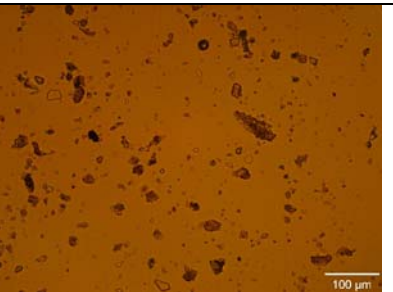
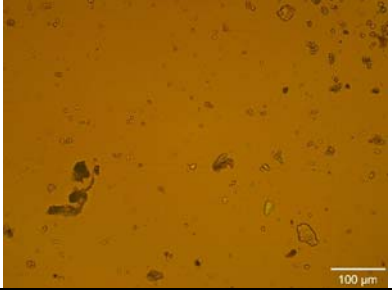
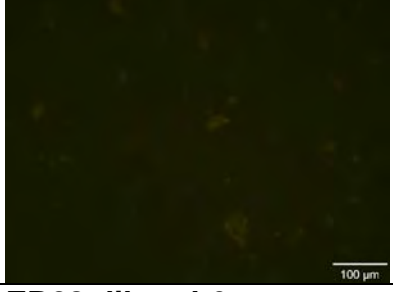
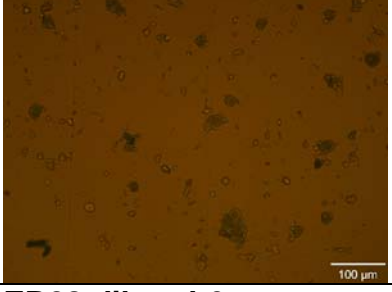
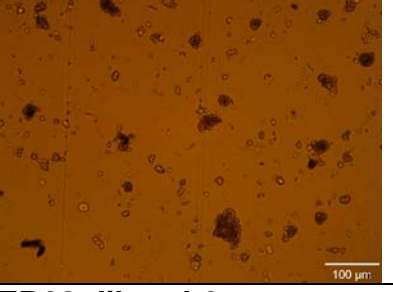
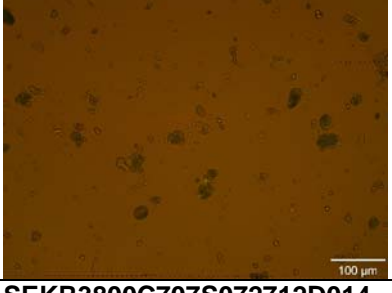
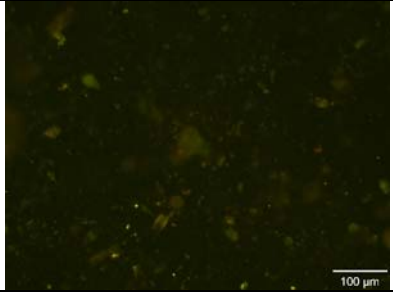
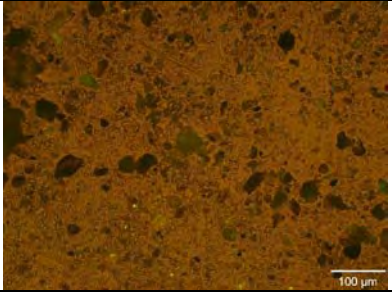
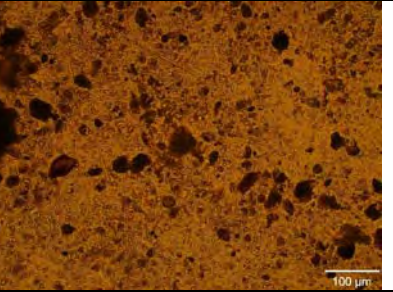
SEKR3775C702S072712D009 EB26-1 A	SEKR3775C702S072712D009 EB26-1 B	SEKR3775C702S072712D009 EB26-1 C
		
EB26-1 at 320x	EB26-1 at 320x	EB26-1 at 320x
		
EB26-2	EB26-2	EB26-2
		
EB26-2 at 320x	EB26-2 at 320x	EB26-2 at 320x
		
EB26-3	EB26-3	EB26-3
		

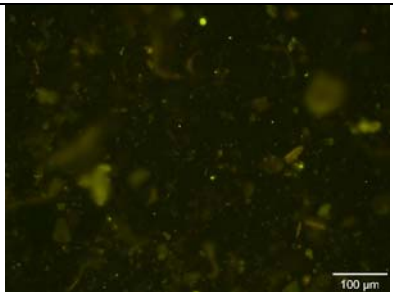
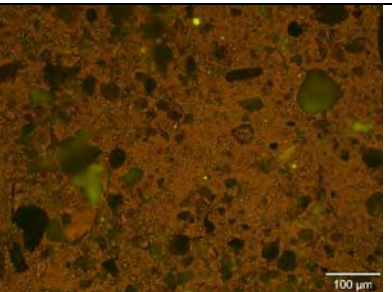
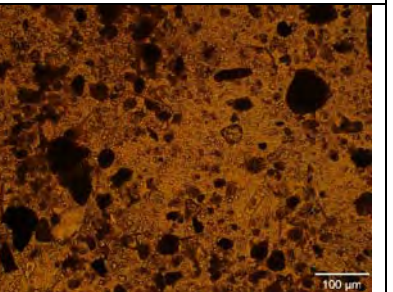
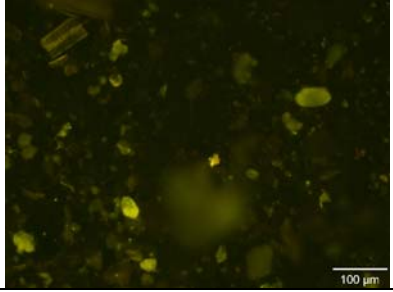
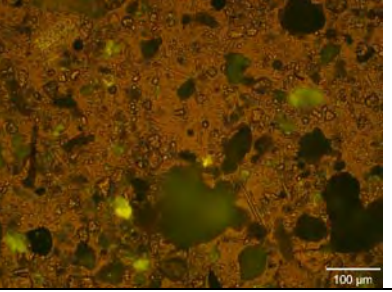
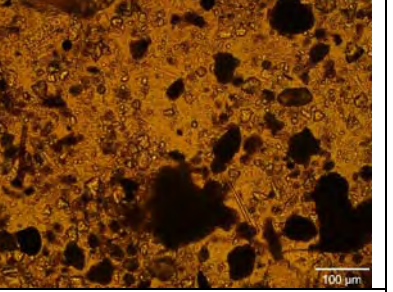
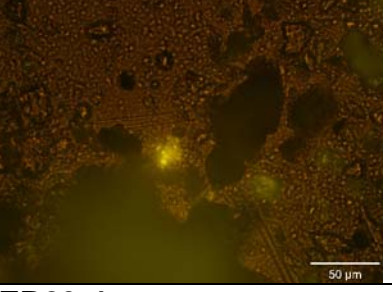
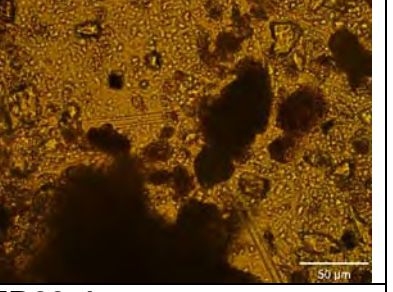
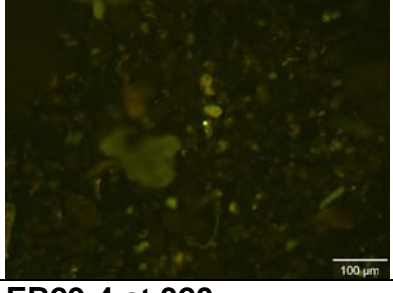
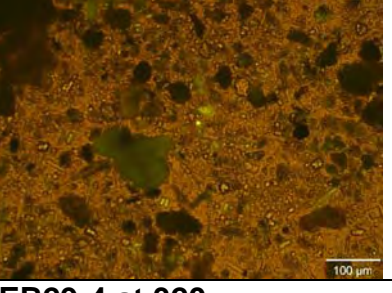
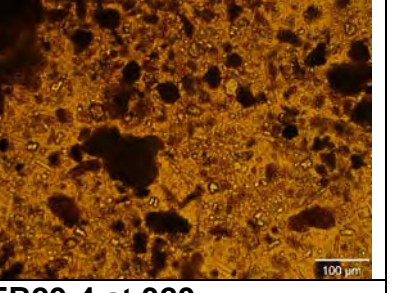
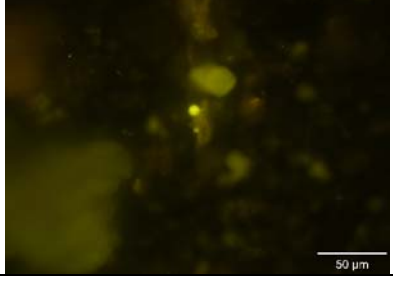
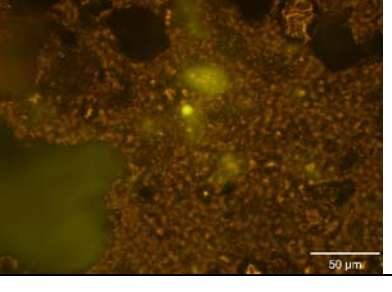
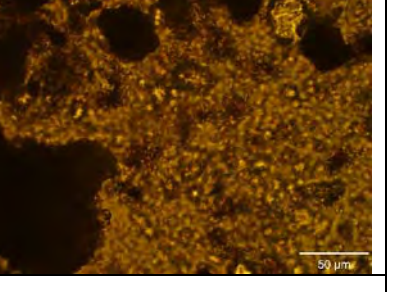
EB26-4 	EB26-4 	EB26-4 
EB26-4 at 320x 	EB26-4 at 320x 	EB26-4 at 320x 
EB26-5 	EB26-5 	EB26-5 
EB26-6 	EB26-6 	EB26-6 
SEKR3950C701S072612D013 EB27-1 A	SEKR3950C701S072612D013 EB27-1 B	SEKR3950C701S072612D013 EB27-1 C
		

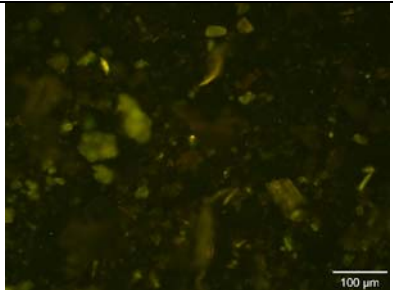
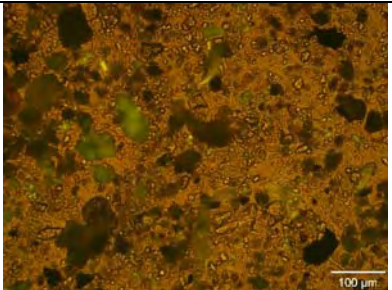
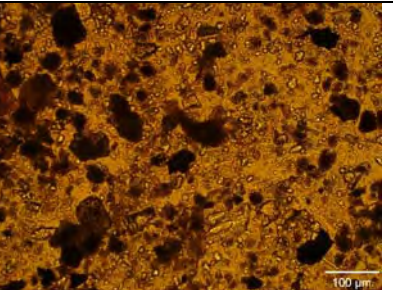
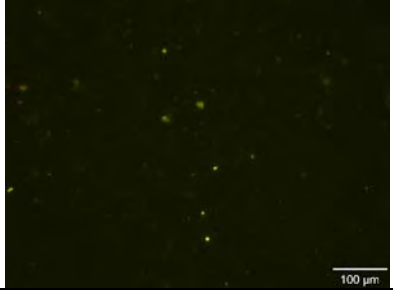
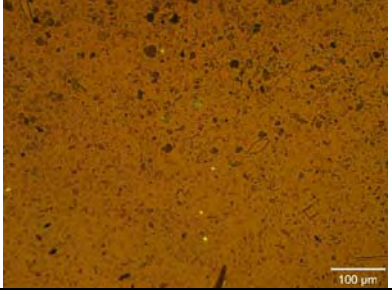
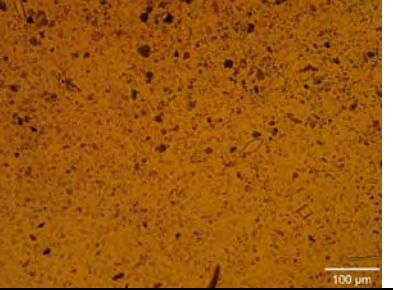
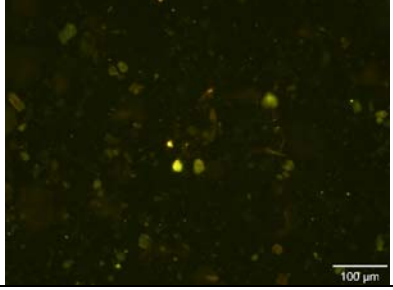
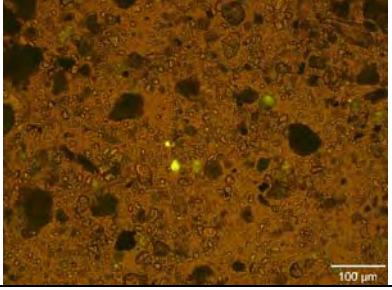
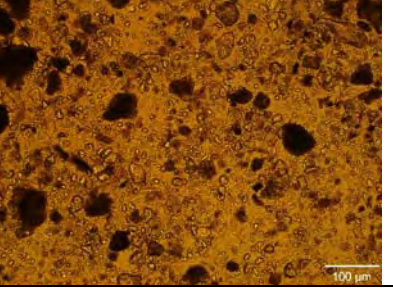
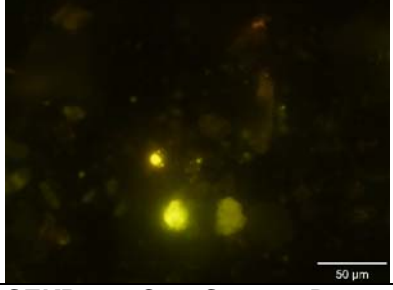
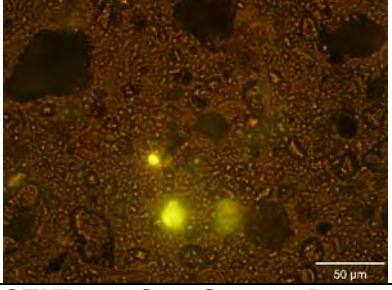
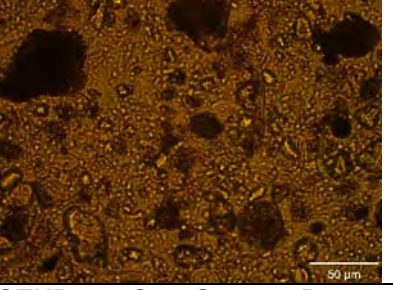
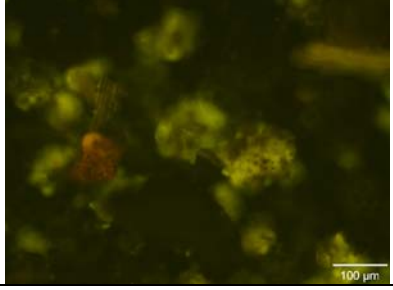
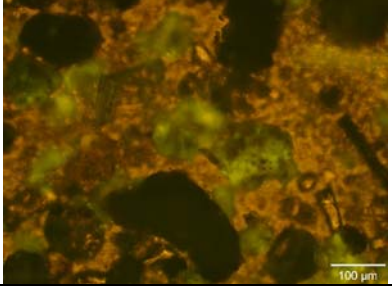
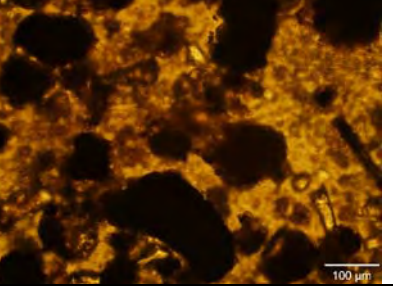
EB27-2  100 μm	EB27-2  100 μm	EB27-2  100 μm
EB27-2 at 320x  50 μm	EB27-2 at 320x  50 μm	EB27-2 at 320x  50 μm
EB27-3  100 μm	EB27-3  100 μm	EB27-3  100 μm
EB27-4  100 μm	EB27-4  100 μm	EB27-4  100 μm
EB27-4 at 320x  50 μm	EB27-4 at 320x  50 μm	EB27-4 at 320x  50 μm

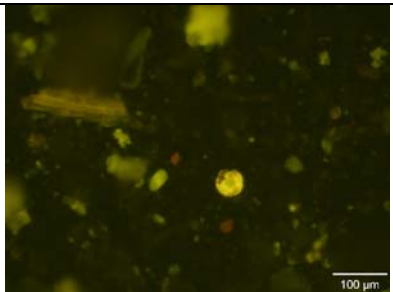
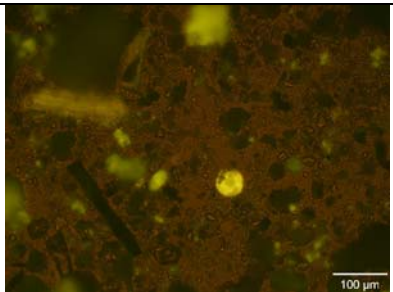
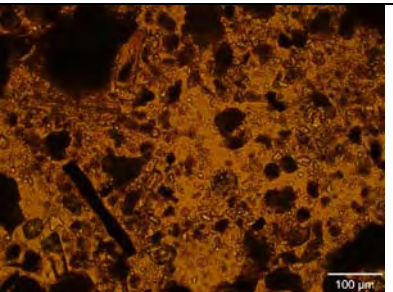
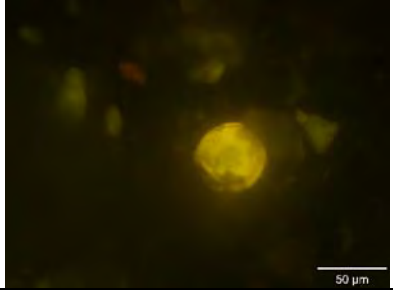
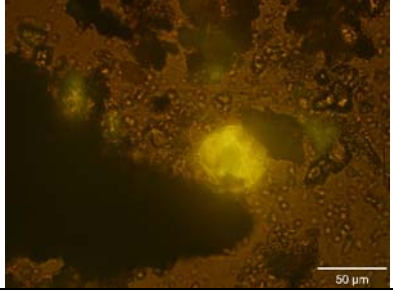
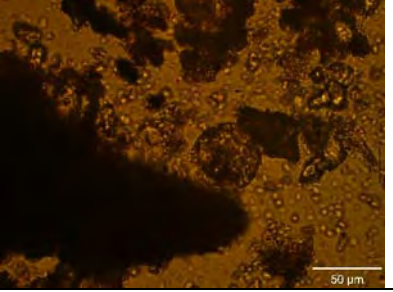
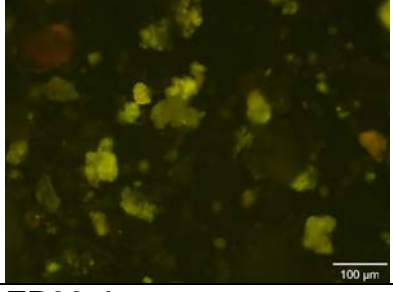
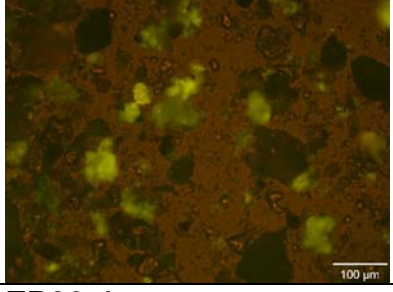
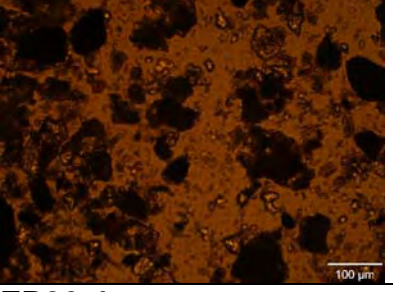
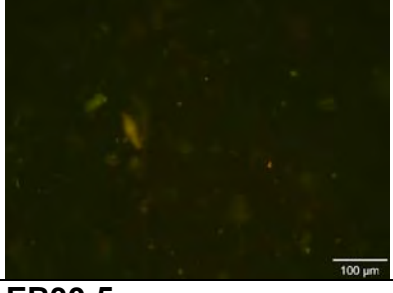
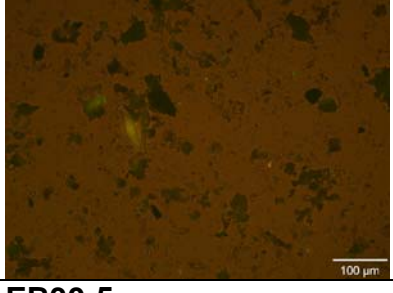
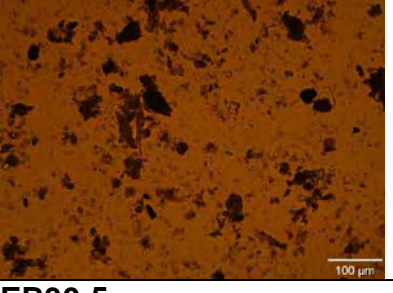
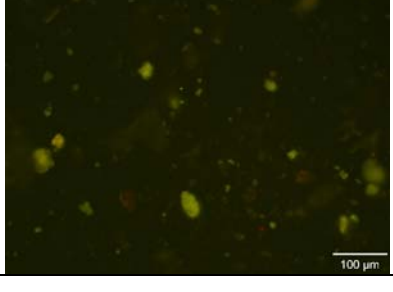
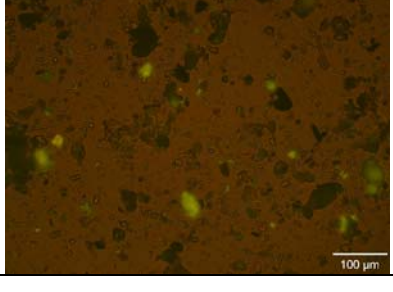
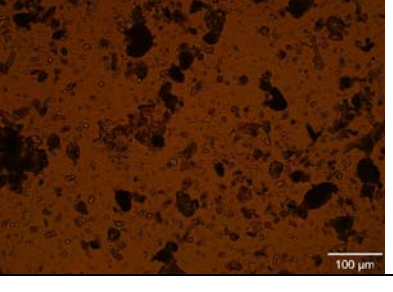
EB27-5  100 µm	EB27-5  100 µm	EB27-5  100 µm
EB27-6  100 µm	EB27-6  100 µm	EB27-6  100 µm
SEKR3650C701S072512D010 EB28-1 A  100 µm	SEKR3650C701S072512D010 EB28-1 B  100 µm	SEKR3650C701S072512D010 EB28-1 C  100 µm
EB28-2  100 µm	EB28-2  100 µm	EB28-2  100 µm
EB28-3  100 µm	EB28-3  100 µm	EB28-3  100 µm

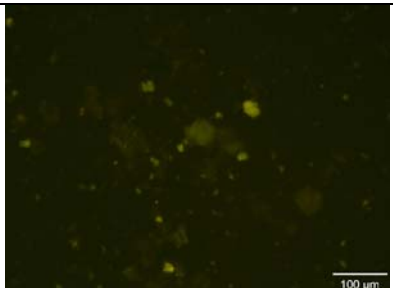
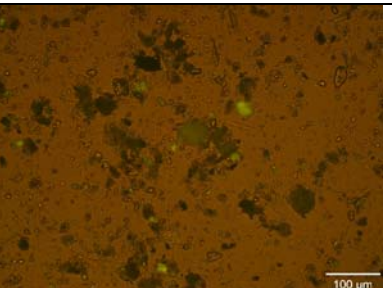
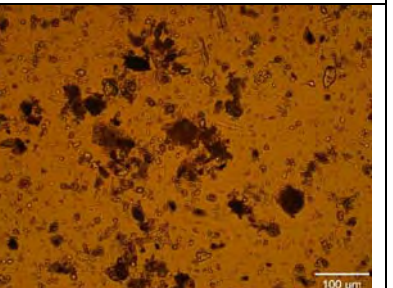
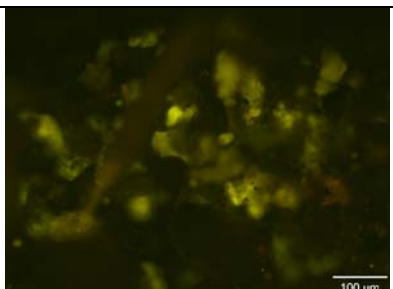
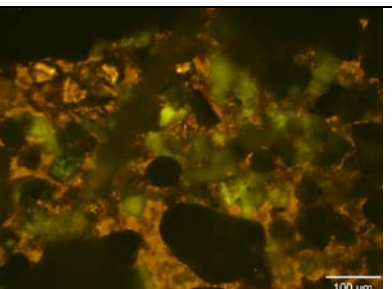
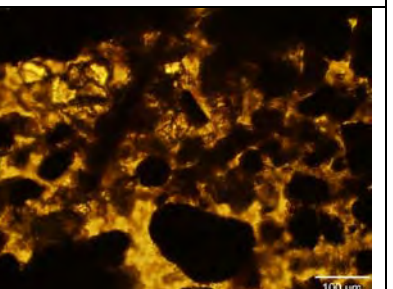
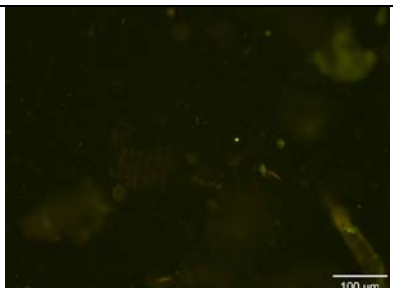
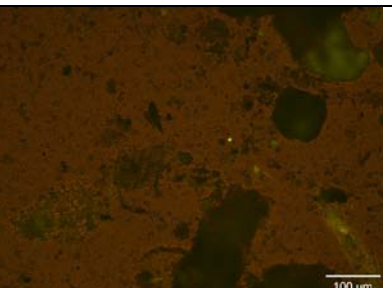
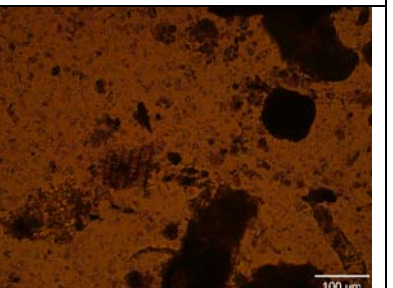
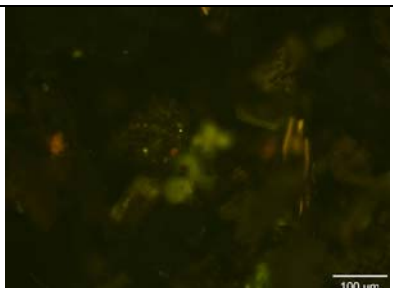
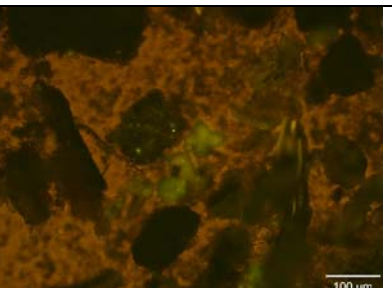
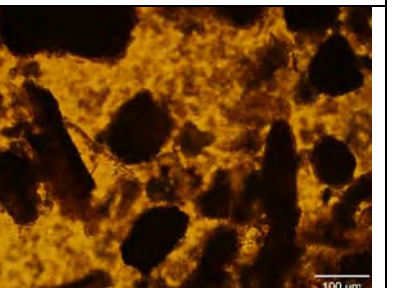
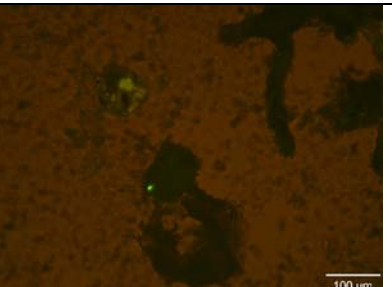
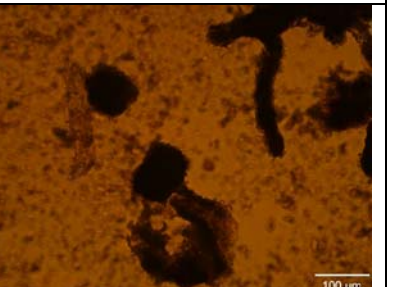
EB28-4 	EB28-4 	EB28-4 
EB28-5 	EB28-5 	EB28-5 
EB28-6 	EB28-6 	EB28-6 
SEKR3650C701S072512D010 EB28 diluted-1 A	SEKR3650C701S072512D010 EB28 diluted-1 B	SEKR3650C701S072512D010 EB28 diluted-1 C
		
EB28 diluted-2 	EB28 diluted-2 	EB28 diluted-2 

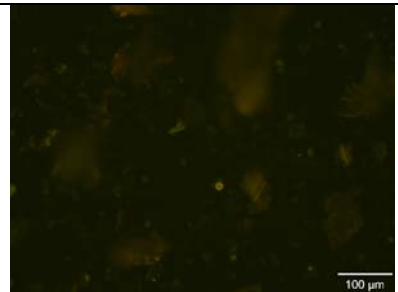
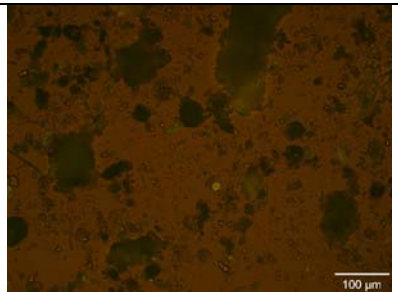
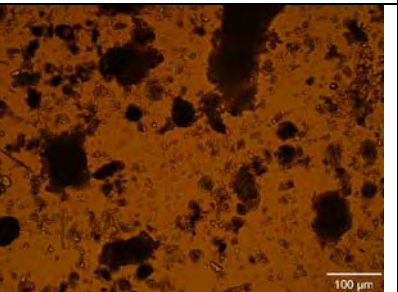
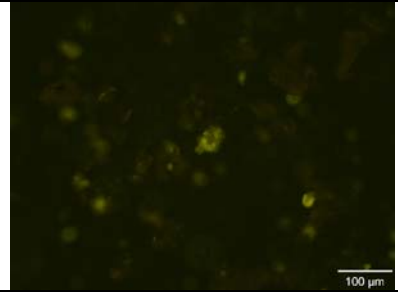
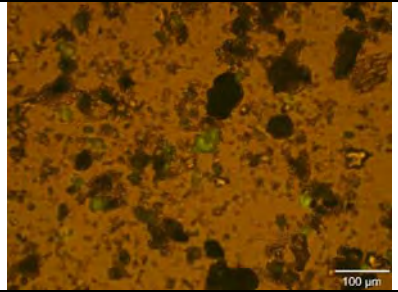
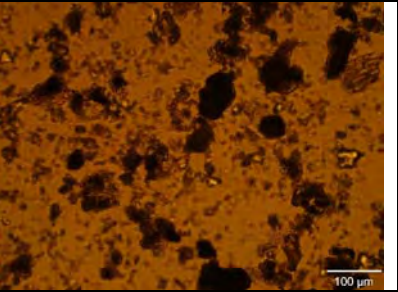
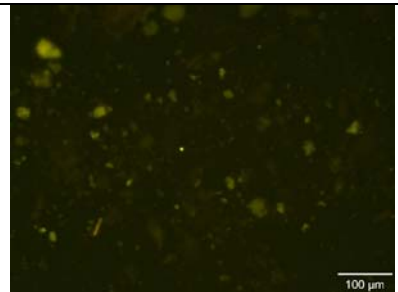
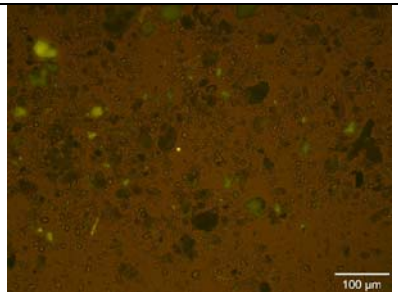
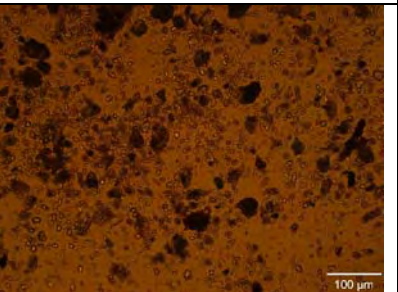
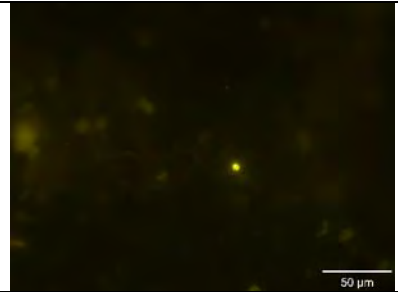
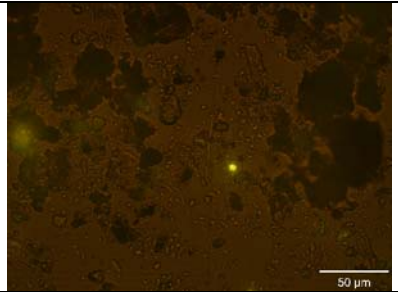
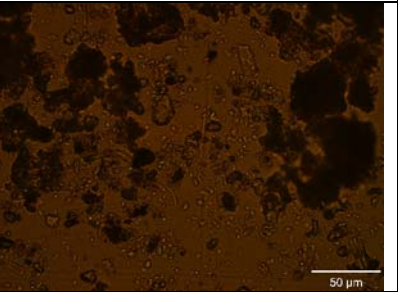
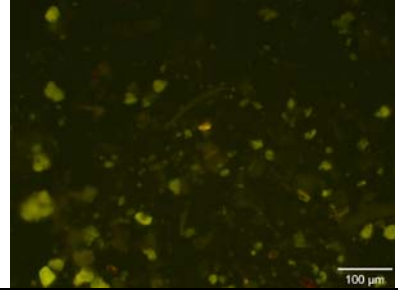
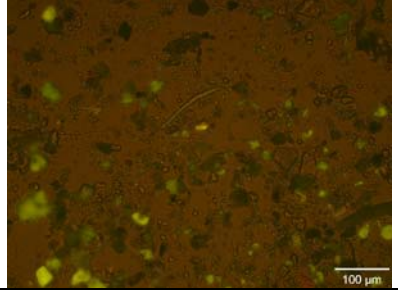
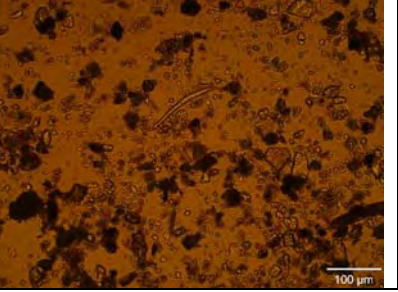
EB28 diluted -3 	EB28 diluted -3 	EB28 diluted -3 
EB28 diluted -4 	EB28 diluted -4 	EB28 diluted -4 
EB28diluted-5 	EB28diluted-5 	EB28diluted-5 
EB28 diluted-6 	EB28 diluted-6 	EB28 diluted-6 
SEKR3800C707S072712D014 EB29-1 A	SEKR3800C707S072712D014 EB29-1 B	SEKR3800C707S072712D014 EB29-1 C
		

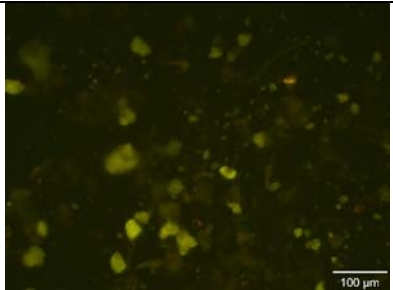
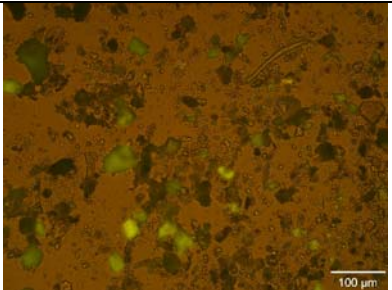
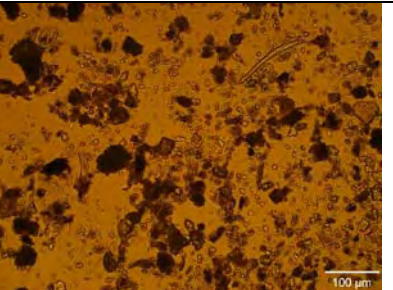
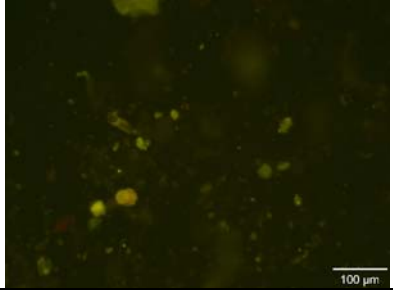
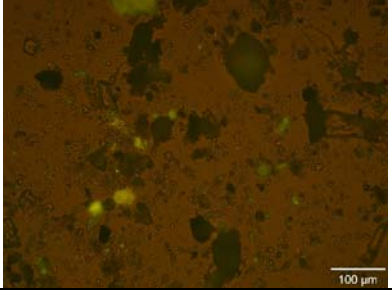
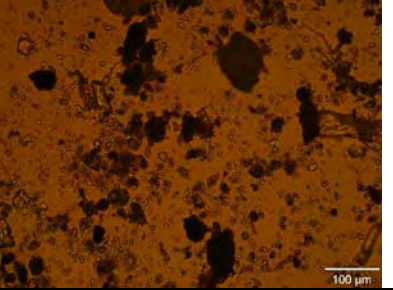
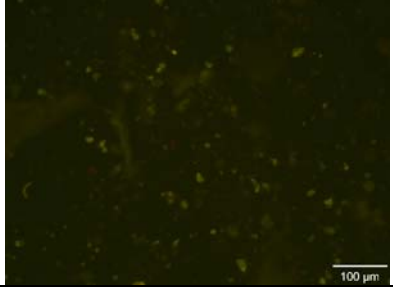
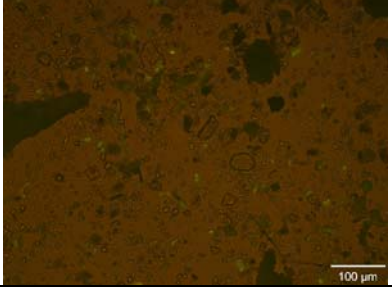
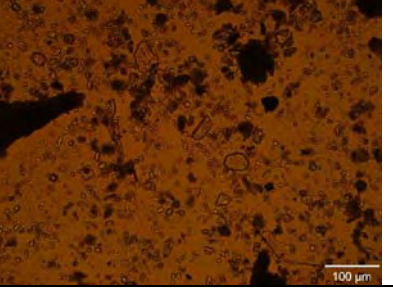
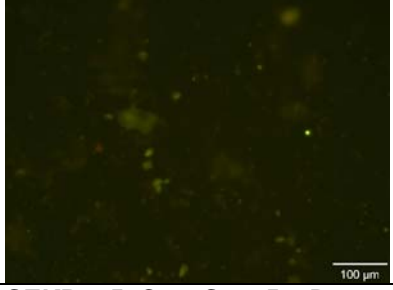
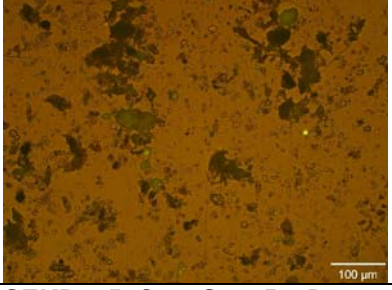
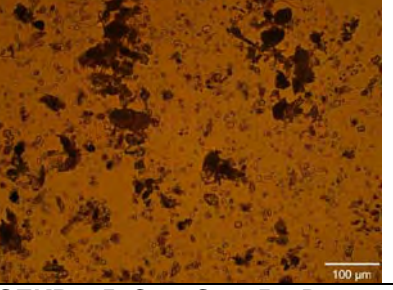
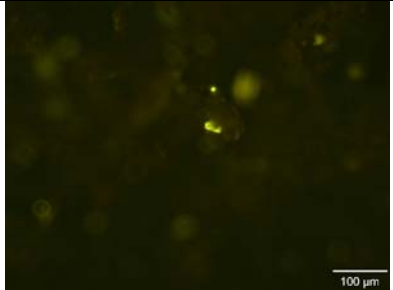
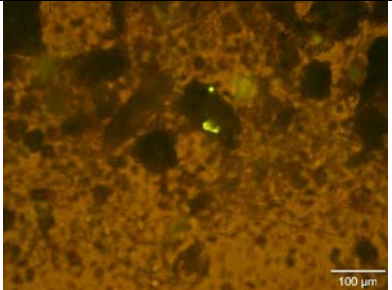
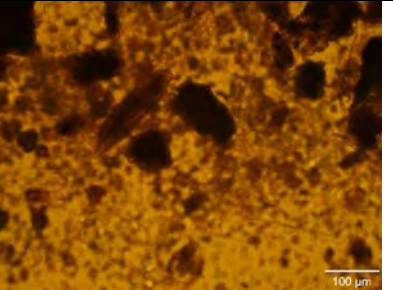
EB29-2 	EB29-2 	EB29-2 
EB29-3 	EB29-3 	EB29-3 
EB29-3 at 320x 	EB29-3 at 320x 	EB29-3 at 320x 
EB29-4 	EB29-4 	EB29-4 
EB29-4 at 320x 	EB29-4 at 320x 	EB29-4 at 320x 

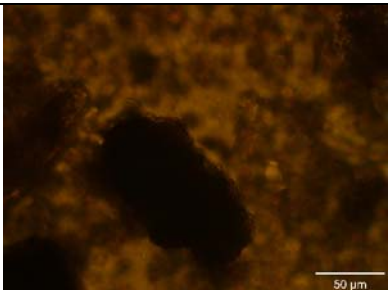
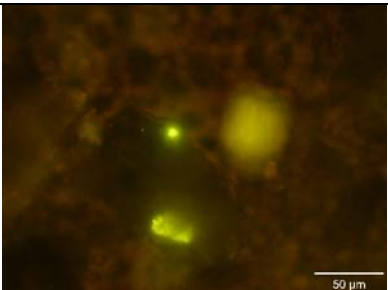
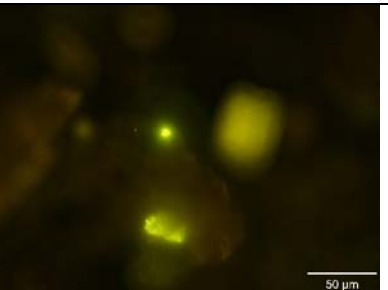
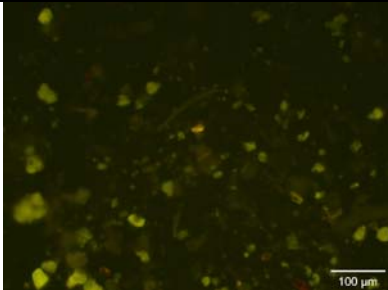
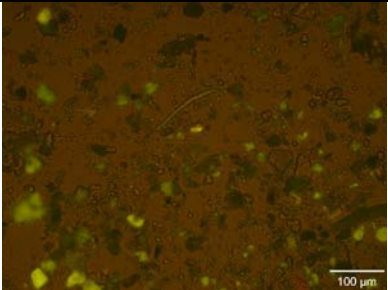
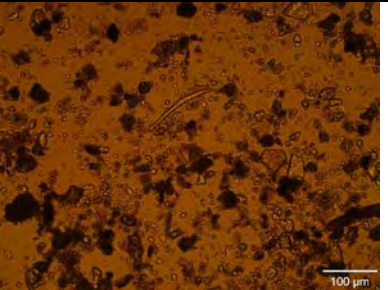
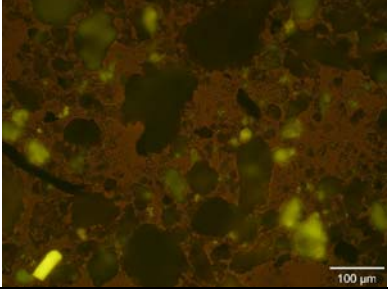
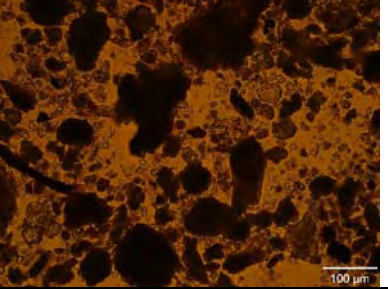
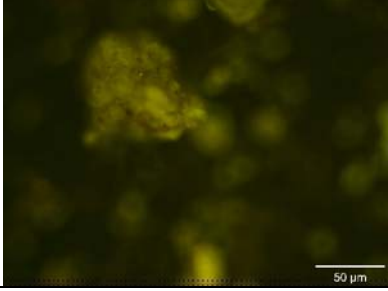
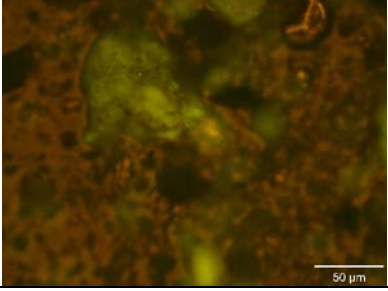
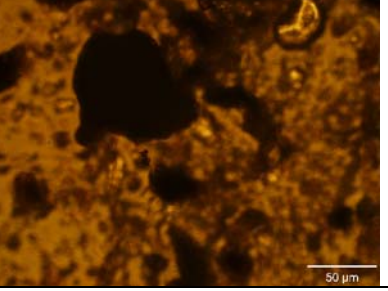
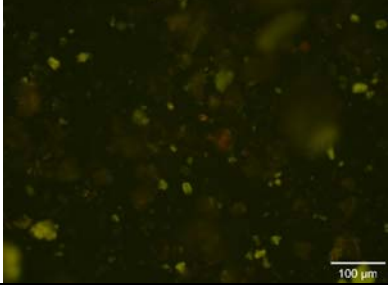
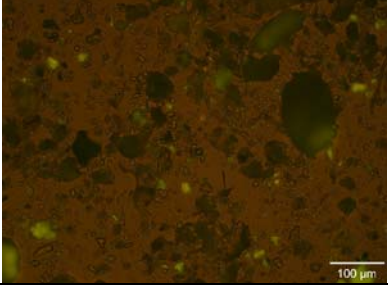
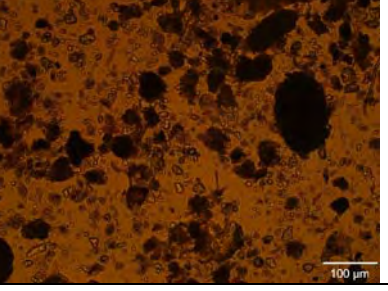
EB29-5 	EB29-5 	EB29-5 
EB29-6 	EB29-6 	EB29-6 
EB29-7 	EB29-7 	EB29-7 
EB29-7 at 320x 	EB29-7 at 320x 	EB29-7 at 320x 
SEKR3800C709S072712D006 EB30-1 A	SEKR3800C709S072712D006 EB30-1 B	SEKR3800C709S072712D006 EB30-1 C
		

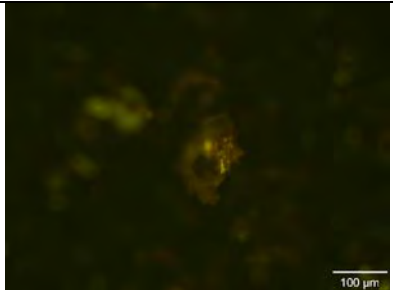
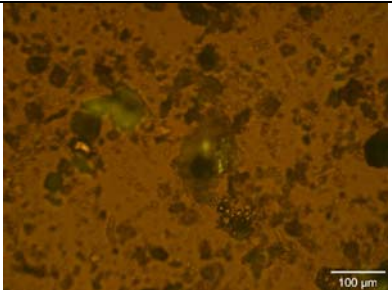
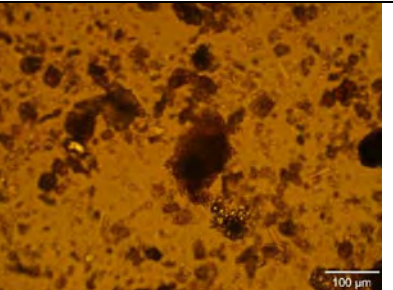
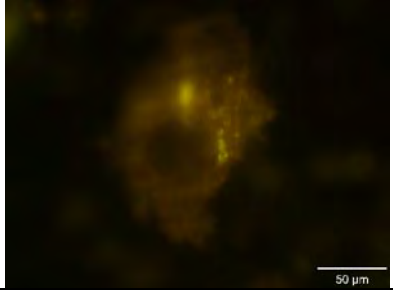
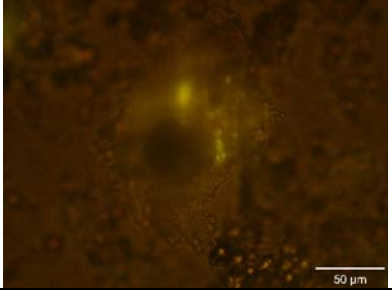
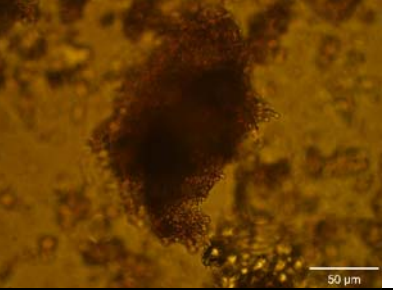
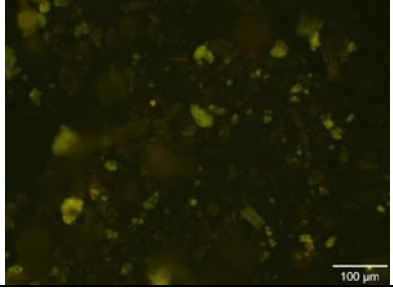
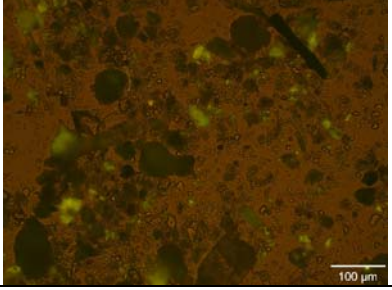
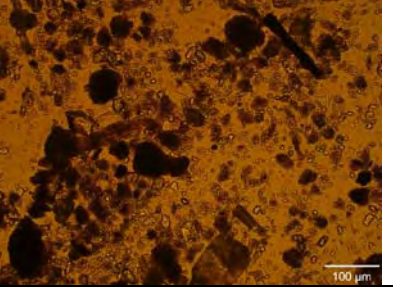
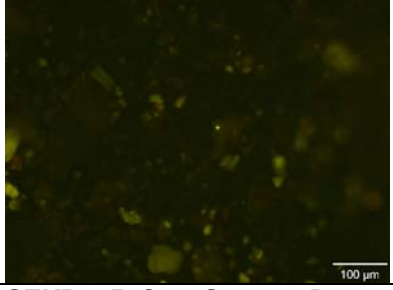
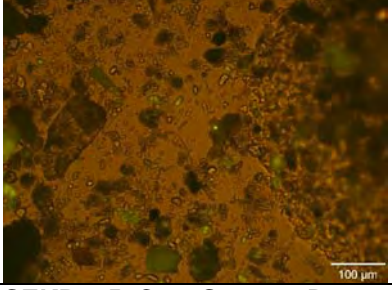
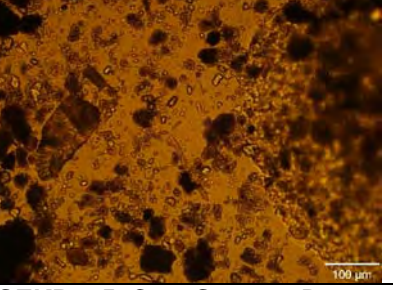
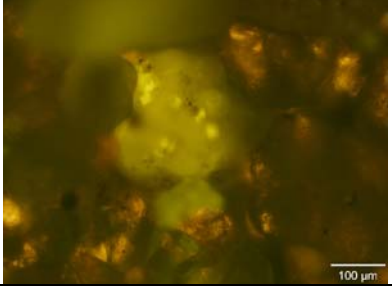
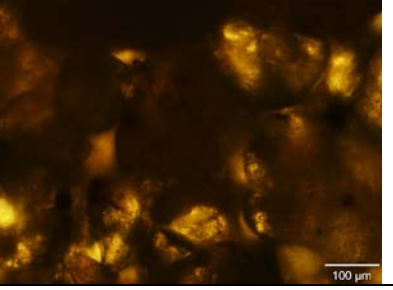
EB30-2 	EB30-2 	EB30-2 
EB30-2 at 320x 	EB30-2 at 320x 	EB30-2 at 320x 
EB30-3 	EB30-3 	EB30-3 
EB30-4 	EB30-4 	EB30-4 
EB30-5 	EB30-5 	EB30-5 

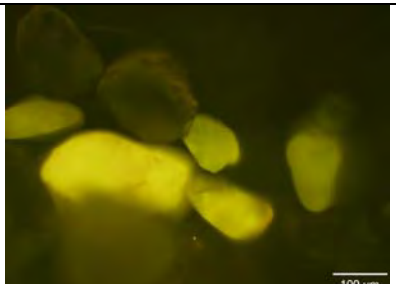
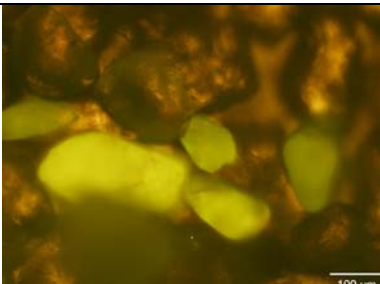
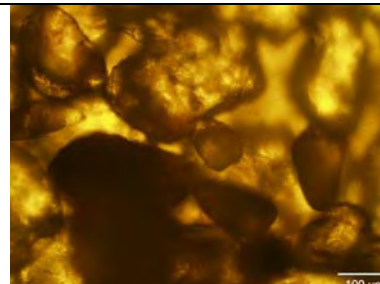
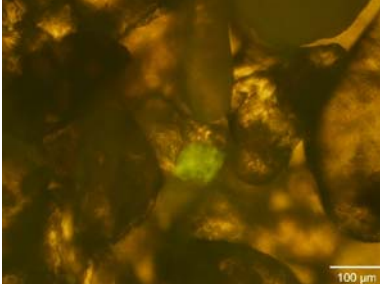
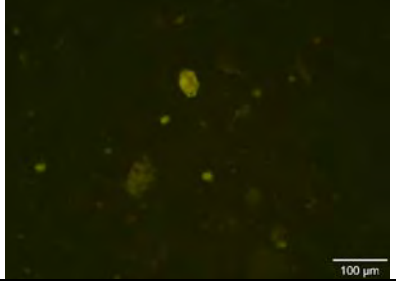
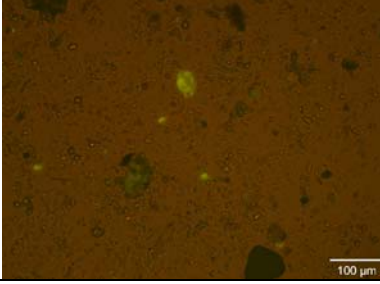
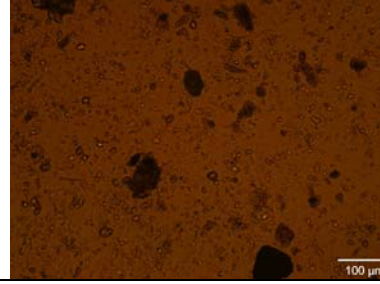
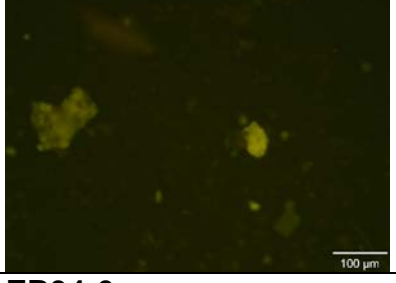
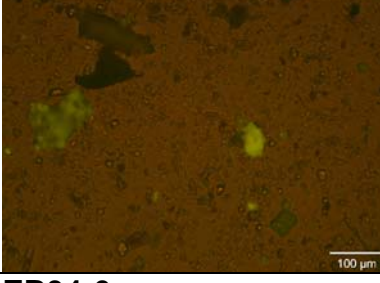
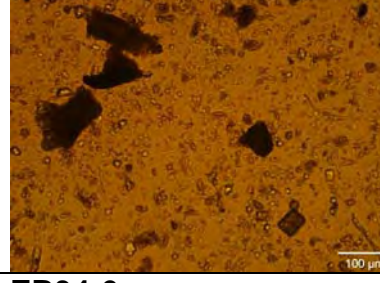
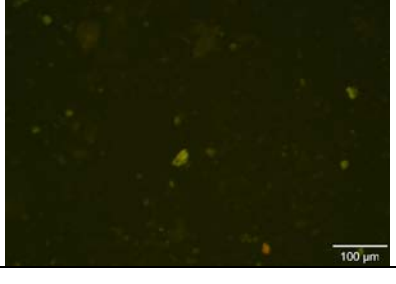
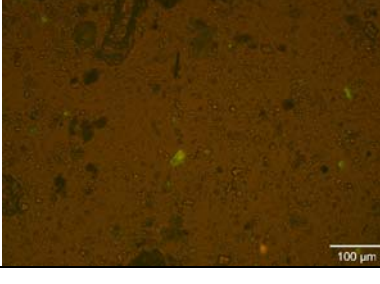
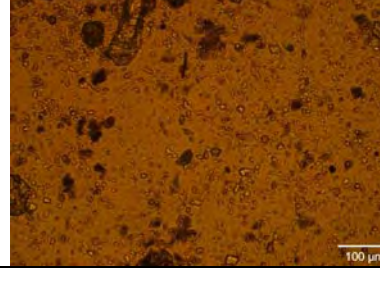
EB30-6	EB30-6	EB30-6
		
SEKR3800C709S072712D011 EB31-1 A	SEKR3800C709S072712D011 EB31-1 B	SEKR3800C709S072712D011 EB31-1 C
		
EB31-2	EB31-2	EB31-2
		
EB31-3	EB31-3	EB31-3
		
EB31-4	EB31-4	EB31-4
		

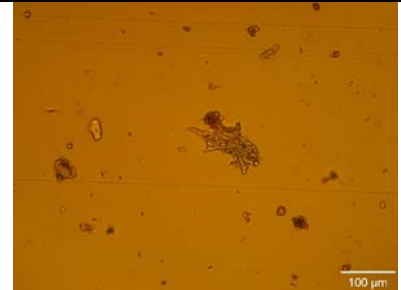
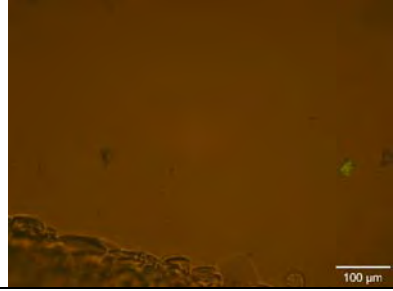
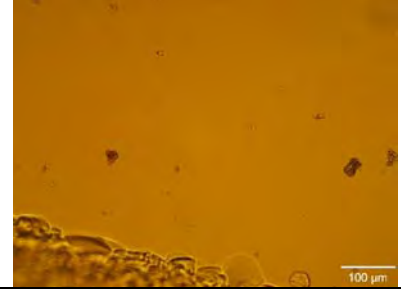
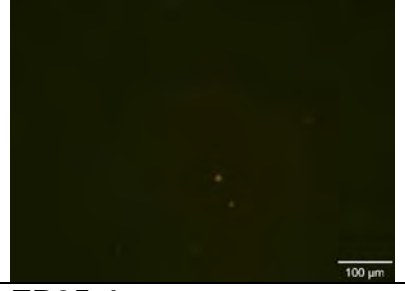
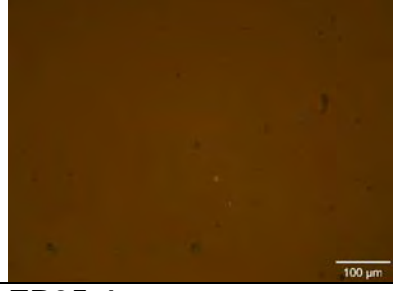
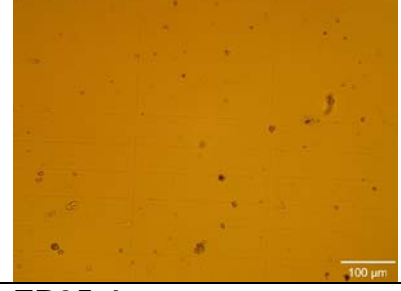
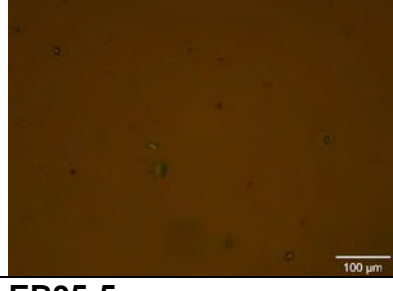
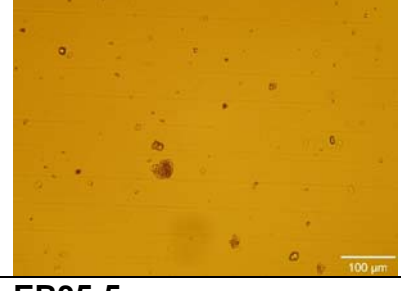
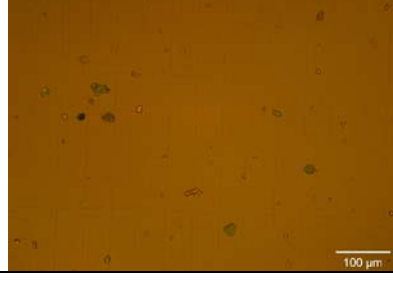
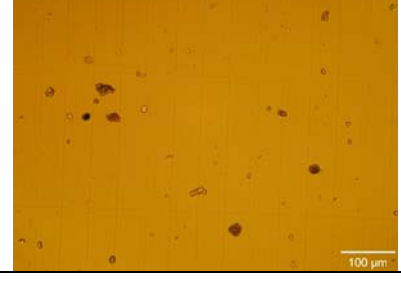
EB31-5 	EB31-5 	EB31-5 
EB31-6 	EB31-6 	EB31-6 
SEKR2850C701S072412DX EB32-1 A 	SEKR2850C701S072412DX EB32-1 B 	SEKR2850C701S072412DX EB32-1 C 
EB32-1 at 320x 	EB32-1 at 320x 	EB32-1 at 320x 
EB32-2 	EB32-2 	EB32-2 

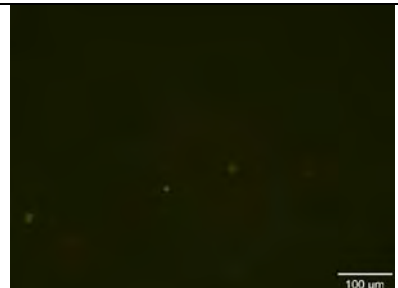
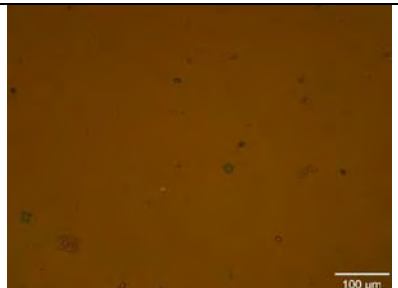
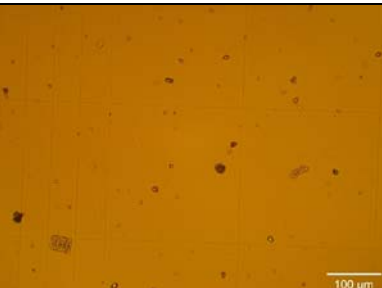
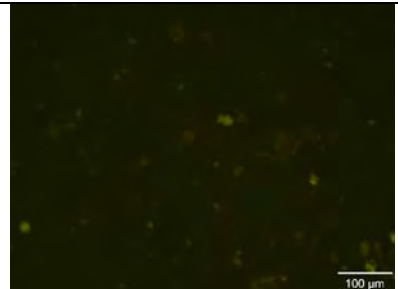
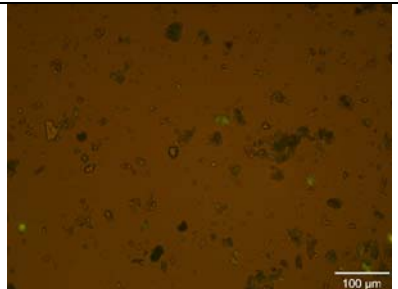
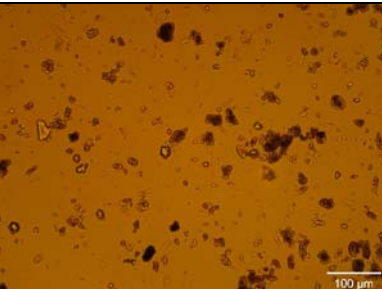
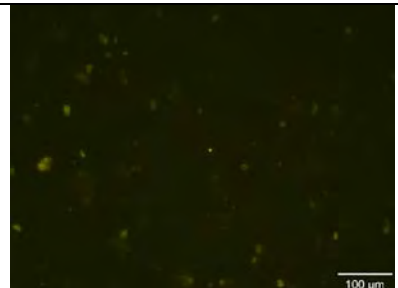
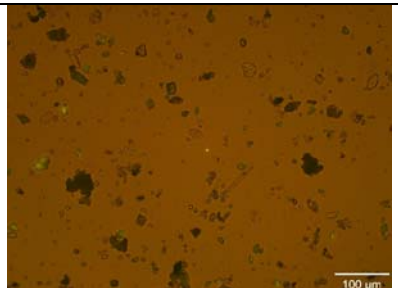
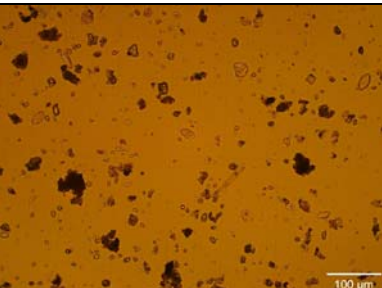
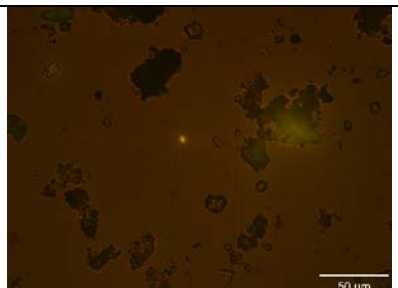
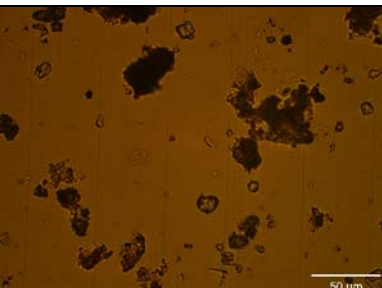
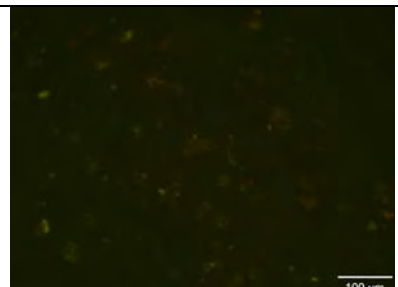
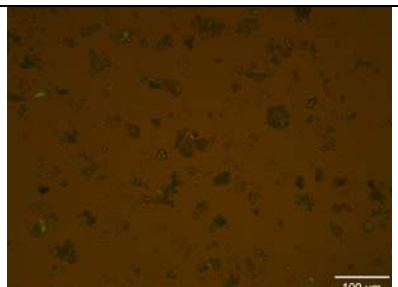
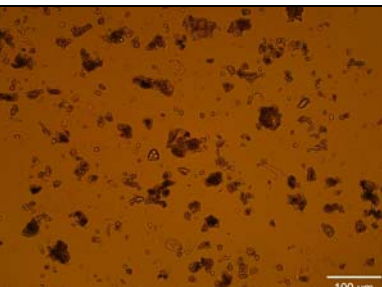
EB32-3 	EB32-3 	EB32-3 
EB32-4 	EB32-4 	EB32-4 
EB32-5 	EB32-5 	EB32-5 
EB32-6 	EB32-6 	EB32-6 
SEKR3750C701S072512D010 EB33-1 A	SEKR3750C701S072512D010 EB33-1 B	SEKR3750C701S072512D010 EB33-1 C
		

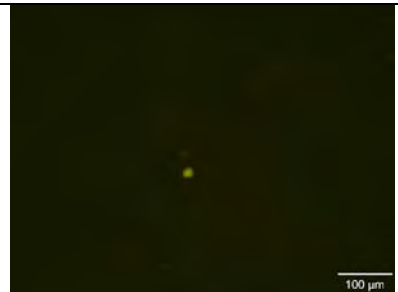
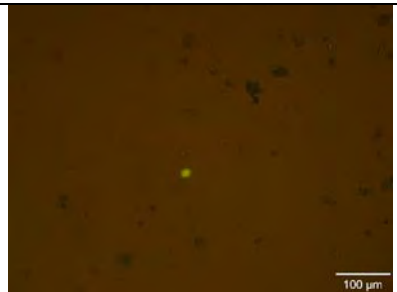
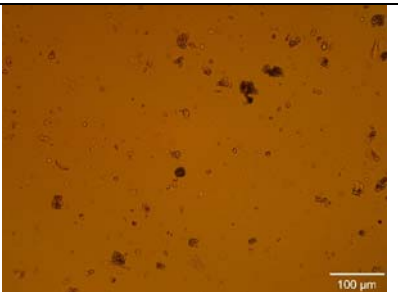
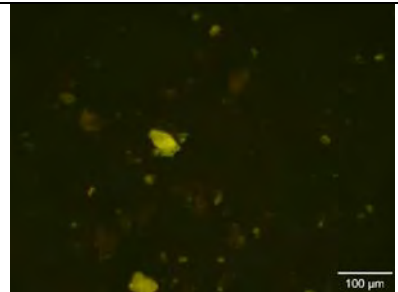
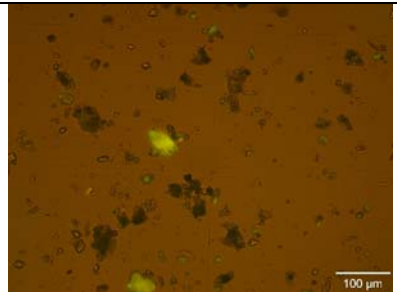
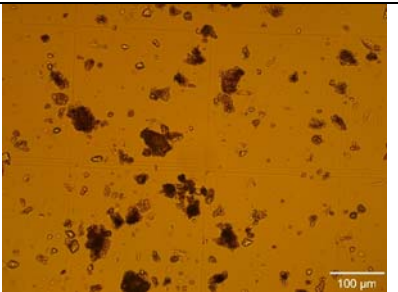
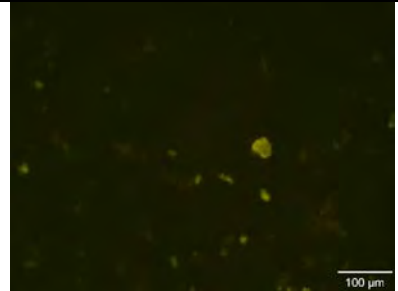
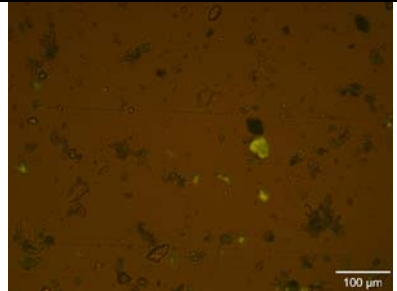
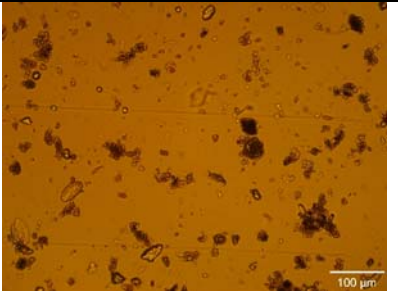
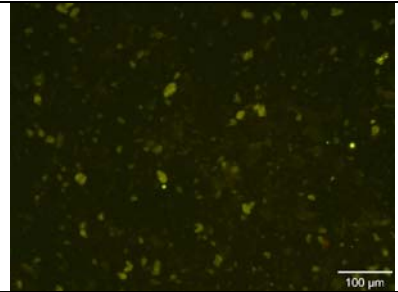
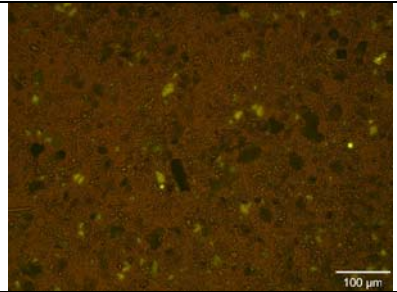
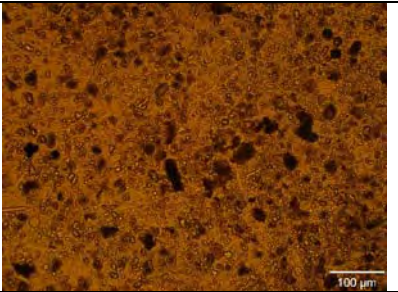
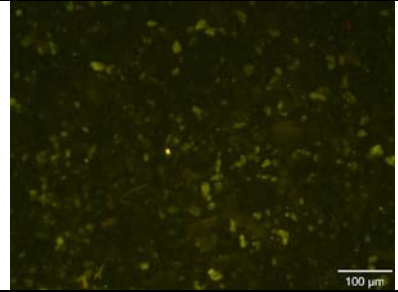
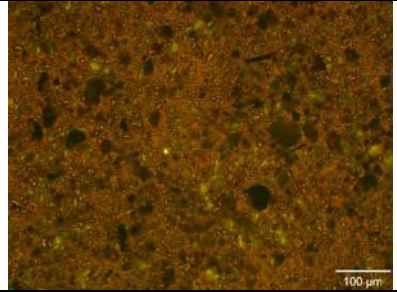
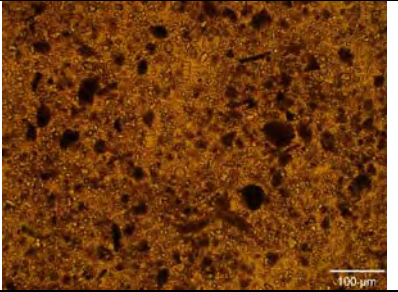
EB33-1 at 320x	EB33-1 at 320x	EB33-1 at 320x
		
EB33-2	EB33-2	EB33-2
		
EB33-3	EB33-3	EB33-3
		
EB33-3 at 320x	EB33-3 at 320x	EB33-3 at 320x
		
EB33-4	EB33-4	EB33-4
		

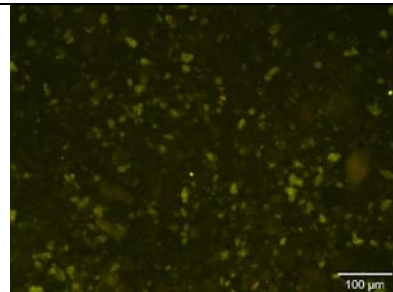
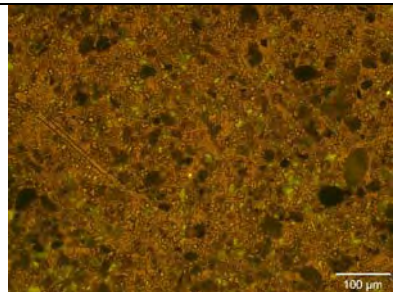
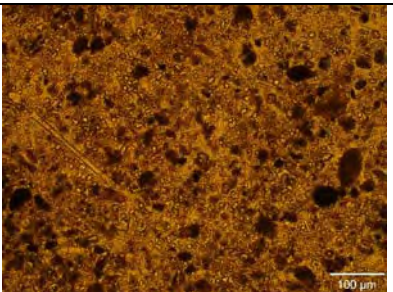
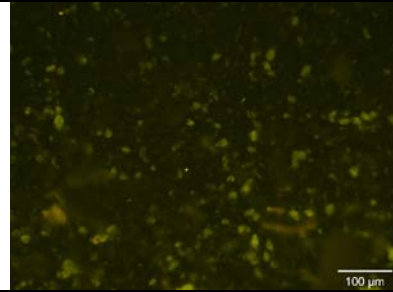
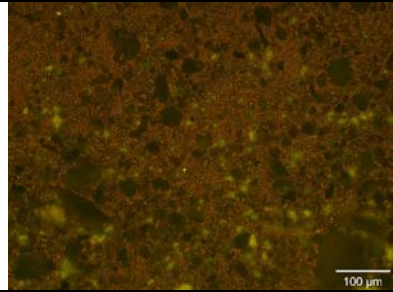
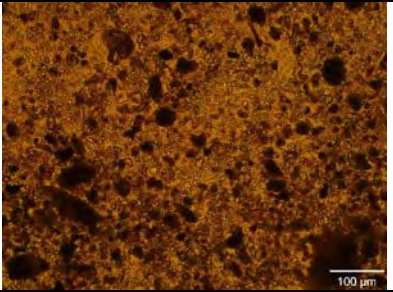
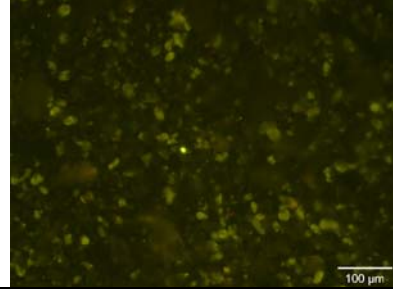
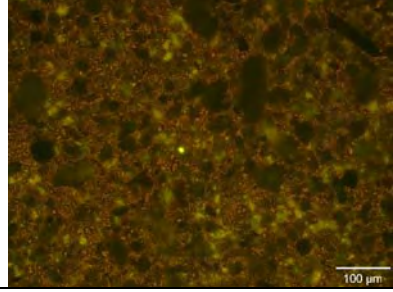
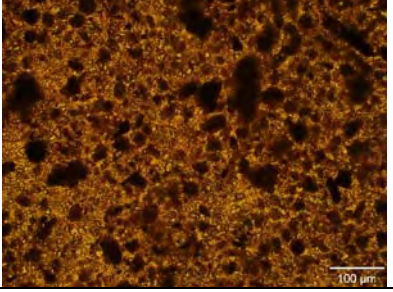
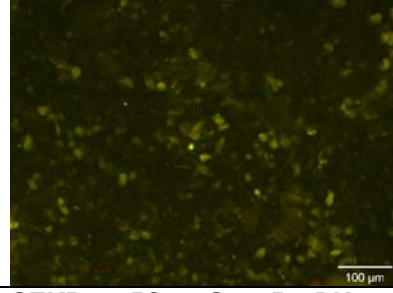
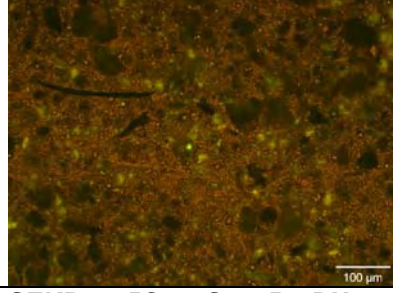
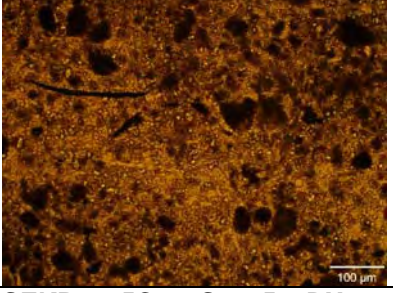
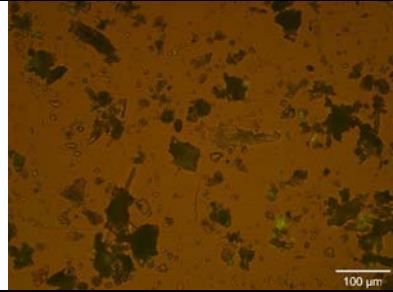
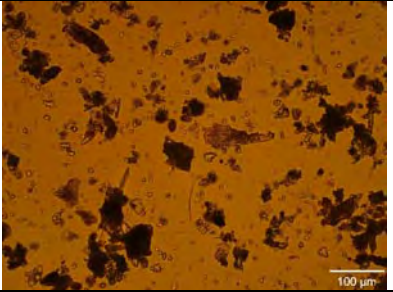
EB33-5 	EB33-5 	EB33-5 
EB33-5 at 320x 	EB33-5 at 320x 	EB33-5 at 320x 
EB33-6 	EB33-6 	EB33-6 
EB33-7 	EB33-7 	EB33-7 
SEKR2850C701S072412D003 EB34-1 A	SEKR2850C701S072412D003 EB34-1 B	SEKR2850C701S072412D003 EB34-1 C
		

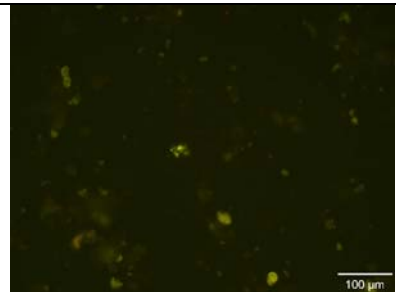
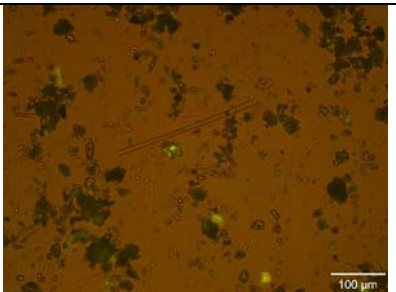
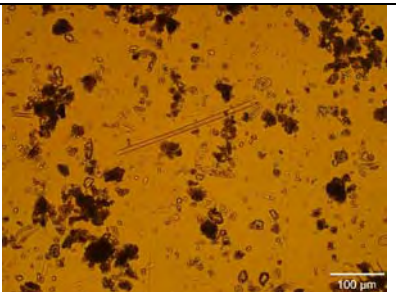
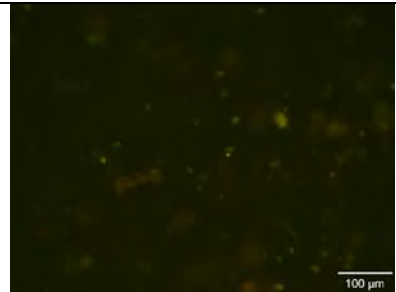
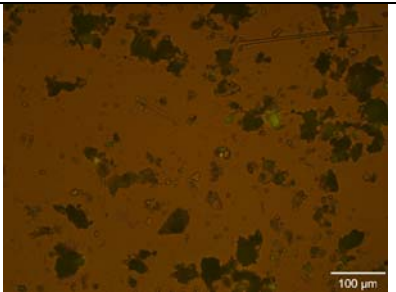
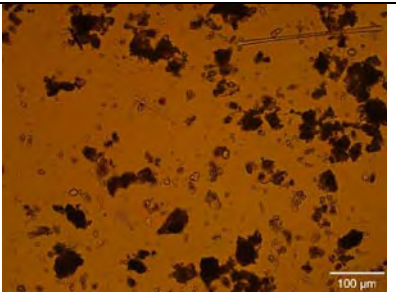
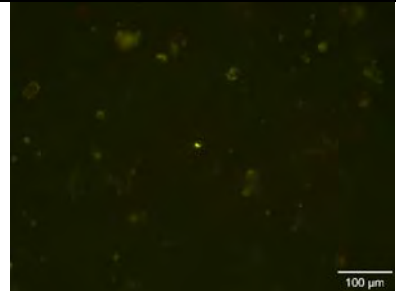
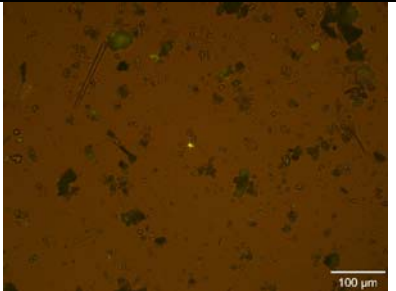
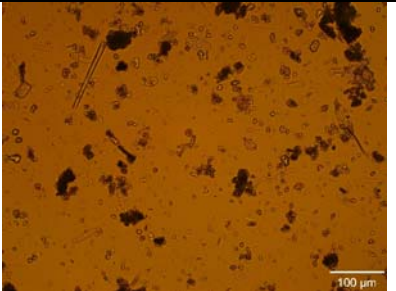
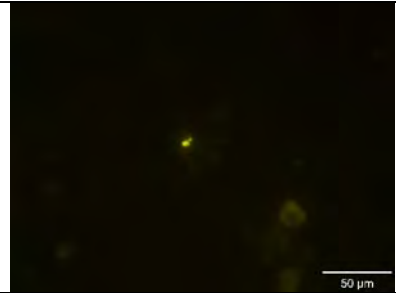
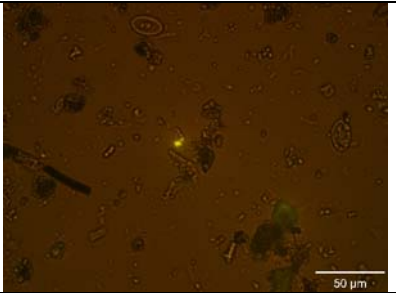
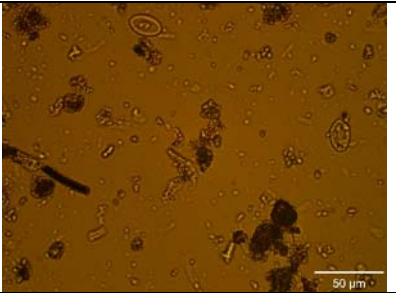
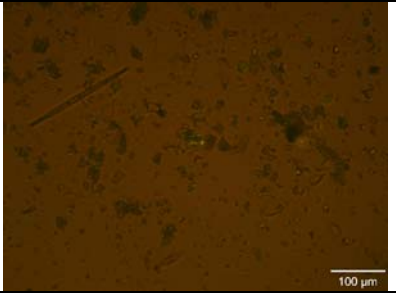
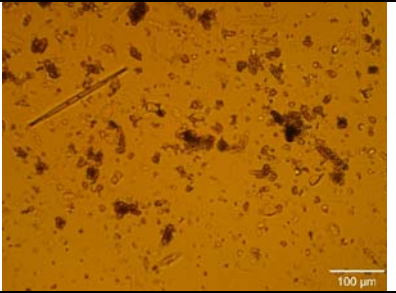
<p>EB34-2</p> 	<p>EB34-2</p> 	<p>EB34-2</p> 
<p>EB34-3</p> 	<p>EB34-3</p> 	<p>EB34-3</p> 
<p>EB34-4</p> 	<p>EB34-4</p> 	<p>EB34-4</p> 
<p>EB34-5</p> 	<p>EB34-5</p> 	<p>EB34-5</p> 
<p>EB34-6</p> 	<p>EB34-6</p> 	<p>EB34-6</p> 

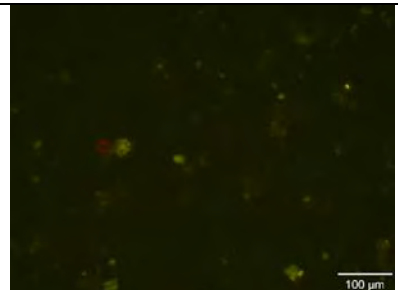
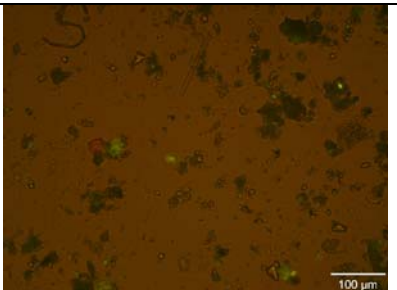
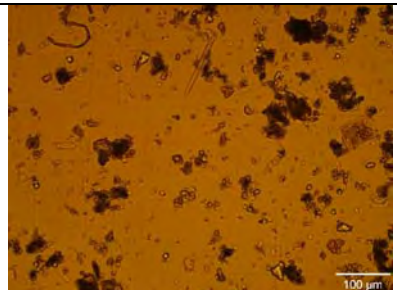
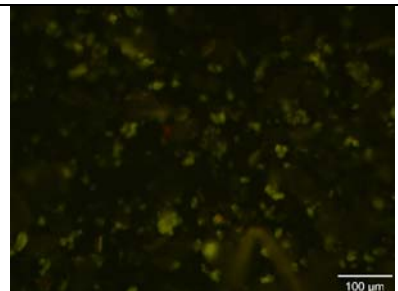
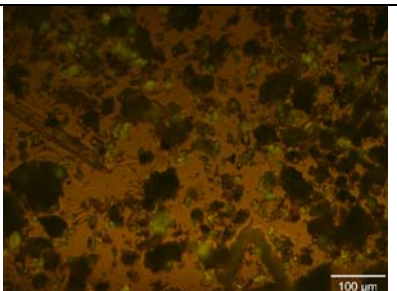
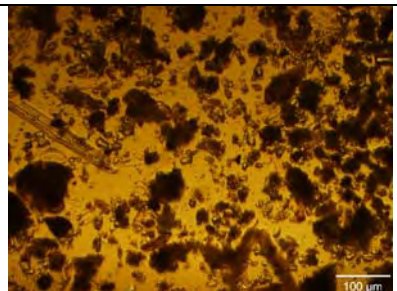
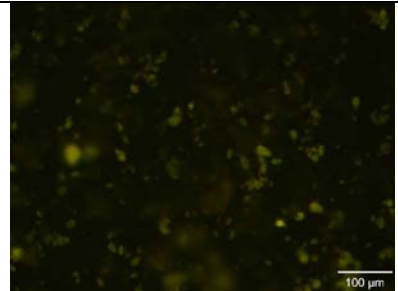
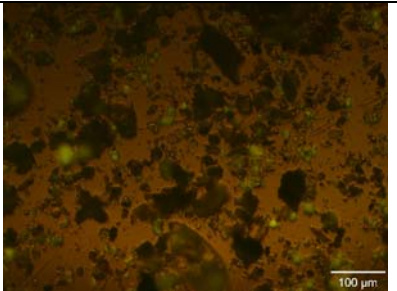
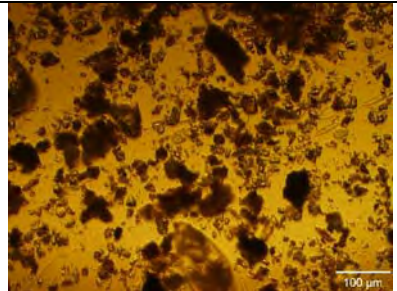
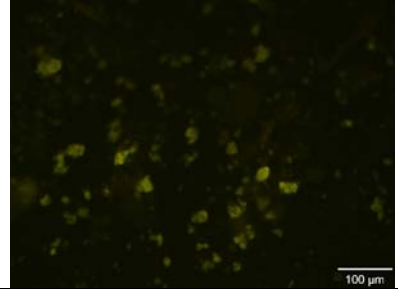
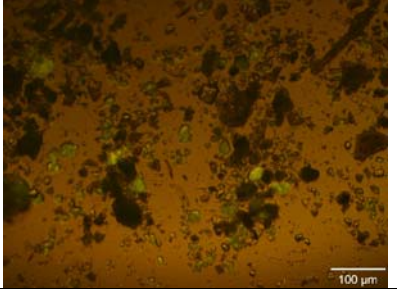
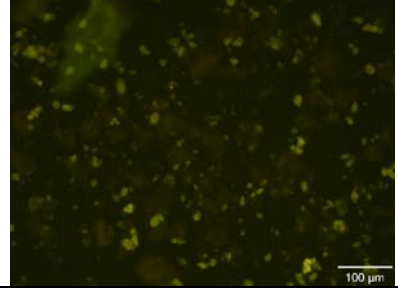
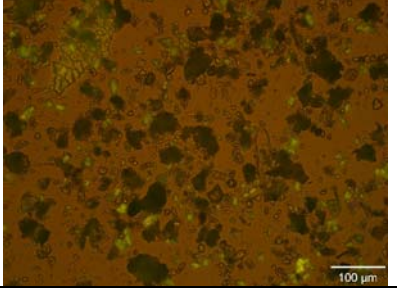
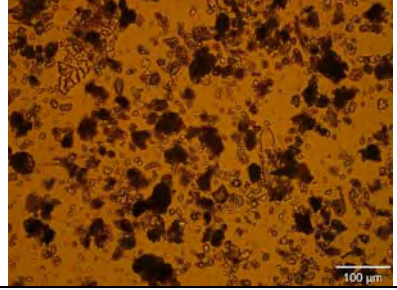
SEKR1900C701S072512D009 EB35-1 A	SEKR1900C701S072512D009 EB35-1 B	SEKR1900C701S072512D009 EB35-1 C
		
EB35-2	EB35-2	EB35-2
		
EB35-3	EB35-3	EB35-3
		
EB35-4	EB35-4	EB35-4
		
EB35-5	EB35-5	EB35-5
		

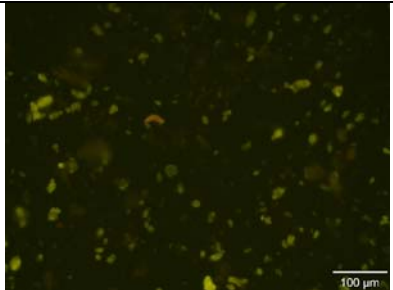
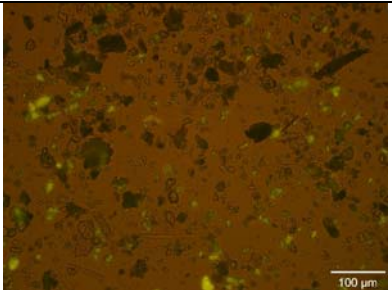
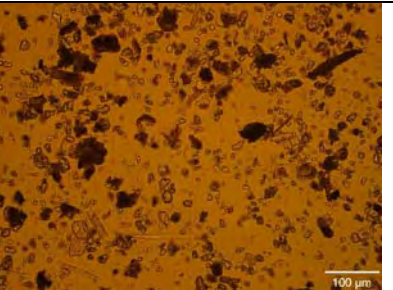
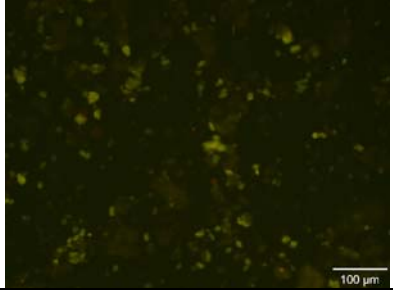
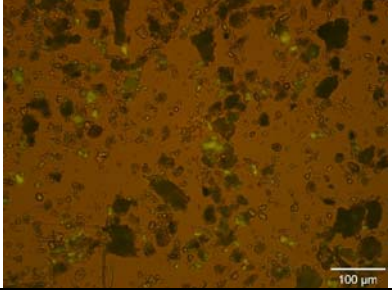
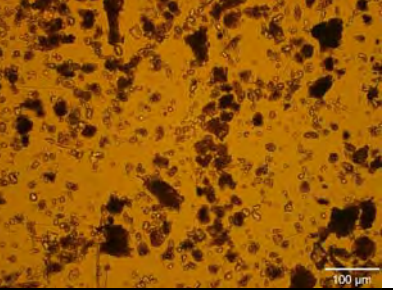
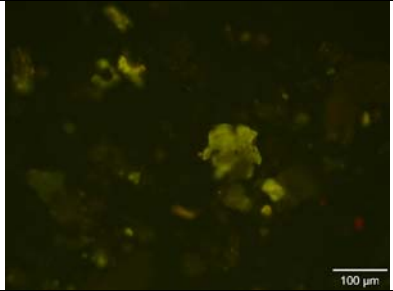
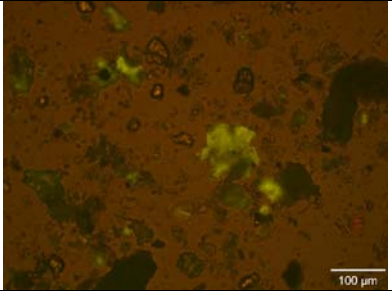
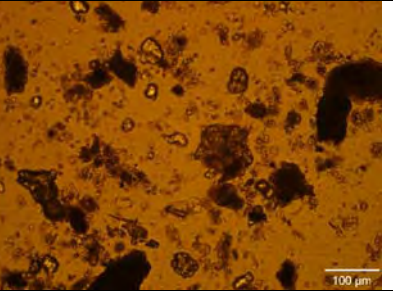
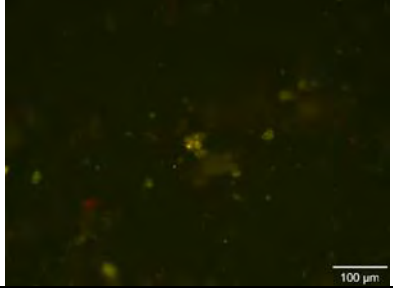
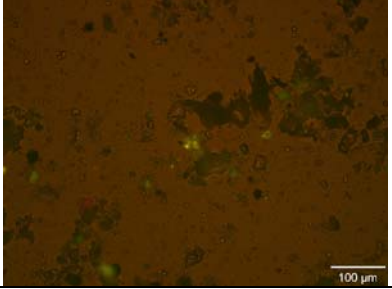
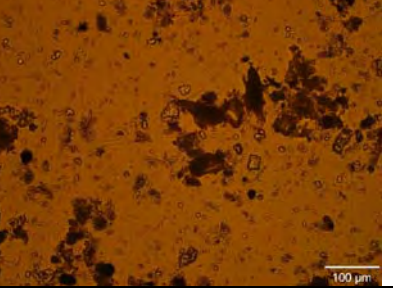
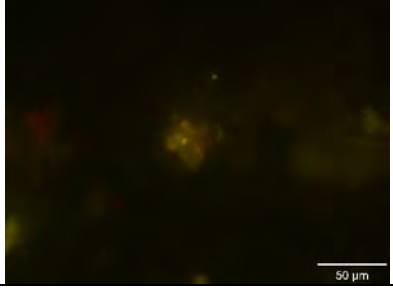
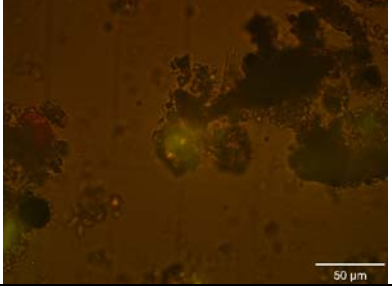
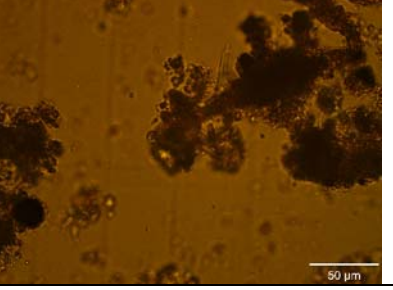
EB35-6 	EB35-6 	EB35-6 
SEKR1900C701S072512DX EB36-1 A 	SEKR1900C701S072512DX EB36-1 B 	SEKR1900C701S072512DX EB36-1 C 
EB36-2 	EB36-2 	EB36-2 
EB36-2 at 320x 	EB36-2 at 320x 	EB36-2 at 320x 
EB36-3 	EB36-3 	EB36-3 

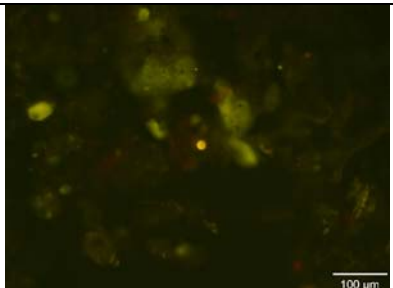
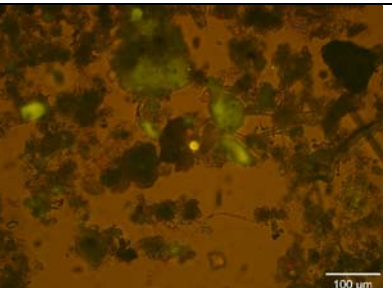
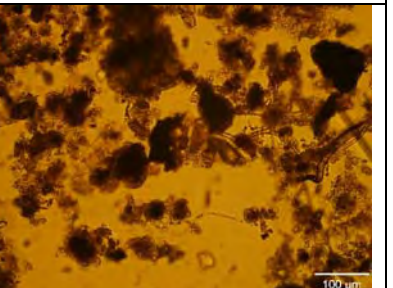
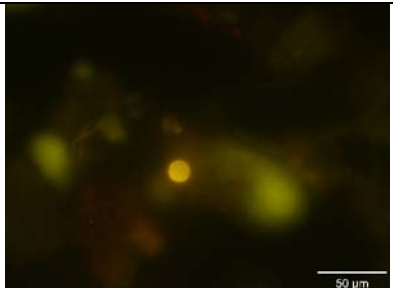
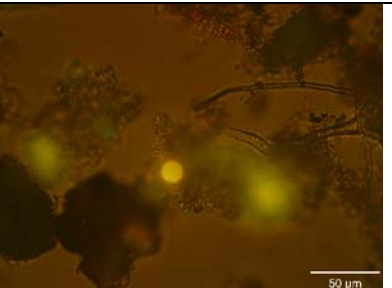
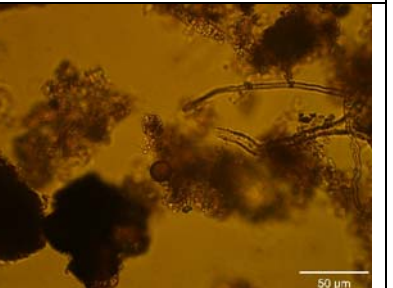
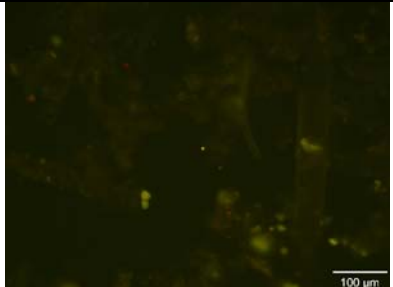
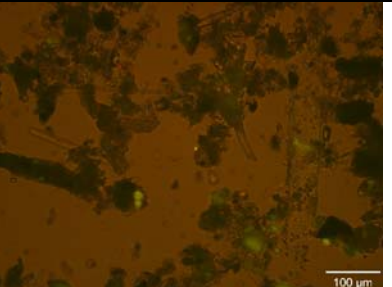
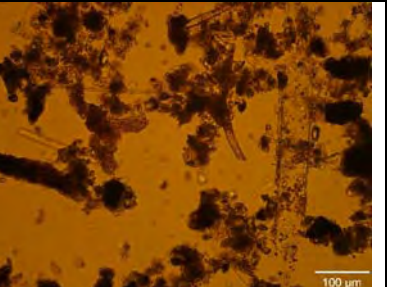
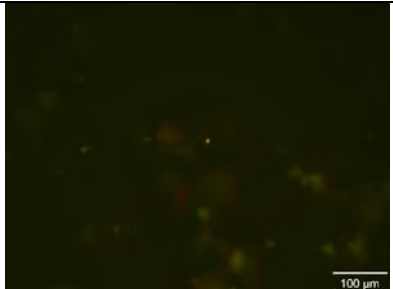
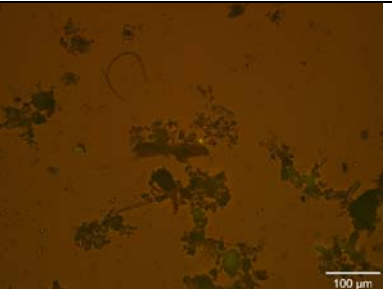
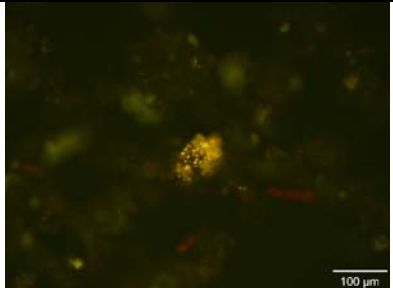
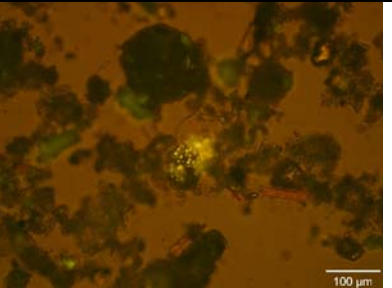
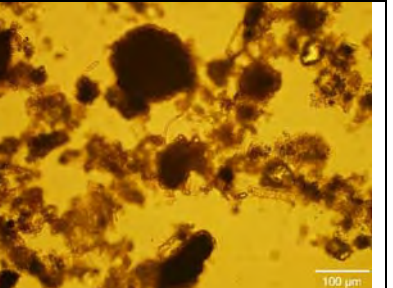
EB36-4 	EB36-4 	EB36-4 
EB36-5 	EB36-5 	EB36-5 
EB36-6 	EB36-6 	EB36-6 
SEKR3950C701S072612D013 EB37-1 A	SEKR3950C701S072612D013 EB37-1 B	SEKR3950C701S072612D013 EB37-1 C
		
EB37-2 	EB37-2 	EB37-2 

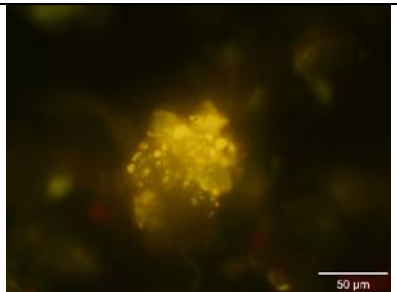
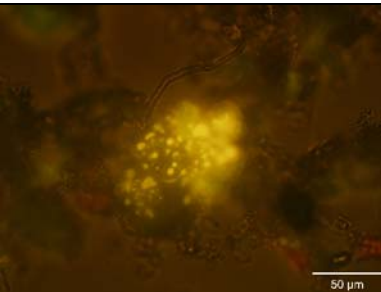
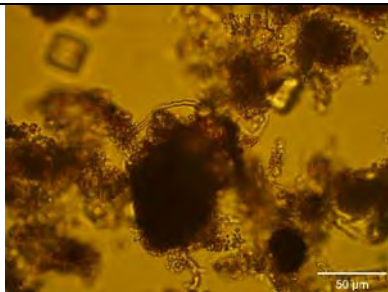
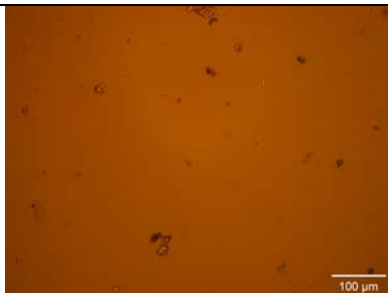
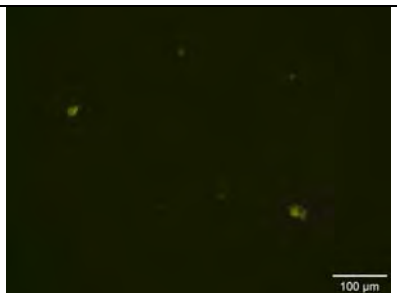
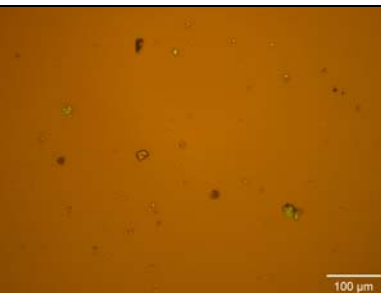
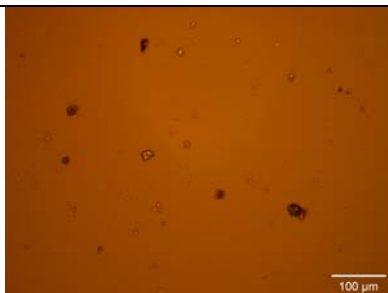
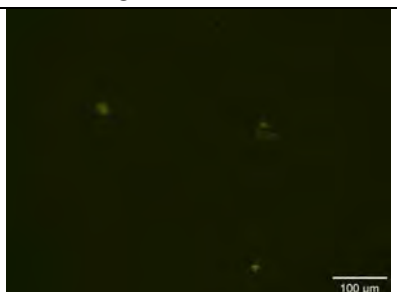
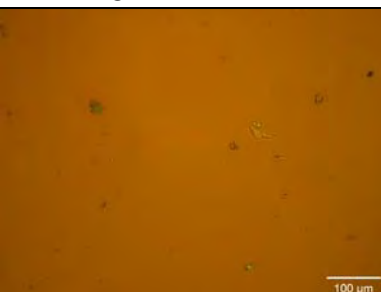
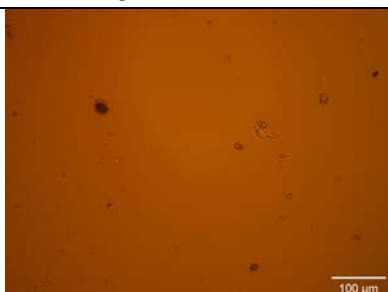
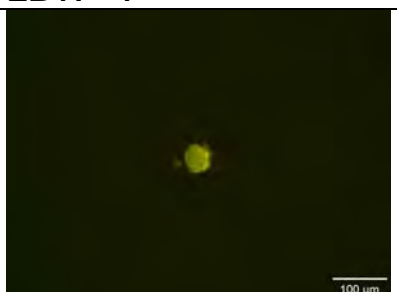
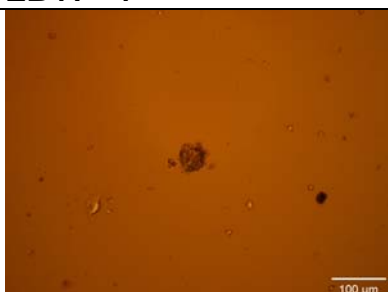
EB37-3 	EB37-3 	EB37-3 
EB37-4 	EB37-4 	EB37-4 
EB37-5 	EB37-5 	EB37-5 
EB37-6 	EB37-6 	EB37-6 
SEKR0425C701S072512DX EB38-1 A	SEKR0425C701S072512DX EB38-1 B	SEKR0425C701S072512DX EB38-1 C
		

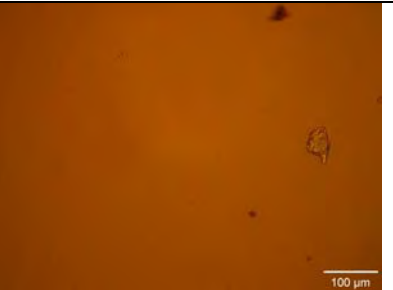
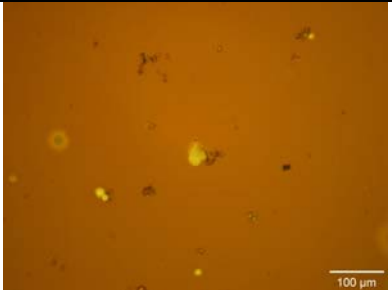
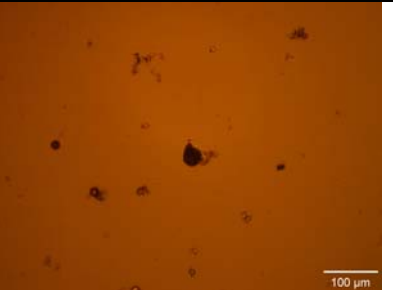
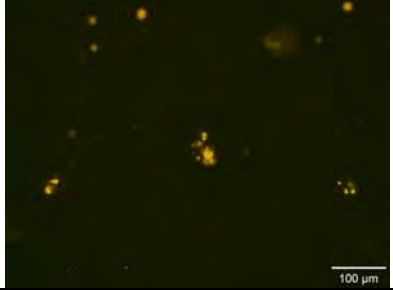
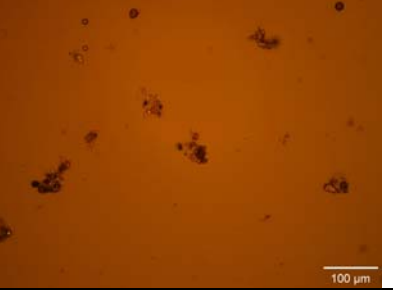
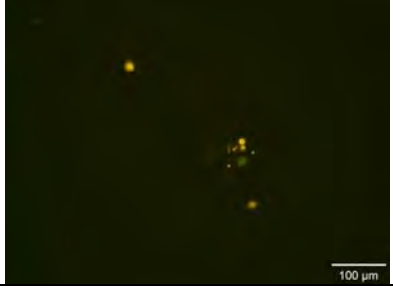
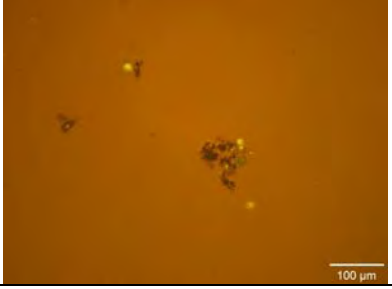
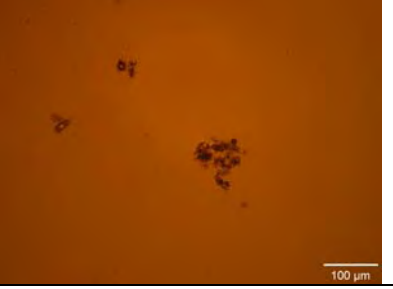
EB38-2 	EB38-2 	EB38-2 
EB38-3 	EB38-3 	EB38-3 
EB38-4 	EB38-4 	EB38-4 
EB38-4 at 320x 	EB38-4 at 320x 	EB38-4 at 320x 
EB38-5 	EB38-5 	EB38-5 

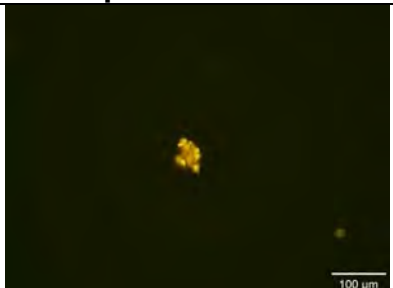
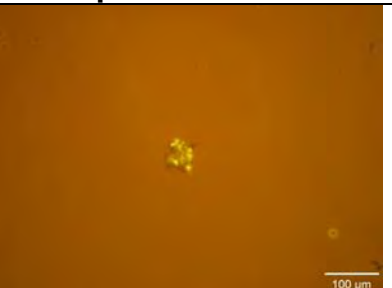
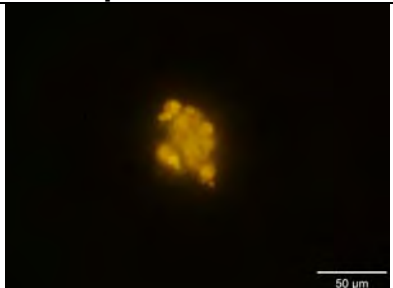
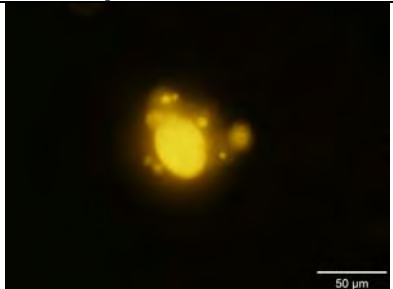
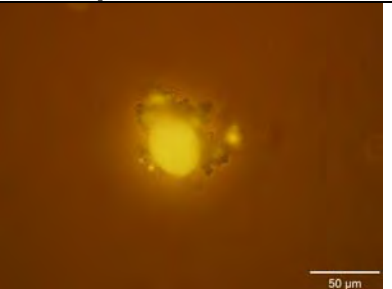
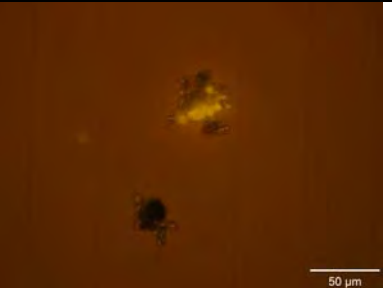
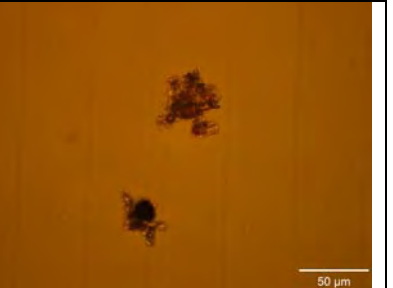
EB38-6	EB38-6	EB38-6
		
SEKR3950C701S072612DX EB39-1 A	E SEKR3950C701S072612DX B39-1 B	SEKR3950C701S072612DX EB39-1 C
		
EB39-2	EB39-2	EB39-2
		
EB39-3	EB39-3	EB39-3
		
EB39-4	EB39-4	EB39-4
		

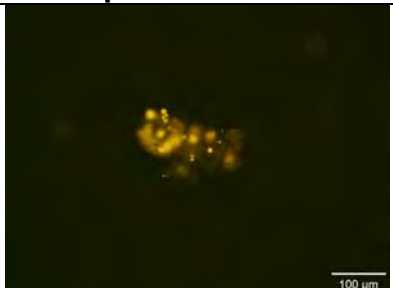
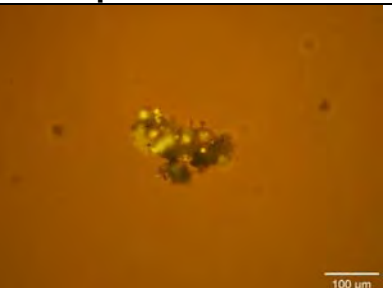
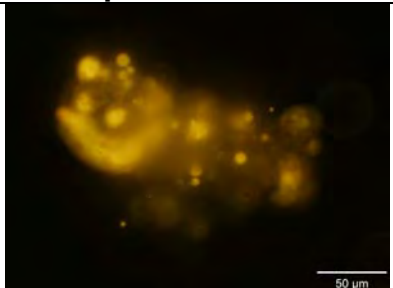
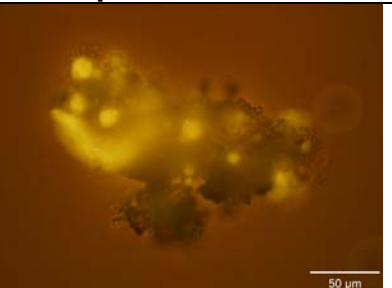
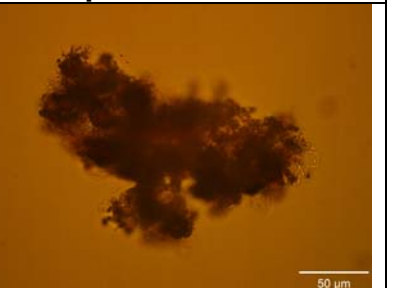
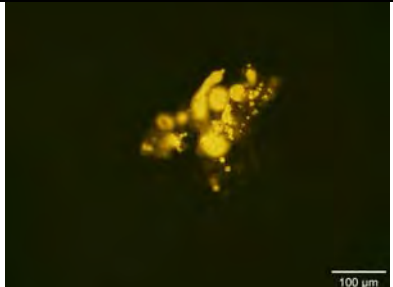
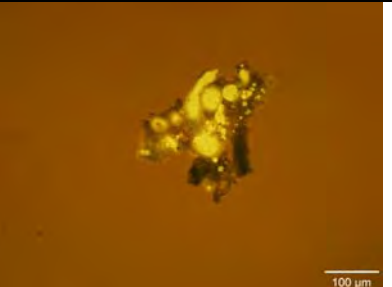
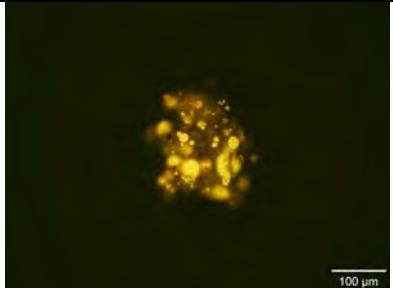
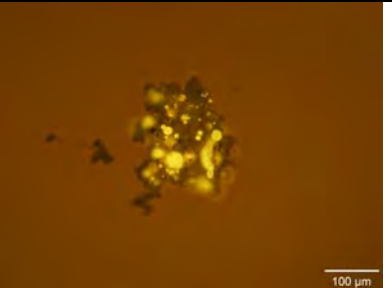
EB39-5	EB39-5	EB39-5
		
EB39-6	EB39-6	EB39-6
		
OxBow EB40-1 A	OxBow EB40-1 B	OxBow EB40-1 C
		
EB40-2	EB40-2	EB40-2
		
EB40-2 at 320x	EB40-2 at 320x	EB40-2 at 320x
		

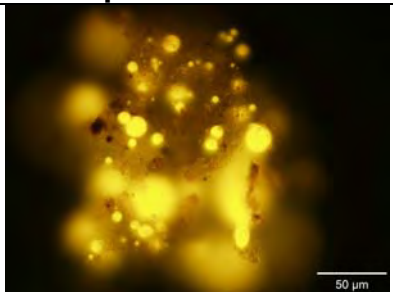
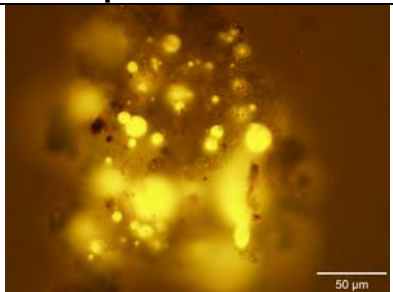
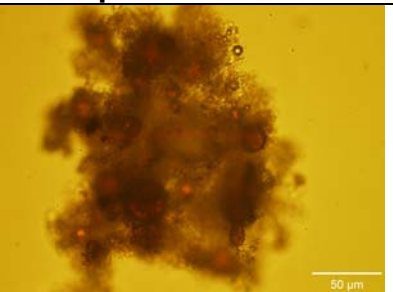
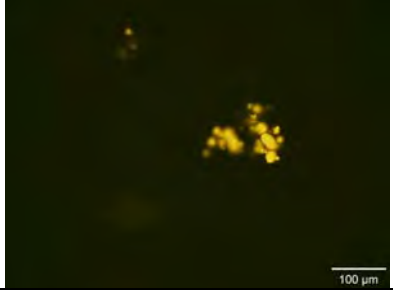
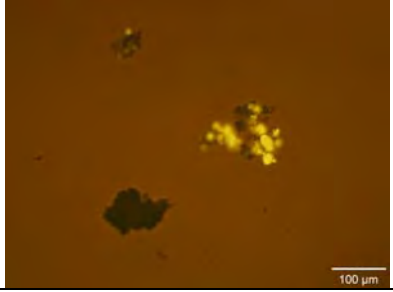
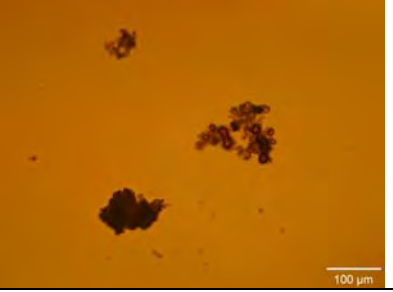
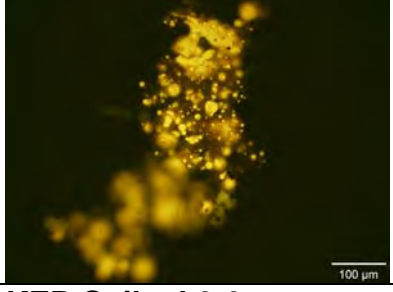
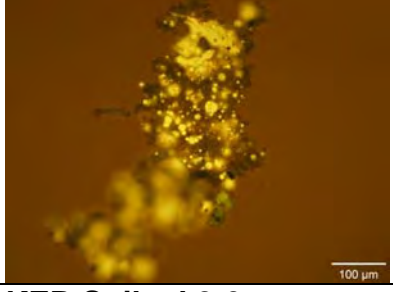
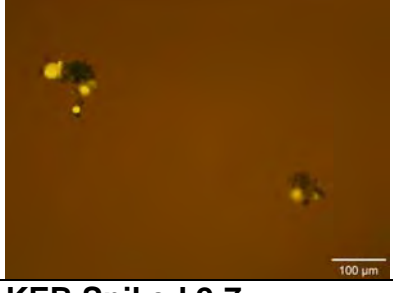
EB40-3 	EB40-3 	EB40-3 
EB40-3 at 320x 	EB40-3 at 320x 	EB40-3 at 320x 
EB40-4 	EB40-4 	EB40-4 
EB40-5 	EB40-5 	EB40-5 
EB40-6 	EB40-6 	EB40-6 

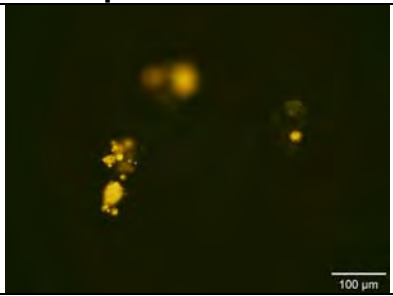
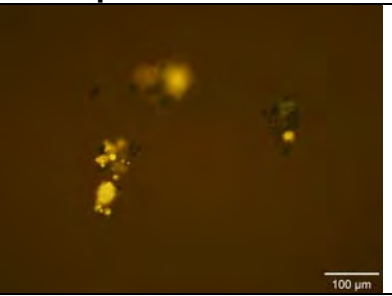
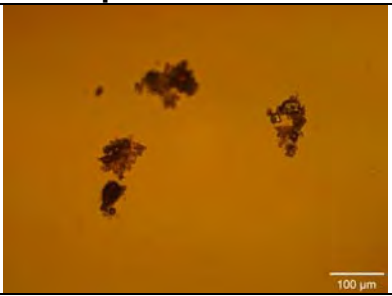
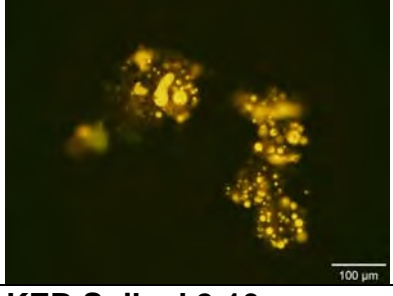
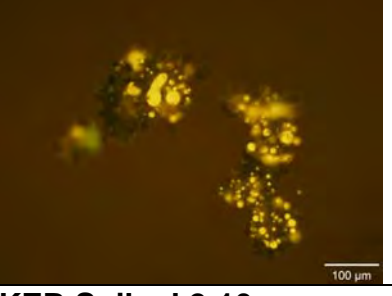
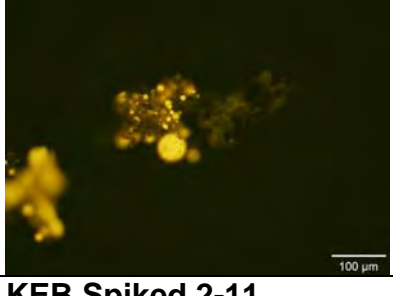
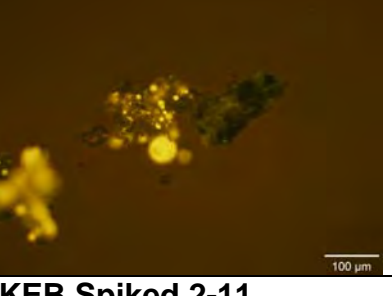
EB40-6 at 320x	EB40-6 at 320x	EB40-6 at 320x
		
SEKR1900C701S072512D005E B41-1 A	SEKR1900C701S072512D005 EB41-1 B	SEKR1900C701S072512D005 EB41-1 C
		
EB41 - 2	EB41 - 2	EB41 - 2
		
EB41 - 3	EB41 - 3	EB41 - 3
		
EB41 - 4	EB41 - 4	EB41 - 4
		

EB41 - 5  100 µm	EB41 - 5  100 µm	EB41 - 5  100 µm
EB41 - 6  100 µm	EB41 - 6  100 µm	EB41 - 6  100 µm
KEB Spiked 1-1 A  100 µm	KEB Spiked 1-1 B  100 µm	KEB Spiked 1-1 C  100 µm
KEB Spiked 1-2  100 µm	KEB Spiked 1-2  100 µm	KEB Spiked 1-2  100 µm
KEB Spiked 1-3  100 µm	KEB Spiked 1-3  100 µm	KEB Spiked 1-3  100 µm

KEB Spiked 1-4	KEB Spiked 1-4	KEB Spiked 1-4
		
KEB Spiked 1-4 at 320x	KEB Spiked 1-4 at 320x	KEB Spiked 1-4 at 320x
		
KEB Spiked 1-5A	KEB Spiked 1-5A	KEB Spiked 1-5A
		
KEB Spiked 1-5A at 320x	KEB Spiked 1-5A at 320x	KEB Spiked 1-5A at 320x
		
KEB Spiked 1-5B at 320x	KEB Spiked 1-5B at 320x	KEB Spiked 1-5B at 320x
		

KEB Spiked 1-6	KEB Spiked 1-6	KEB Spiked 1-6
		
KEB Spiked 1-6 at 320x	KEB Spiked 1-6 at 320x	KEB Spiked 1-6 at 320x
		
KEB Spiked 2-1	KEB Spiked 2-1	KEB Spiked 2-1
		
KEB Spiked 2-2	KEB Spiked 2-2	KEB Spiked 2-2
		
KEB Spiked 2-3	KEB Spiked 2-3	KEB Spiked 2-3
		

KEB Spiked 2-3 at 320 x	KEB Spiked 2-3 at 320 x	KEB Spiked 2-3 at 320 x
		
KEB Spiked 2-4	KEB Spiked 2-4	KEB Spiked 2-4
		
KEB Spiked 2-5	KEB Spiked 2-5	KEB Spiked 2-5
		
KEB Spiked 2-6	KEB Spiked 2-6	KEB Spiked 2-6
		
KEB Spiked 2-7	KEB Spiked 2-7	KEB Spiked 2-7
		

KEB Spiked 2-8	KEB Spiked 2-8	KEB Spiked 2-8
		
KEB Spiked 2-9	KEB Spiked 2-9	KEB Spiked 2-9
		
KEB Spiked 2-10	KEB Spiked 2-10	KEB Spiked 2-10
		
KEB Spiked 2-11	KEB Spiked 2-11	KEB Spiked 2-11
